**Laboratory Testing of Transverse Joints in Precast-Panel Bridge-Deck Replacement Systems**

by

Jamieson D. Matthews

A thesis submitted to the Graduate Faculty of
Auburn University
in partial fulfillment of the
requirements for the Degree of
Master of Science

Auburn, Alabama
December 16, 2017

Keywords: Bridge; Deck, Grid-Reinforced Concrete; Deck, Exodermic; Fatigue; Grout; Joint; Rehabilitation; Key, Shear; Reinforcement

Approved by

Robert W. Barnes, Chair, Associate Professor of Civil Engineering
Anton K. Schindler, Professor of Civil Engineering
J. Michael Stallings, Professor of Civil Engineering

## Abstract

Out of the 614,387 bridges in the United States, 56,007 are structurally deficient (FHWA 2016). In many instances this structural deficiency relates to the deck of the bridge. Deck degradation is very common in bridges over 25 years old (Biswas 1986). Many decks fail several years before the rest of the bridge superstructure and substructure reach the end of their useful life (Bettigole and Robison 1997). An effective solution to this problem is to rapidly replace the bridge deck with precast panels. An important aspect of any deck system is the behavior of its transverse joints. The long-term success of a deck replacement project is dependent on the durability of the deck joints.

The Alabama Department of Transportation does not have any standards to test or evaluate the performance of transverse joints in precast-panel bridge deck systems. This thesis describes the development of test methods and performance criteria to compare behavior of various precast-panel transverse joints and determine their acceptability. The test methods and performance criteria were implemented on a proprietary deck system in the laboratory. The two joint types tested for the Exodermic® deck system were the unreinforced shear key joint and the staggered hook reinforced joint. The transverse joints were tested in quasi-static and fatigue loading for positive bending, negative bending, and a newly developed test of shear reversal under constant positive bending. Data were collected and analyzed to determine the in-service and long-term performance of the joints. The results were based on capacity, midspan deflection, and crack opening of the specimens. A practical test method for future implementation was produced

successfully. However, correlation between the quasi-static and fatigue test results could not be determined due to the small range of specimens tested.

## Acknowledgements

I would first like to thank my advisor, Dr. Robert Barnes, for his guidance on my thesis and instruction in the classroom. I would also like to thank my committee members, Dr. Anton Schindler and Dr. Michael Stallings, for their input and advice on this thesis. Special thanks go to all my teachers and mentors from college and high school who have helped me along my journey in learning more about myself and structural engineering. Thank you also to Mark Kaczinski at D.S. Brown Company for donating the steel grids for the research project. I am very appreciative of the dozen or so undergraduate and graduate students who helped in the construction process of the specimens and working in the laboratory, especially Yohance Stringfield and Rob Crosby. Finally, I would like to thank my family for all their love and support. Thanks, Mom, Dad, Michael, Mamaw, Grandad, Nana, and Pop.

## Table of Contents

## List of Tables

## List of Figures

## List of Abbreviations

| | |
|---|---|
| AASHTO | American Association of State Highway and Transportation Officials |
| ALDOT | Alabama Department of Transportation |
| ASTM | American Society of Testing Materials |
| BGFMA | Bridge Grid Flooring Manufacturers Association |
| CIP | Cast-In-Place |
| FHWA | Federal Highway Administration |
| GDOT | Georgia Department of Transportation |

# CHAPTER 1: INTRODUCTION

## 1.1 General Background

Out of the 614,387 bridges in the United States, 56,007 are structurally deficient (FHWA 2016). In many instances this structural deficiency relates to the deck of the bridge. Deck degradation is very common in bridges over 25-years old (Biswas 1986). Many decks fail several years before the rest of the bridge superstructure and substructure reach the end of their useful life (Bettigole and Robison 1997). Deck deterioration is due to several causes including thermal shrinkage cracking, weathering from wet-dry cycles, and fatigue effects from truck traffic (Ramey and Oliver 1998). An effective solution to this problem is to rapidly replace the deteriorated bridge deck with precast panels. By utilizing this replacement method, work can be completed over a weekend or even overnight, which limits the disruption to traffic.

Various types of prefabricated panels have been implemented on bridge deck replacement projects. Some examples of deck panels include full-depth precast concrete, steel grid partially filled with precast concrete, and open steel grid (Bettigole and Robison 1997). Figure 1.1 shows the important details of a typical full-depth precast concrete deck system. The panels span transversely relative to the direction of traffic and are connected to the girders via shear pockets which create horizontal shear resistance for the entire system. The panels are connected to each other via transverse joints, which run transversely relative to the direction of traffic (and parallel to the span of the panel). In some systems these joints are given additional strength by post-tensioning the panels together (Bowers 2007).

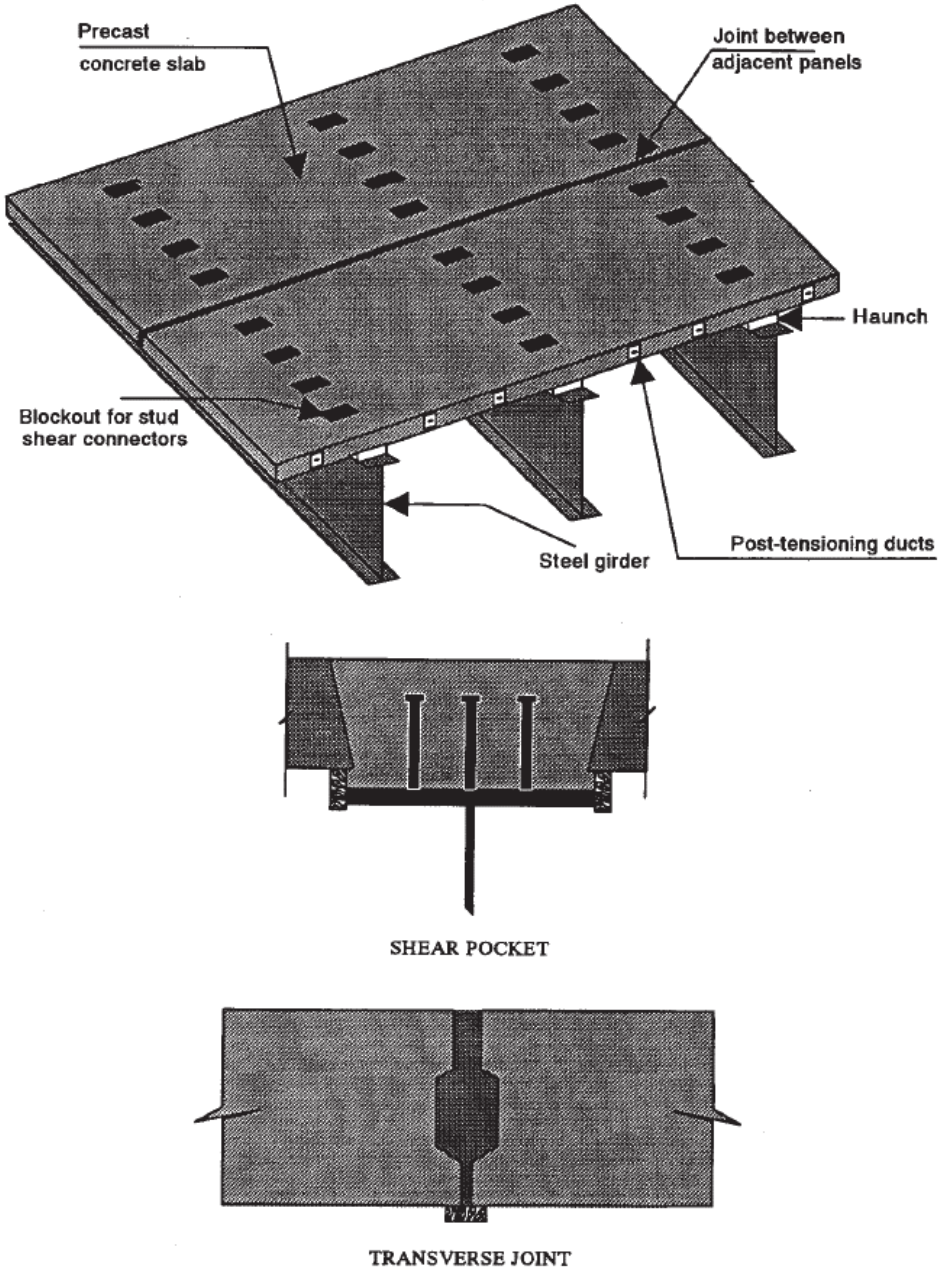


**Figure 1.1: Full-Depth Precast Deck System (Issa, Yousif and Issa 2000)**

An important aspect of any deck system is the behavior of its transverse joints. Durability of the joints is required for the success of a deck replacement project. The Alabama Department of Transportation (ALDOT) does not have any standards to test or evaluate the performance of

transverse joints proposed for prefabricated panel bridge deck systems. The goal of this research project is to develop test methods and performance criteria to compare behavior of various precast-panel transverse joints and determine their successfulness. The test methods and performance criteria were developed by analyzing stress demands from typical bridge deck transverse joints and by testing two joint types of a proprietary deck system in the laboratory.

One type of proprietary prefabricated panel system is the Exodermic® grid-reinforced concrete deck system which is owned by the D.S. Brown Company. Figure 1.2 shows an isometric view of all the components in the Exodermic deck system. The system consists of a reinforced concrete slab on top of a two-way steel grid. Main WT4x5 bars extend 1 in. into concrete slab and the tops of the main bars have ¾ in. punched holes to enhance horizontal shear resistance and composite action (D.S. Brown Company 2007) in the direction of the panel span.

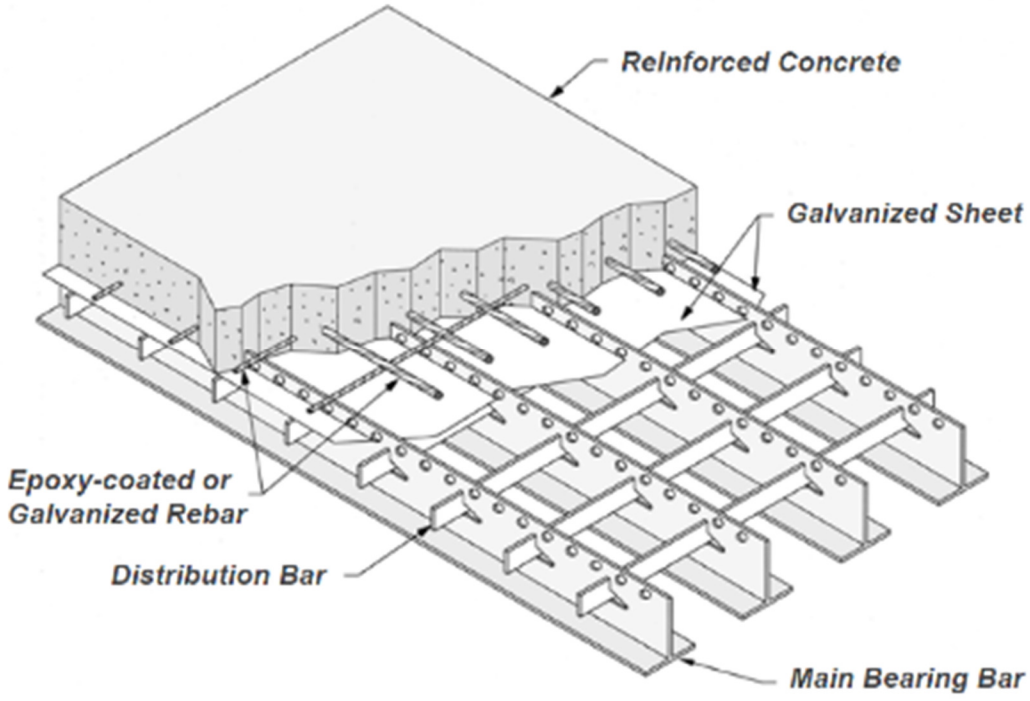


**Figure 1.2: Exodermic Deck System (D.S. Brown Company 2007)**

The two types of transverse joints tested in this study were the unreinforced shear key joint and the staggered hook reinforced joint as shown in Figure 1.3 and Figure 1.4, respectively. Both joint types were suggested by the D.S. Brown Company (2007) for precast Exodermic panels. The joints are designed to be filled with a rapid-setting non-shrink grout.

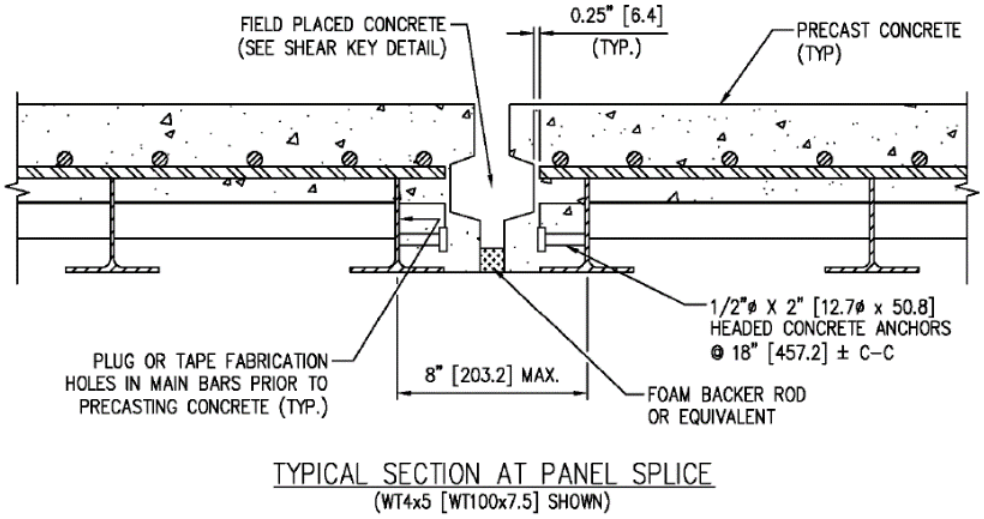


**Figure 1.3: Unreinforced Shear Key Transverse Joint (D.S. Brown Company 2007)**

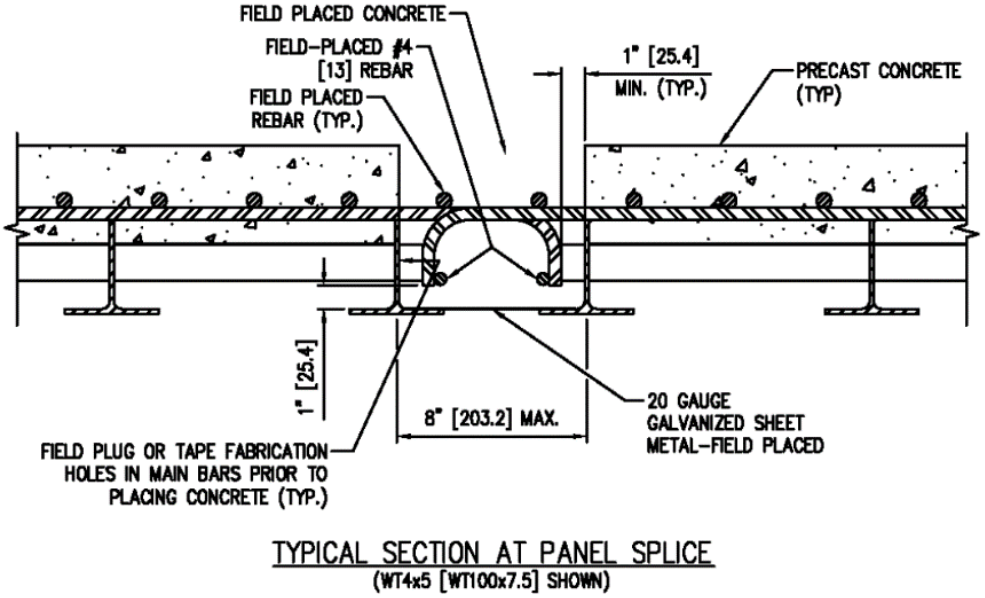


**Figure 1.4: Staggered Hook Reinforced Transverse Joint (D.S. Brown Company 2007)**

## 1.2 Research Objectives

The main objectives of this research project included the following:

- Develop a testing procedure that can be used to assess the in-service and long-term performance of various precast-panel bridge-deck transverse joints.
- Propose performance criteria that account for the joint propensity to cracking, its stiffness and strength degradation, and the effect of loading conditions.

## 1.3 Scope

The research tasks performed to achieve the research objectives included the following:

- Determine typical stress demands in bridge deck transverse joints.
- Design relatively simple laboratory test configurations and loadings to mimic the stress demands.
- Construct transverse joint bridge deck specimens.
- Perform laboratory tests on transverse joints for ultimate strength and fatigue durability.
- Generate experimental data and compare the performance between joint types.
- Make recommendations and propose test standard and performance criteria.

## 1.4 Organization of Thesis

The organization of the thesis is separated into six chapters which includes the first chapter, "Introduction."

Chapter 2 is titled "Background." This chapter covers background information related to transverse joint testing of precast deck panels. The literature review conducted describes rapid rehabilitation and replacement of bridge decks, stress demands on transverse joints, laboratory testing of transverse joints including tensile, shear, and flexural tests, and information on the precast Exodermic bridge deck system.

Chapter 3 is titled "Design of Experimental Program." This chapter covers aspects of the testing program ranging from test assembly, loading procedure, instrumentation, and data acquisition.

Chapter 4 is titled "Specimen Construction." This chapter covers aspects of the construction process of the test specimens ranging from detailed drawings, delivery of materials, fabrication of the specimens, to testing the properties of the materials.

Chapter 5 is titled "Results and Discussion." This chapter covers the quasi-static and fatigue test results and discussion of the twelve specimens tested by presenting the visual inspection, external instrumentation, and internal instrumentation results.

Chapter 6 is titled "Summary, Conclusions, and Recommendations." This chapter summarizes the overall research project, provides conclusions of the two joint types based on the data collected, and recommends performance criteria and future work.

# CHAPTER 2: BACKGROUND

## 2.1 Overview

This chapter covers background information related to transverse joint testing of precast deck panels. A review of literature on the following topics was conducted: rapid rehabilitation and replacement of bridge decks, stresses on typical bridge deck transverse joints, previous laboratory testing of transverse joints including tensile, shear, and flexural tests, and the precast Exodermic bridge deck system.

## 2.2 Rapid Rehabilitation/Replacement of Bridge Decks

Out of the 16,098 bridges in Alabama, 1,229 are structurally deficient (FHWA 2016). The term structurally deficient means that a bridge has at least one structural defect which may indicate that a structural component does not satisfy current code requirements or that a structural component is damaged and thus has a reduction in structural capacity. In many instances this structural deficiency relates to the deck of the bridge. Deck degradation is very common in bridges over 25 years old (Biswas 1986). Many decks fail several years before the rest of the bridge superstructure and substructure reach the end of their useful life (Bettigole and Robison 1997). Figure 2.1 shows the deterioration of a typical bridge deck.

**Figure 2.1: Typical Deck Deterioration (Umphrey 2006)**

Per Ramey and Oliver (1998) causes of deck degradation are due to:

- early drying and thermal shrinkage cracking,
- weathering from freeze-thaw, wet-dry, and hot-cold cycles, and
- impact and fatigue loading from truck traffic.

The two main solutions to repair deteriorated decks are rehabilitation or replacement. Typically, rehabilitation is accomplished by adding an overlay to the deck. This procedure creates a uniform appearance, corrects uneven surfaces caused by wear, provides a nonskid riding surface, protects against heavy truck traffic, prevents carbonation, and protects further intrusion of other contaminants such as gasoline and chlorides. However, this is only a short-term solution since overlays can debond and create additional maintenance issues (Ramey and Oliver 1998). For instance, when cracks form within the deck they are reflected up through the overlay.

The other option to repair deteriorated decks is replacement. The two main replacement methods for concrete decks are cast-in-place (CIP) and precast (PC). In both cases the old deck is completely removed and replaced. The construction time for CIP decks takes considerably longer because the concrete is cast on the site and the concrete may require several days or weeks to reach the required strength (Sullivan 2003). In addition, installation and removal of the formwork is time-consuming and labor-intensive (Culmo 2000).

Precast deck replacement, however, can be completed over a weekend or even overnight. In many cases this process is completed in stages by replacing one lane of a bridge at a time to limit disruption to traffic. The deck panels are fabricated off site at a plant, which allows higher quality control, more controlled curing environment, and allows shrinkage to stabilize (Bettigole and Robison 1997). Once the panels reach the required strength, they are transported to the bridge construction site and placed on the supporting girder system. This reduces construction time of the bridge and reduces exposure of the laborers to any risks involved (Sullivan 2003). Transportation restrictions limit the deck panels to approximately eight feet wide (Ahmadi 1997).

Various types of precast panels have been implemented on bridge deck replacement projects. Some examples of deck panels include full-depth precast concrete, half-filled precast concrete with steel grid, and open steel grid. Figure 2.2 shows the important details of a typical full-depth precast concrete deck system such as shear pockets and transverse joints. The panels are connected via longitudinal joints (parallel to the direction of traffic) and transverse joints (perpendicular to the direction of traffic) to allow the deck to behave as one unit and transfer the load from one panel to the next. In many cases the panels are post-tensioned longitudinally to increase the strength of the transverse joints and avoid cracking and leaking which can lead to

rusting of the girders below (Bowers 2007). To make the deck composite with the superstructure, headed shear studs are welded to the top flanges of the girders and rapid-setting non-shrink grout is placed in the shear pockets (Bettigole and Robison 1997).

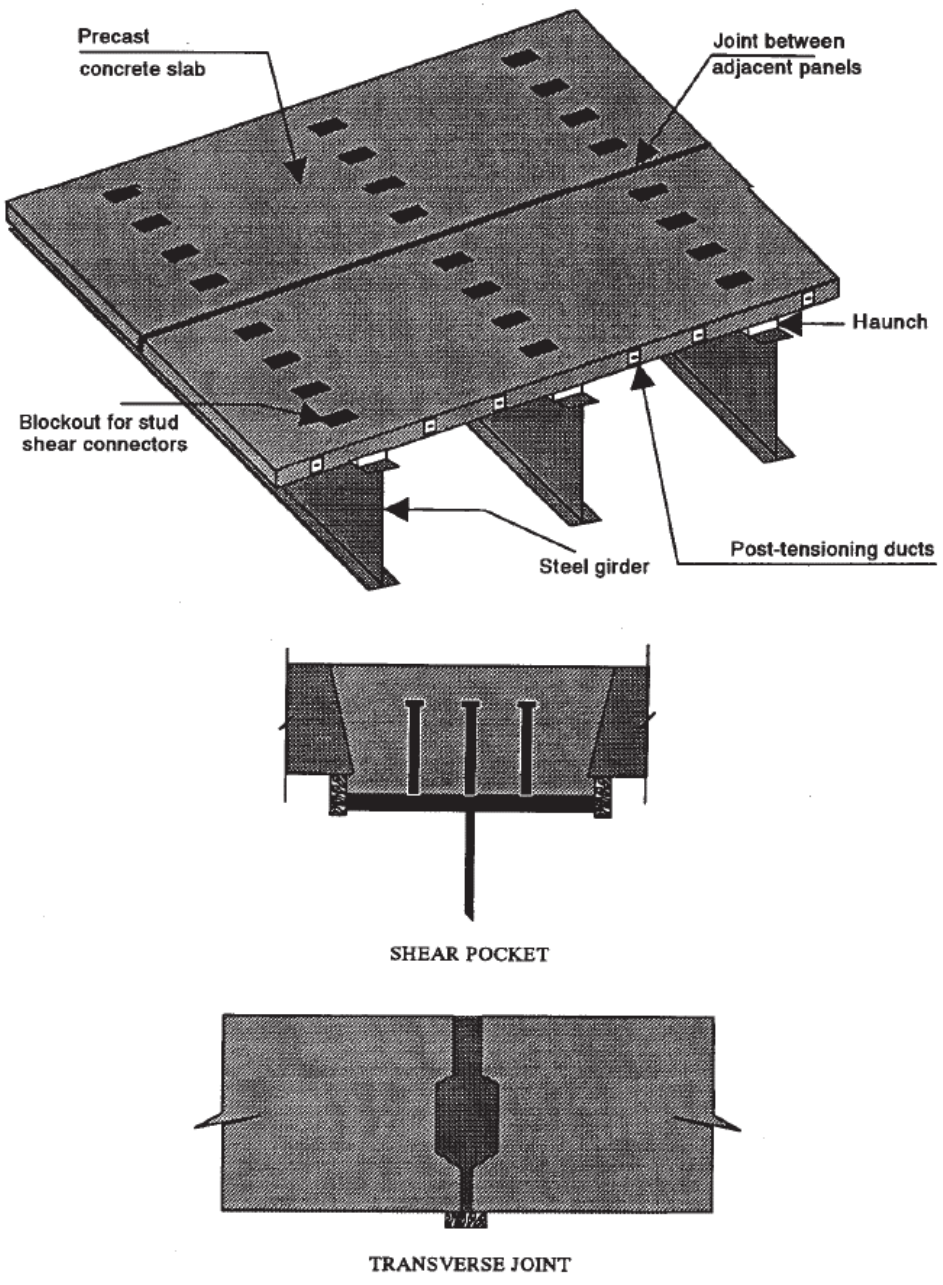


**Figure 2.2: Full-Depth Precast Deck System (Issa, Yousif and Issa 2000)**

## 2.3 Stress Demand on Transverse Joints

The target forces and stresses for this project were based on previous research conducted by Brian Rhett at Auburn University in the thesis "An Analytical Investigation of Transverse Joints in Precast-Panel Bridge-Deck Replacement Systems" (2012). Three bridges were modeled and analyzed using the finite-element program SAP2000. The girders and deck were modeled as shell elements. The bridges were standard two-lane ALDOT bridges with steel girders. The first bridge was simply supported with a 56 ft span. The second bridge was a continuous three span (60-80-60 ft). The third bridge was a continuous three span (80-100-80 ft). The bridges were loaded with an HS20 design truck in accordance with AASHTO LRFD truck loading provisions. The loading was done in accordance with the AASHTO 3.6.1.4 Fatigue Load condition. The analysis was conducted without the use of dynamic load allowance (IM) per AASHTO LRFD 3.6.2 and without the application of multiple presence factors (m), Section 3.1.1.2. The dimensions and forces of the three-axle load truck are shown in Figure 2.3. The truck was systematically placed longitudinally and transversely along the bridges to determine the critical locations for stresses acting on potential transverse joints in the 8 in. thick concrete deck. An 8 in. thick deck is typical in ALDOT bridges. The stresses found in this deck can be applied to other deck joints with varying thicknesses. The continuous three-span (60-80-60 ft) bridge yielded the highest demand for the transverse joints. The deck acted as a two-way system. However, only the stresses in the transverse direction were of concern for this research project. Figure 2.4 shows the longitudinal positions for critical stresses as CL-1 at (interior) Bent 1 and CL-2 which is 5 ft beyond the bent for negative and positive flexure stresses, respectively. Figure 2.5 and Figure 2.6 diagram the transverse truck positions where the wheel loads either straddle or directly align with the girders.

The naming convention of the truck positions correlates with the distance between the location of the center of the truck relative to the center of the bridge. Figure 2.7 and Figure 2.8 illustrate the longitudinal truck position for extreme positive-flexure and negative-flexure transverse stresses in the deck across a potential transverse joint, respectively.

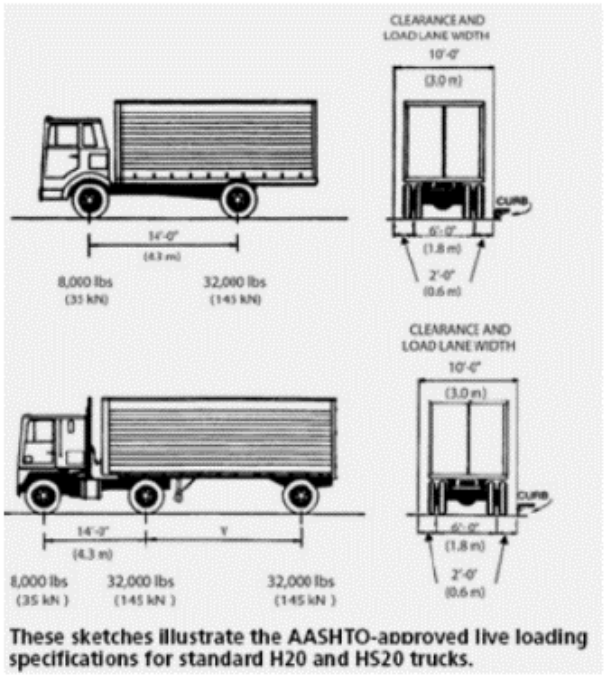


**Figure 2.3: AASHTO Truck Loading Scenarios (AASHTO 2007)**

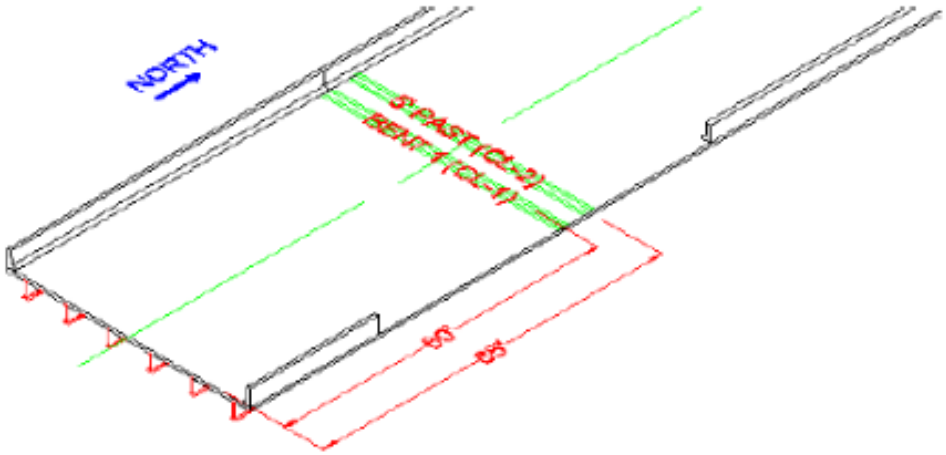


**Figure 2.4: Critical Locations for Continuous Bridge (Rhett 2012)**

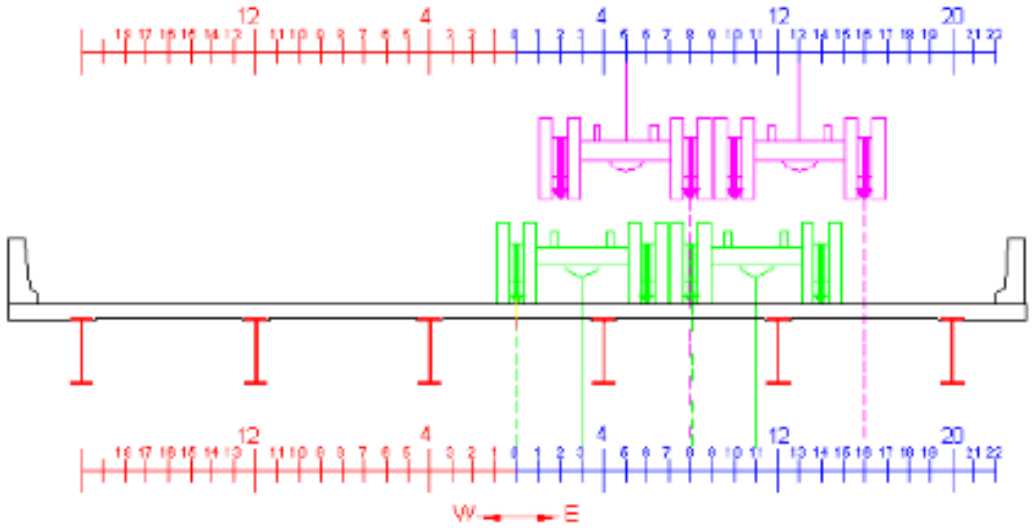


**Figure 2.5: Transverse Truck Positions TR-3, 5, 11, and 13 Loading the Exact Middle between Girders (Rhett 2012)**

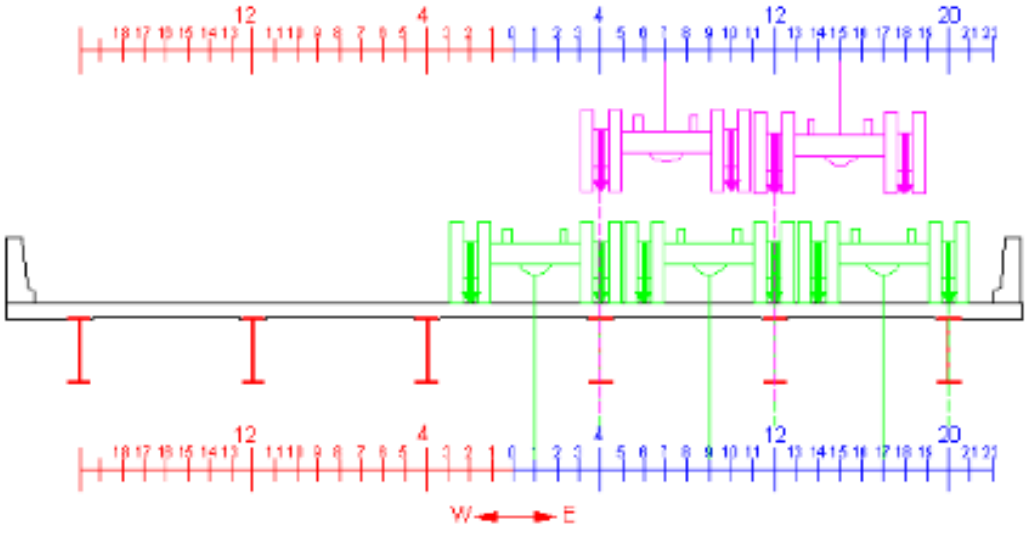


**Figure 2.6: Transverse Truck Positions TR-1, 7, 9, 15, and 17 Loading Girders (Rhett 2012)**

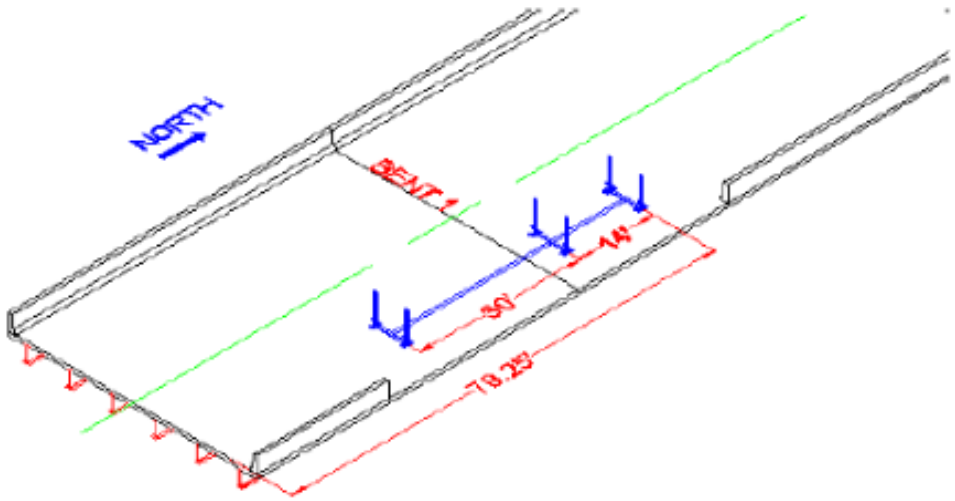


**Figure 2.7: Longitudinal Position of Truck for Extreme Positive-Flexure Stresses (Rhett 2012)**

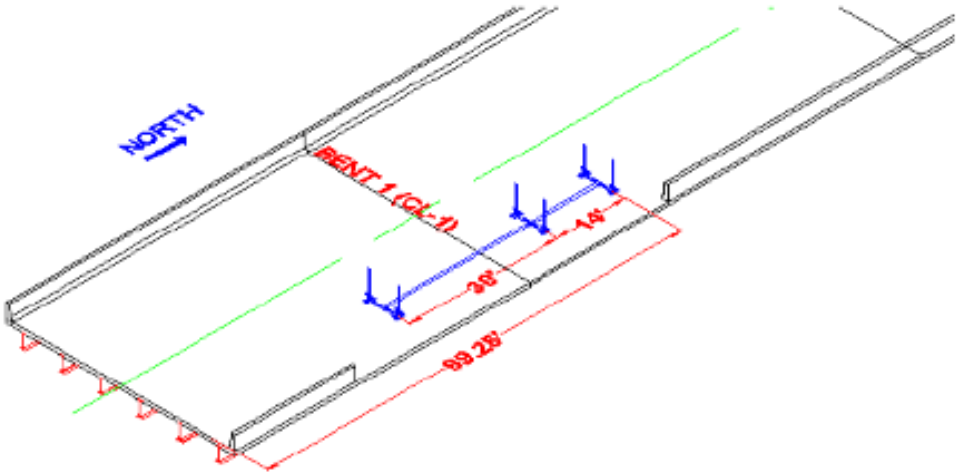


**Figure 2.8: Longitudinal Position of Truck for Extreme Negative-Flexure Stresses (Rhett 2012)**

From the analysis of the bridge model it was determined that the extreme positive-flexure stress in the deck occurred at CL-2 with truck location at TR-13 and stress location at TR-16 while the extreme negative-flexure stress occurred at CL-1 with truck location at TR-18 and stress location at TR-20. Note that the extreme positive-flexure stress occurred 5 ft past the first bent

and between the two outermost girders while the extreme negative-flexure stress occurred above the first bent and above the outermost girder. In addition, the analysis showed that the positive flexure case also depicted a reversal in the shear at the location of critical stress as the wheel group passed across this joint location. However, the maximum negative flexure case did not depict a shear reversal since the location was directly over a bent.

Table 2.1 summarizes the extreme forces and stresses resulting from Rhett's research that were then implemented for this current project. Note that for the positive bending stress demands the computed shear listed contained two values. This represented the shear reversal experienced at the transverse joint. Also, note that the smallest moment-to-shear ratio for either case was 40 in. This ratio was implemented in the load configuration of the test assembly in Section 3.2.

**Table 2.1: Computed Stress Demands (Rhett 2012)**

| Critical Stress | Bending Stress (ksi) | | Moment | Shear | Moment/Shear |
|---|---|---|---|---|---|
| | Top Fiber | Bottom Fiber | (kip-in) | (kips) | (in.) |
| **Positive Bending** | -0.184 | 0.226 | 28.9 | 0.728/-0.425 | 40/-68 |
| **Negative Bending** | 0.256 | -0.084 | -32.7 | -0.452 | 73 |

## 2.4 Laboratory Testing of Transverse Joints

Transverse joints experience a combination of stresses ranging from tension, shear, and flexural. Tension occurs in joints when the deck is made composite with girders and is experiencing negative flexure. In this situation, the neutral axis is below the deck so the entire joint is in tension. Shear stresses at the joint occur when loads are transferred from one panel to the other, vertically. Maximum positive bending of transverse joints occurs when the deck is loaded so that it deflects

downwards between bents and between girders. Negative bending occurs when the deck joint is loaded over a bridge bent, typically.

In previous deck research, ASTM D6275 "Standard Practice for Laboratory Testing of Bridge Decks" (ASTM 1998) was referenced as the standard method to test bridge decks, but has since been discontinued. The standard required that the applied load be represented by a truck-tire footprint. For fatigue tests the load should be applied for 2,000,000 cycles at no more than 5.0 Hz to represent an infinite life test. There are no standards regarding deck joint testing, so many research projects base some aspects of their testing on the methods described in ASTM D6275.

Other references for projects are from practices conducted by previous research in deck joint testing. A wide range of research projects on full-depth precast deck joints have been conducted in the past. To limit the scope of this subsection, small-scale tensile, shear, and bending tests are discussed here.

### 2.4.1 Tensile Tests

To quantify the behavior of transverse bridge deck joints in tension, several research projects have focused on this specific element. Chapman (2010) conducted research at the University of Tennessee on small-scale specimens. The specimens were tested in pure tension to simulate the negative bending of a bridge deck composite with girders. The joint tested was a U-bar joint which consisted of No. 5 reinforcing bar with a tight 180° bend staggered and extended beyond the precast deck into the joint, as shown in Figure 2.9. The deck was 7 ¼ in. thick with No. 4 and No. 5 reinforcing bars utilized as the top and bottom layers, respectively. Figure 2.10 shows the test set-up. The test placed the specimen vertically and applied an increasing monotonic tensile force until the specimen failed. Figure 2.11 shows tensile cracks of the specimen at failure. The test was

conducted with a total of four specimens including the control specimen. The variables for the project were concrete strength, joint overlap length, and reinforcement spacing. The testing showed that reducing the concrete strength decreased the tensile capacity by 5%, decreasing the joint overlap length decreased the tensile capacity by 18.9%, and increasing the reinforcing steel spacing increased the tensile capacity by 14.3% (Chapman 2010).

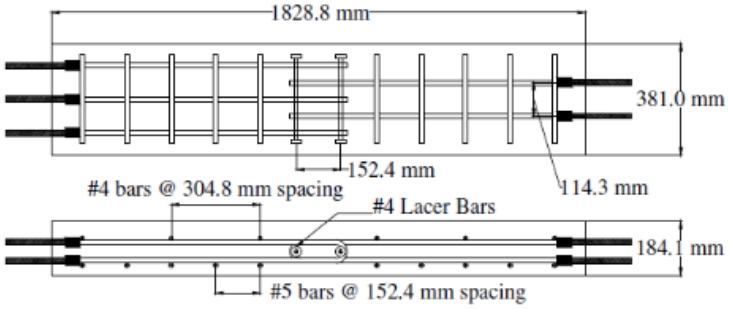


**Figure 2.9: Tension Specimen (Chapman 2010)**

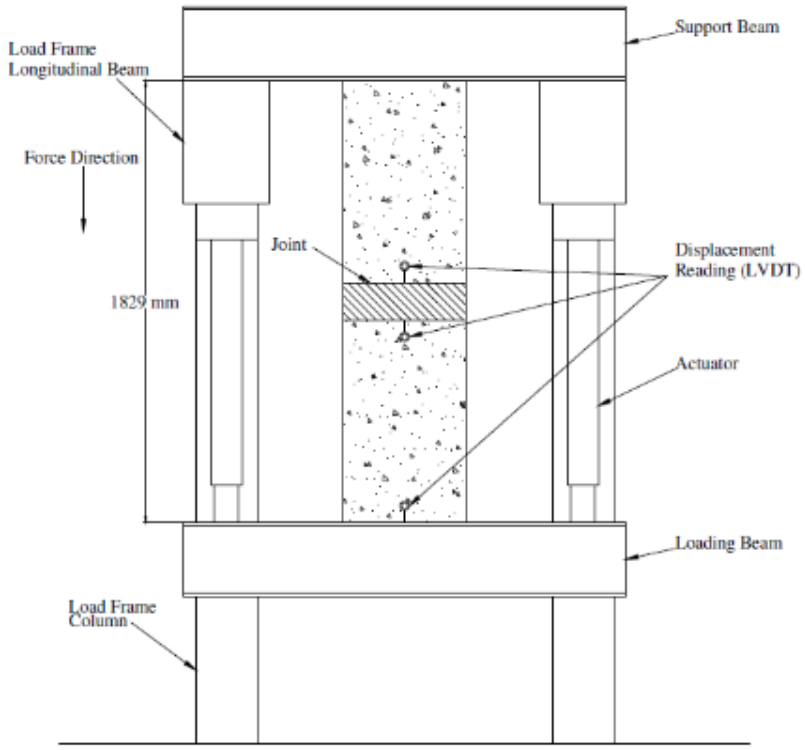


**Figure 2.10: Tension Test Set-Up (Chapman 2010)**

**Figure 2.11: Tensile Cracks at Failure (Chapman 2010)**

Zhu et al. (2012) expanded upon Chapman's research with similar specimens and an identical test-set up. The specimens were constructed per the recommended overlap length and spacing from Chapman's conclusions. Four U-bar joint specimens were tested in pure tension. The variables for the project were the joint grout and loading program. The joint grout utilized was an overnight cure material and a seven-day cure material. The loading program was static (monotonic until failure) and fatigue. To determine an accurate load level for the test a bridge was modeled and analyzed with a computer program to determine the stress demands on the deck transverse joints. The fatigue load case was considered. Load was applied to the model with the design load truck and design lane load according to AASHTO LRFD. The maximum negative moment in the deck occurred over an interior girder over an interior pier. The stress in the extreme top fiber of the transverse joint was 0.306 ksi. This value determined the applied load for the small-scale tension test. The applied load ranged from 0.0 to 12.8 kips. Although not explicitly

referenced, it appeared that the project followed the precedent set by ASTM D6275 by loading the fatigue tests at 2,000,000 cycles at 4.0 Hz. Static tests were conducted at the 1st, 500,000th, 1,000,000th, 1,500,000th, and 2,000,000th cycle to record the joint degradation throughout the fatigue tests. The performance of the specimens were judged on tension capacity, cracking, and steel strain. The U-bar joint was deemed a promising system, and the seven-day cure material performed better than the overnight-cure material (Zhu et al. 2012).

### 2.4.2 Shear Tests

To quantify the behavior of transverse bridge deck joints in shear, several research projects have focused on this specific element. Porter (2009) conducted research at Utah State University on small-scale specimens. Figure 2.12 shows a drawing of one of the shear specimens in the test-set up. The specimens were 6 in. wide "L" shaped with non-shrink grout connection. The connections tested were welded stud, welded reinforcing steel, unreinforced shear key, and post-tensioned joints. The specimens were reinforced with two layers of No. 3 bars. The specimens were tested in pure shear to simulate load transferred from one deck panel to the other, vertically. The tests included four static (monotonic until failure) loading tests and two fatigue loading tests. The applied load for the cyclic tests was calculated as 90% of the mean minus one standard deviation of the ultimate load from the monotonic tests. This load was selected because the specimens would not fail under the first cycle. While at the same time, the specimens would fail after a reasonable number of cycles. Figure 2.13 shows shear cracks from one of the unreinforced shear key specimens at failure. The deflections, cracking, and ultimate loads were recorded. The post-tensioned joint demonstrated the highest ultimate load capacity and cracked under higher loads than the other joint types tested (Porter 2009). This type of pure shear test is limited in scope

because they do not represent realistic stress demands in bridge decks where the transverse joints experience flexure and shear simultaneously.

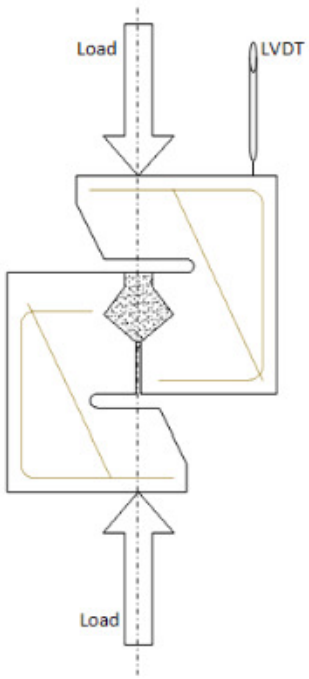


**Figure 2.12: Shear Test Set-Up (Porter 2009)**

**Figure 2.13: Shear Cracks at Failure (Porter 2009)**

### 2.4.3 Flexural Tests

To quantify the behavior of transverse bridge deck joints in bending, several research projects have focused on this specific element. The two main types of bending tests for small-scale specimens involve either a three-point bending or four-point bending configuration. Three-point bending is where the specimen is simply supported with a load applied in the middle at the joint location. This creates a bending moment as well as a shear force at the middle where the joint is located. Four-point bending is where the specimen is simply supported with two loads applied symmetrically on either side of the midspan where the joint is located. This creates pure flexure in the middle of the beam at the joint region without any shear force effects.

Au, Lam, and Tharmabala (2011) conducted research at the Ministry of Transportation of Ontario on joints in three-point bending. Figure 2.14 shows a detail drawing of the three-point bending specimen, and Figure 2.15 shows the three-point bending test set-up. The specimens were two-third scale models of standard bridge decks in Ontario. The joints consisted of U-shaped bars, L-shaped bars, and welded straight bars. Control specimens without joints were also cast. The specimens were 72 in. long, 24 in. wide, and 6 in. thick concrete slabs. Top and bottom layers of reinforcement consisted of No. 3 reinforcement spaced at 6 in. in both transverse and longitudinal directions. The joint width was 12 in. Load was applied by a 4 in. square pad to simulate a wheel footprint. The loading program was static tests (monotonic until failure) and fatigue tests. The fatigue tests were loaded for 3,000,000 cycles at 1.0 Hz. The applied load ranged from 0.0 to 4.0 kips which simulated a factored wheel load scaled to correspond to the two-third geometric scaling of the specimen. Due to this applied load, the calculated stress at the extreme bottom fiber of the specimen yielded a value close to the nominal cracking stress of concrete. Static tests were

conducted at the 1st, 1,000,000th, 2,000,000th, and 3,000,000th cycle to record the joint degradation throughout the fatigue tests. The results indicated that the U-shaped reinforcing steel, L-shaped bar, and welded reinforcement all had similar performance. The specimens experienced a reduction in stiffness due to the cyclic loading relative to the control specimens (Au, Lam and Tharmabala 2011).

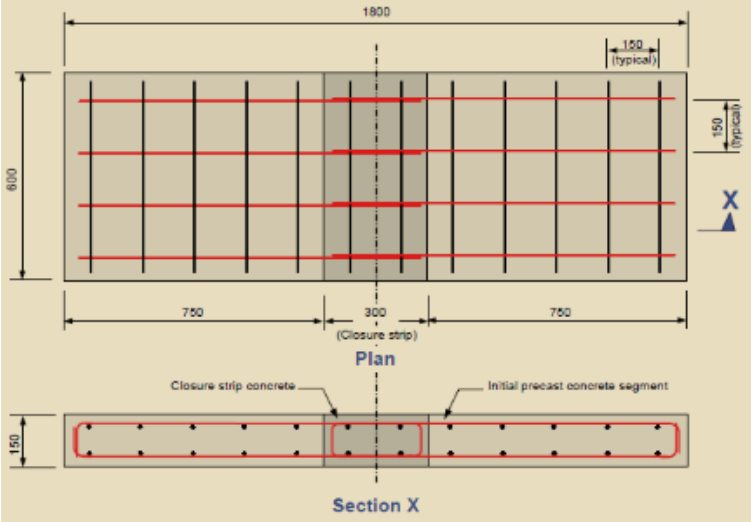


**Figure 2.14: Three-point Bending Specimen (Au, Lam, and Tharmabala 2011)**

**Figure 2.15: Three-point Bending Test Set-Up (Au, Lam, and Tharmabala 2011)**

Ryu, Kim, and Chang (2007) conducted research at Seoul National University on joints in four-point bending. Figure 2.16 shows a detail drawing of the four-point bending specimen, and Figure 2.17 shows the four-point bending test set-up. The specimens were loop-bar joints. The variables for the project were diameter of the looped reinforcement and width of the joint. Control specimens without joints were also cast. The specimens were 800 mm (32 in.) wide, 250 mm (10 in.) thick, and 2.1 m (83 in.) long. The load was applied by a line load extending across the entire width of the specimen. The loading program was static (monotonic until failure) and fatigue. Although not explicitly referenced, it appeared that the project followed the precedent set by ASTM D6275 by loading the fatigue tests at 2,000,000 cycles at 3.0 Hz. The fatigue tests were loaded at either 30%, 50%, or 70% of the ultimate load as determined from the static tests. Static tests were conducted at the $1^{st}$, $100^{th}$, $1{,}000^{th}$, $10{,}000^{th}$, $100{,}000^{th}$, $1{,}000{,}000^{th}$, and $2{,}000{,}000^{th}$ cycle to record the joint degradation throughout the fatigue tests. Figure 2.18 shows bending cracks at failure from fatigue loading for one of the specimens. Cracking, ultimate behavior, ductility, and fatigue behavior were compared to the control specimens. It was concluded that the loop-bar joints demonstrated similar ultimate strength capacity and ductility as the control specimens. Also, the larger the reinforcing steel diameter specimens resulted in higher ultimate strength capacities and lower midspan deflections (Ryu, Kim, and Chang 2007).

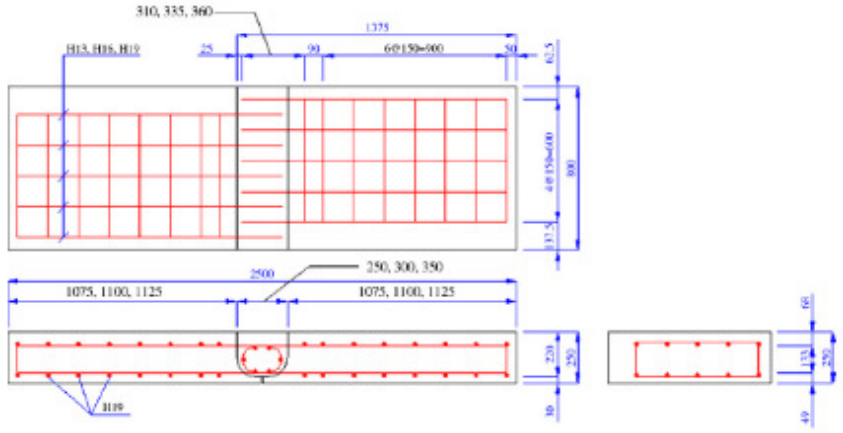


**Figure 2.16: Four-point Bending Specimen (Ryu, Kim, and Chang 2007)**

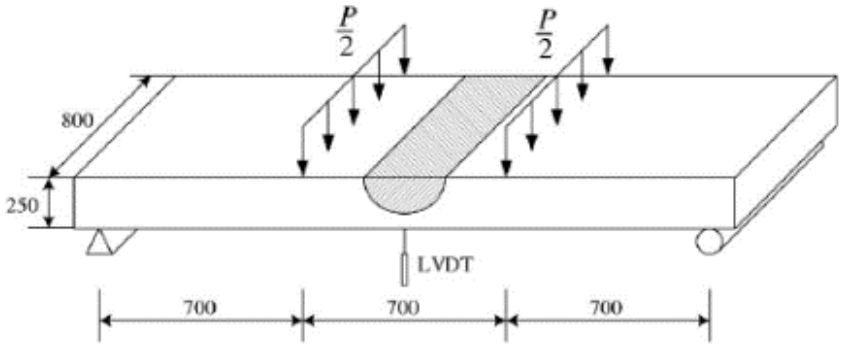


**Figure 2.17: Four-point Bending Test Set-Up (Ryu, Kim, and Chang 2007)**

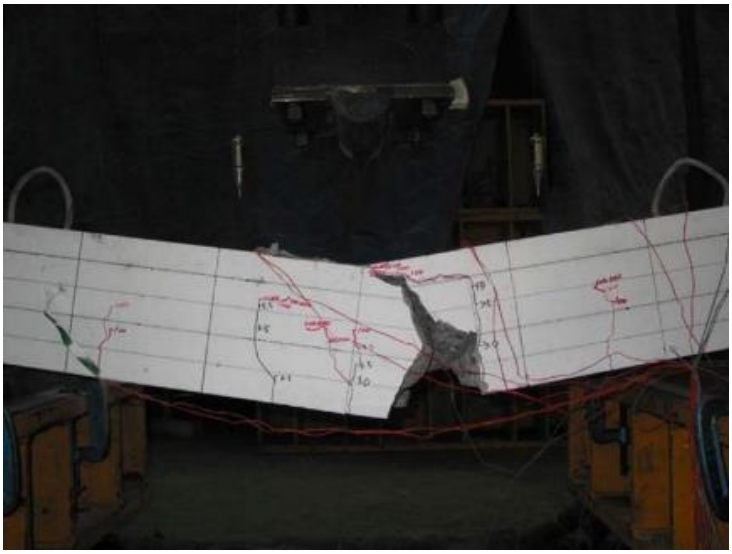

**Figure 2.18: Bending Cracks at Failure from Fatigue Loading (Ryu, Kim, and Chang 2007)**

## 2.5 Precast Exodermic Deck System

ALDOT is interested in rapid replacement of deteriorated decks. The deck systems to be implemented were required to meet the following criteria (Rhett 2012):

- Suited for rapid replacement
- Proven concept
- Provide composite action between the deck and the supporting steel girders
- Avoid the use of longitudinal post-tensioning
- Avoid the use of an overlay

From previous research conducted at Auburn University (Ramey and Oliver 1998, Umphrey 2006, and Harvey 2011) it was determined that the precast Exodermic type of grid-reinforced deck system fulfilled the criteria. For this research project, the Exodermic deck system

was used to develop test methods and performance criteria to compare behavior of various precast-panel transverse joints and determine their successfulness.

The Exodermic system is a proprietary grid-reinforced deck system owned by the D.S. Brown Company. Originally designed in the 1980's, the system in its current form consists of a reinforced concrete slab on top of a two-way steel grid. Figure 2.19 shows an isometric view of all the components in the Exodermic deck system. The panels typically span across girders in the direction that the main WT4x5 bars are oriented. Figure 2.20 shows construction drawings depicting how the panels span in a standard ALDOT bridge. The drawings were part of previous research at Auburn University by Harvey (2011) to propose construction methods for deck replacement of a bridge along I-59 in Collinsville, Alabama. The WT4x5 bars extend 1 in. into concrete slab and the tops of the main bars have ¾ in. punched holes to provide horizontal shear resistance and composite action (D.S. Brown Company 2007). The panels are made composite with the superstructure in similar fashion as other precast decks by welding headed shear studs to the top flanges of the girders and placing rapid-setting non-shrink grout in the shear pockets. The Exodermic panels are not post-tensioned longitudinally. Typical overall thickness of the panels ranges from 6 ¼ in. to 9 ¼ in. (BGFMA 2013).

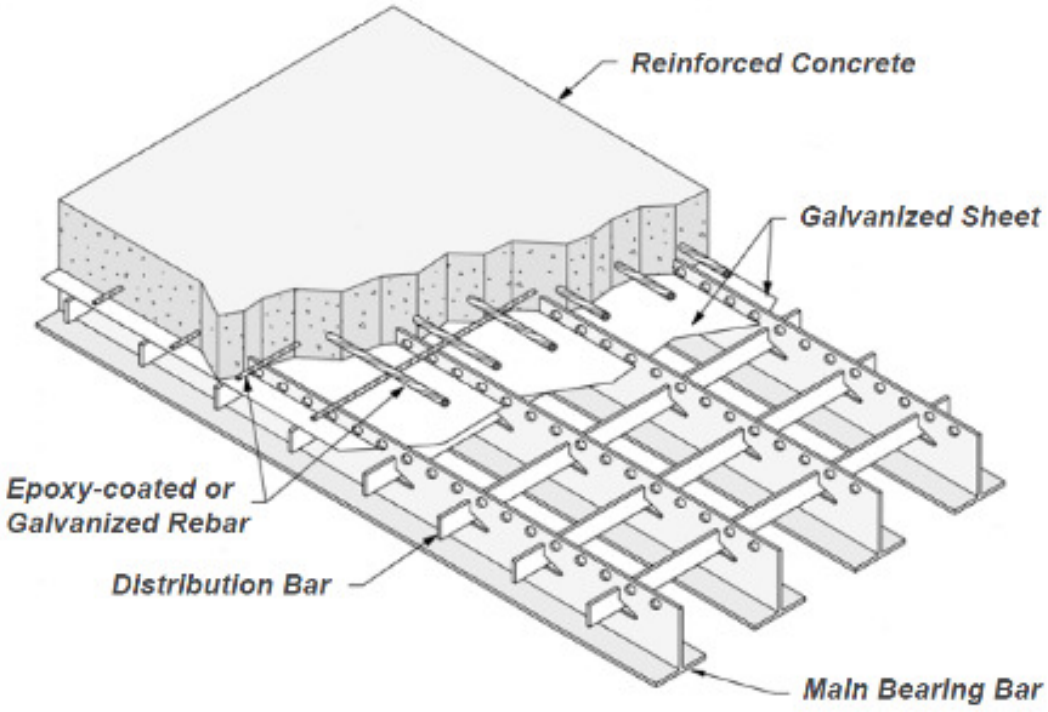


**Figure 2.19: Exodermic Deck System (D.S. Brown Company 2007)**

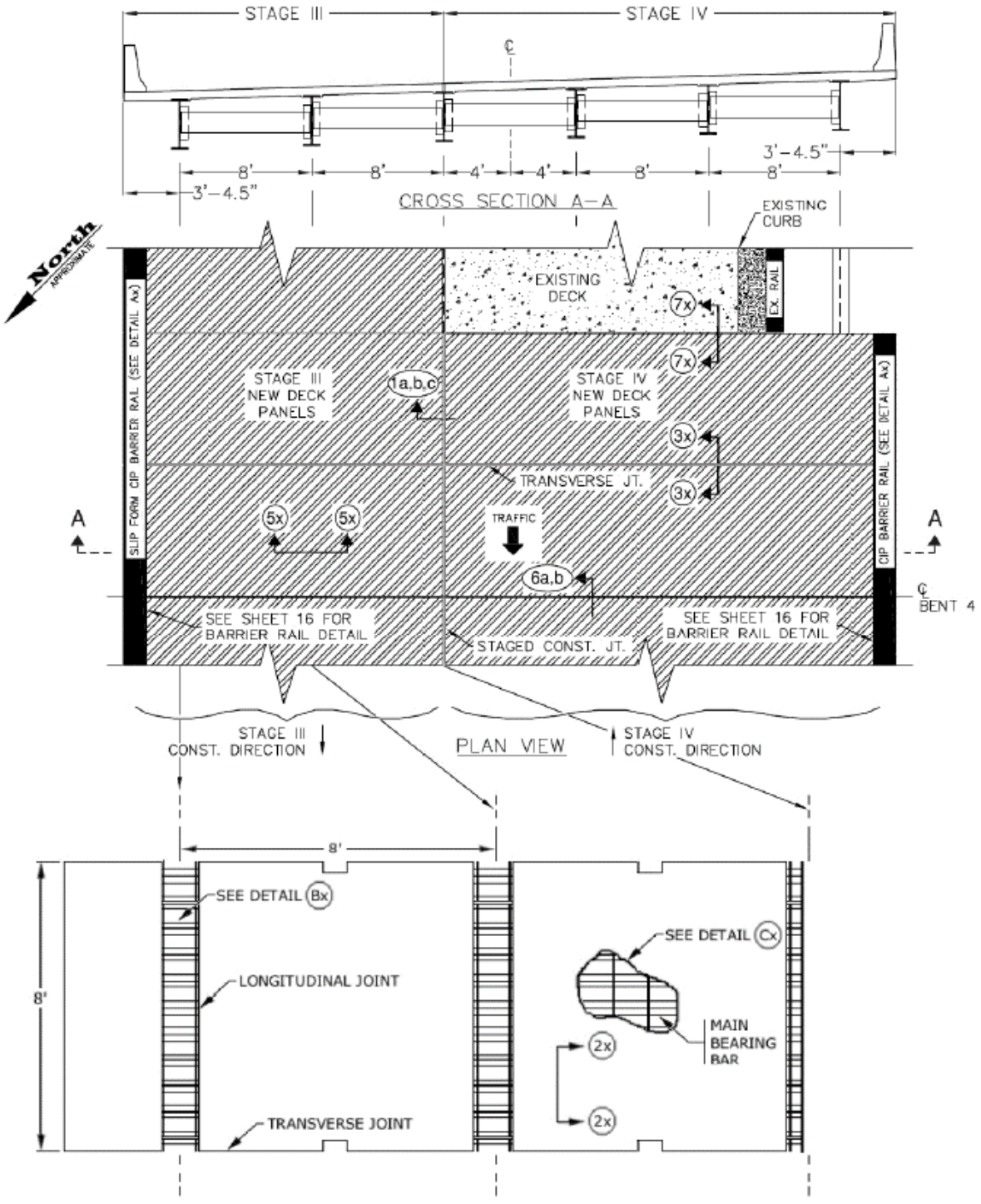


**Figure 2.20: Exodermic Precast Deck System Replacement Drawings (Harvey 2011)**

By reducing the thickness of the concrete in the deck system compared to full-depth precast panels, the dead load is reduced. This can help structurally deficient bridges to conform to current code requirements if the substructures are deficient. Typical weight of the panels range from 58 to 70 pounds per square foot which is an approximate 30 to 42% weight reduction compared to typical 8 in. thick full-depth precast panels (D.S. Brown Company 2007).

The Exodermic deck system also efficiently uses the concrete and steel materials in the panel. For instance, when the panel experiences positive bending, as shown in Figure 2.21, the top concrete portion of the panel is in compression while the bottom steel portion of the panel is in tension. Similarly, when the panel experiences negative bending, as shown in Figure 2.22, the reinforcing steel in the top concrete portion of the panel is in tension while the bottom steel portion of the panel is in compression (D.S. Brown Company 2007). For both of the figures shown the panels are spanning across girders.

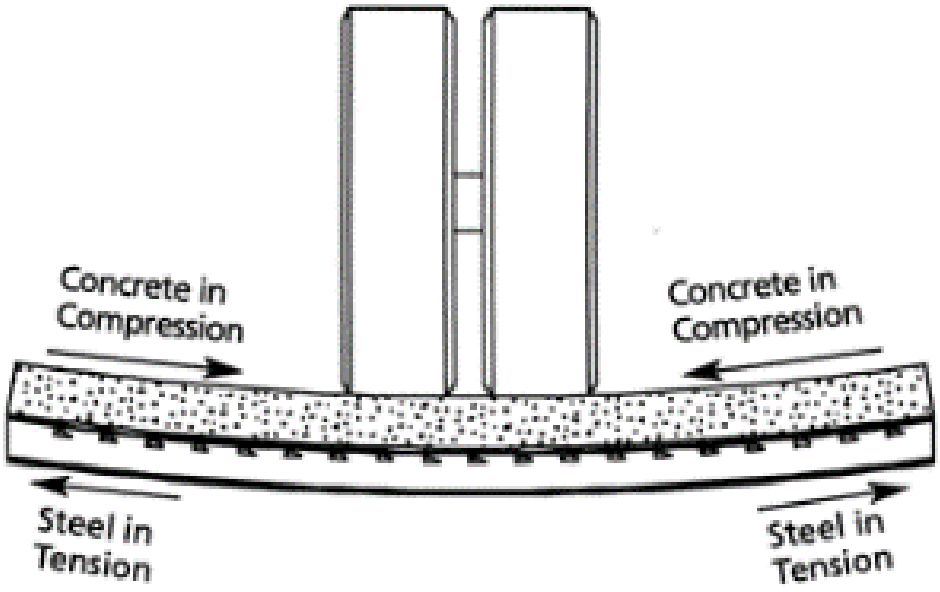


**Figure 2.21: Exodermic Panel in Positive Bending (D.S. Brown Company 2017a)**

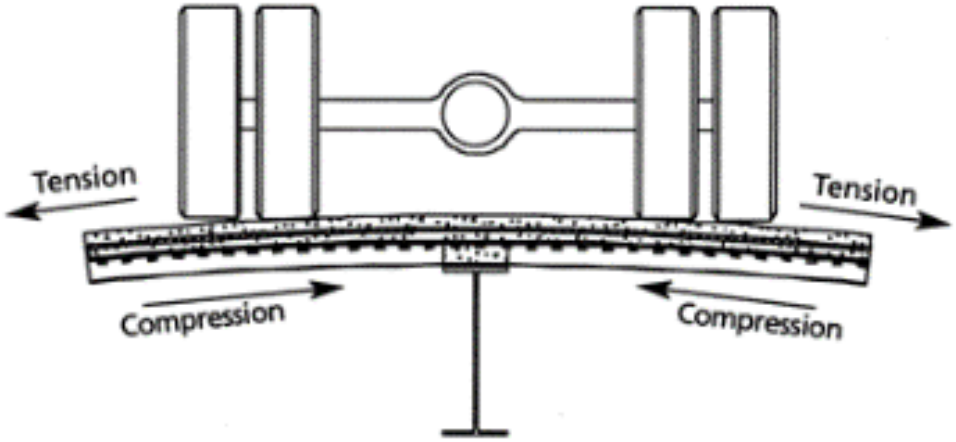


**Figure 2.22: Exodermic Panel in Negative Bending (D.S. Brown Company 2017a)**

Another important aspect of any deck system is the behavior of its transverse joints. The reduction of the load-sharing mechanism between panels results in deck degradation over time which leads to durability and performance issues. The durability of the joints is directly related to the success of a deck replacement project.

The two precast Exodermic transverse joint types suggested by D.S. Brown are the unreinforced shear key joint and the staggered hook reinforced joint as shown in Figure 2.23 and Figure 2.24, respectively. The unreinforced shear key joint consists of a female-to-female shear key. The top opening of the shear key is 1 ½ in. wide, opens to 3 ½ in. in the middle, and narrows to 1 in. at the bottom. A foam backer rod is placed at the bottom to serve as a stay-in-place form. The staggered hook reinforced joint consists of an 8 in. wide space between the precast panels with hooked No. 4 bars extending into the joint at staggered intervals. A metal sheet rests on the WT flanges at the bottom to serve as a stay-in-place form. Both joint types are designed to be filled with a rapid-setting non-shrink grout with 3/8 in. maximum coarse aggregate (D.S. Brown Company 2007).

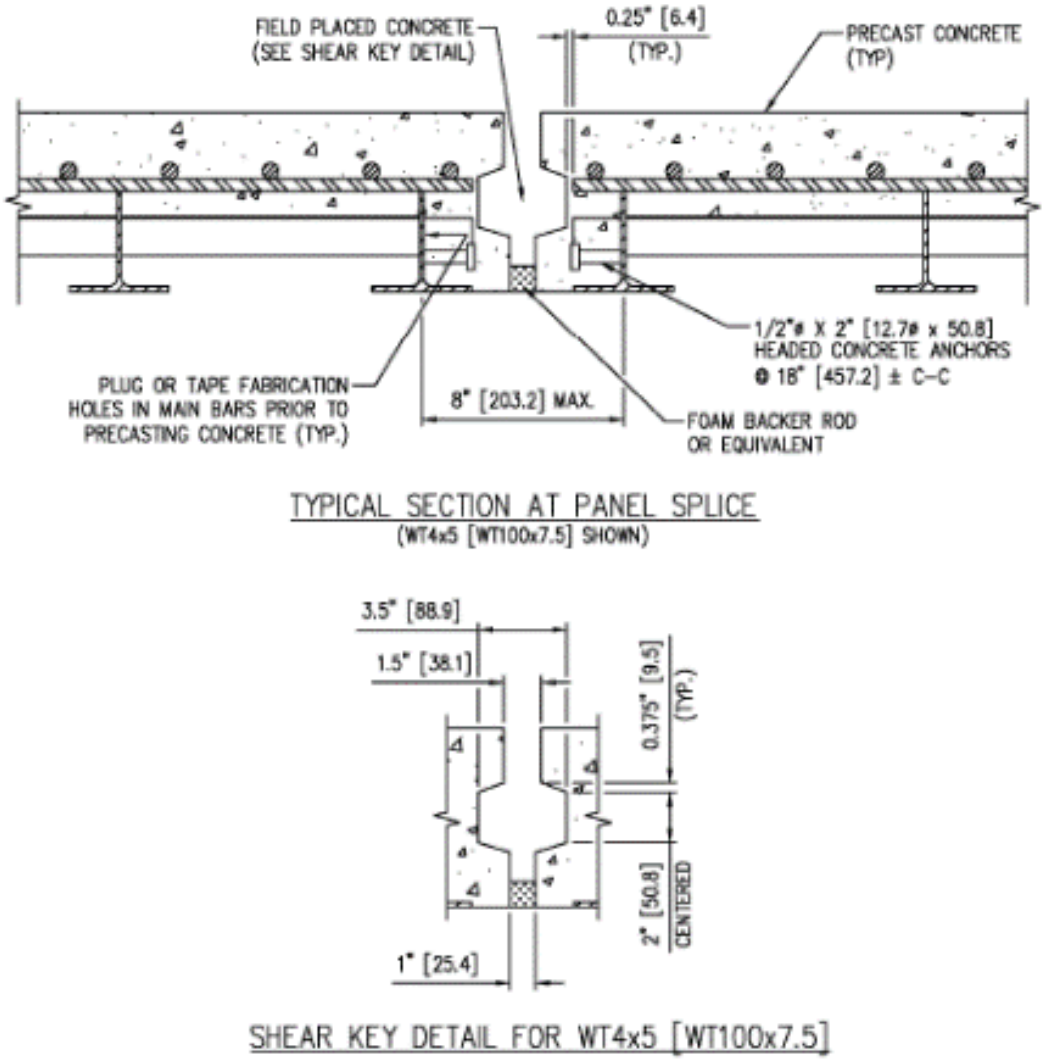


**Figure 2.23: Unreinforced Shear Key Transverse Joint (D.S. Brown Company 2007)**

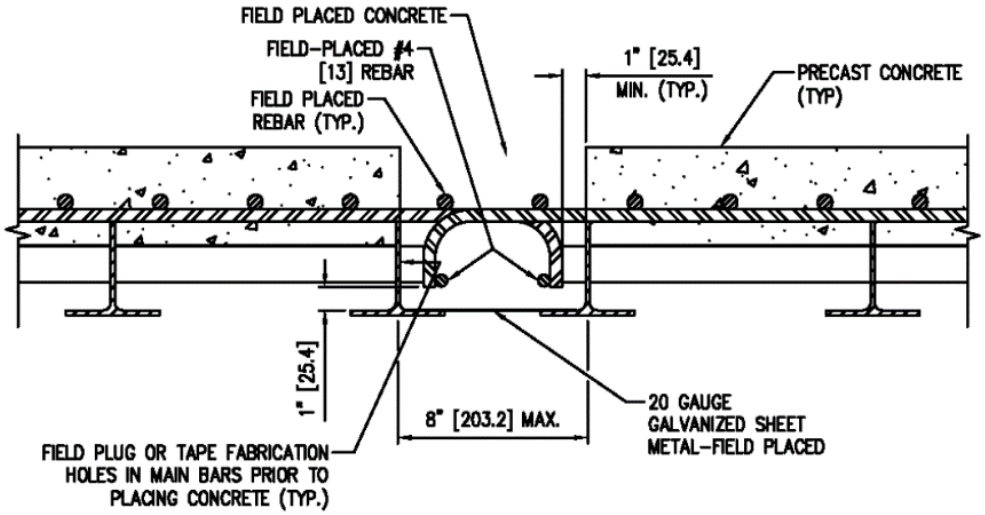


TYPICAL SECTION AT PANEL SPLICE
(WT4x5 [WT100x7.5] SHOWN)

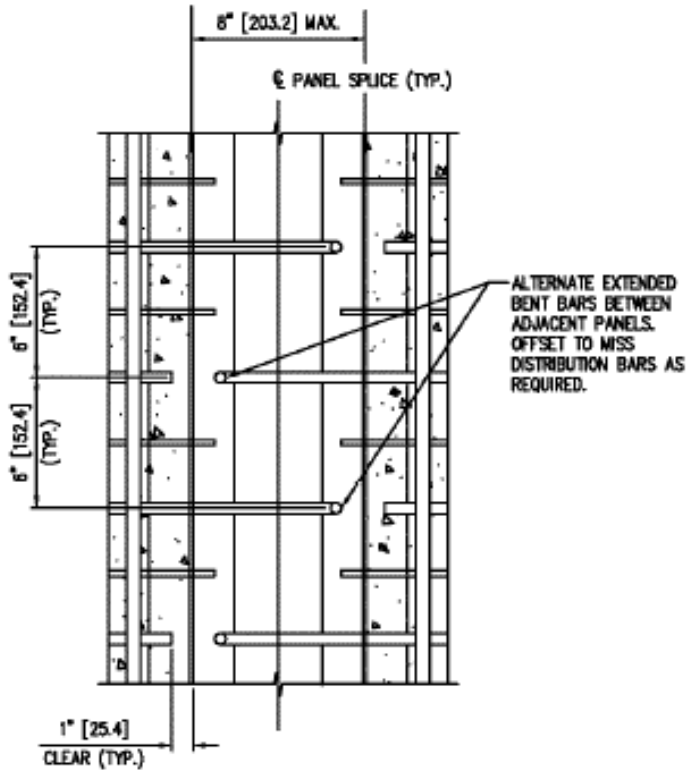


VIEW A-A: BENT REBAR STAGGERED SPACING SCHEMATIC
(FIELD PLACED REBAR NOT SHOWN)

**Figure 2.24: Staggered Hook Reinforced Transverse Joint (D.S. Brown Company 2007)**

The precast Exodermic deck system has been implemented in over 100 rapid deck replacement projects (Battaglia and Bischoff 2010). The first project was in 1984 with the Driscoll Bridge along the Garden State Parkway in New Jersey. The roadway was widened and 500 precast panels were installed successfully within just six days (Bettigole and Robison 1997).

One of the more prominent deck replacement projects was in 1998 with the New York Thruway Authority's Tappan Zee Bridge along I-87 over the Hudson River (Ramey and Oliver 1998). The bridge was originally built between 1951 and 1955. Due to increased traffic demand and deck deterioration, it was required that the deck be replaced and widened to seven lanes. Figure 2.25 shows placement of one of the Exodermic panels on the Tappan Zee Bridge. Utilizing this deck system allowed the construction to be completed in stages overnight without disrupting traffic flow (Rao, Tajirian, and Stubstad 2003). Construction lasted over several nights from 8:00 p.m. to 6:00 a.m. (Bettigole 1998). As an incentive to complete the work on time and not disrupt morning rush-hour traffic, the contractors were penalized $1,300 per minute if all lanes were not opened by 6:00 a.m. each morning. The replacement project was completed successfully and the Exodermic bridge deck panels have performed well (Rao, Tajirian, and Stubstad 2003).

**Figure 2.25: Tappan Zee Bridge Deck Placement (D.S. Brown Company 2017b)**

Another more recent Exodermic deck replacement project was conducted by the Georgia Department of Transportation (GDOT) in 2005. The project included two bridges in Gainesville, Georgia (Longstreet Bridge and Bells Mill Bridge) and two bridges in Atlanta, Georgia (I-285 Bridge over Buford Highway and I-285 Bridge over U.S. 41). Figure 2.26 shows the existing deck removed from the Longstreet Bridge, and Figure 2.27 shows the placement of rapid-setting concrete in the joints of the Longstreet Bridge.

The bridges in this deck replacement project were similar in many ways, however they also had their differences. The Longstreet Bridge and I-285 Bridges over U.S. 41 were simply supported while the Bells Mill Bridge and I-285 Bridges over Buford Highway were continuous span. The two Gainesville bridges were full deck replacement projects while the two Atlanta bridges were partial deck replacement projects (Umphrey 2006).

The Longstreet Bridge had two lanes, and the support structure for the bridge consisted of a concrete deck supported by longitudinal stringers that ran the entire length of the bridge which were simply-supported on cross-girders. Several transverse cracks were identified in the deck so a replacement was necessary. The entire bridge was closed to traffic during each night of construction from 9:00 p.m. to 5:00 a.m. Construction lasted from July to September 2005 (Umphrey 2006).

The Bells Mill Bridge also had two lanes, and the supporting structure for the bridge consisted of a concrete deck supported by longitudinal girders that were continuous span. The deck was in need of rehabilitation. The bridge was closed from 9:00 p.m. to 5:00 a.m. to traffic during each work night. Construction lasted from March to July 2005 (Umphrey 2006).

The I-285 Bridges over Buford Highway were sister bridges that were originally two lanes wide each which were widened over time to 7 lanes eastbound and 6 lanes westbound. Only the decks for the original lanes were replaced. The supporting structure for the bridge was a concrete deck on steel girders. The bridge remained opened partially during the construction process. Work on the original lanes was conducted over weekend sessions from 9:00 p.m. Friday to 5:00 a.m. Monday (Umphrey 2006).

The I-285 Bridges over U.S. 41 were sister bridges with four lanes each where only the two original lanes needed to be replaced. The supporting structure consisted of full-depth concrete decks on longitudinal girders that were simply supported on each of the four spans. Deck replacement was needed because the deck surface was spalling. The bridge remained opened partially during the construction process. Work on the original lanes was conducted over twelve weekend sessions from 9:00 p.m. Friday to 5:00 a.m. Monday. Construction lasted from July to September 2005 (Umphrey 2006).

The construction process for each bridge followed similar steps during a single work period. First, transverse and longitudinal saw cuts were made around the designated deck area. Then, the deck portion was removed and the steel flanges below were cleaned. Next, the precast Exodermic deck panels were aligned and positioned at the correct location. The formwork for the closure pours and haunches was installed, and studs were welded to the top surface of the supporting steel girders. Rapid-setting concrete was then placed in the joints. The bridge was reopened to traffic as soon as the joint material reached a compressive strength of at least 3,500 psi. Typically, one lane was replaced at a time during an individual work session (Umphrey 2006).

The results from each of the four deck replacement projects conducted by the GDOT proved to be quite successful. The construction was efficiently completed within the required timeframe. In addition, there was limited disruption to traffic (Umphrey 2006).

**Figure 2.26: Existing Deck Removed from the Longstreet Bridge (Umphrey 2006)**

**Figure 2.27: Placement of Rapid-Setting Concrete in the Joints of the Longstreet Bridge (Umphrey 2006)**

## 2.6 Summary

The precast deck panel system is an efficient replacement system for deteriorated bridge decks. In order for ALDOT to judge the performance of potential deck joint systems for implementation in the field, small-scale specimens need to be tested in the laboratory with standard practices and criteria. The following summarizes major findings from past research and highlights information that is lacking with respect to transverse joint demand, behavior, and testing.

Transverse joints experience a combination of stresses ranging from tension, shear, and flexural. Tension occurs in joints when the deck is made composite with girders and is experiencing negative flexure. In this situation, the neutral axis is below the deck so the entire joint is in tension. Shear stresses at the joint occur when loads are transferred from one panel to the other, vertically. Maximum positive bending of transverse joints occurs when the deck is loaded so that it deflects downwards between bents and between girders. Negative bending occurs when the deck joint is loaded over a bridge bent, typically.

Research conducted in the past has typically only focused on a single force effect at a time such as testing in pure tension, pure shear, or pure bending. From research conducted by Rhett (2012) it was determined that for a standard ALDOT bridge, the deck experiences bending stresses simultaneous with shear stresses. Specifically, when a deck is in positive bending there is a reversal in shear, and when a deck experiences negative flexure there is a shear stress in the deck.

In addition, some research projects tested deck specimens for ultimate strength or fatigue durability with no regard for the actual stress demands from the effects of a deck joint loaded on a bridge. For instance, the applied load for the cyclic pure shear tests conducted by Porter (2009) was calculated as 90% of the mean minus one standard deviation of the ultimate load from the

previous monotonic tests. This load was selected because the specimens would not fail under the first cycle. While at the same time, the specimens would fail after a reasonable number of cycles. Also, the fatigue pure bending tests conducted by Ryu, Kim, and Chang (2007) were loaded at either 30%, 50%, or 70% of the ultimate load as determined from the previous static tests.

In contrast, the pure tension tests conducted by Zhu et al. (2012) the load was applied to the model with the design load truck and design lane load according to AASHTO LRFD. The maximum negative moment in the deck occurred over an interior girder over an interior pier. The stress in the extreme top fiber of the transverse joint was 0.306 ksi. This value was similar to the 0.256 ksi stress experienced in the top fiber of the bridge deck analyzed by Rhett (2012). Also, for the fatigue positive bending with simultaneous shear tests conducted by Au, Lam, and Tharmabala (2011) the applied load simulated a factored wheel load scaled to correspond to the two-third geometric scaling of the specimen.

Many research projects tested the specimens in both static tests (monotonic until failure) and fatigue tests. For the fatigue tests it appeared that the loading procedure followed the precedent set by ASTM D6275 where the applied load was applied for 2,000,000 cycles at no more than 5.0 Hz.

# CHAPTER 3: DESIGN OF EXPERIMENTAL PROGRAM

## 3.1 Overview

This chapter covers all aspects of the test method utilized in this project ranging from test assembly, loading procedure, instrumentation, and data acquisition. The experimental program was designed to apply for any type of proposed deck panel and joint combination. However, the Exodermic deck system used in this research project exhibited a joint strength capacity limitation that warranted adjusting the experimental program. The differences in the proposed experimental program and actual experimental program used in this project are clearly noted in the following chapters as they appear.

## 3.2 Test Assembly

This section covers all aspects of the test assembly ranging from load configuration, load application, and supports.

### 3.2.1 Load Configuration

As referenced in Section 2.3, transverse joints experience a combination of stresses ranging from tension, shear, and flexure dependent upon the location of the joint with relation to the girders and piers. Tension occurs in joints when the deck is made composite with girders and is experiencing negative flexure. In this situation, the neutral axis is below the deck so the entire joint is in tension. Shear stresses at the joint occur when loads are transferred from one panel to the other, vertically. Maximum positive bending of transverse joints occurs when the deck is loaded so that it deflects downwards between bents and between girders. Negative bending occurs when the deck joint is

loaded over a bridge bent, typically. Laboratory testing conducted in the past has typically only focused on a single force effect at a time such as testing in pure tension, pure shear, or pure bending. However, for this research project, testing will include a realistic combination of stresses.

From previous research conducted by Rhett (2012) at Auburn University it was determined from finite element analysis that the extreme stresses experienced by transverse joints in typical ALDOT bridges included two main cases: positive bending simultaneous with a reversal in shear and negative bending with a shear component. The extreme positive-flexure stress occurred 5 ft past the first bent and between the two outermost girders while the extreme negative-flexure stress occurred above the first bent and above the outermost girder. Stress values from the analysis are summarized in Table 3.1. Note that for the positive bending stress demands the computed shear listed contained two values. This represented the shear reversal experienced at the transverse joint. Also, note that the smallest moment-to-shear ratio for either case was 40 in. The service-level moments in the positive bending and negative bending cases were fairly similar while the service-level shear in the positive bending case was more extreme than in the negative bending case. To simplify and conservatively utilize the same service-level moments and shears for all of the tests in this proposed experimental program, the values from the positive bending case were implemented. Therefore, for the positive bending tests the service-level moment, $M_{service}$, was 28.9 kip-in per unit width and the service-level shear, $V_{service}$, was 0.728 kips per unit width. For the negative bending tests the service-level moment, $M_{service}$, was -28.9 kip-in per unit width and the service-level shear, $V_{service}$, was -0.728 kips per unit width.

**Table 3.1: Computed Stress Demands (Rhett 2012)**

| Critical Stress | Bending Stress (ksi) | | Moment (kip-in) | Shear (kips) | Moment/Shear (in.) |
|---|---|---|---|---|---|
| | Top Fiber | Bottom Fiber | | | |
| **Positive Bending** | -0.184 | 0.226 | 28.9 | 0.728/-0.425 | 40/-68 |
| **Negative Bending** | 0.256 | -0.084 | -32.7 | -0.452 | 73 |

Rhett (2012) closely examined the shear and moment behavior of transverse joints as a wheel load crossed the joint. Figure 3.1 graphically illustrates the interaction of shear and negative moment. As the load approached the center of the joint the shear increased as well as the negative moment. There was not a reversal of the shear as the load reached the center of the joint. Figure 3.2 illustrates the interaction of shear and positive moment. For this case as the load approached the center of the joint the shear increased in one direction and reversed in another. Also, as the load approached the center of the joint the moment showed minimal negative moment at first followed by a sharp positive moment at the center of the joint. The important aspect of the second figure is that the transverse joint experienced positive flexure combined with a reversal in the shear. This type of interaction has seldom, if ever, been investigated in a laboratory environment. Therefore, this research project included this unique interaction in the experimental program.

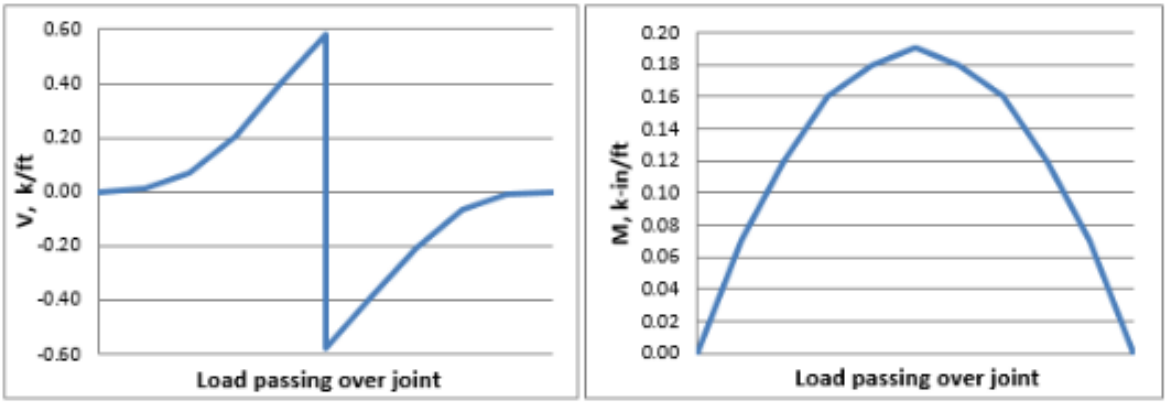


(a) Shear (b) Negative Moment

**Figure 3.1: Simultaneous Shear and Negative Moment Diagrams (Rhett 2012)**

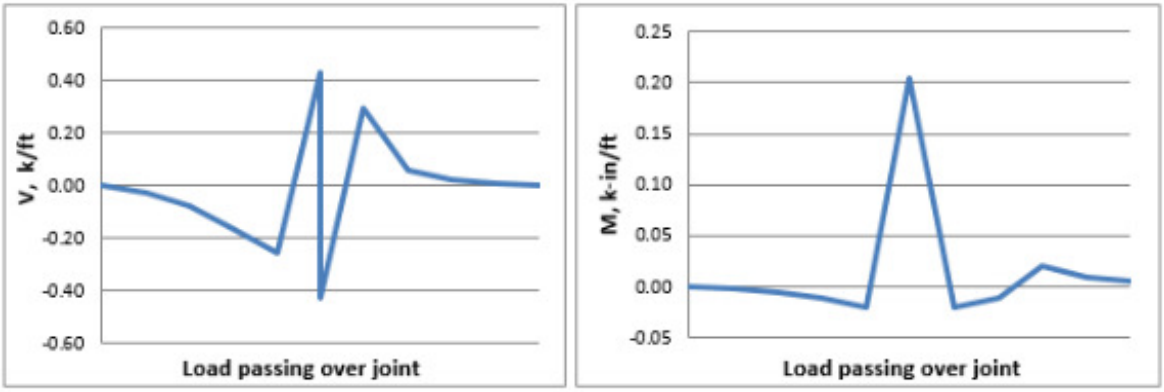


(a) Shear (b) Positive Moment

**Figure 3.2: Simultaneous Shear and Positive Moment Diagrams (Rhett 2012)**

Three different load configurations were implemented to test transverse deck joints. Figure 3.3, 3.4, and 3.5 show the load configuration for the positive bending, negative bending, and shear reversal tests, respectively. The configurations described are applicable for any future experimental program as well as what was actually used in this project. The tests were set-up as simply supported beams with a span length of 72 in. The span of the specimens was parallel to the direction of traffic on a bridge so that the transverse joint was transverse to the flow of traffic. There was one point of loading for the bending tests and two independent points of loading for the shear reversal test. The negative bending test had a similar load configuration as the positive bending test with the only difference being that the test specimen was positioned upside down to achieve a negative moment in the joint.

As noted earlier the most extreme moment-to-shear ratio from the Rhett (2012) research was 40 in. Due to physical constraints in the laboratory and to conservatively apply this ratio for flexural testing, the value was modified to 36 in. This value represented the distance from the center of the joint to the support on the opposite side of the load.

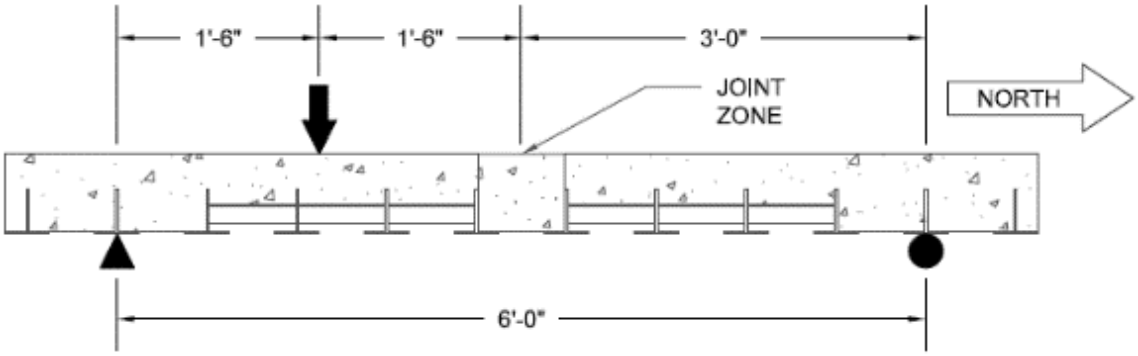


**Figure 3.3: Load Configuration for Positive Bending Test**

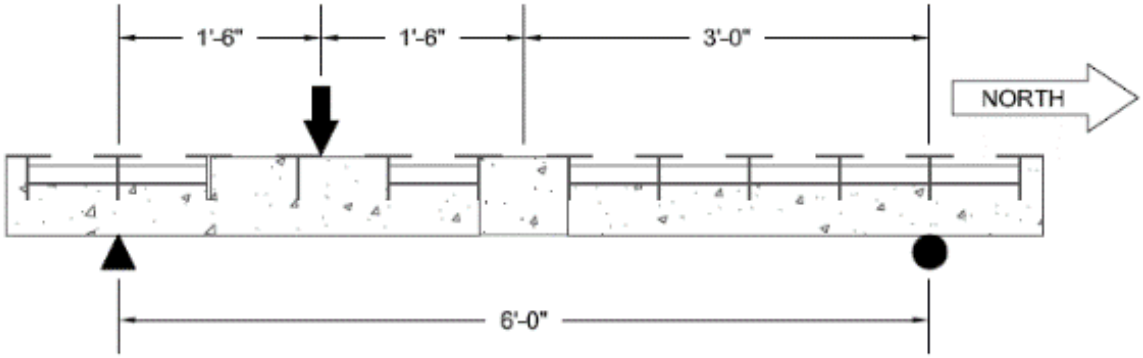


**Figure 3.4: Load Configuration for Negative Bending Test**

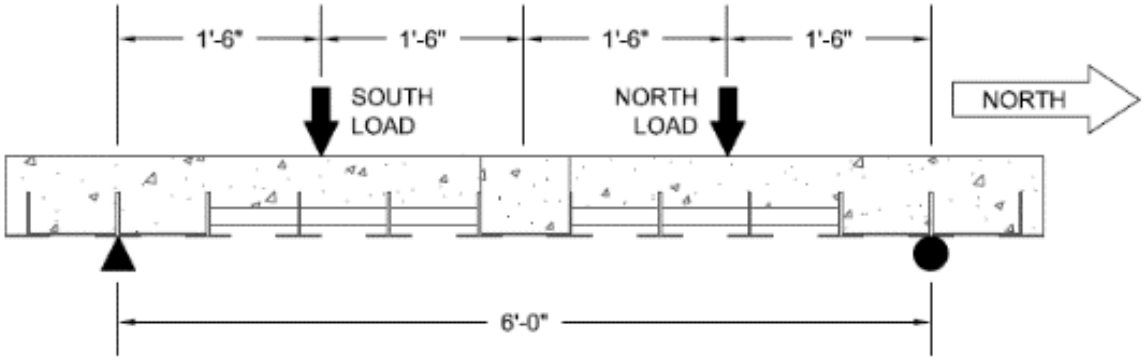


**Figure 3.5: Load Configuration for Shear Reversal Test**

### 3.2.2 Load Application

This section covers all aspects of the load application ranging from the reaction frame, hydraulic actuator, and spreader beam. A steel reaction frame was post-tensioned to the laboratory strong floor to ensure the load application system was secure. Hydraulic actuators were then attached to the reaction frame. The MTS Model 243.35 actuators had a capacity ranging from 54 kips in tension to 82 kips in compression and a stroke range of 10 in. The actuators could be load controlled or force controlled by the MTS Series 793 Controller software with Flex Test 60 hardware. A W8x31 beam with 3/8 in. stiffeners was utilized to spread the load across the width of the test specimen. Finally, the spreader beam rested on a 1 in. diameter rod welded to ½ in. x 4 in. steel plate which was seated in gypsum cement on the specimen surface.

The specimens used in this research project were 24 in. wide. This width was based on the reinforcing steel geometry specified by the Exodermic deck system, which was used for this project. The reinforcing bars that extended out of the deck panel and into the joint were spaced at 12 in. on center. To maintain a representative concrete to steel ratio at the joint, the specimen width could be multiples of 12 in. A width of 24 in. was selected so that each panel contained two reinforcing bars which allowed some redundancy if any strain gages attached to the steel happened to fail. A specimen width of 24 in. is recommended for any future experimental programs but not required. The applied load must increase proportionally with the increase in specimen width. More details regarding the geometry of the deck panels used in this research project are described in Section 4.2.

### 3.2.3 Supports

Two large concrete reaction blocks rested on the strong floor in the laboratory shown in Figure 3.6. The supports for the test were seated in gypsum cement on top of the blocks. Figure 3.7 shows the two supports. The south support served as a roller which consisted of a 1 in. diameter rod welded to ½ in. x 4 in. x 24 in. steel plate. The north support served as a rocker which consisted of a 1 in. diameter rod in between two ½ in. x 4 in. x 24 in. beveled out plates of steel. The high radius of the bevel allowed the rod to translate and rotate small amounts while preventing sudden lateral displacement. Similar set-up of the supports for future experimental programs is recommended but not required.

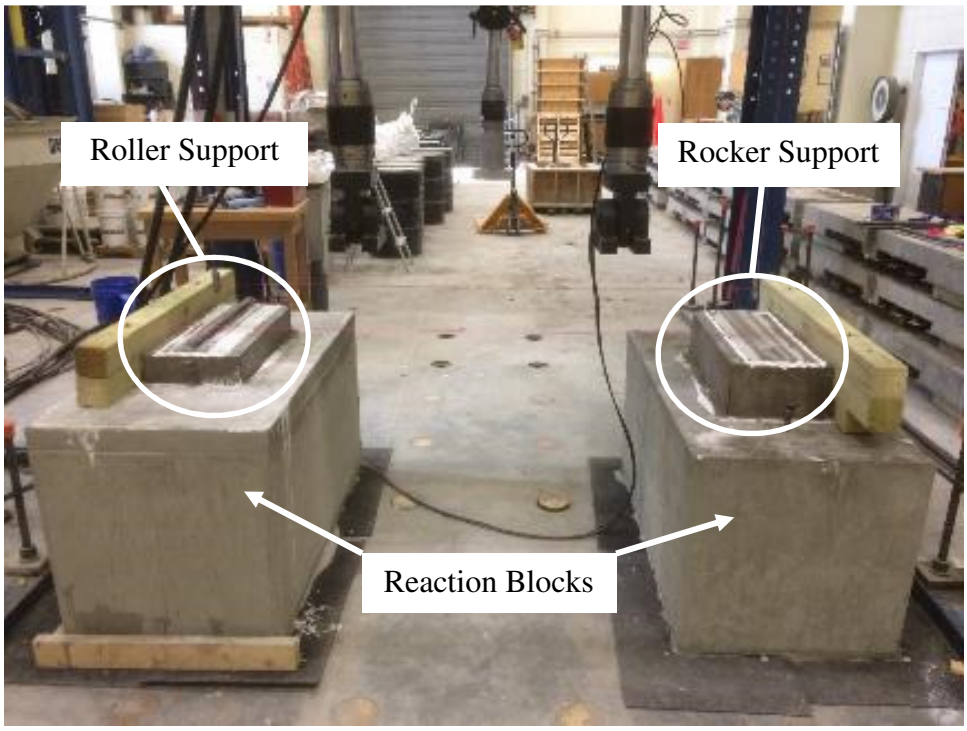


**Figure 3.6: Reaction Blocks**

**Figure 3.7: Supports**

## 3.3 Loading Procedure

The loading procedure proposed for future experimental programs as well as this research project was separated into two categories: quasi-static loading and fatigue loading. Table 3.2 and Table 3.3 show the test schedule for the unreinforced shear key and staggered hook reinforced specimens used in this project, respectively. For each joint type and test configuration there was an additional "backup" specimen that was kept in reserve in case a panel was damaged prematurely.

The purpose of the quasi-static tests was to understand the static loading behavior of the joints and to determine if there was any correlation between the quasi-static behavior and the fatigue behavior of the specimens. The quasi-static test was a simpler and faster test. So, if there was a correlation between the two tests, then it may be possible to only perform the quasi-static test to judge whether a proposed deck-joint system was acceptable or not.

The purpose of the fatigue tests was to quantify the fatigue durability of the joints under service level loads. This type of test is time-consuming and potentially expensive. So, a replacement test that can represent the joint behavior in a shorter amount of time is desirable.

**Table 3.2: Test Schedule for Unreinforced Shear Key Joints**

| Specimen Name | Test Configuration | Loading Procedure |
|---|---|---|
| U-POS-Q | Positive Bending | Quasi-Static |
| U-POS-F | Positive Bending | Fatigue |
| U-POS-B | Positive Bending | Backup |
| U-NEG-Q | Negative Bending | Quasi-Static |
| U-NEG-F | Negative Bending | Fatigue |
| U-NEG-B | Negative Bending | Backup |
| U-REV-Q | Shear Reversal | Quasi-Static |
| U-REV-F | Shear Reversal | Fatigue |
| U-REV-B | Shear Reversal | Backup |

**Table 3.3: Test Schedule for Staggered Hook Reinforced Joints**

| Specimen Name | Test Configuration | Loading Procedure |
|---|---|---|
| R-POS-Q | Positive Bending | Quasi-Static |
| R-POS-F | Positive Bending | Fatigue |
| R-POS-B | Positive Bending | Backup |
| R-NEG-Q | Negative Bending | Quasi-Static |
| R-NEG-F | Negative Bending | Fatigue |
| R-NEG-B | Negative Bending | Backup |
| R-REV-Q | Shear Reversal | Quasi-Static |
| R-REV-F | Shear Reversal | Fatigue |
| R-REV-B | Shear Reversal | Backup |

### 3.3.1 Quasi-Static Tests

The quasi-static tests were performed to better understand the static loading behavior of the joints and to determine if there was any correlation between the quasi-static behavior and the fatigue behavior of the specimens.

Given the prescribed load configuration mentioned previously in Section 3.2.1, Figures 3.8, 3.9, and 3.10 show a typical load cycle with applied load, shear at joint, and moment at joint interaction for positive bending, negative bending, and shear reversal, respectively. The period of each cycle depends on the test type: quasi-static or fatigue. For the positive bending test as the applied load increased the shear and moment also increased, and as the applied load decreased the shear and moment also decreased. Similarly, for the negative bending test as the applied load increased the shear and moment also increased in magnitude, and as the applied load decreased the shear and moment decreased in magnitude. The shear reversal test was different, however. Two actuators each applied load to the specimen independently. One was on the north side and the other was on the south side of the joint. The two actuators applied load 180 degrees out of phase with each other such that when the north actuator was at a maximum load magnitude the south actuator was at a minimum load magnitude and vice versa. The applied load from the actuators was calculated such that the joint experienced a constant magnitude of positive bending for the entire cycle while the shear at the joint reversed as the applied load increased and decreased on each side of the joint throughout a typical cycle.

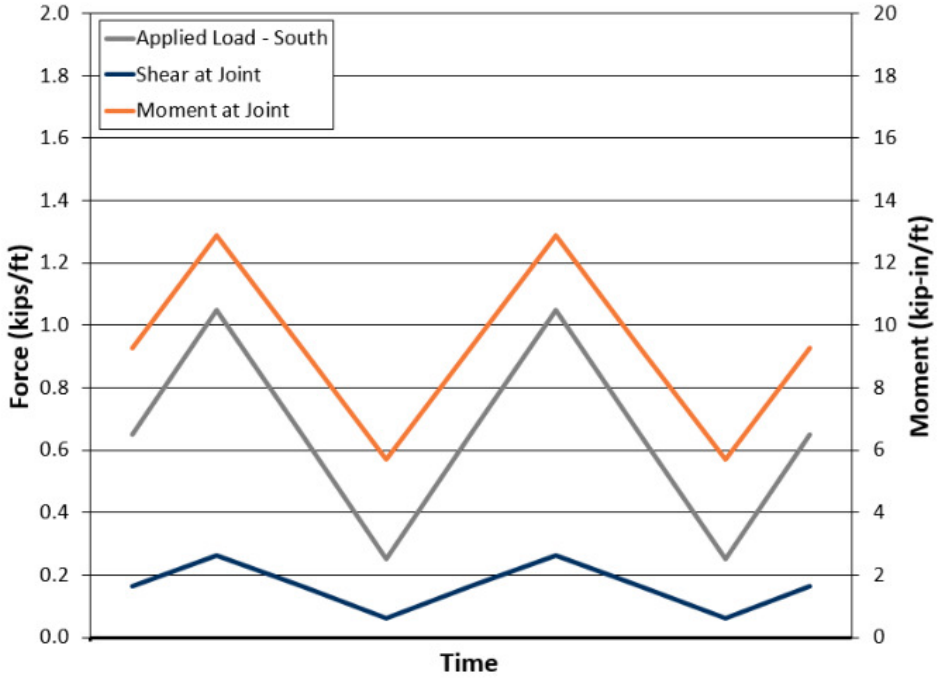


**Figure 3.8: Typical Positive Bending Load Cycle**

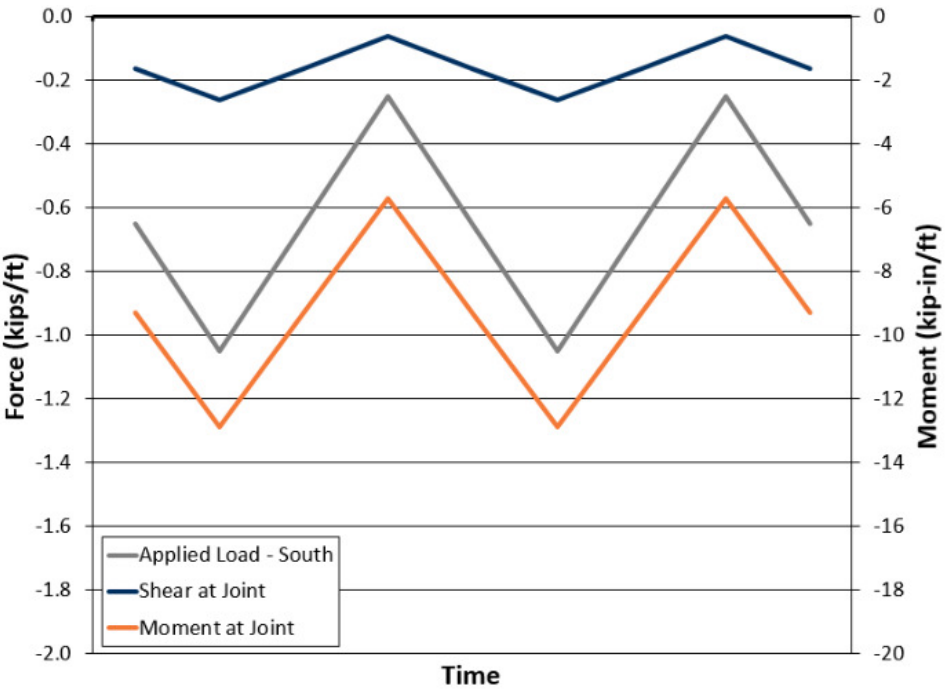


**Figure 3.9: Typical Negative Bending Load Cycle**

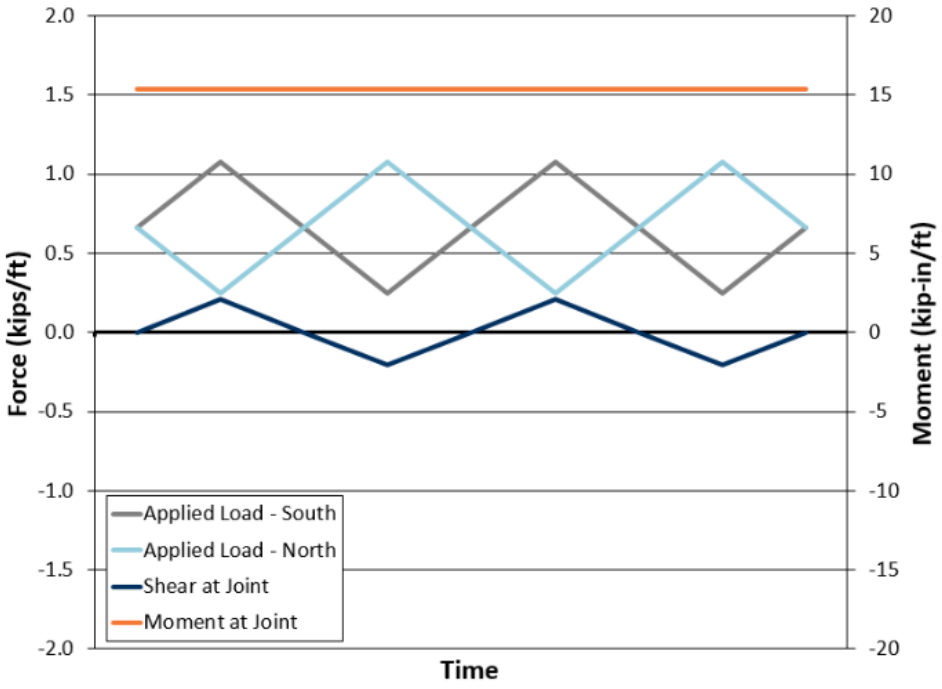


**Figure 3.10: Typical Shear Reversal Load Cycle**

Overall, the applied load was based on service-level stress demands that resulted from the Rhett (2012) analysis. As referenced previously in Section 3.2.1 for the positive bending tests the service-level moment, $M_{service}$, was 28.9 kip-in per unit width, for the negative bending tests the service-level moment, $M_{service}$, was -28.9 kip-in per unit width, and for the shear reversal tests the service-level shear, $V_{service}$, was +/-0.728 kips per unit width where the positive and negative sign indicate a reversal in the shear. Instead of immediately applying the full service-level loads to the specimens the loads were incrementally increased in a quasi-static manner. With this technique, the applied load was increased in "load steps" so that the behavior of the specimen could be studied at varying levels of load. The load steps for the tests were a function of theoretical joint behavior. For the flexure tests the defining factor was the cracking moment, $M_{cr}$, while for the shear reversal tests the defining factor was the shear strength of the concrete, $V_n$. The defining factors were based

on the measured average compressive strength of the deck concrete and the dimensions of a unit width of deck joint. These values could be calculated with the following equations:

$$M_{cr} = f_r S \quad \textbf{Equation 3.1}$$

$$V_n = 2\lambda\sqrt{f'_c}bd \quad \textbf{Equation 3.2}$$

$$S = \frac{1}{6}bh^2 \quad \textbf{Equation 3.3}$$

$$f_r = 7.5\sqrt{f'_c} \quad \textbf{Equation 3.4}$$

$$d = 0.8h \quad \textbf{Equation 3.5}$$

where

$M_{cr}$ = cracking moment of concrete deck
$V_n$ = shear strength of concrete deck
$f_r$ = modulus of rupture of concrete
S = section modulus
$f'_c$ = compressive strength of concrete
b = unit width of deck
h = overall depth of joint
d = effective depth of joint from compression fiber

The (one-way) shear strength and modulus of rupture relationships are from ACI 318-11. The effective depth, d, was selected as a simple, approximate calculation for both unreinforced and reinforced joints. Referring to Rhett's research on the finite element analysis of a typical ALDOT bridge, the unit width of the deck was 12 in., height of the deck was 8 in. The average compressive strength of the deck concrete used in this research project was 4,500 psi. By following the equations from above, $M_{cr}$ = 64.4 kip-in per unit width and $V_n$ = 10.3 kips per unit width.

Table 3.4 and Table 3.5 show the load steps with the calculated shear and moment per unit width at the joint for the flexure and shear-reversal tests, respectively. Self-weight of the specimens was accounted for which was 63.8 pounds per square foot. For the quasi-static tests,

the loading was incrementally increased throughout the test in proportion to $M_{cr}$ and $V_n$. For instance, the load steps for the flexure tests (U-POS-Q, U-NEG-Q, R-POS-Q, and R-NEG-Q) corresponded to 10% of $M_{cr}$, 20% of $M_{cr}$, 30% of $M_{cr}$, etc. Likewise, the load steps for the shear-reversal tests (U-REV-Q and R-REV-Q) corresponded to 1% of $V_n$, 2% of $V_n$, 3% of $V_n$, etc. For each load step, the load cycled five times up to the calculated value and down to the minimum load. A minimum load of 0.25 kips per unit width was used to maintain constant contact between the spreader beam and test specimen.

**Table 3.4: Load Steps for Flexure Tests**

| | **Applied Load (kips/ft)** | **$V_{joint}$ (kips/ft)** | **$M_{joint}$ (kip-in/ft)** |
|---|---|---|---|
| **10% of $M_{cr}$** | 0.33 | 0.08 | 6.4 |
| **20% of $M_{cr}$** | 1.05 | 0.26 | 12.9 |
| **30% of $M_{cr}$** | 1.76 | 0.44 | 19.3 |
| **40% of $M_{cr}$** | 2.48 | 0.62 | 25.8 |
| **50% of $M_{cr}$** | 3.19 | 0.80 | 32.2 |
| **60% of $M_{cr}$** | 3.91 | 0.98 | 38.6 |
| **70% of $M_{cr}$** | 4.63 | 1.16 | 45.1 |

**Table 3.5: Load Steps for Shear-Reversal Tests**

| | Applied Load (kips/ft) | $V_{joint}$ (kips/ft) | $M_{joint}$ (kip-in/ft) |
|---|---|---|---|
| **1% of $V_n$** | 0.66 | 0.10 | 11.7 |
| **2% of $V_n$** | 1.07 | 0.21 | 15.4 |
| **3% of $V_n$** | 1.49 | 0.31 | 19.1 |
| **4% of $V_n$** | 1.90 | 0.41 | 22.8 |
| **5% of $V_n$** | 2.31 | 0.52 | 26.5 |
| **6% of $V_n$** | 2.72 | 0.62 | 30.2 |
| **7% of $V_n$** | 3.14 | 0.72 | 33.9 |

The loading of the specimens was intended to be quasi-statically therefore, the loading rate was very slow such that the frequency of each cycle was 0.02 Hz. After each load step the test was paused to document any crack propagation. The load incrementally increased until the test specimen failed. Similar procedure should be followed for future experimental programs.

Figures 3.11, 3.12, and 3.13 show the loading procedure in relation to the theoretically calculated shear and moment at the joint per unit width for the positive bending, negative bending, and shear reversal tests, respectively.

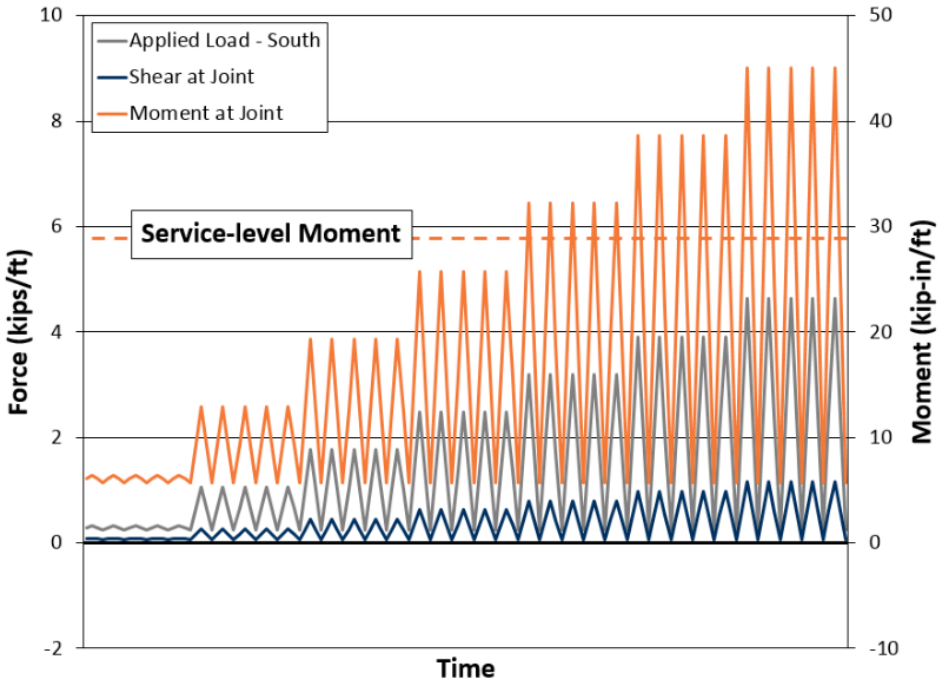


**Figure 3.11: Positive Bending Quasi-Static Loading Procedure**

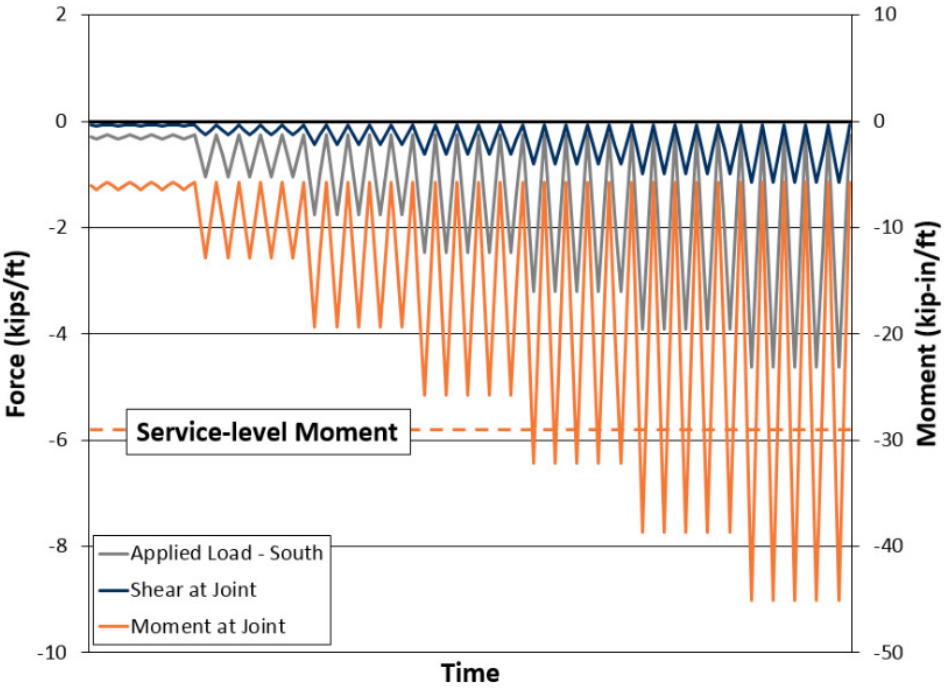


**Figure 3.12: Negative Bending Quasi-Static Loading Procedure**

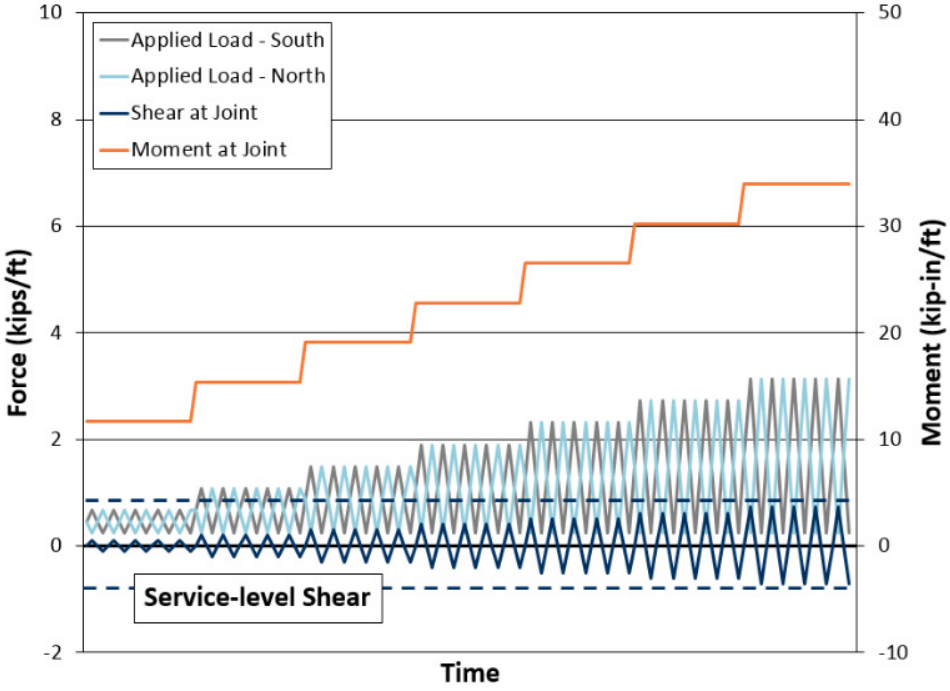


**Figure 3.13: Shear Reversal Quasi-Static Loading Procedure**

### 3.3.2 Fatigue Tests

The fatigue tests were performed to quantify the fatigue durability of the joints under service level loads and to determine if there was any correlation between the quasi-static behavior and the fatigue behavior of the specimens. The fatigue type test was time-consuming and potentially expensive. So, a replacement test that could represent the joint behavior in a shorter amount of time is desirable. More discussion on the correlation between the two test types is found in Section 5.4.

For future experimental programs the fatigue test loading is based on the service-level stresses from Rhett (2012) results where $M_{service}$ was 28.9 kip-in per unit width and $V_{service}$ was 0.728 kips per unit width. Therefore, the applied loading for the positive bending test should calculate to a moment at the joint of 28.9 kip-in/ft. The applied loading for the negative bending

test should calculate to a moment at the joint of -28.9 kip-in/ft. The applied loading for the shear reversal test should calculate to a shear at the joint of +/- 0.728 kips/ft where the positive and negative signs indicate a reversal in the shear. All fatigue tests should be cycled up to the calculated value and down to a minimum load of 0.25 kips/ft. The test should run for 2,000,000 cycles at 1.0 to 2.0 Hz and pause at discrete intervals to record the degradation of the joint at the $1^{st}$, $10^{th}$, $100^{th}$, $1{,}000^{th}$, $10{,}000^{th}$, $100{,}000^{th}$, $1{,}000{,}000^{th}$, and $2{,}000{,}000^{th}$ cycle.

For this research project the intention was to adhere to the fatigue loading procedure mentioned above. However, after conducting the quasi-static tests it was determined in general that the Exodermic panel specimens used in this project did not possess the ultimate strength required to resist the service-level stresses in this one-way framing configuration. This was due to the decreased effective cross section inherent in the Exodermic deck system design. Only three out of the six specimens tested quasi-statically had enough capacity to resist the service-level stresses. More information regarding the quasi-static and fatigue test results is found in Chapter 5.

By referring to the quasi-static test results, it was determined what loading on average caused the first crack in the specimens, the reinforcing steel to yield, and the failure of the specimens. Therefore, a load was selected for the fatigue tests so that the specimen did not crack nor yield the reinforcement upon initial loading. Figures 3.14, 3.15, and 3.16 show the loading procedure in relation to the theoretically calculated shear and moment at the joint per unit width for the positive bending, negative bending, and shear reversal tests, respectively. The load for the flexure tests (U-POS-F, U-NEG-F, R-POS-F, and R-NEG-F) corresponded to 30% of $M_{cr}$ which was approximately 67% of $M_{service}$. The load for the shear-reversal tests (U-REV-F and R-REV-

F) corresponded to 3% of $V_n$ which was approximately 42% of $V_{service}$. For each test the load cycled up to the calculated value and down to the minimum load of 0.25 kips/ft.

The test ran for 2,000,000 cycles and paused at discrete intervals to record the degradation of the joint at the 1st, 10th, 100th, 1,000th, 10,000th, 100,000th, 1,000,000th, and 2,000,000th cycle. The frequency of the discrete interval loading was 1.0 Hz while the frequency of the cycles intermediate the discrete intervals (i.e., cycles 2-9, 11-99, 101-999, etc.) was 2.0 Hz. The test continued until the specimen failed or it reached the end of 2,000,000 cycles.

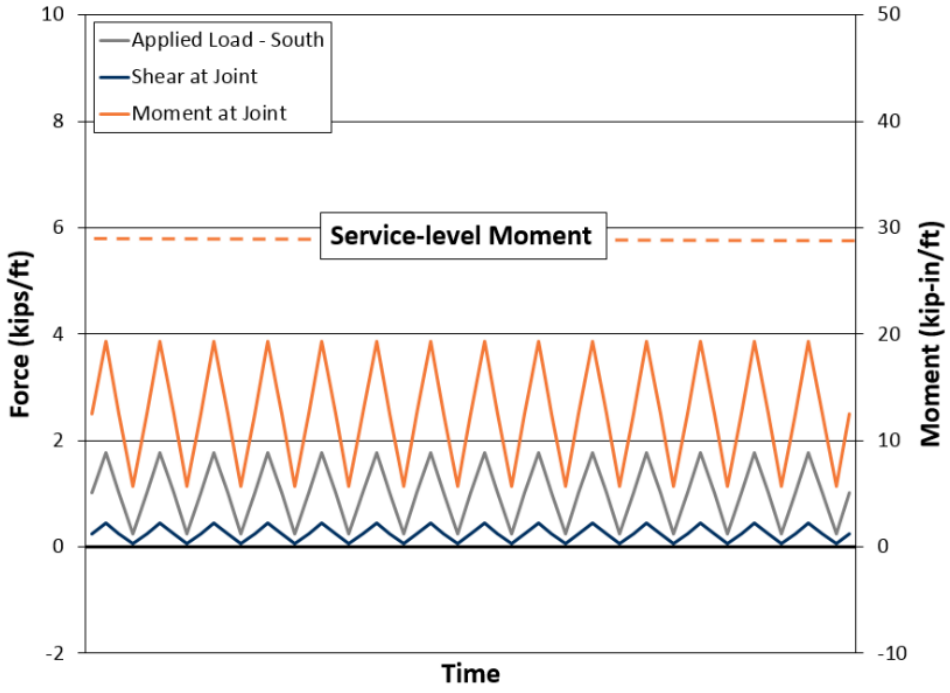


**Figure 3.14: Positive Bending Fatigue Loading Procedure**

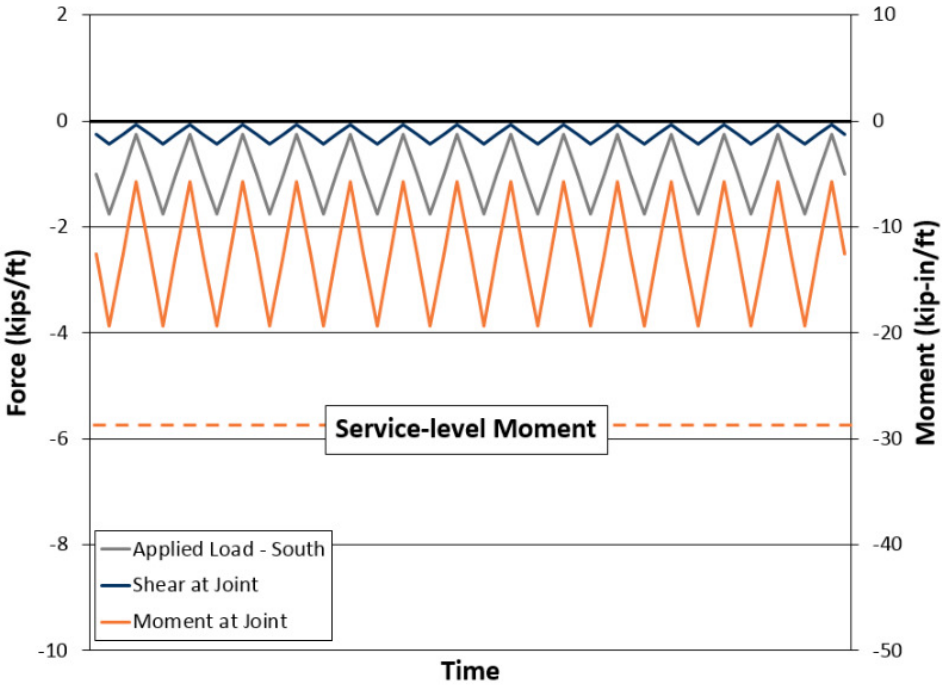


**Figure 3.15: Negative Bending Fatigue Loading Procedure**

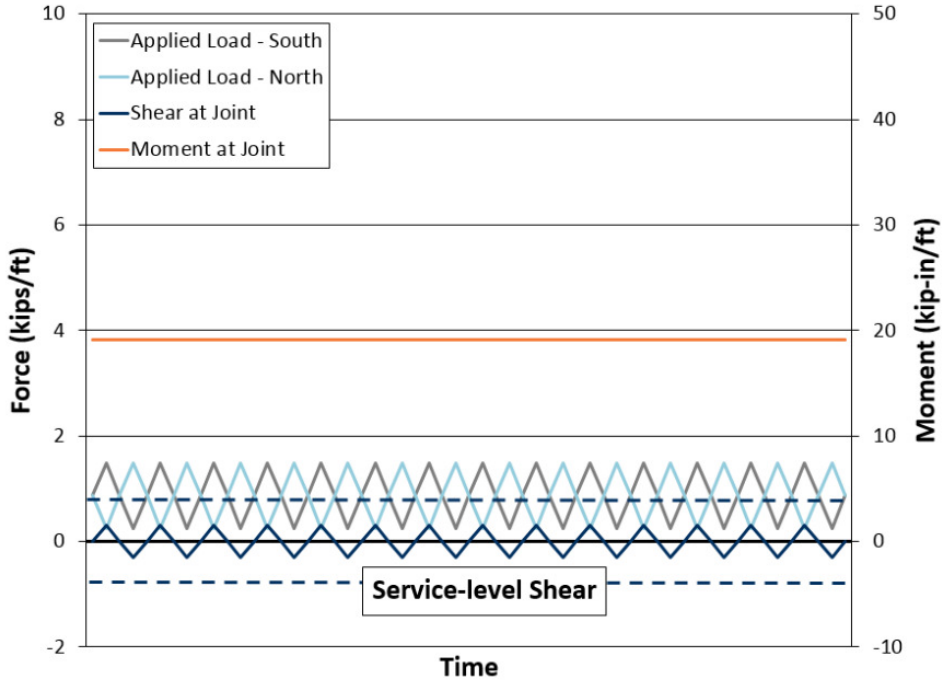


**Figure 3.16: Shear Reversal Fatigue Loading Procedure**

## 3.4 Instrumentation

This section covers the internal and external instrumentation utilized in this research project. Several sensors and instruments were used to help quantify the behavior of the joint by measuring the strain in the reinforcing steel, displacement of the specimen, and crack opening at the joint-deck interface. Not all of the instrumentation described in the following sections are necessary for future acceptance testing of potential bridge deck joints. For future testing, only the top wire potentiometers used to measure midspan deflection are needed. More details about the top wire potentiometer set-up is described in Section 3.4.2.

### 3.4.1 Internal Instrumentation

The internal instrumentation for this project consisted of attaching strain gages to the four hooked reinforcing bars in the staggered hook reinforced joints. Figure 3.17 shows the internal instrumentation locations. The 6 mm electronic resistance strain gages were attached at approximately ½ in. from the surface of the concrete where they extended out of the deck panels and into the joint. Additional description and figures regarding the gage attachment process is found in Section 4.5.1. Since the unreinforced shear key joints did not contain any reinforcement extending through the joint, there was no strain gages instrumented in these specimen types.

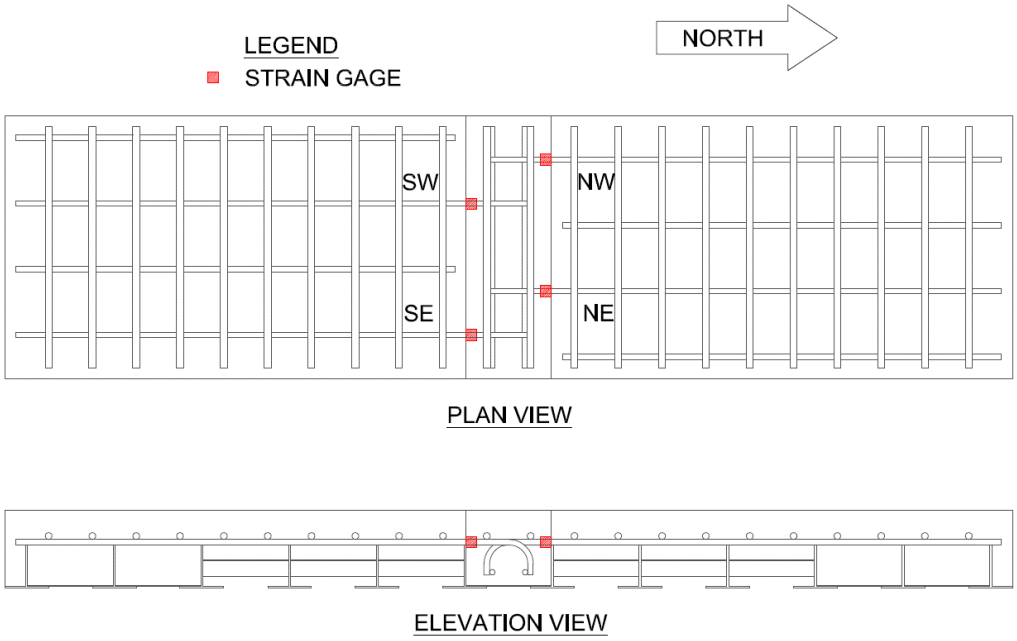


**Figure 3.17: Internal Instrumentation Locations**

### 3.4.2 External Instrumentation

The external instrumentation for this project consisted of attaching wire potentiometers (wirepots) and displacement transducers (crack gages) to the specimen to measure displacement and crack opening of the specimen when loaded. The external instrumentation locations for positive bending, negative bending, and shear reversal are shown in Figures 3.18, 3.19, and 3.20, respectively.

Figure 3.21 shows the wirepot deflection frame resting on the reaction blocks. Figure 3.22 shows the set-up of a typical top wirepot. Finally, Figure 3.23 shows a typical side wirepot set-up. Two Micro-Epsilon WDS-1000-P60-CR-P wirepots were attached from a deflection frame above the north support, two above the south support, and two above the center of the joint. This set-up allowed the effects of torsion to be averaged, and it allowed a measurement of the displacement of the joint relative to the supports to be calculated. These wirepots had a range of

about 1 ¼ in. Also, two wirepots were placed below the center of the joint to measure joint displacement. These wirepots had a range of about 4 in. and were implemented when a specimen had large deflection and the top wirepots exceeded their range limit. The side wirepots were mounted on brackets on the side of the specimen to measure crack opening at the joint interface. The wirepots were placed at the same height as the reinforcing steel locations within the specimens. For the flexure tests there were only side wirepots on the south side near the load location while for the shear-reversal tests there were side wirepots on the south and north joint interfaces.

Tokyo Sokki Kenkyujo PI-2-50 crack gages were only utilized for the staggered hook reinforced specimens with negative bending. Figure 3.24 shows the set-up for the crack gages. The crack gages were attached below the reinforcing steel locations to measure the crack opening at the joint interface.

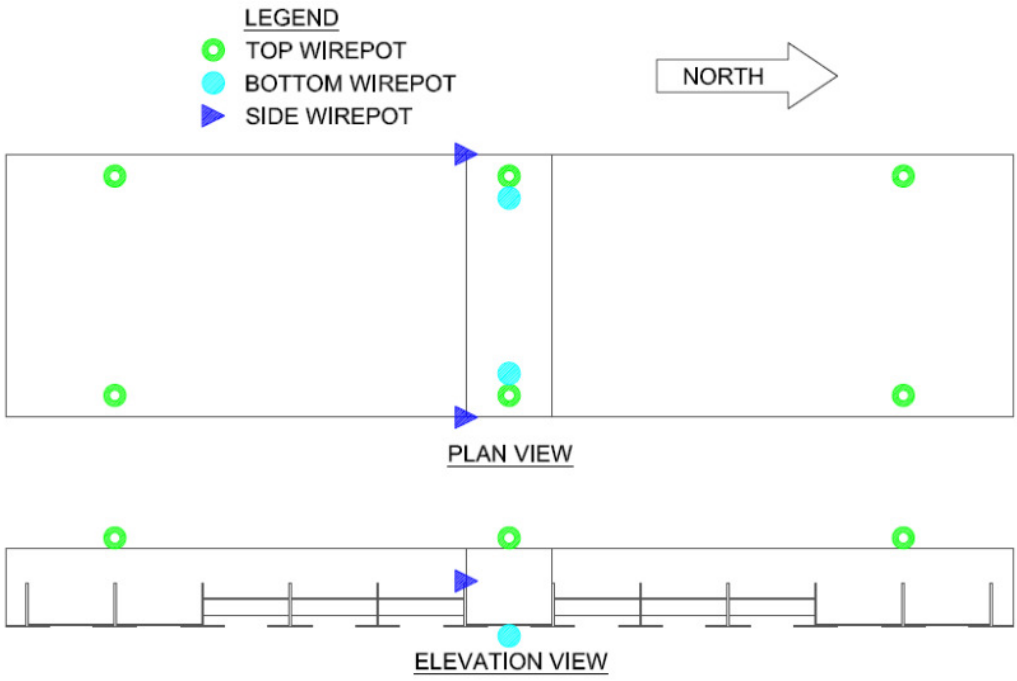


**Figure 3.18: External Instrumentation Locations – Positive Bending Test**

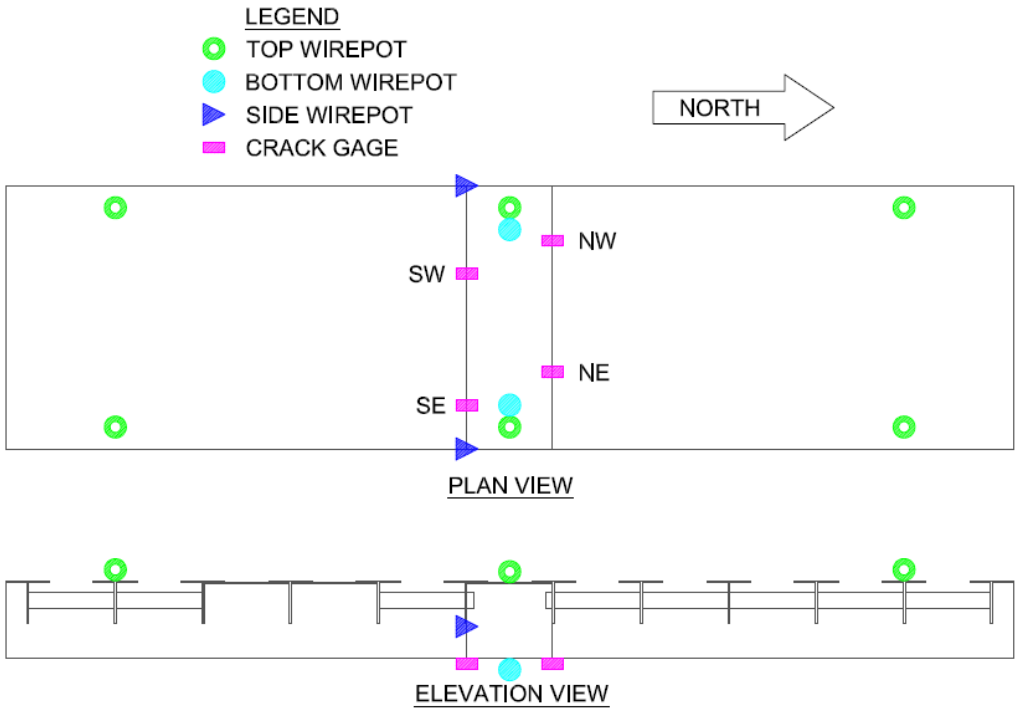


**Figure 3.19: External Instrumentation Locations – Negative Bending Test**

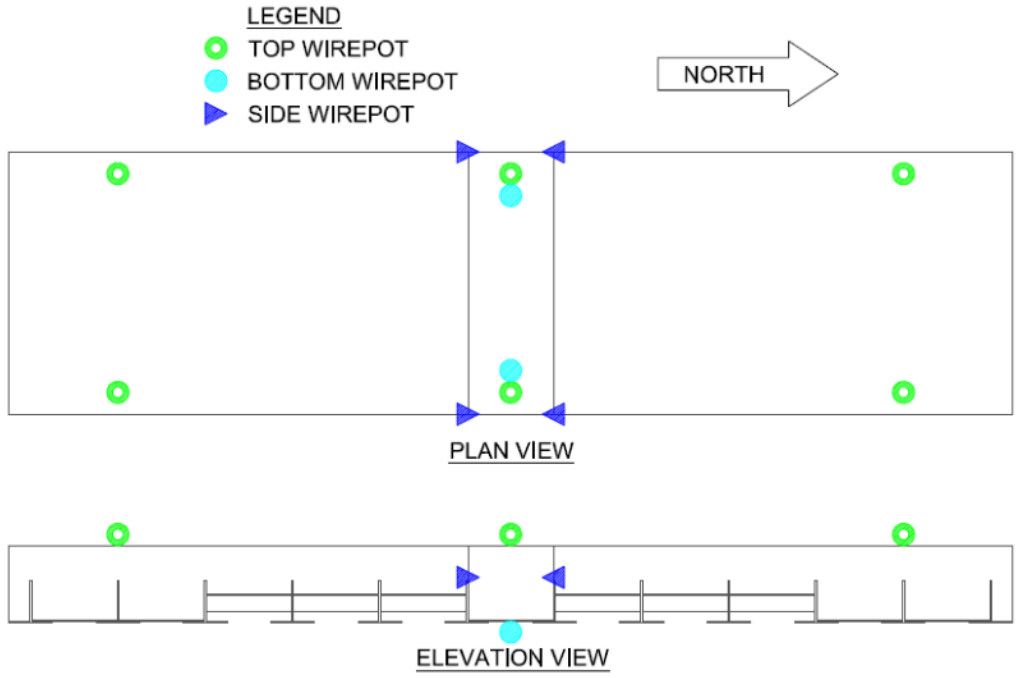


**Figure 3.20: External Instrumentation Locations – Shear Reversal Test**

**Figure 3.21: Wire Potentiometer Deflection Frame**

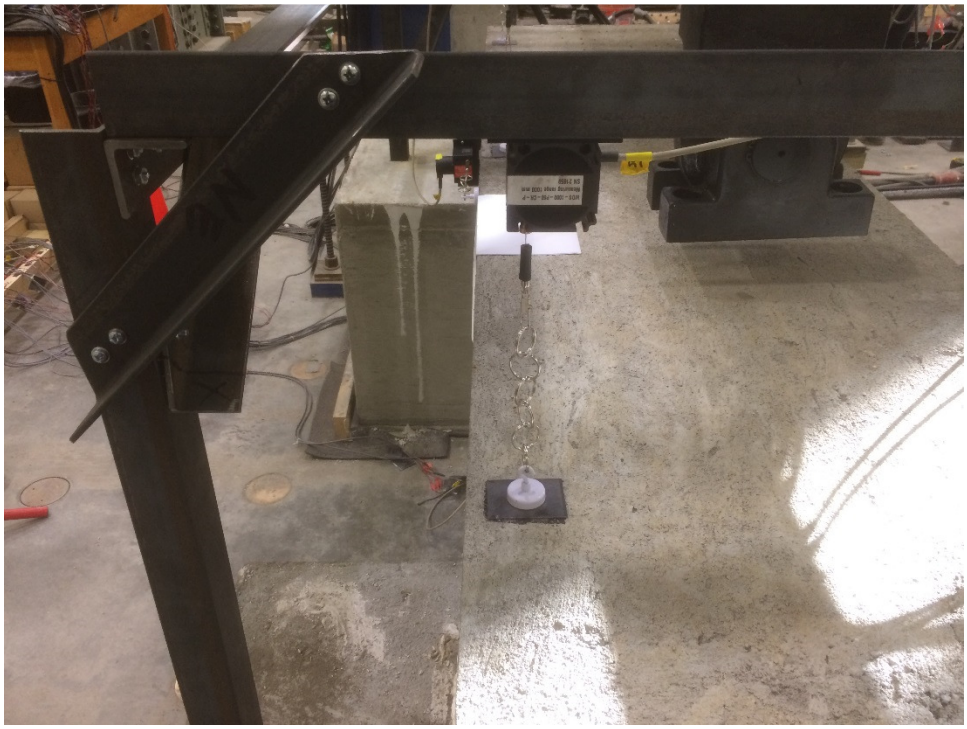

**Figure 3.22: Top Wire Potentiometer Set-Up**

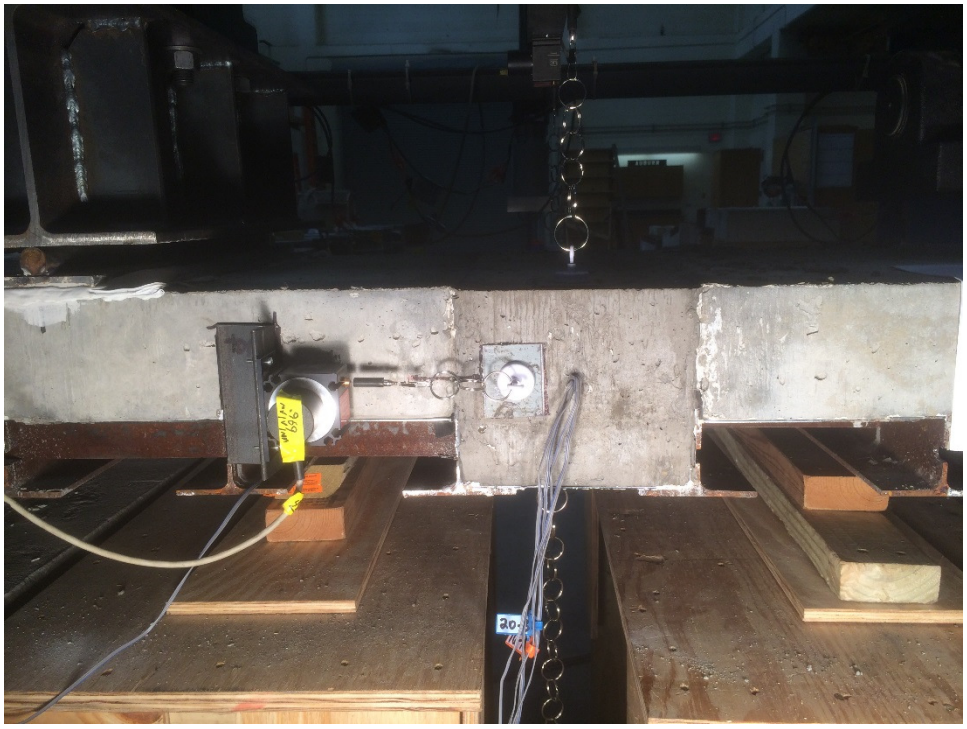

**Figure 3.23: Side Wire Potentiometer Set-Up**

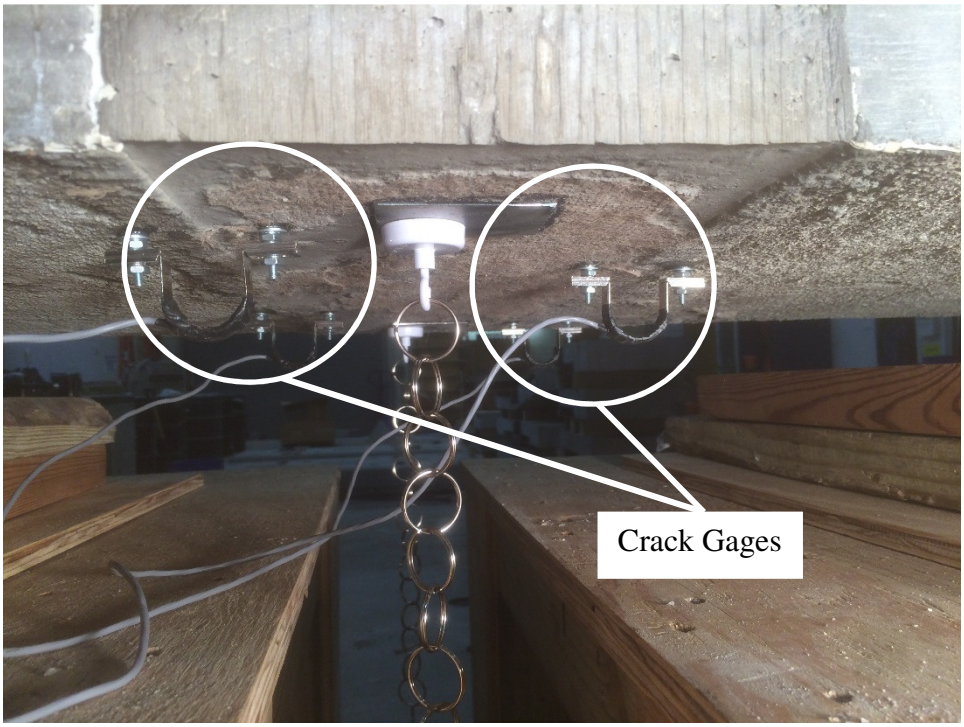


**Figure 3.24: Crack Gage Set-Up**

## 3.5 Data Acquisition

Data acquisition was completed with a Pacific Instruments 6000 Series Data Acquisition System. For the quasi-static tests the load cycled at 0.02 Hz. So, recording the data at a sampling rate of 10 samples/second was satisfactory. For the fatigue tests, the discrete test interval loads were cycled at 1.0 Hz. So, recording the data at a sampling rate of 100 samples/second was satisfactory. However, during the fatigue tests between the discrete test intervals (i.e. cycles 2-9, 11-99, 101-999, etc.), the load was cycled at 2.0 Hz. Since the measurement of the precise behavior of the specimen was not critical for each of these intermediate cycles, data was only recorded and monitored at a rate of 10 samples/second. Similar data acquisition techniques are recommended for future experimental programs.

# CHAPTER 4: SPECIMEN CONSTRUCTION

## 4.1 Overview

This chapter covers all aspects of the construction process of the test specimens used in this research project ranging from detailed drawings, delivery of materials, fabrication of the specimens, to testing the properties of the materials.

## 4.2 Detailed Drawings

Construction drawings of the specimens were drafted to serve as a reference when building the panels. The project called for 18 unreinforced shear key panels and 18 staggered hook reinforced panels. Figure 4.1 shows the reinforcing steel layout of the unreinforced shear key joint panel while Figure 4.2 shows the plan and elevation views of the joined panels. A detailed view of the unreinforced shear key joint dimensions is shown in Figure 4.3. Figure 4.4 shows the reinforcing steel layout of the staggered hook reinforced joint panel while Figure 4.5 shows the plan and elevation views of the joined panels. A detailed view of the staggered hook reinforced joint dimensions is shown in Figure 4.6.

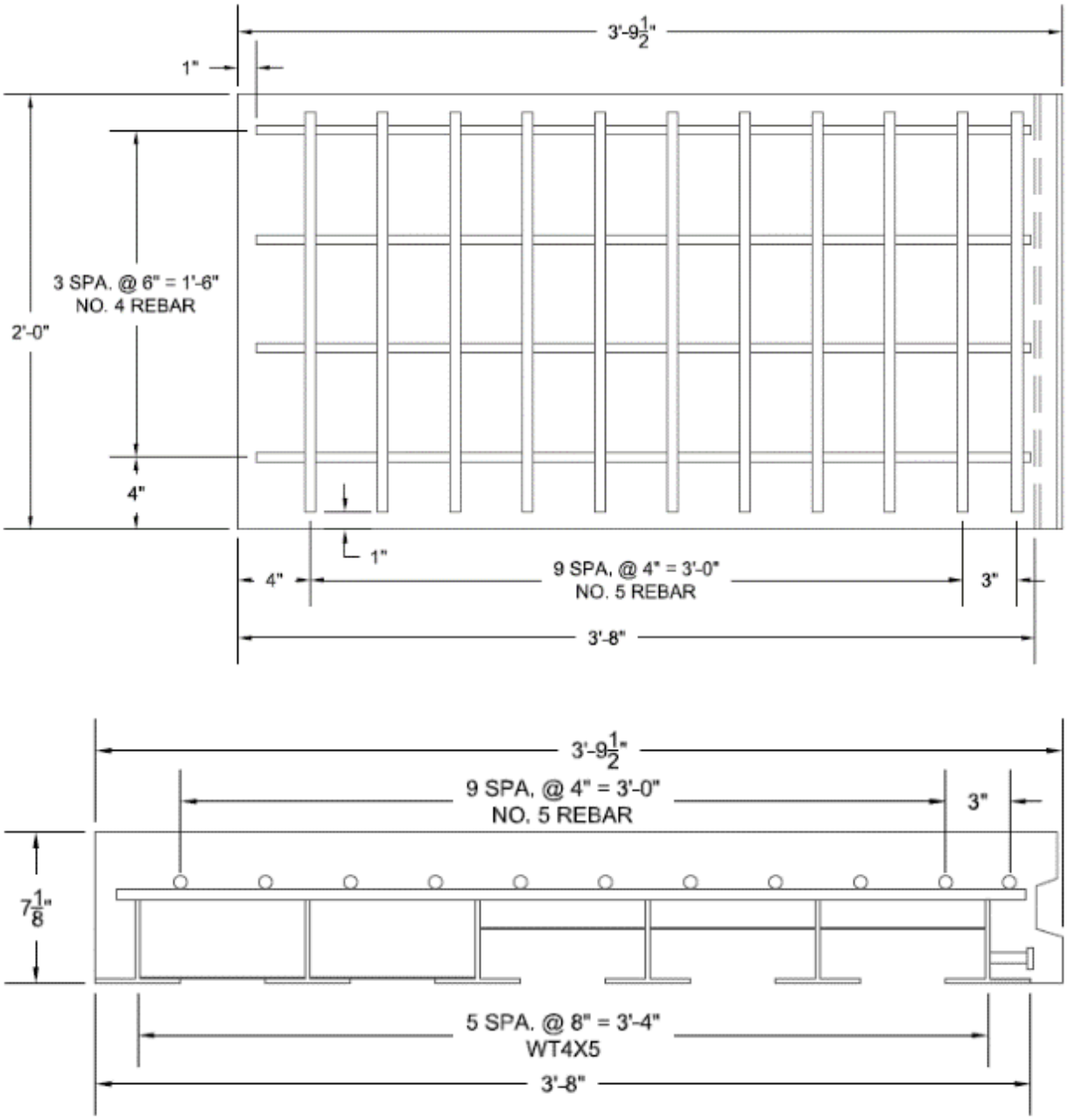


**Figure 4.1: Reinforcing Steel Layout for Unreinforced Shear Key Panel**

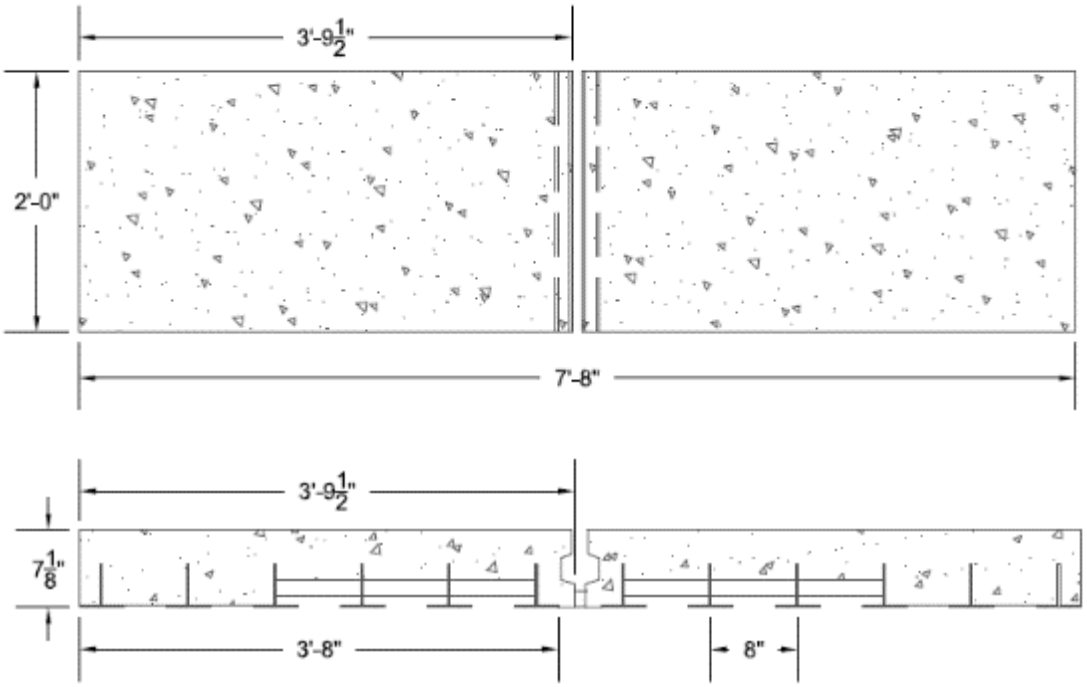


**Figure 4.2: Unreinforced Shear Key Joined Panels Plan and Elevation**

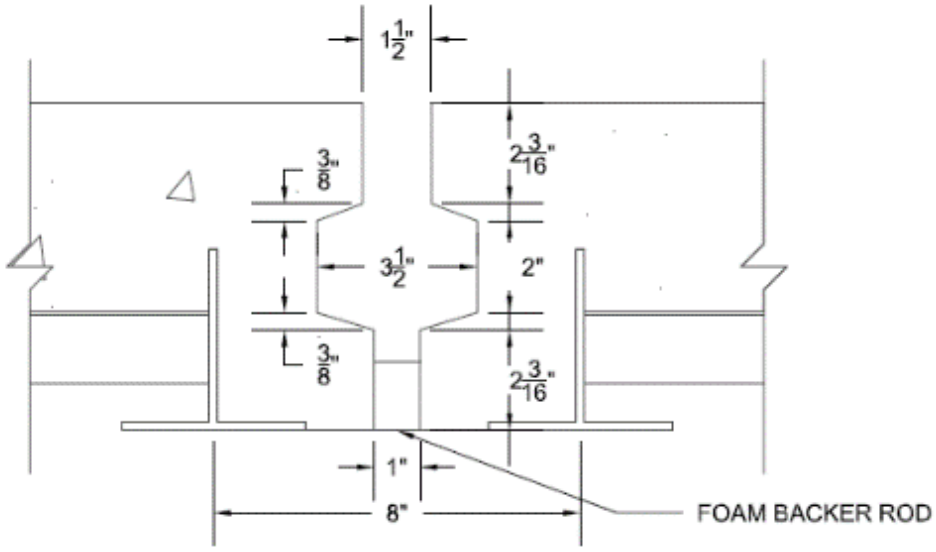


**Figure 4.3: Unreinforced Shear Key Joint Dimensions**

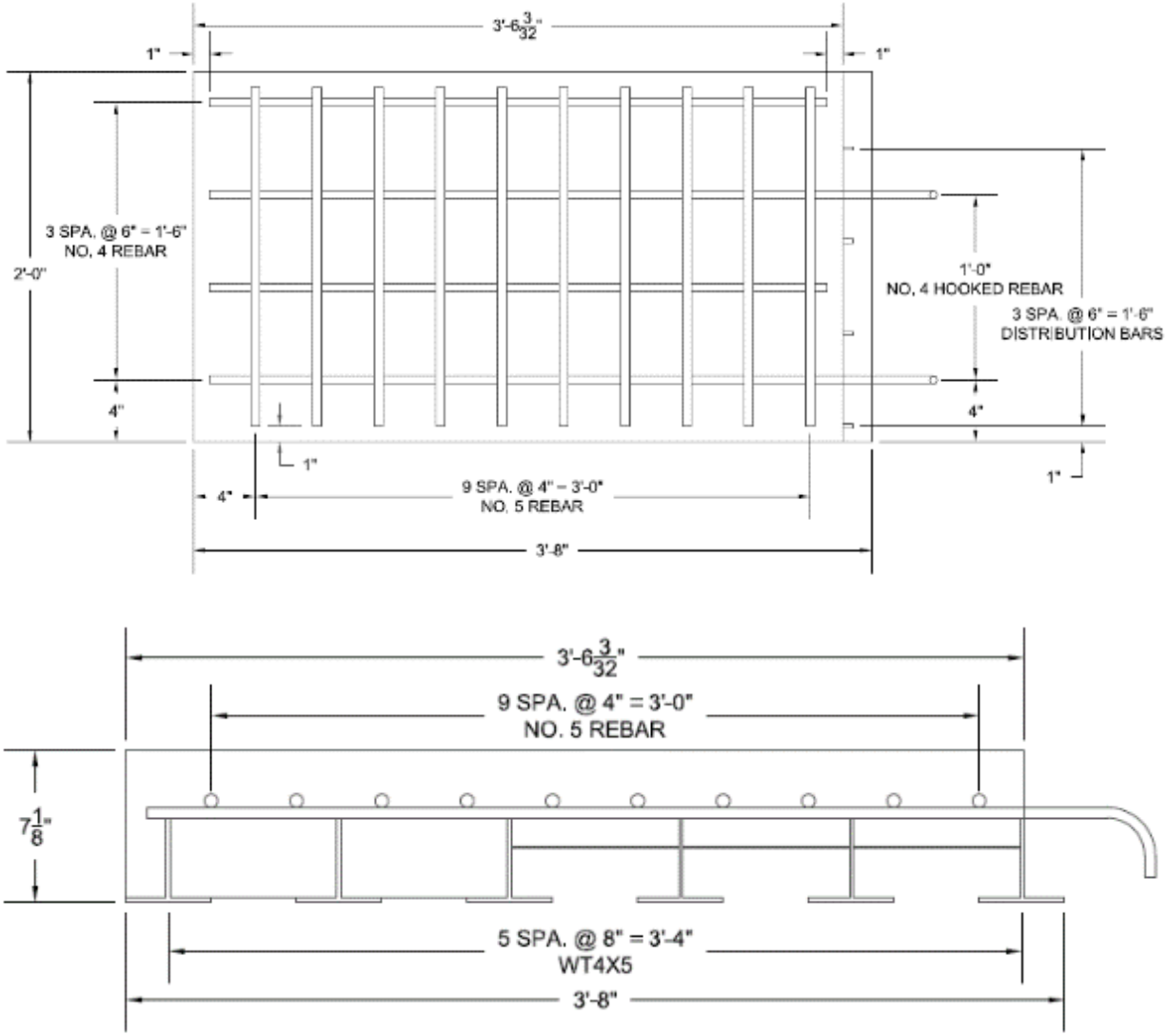


**Figure 4.4: Reinforcing Steel Layout for Staggered Hook Reinforced Panel**

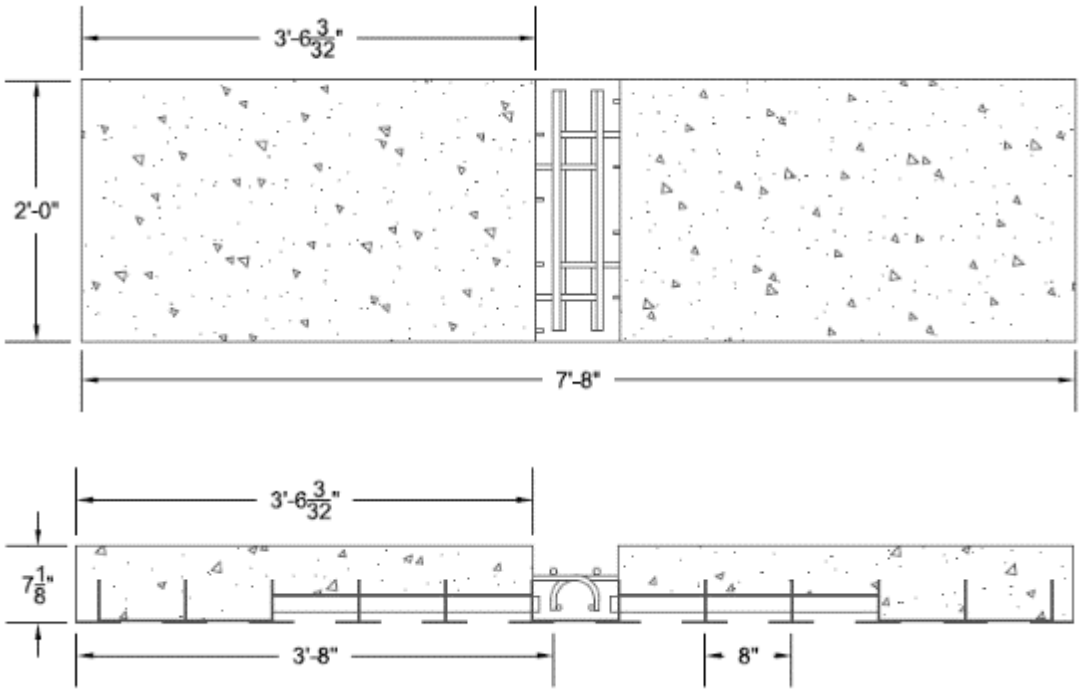


**Figure 4.5: Staggered Hook Reinforced Joined Panels Plan and Elevation**

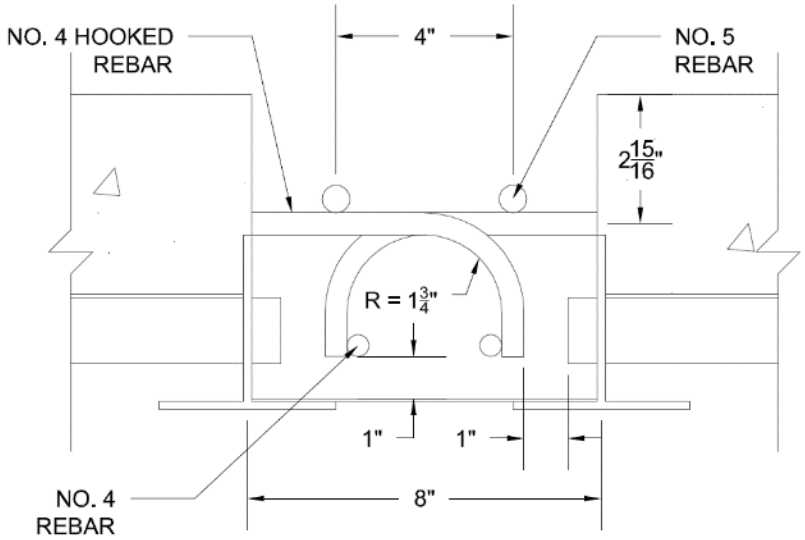


**Figure 4.6: Staggered Hook Reinforced Joint Dimensions**

## 4.3 Exodermic Steel Grids

The D.S. Brown Company donated five Exodermic steel grids with dimensions approximately 8 ft x 14 ft  The steel grids were shipped from North Baltimore, Ohio to Auburn, Alabama on a hot shot trailer as seen in Figure 4.7.


**Figure 4.7:  Shipment of Exodermic Steel Grids**

The grids were exposed to the weather on the D.S. Brown Company property for several years.  Although light surface rusting had developed, the grids were still in adequate shape.  Two of the five grids were designed for the unreinforced shear key joint decks while the other three grids were designed for the staggered hook reinforced joint decks.  Figure 4.8 shows the difference between the steel grids.  The two steel grids designed for the unreinforced shear key joint decks contained an additional attribute, specifically, ½ in. x 2 in. welded studs at 6 in. on center.


**Figure 4.8: Comparison of the Steel Grids**

The steel grids were cut to proper size with a 9-in. handheld circular saw that was designed for machine cutting. Figure 4.9 shows this process.

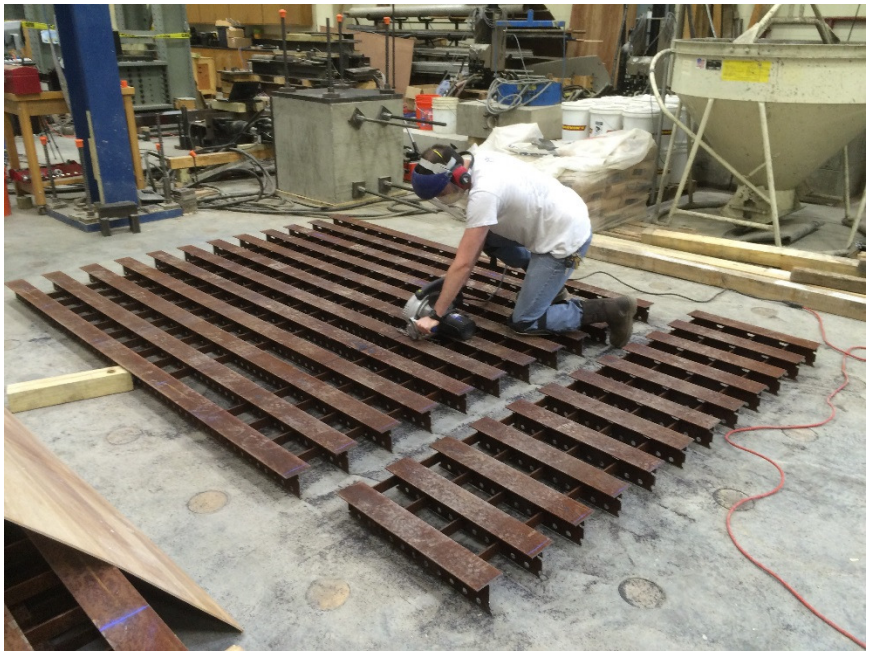

**Figure 4.9: Cutting the Steel Grids**

## 4.4 Deck Concrete

The next step in the construction process was to place the (precast) deck concrete for the test specimens. Along with other tasks this included fabricating the formwork, placing the concrete, and curing the panels.

### 4.4.1 Preliminary Tasks

Before the deck concrete was placed several tasks were completed in preparation. For instance, the slotted holes in the steel grid were taped to prevent concrete from flowing out as shown in Figure 4.10. Also, 16 gage hot-rolled sheets were positioned on the steel grid at their prescribed locations between the WT4x5 members.

A sizable quantity of No. 4 grade 40 reinforcing steel was available in the laboratory. This reinforcement was used as the hooked bars in the test specimens. The remaining No. 4 and No. 5 grade 60 reinforcing steel required was ordered from a local supplier. The bars were cut and bent in the laboratory per the construction drawings. Figure 4.11 shows the reinforcing steel tied on the steel grid.

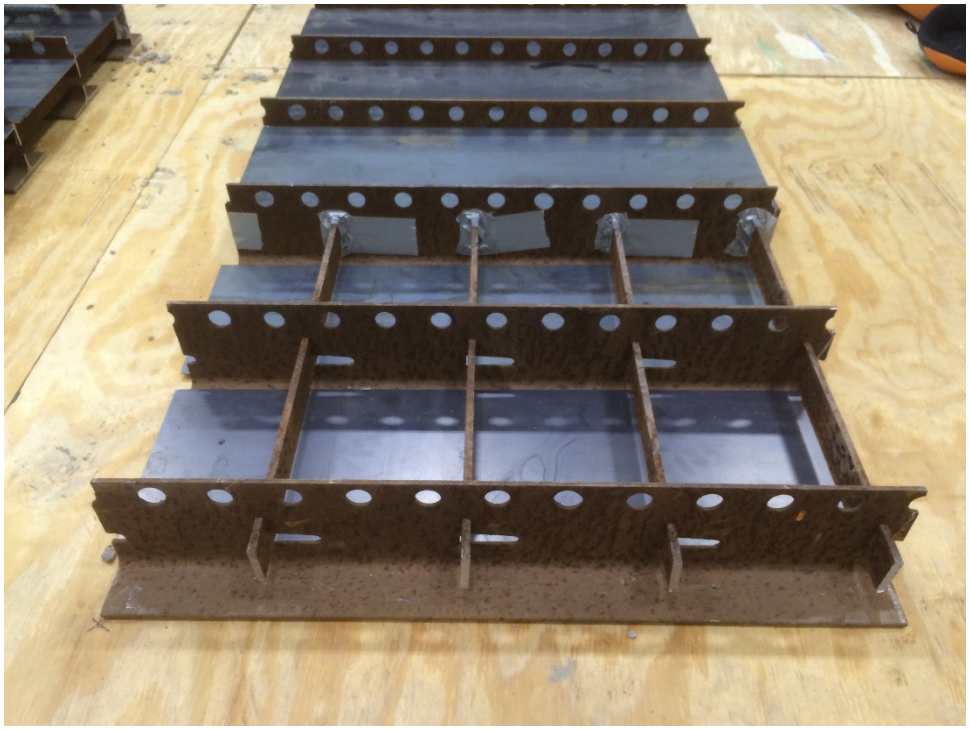

**Figure 4.10: Taping Slotted Holes in Steel Grid**

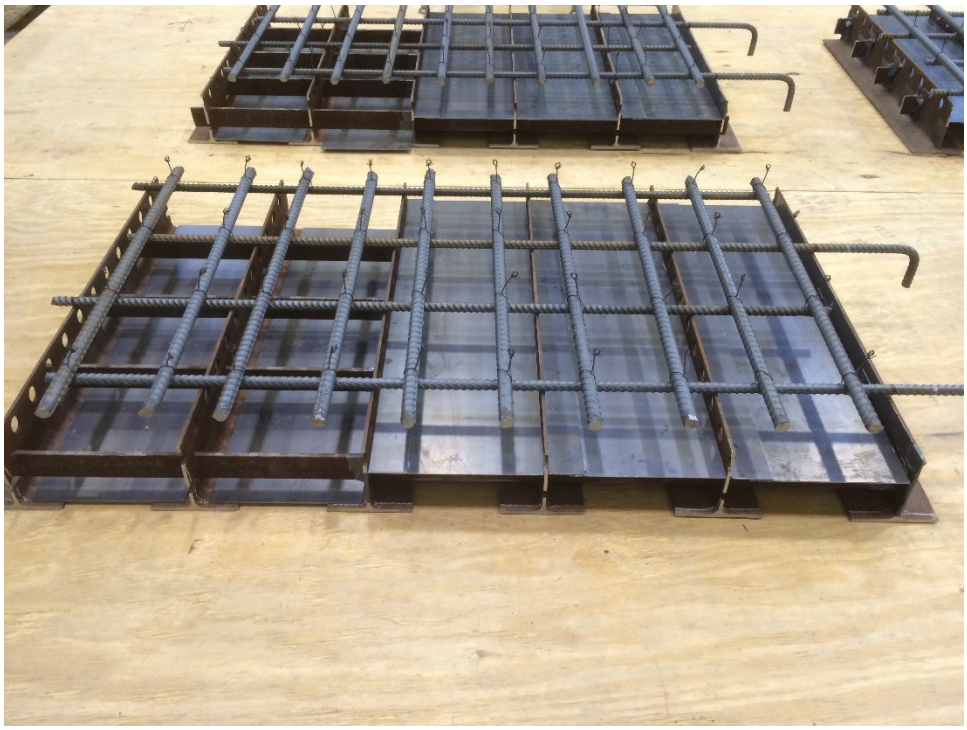

**Figure 4.11: Reinforcement Positioned on Steel Grid**

### 4.4.2 Formwork

A temporary plywood floor was placed in the laboratory to provide a base to attach the panel forms. The forms were constructed out of ½ in. plywood sheets and 2x4 dimensional lumber. The unreinforced shear key joint end caps were constructed out of 2x8 dimensional lumber which were cut to size by a table saw as shown in Figure 4.12. Three coats of spar urethane were applied to the inner sides of the forms. This sealed the wood from absorbing moisture which would dry out the concrete. Once the four sides of the forms were attached to each other and secured to the floor, Type 2 silicone was used to seal the edges to prevent any water or concrete from leaking. This procedure included running a bead of caulk at form-to-form joints, form-to-steel joints, and steel-to-steel joints as shown in Figure 4.13. The forms were sturdy enough so that a person could stand on them during concrete placement. A close-up view of the completed forms can be seen in Figure 4.14.

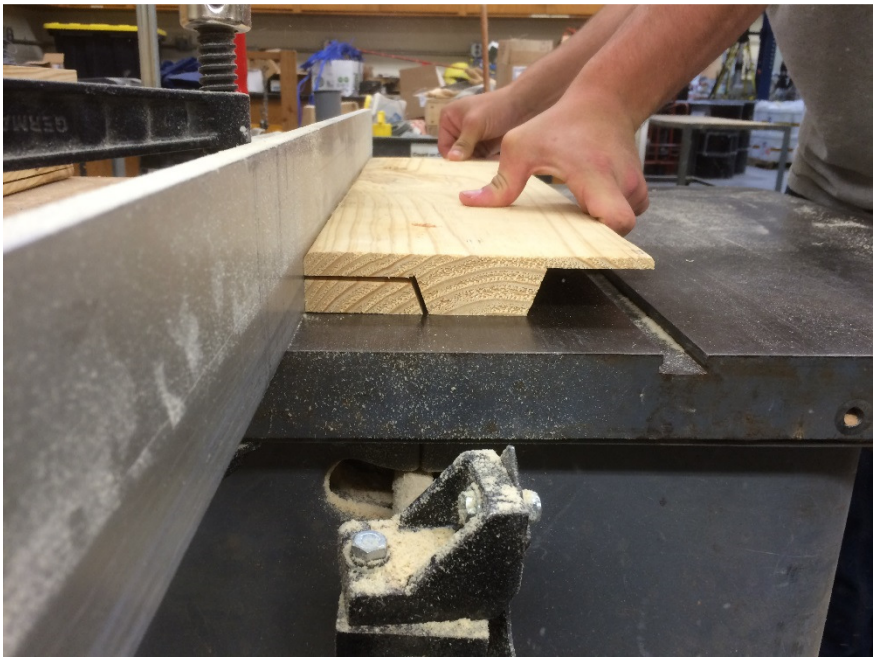

**Figure 4.12: Unreinforced Shear Key Joint End Cap**

**Figure 4.13: Caulking the Forms**

**Figure 4.14: Close-up View of Completed Forms**

### 4.4.3 Placement

Approximately six cubic yards of ready-mixed concrete was ordered from a local supplier. The delivery of the concrete from the truck is shown in Figure 4.15. The mixture design was Class B which is a typical bridge superstructure concrete per the ALDOT Bridge Specification. Table 4.1 shows the deck concrete mixture proportions with aggregate weights reported in the saturated, surface-dry condition.


**Figure 4.15: Delivery of Ready-Mixed Deck Concrete**

**Table 4.1: Deck Concrete Mixture Proportions**

| Item | Supplier | Per CY | Units |
|---|---|---|---|
| Cement I/II | Lehigh | 465.0 | lbs |
| P2 Class Fly Ash | Headwaters-Mi | 158 | lbs |
| 57 Limestone (SSD) | Martin Marietta | 1,912 | lbs |
| Concrete Sand (SSD) | Lambert | 1,213 | lbs |
| Air Entrainer | BASF | 3.83 | lq oz |
| Reduce/Retard | BASF | 19 | lq oz |
| Water | (potable) | 228 | lbs |

The concrete was placed with a 1.5 $yd^3$ hopper and overhead crane as shown in Figure 4.16. Once the proper amount of concrete was placed and spread throughout the forms a handheld mechanical vibrator evenly vibrated the material as seen in Figure 4.17. Then, two people used a damp 2x4 board to screed off the excess concrete in a sawing motion as shown in Figure 4.18. Fourteen students and two professors helped during the concrete placement as seen in Figure 4.19.


**Figure 4.16: Placement of Concrete**


**Figure 4.17: Vibrating the Concrete**


**Figure 4.18: Screeding off the Excess Concrete**


**Figure 4.19: Overview of Concrete Placement**

Sampling of freshly mixed concrete was conducted per ASTM C172 where samples were taken before the second, fourth, and sixth yards were placed. Concrete cylinder test specimens were made per ASTM C31 as seen in Figure 4.20. Slump, unit weight, air content, and temperature measurements were conducted per ASTM C143, C138, C231, and C1064, respectively. Table 4.2 shows the material properties of the fresh deck concrete.


**Figure 4.20: Material Testing of Deck Concrete**

**Table 4.2: Deck Concrete Properties**

| Item | Value | Units |
|---|---|---|
| Slump | 5.25 | in. |
| Unit Weight | 152.9 | pcf |
| Air Content | 2.3 | % |
| Temperature | 83 | °F |

### 4.4.4 Curing Procedure

Wet burlap was placed over the specimens approximately two hours after the final specimen was poured. Plastic sheeting was then placed over the wet burlap to maintain even moisture and temperature while the concrete cured as seen in Figure 4.21.

**Figure 4.21: Wet Burlap and Plastic Sheeting over Panels**

Per Exodermic deck systems construction specifications, the precast panels shall not be removed from the forms or moved until the concrete reached 3,500 psi. This strength was achieved in the cylinder samples at the 7-day mark. Also, per Exodermic deck systems construction specifications, the precast panels were moist cured until the concrete reached its 28-day design strength of 4,000 psi. The plastic sheeting was removed and the burlap was sprayed with water every day to maintain moisture. Concrete cylinder specimens were tested at 14 days which resulted in compressive strengths exceeding 4,000 psi. The plastic sheeting and burlap were permanently removed at that time.

Half of the 6 in. x 12 in. cylinder samples were cured in a moisture room while the other half were cured in the normal lab environment along with the deck panels. The compressive strengths of the deck concrete from moist curing and lab-environment curing are shown in Table 4.3 and Table 4.4, respectively. The tests were conducted in accordance to ASTM C39. Figure 4.22 shows the exposed surfaces of the panels after the formwork was removed.

**Table 4.3: Deck Concrete Compressive Strengths from Moist Curing**

| Day | Compressive Strength (psi) |
|---|---|
| 7 | 3,490 |
| 28 | 4,640 |
| 56 | 5,660 |

**Table 4.4: Deck Concrete Compressive Strengths from Lab-Environment Curing**

| Day | Compressive Strength (psi) |
|---|---|
| 7 | 3,540 |
| 14 | 4,230 |
| 28 | 4,600 |
| 56 | 4,780 |

**Figure 4.22: Unreinforced Shear Key Joint and Staggered Hook Reinforced Joint Panels with Forms Removed**

## 4.5 Joint Grout

The next step in the construction process was to pour the joint grout for the test specimens. Along with other tasks this included fabricating the formwork, placing the grout, and curing the joints.

### 4.5.1 Preliminary Tasks

Before the joint grout was placed several tasks were completed in preparation. For instance, the panels were positioned with their respective mate so that the joint spacing matched the dimensions in the construction drawings. Figure 4.23 shows an aerial view of the panels and Figure 4.24 shows a close-up on the unreinforced shear key and staggered hook reinforced joint.

**Figure 4.23: Overview of Panels before Grout Pour**

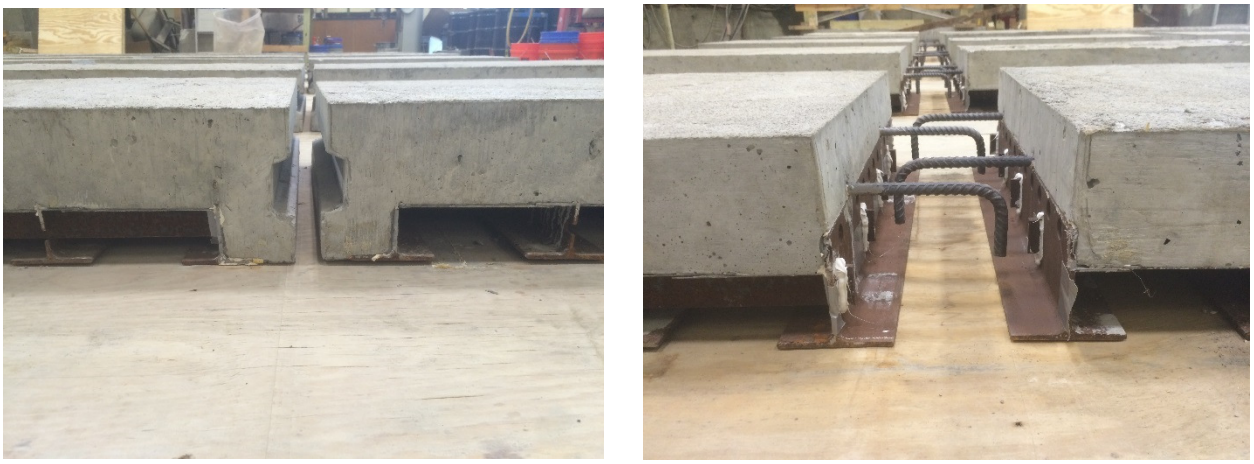

**Figure 4.24: Close-up View of Panels before Grout Pour**

To determine the behavior of the reinforcing steel when tested, 6 mm electronic resistance strain gages were installed. A close-up view of the gage is shown in Figure 4.25. The first step in attaching the strain gages was to grind the ribs of the reinforcing steel with a mechanical grinder.

Next, gages were bonded to the steel by following the cleaning and adhesion steps per the manufacturer. Mastic tape was placed between the lead wires and bar to prevent a shorting of the circuit. Then, yellow nitrile rubber was applied to the gage to provide protection. Finally, heat shrink tubing surrounded the gage to protect from moisture.

A sample of reinforcing steel was instrumented with strain gages and tested in tension to determine the material properties. The reinforcing steel was designated as grade 40; however, previous tensile testing of sample bars indicated a yield stress of 50 ksi, as shown in Figure 4.26.

The strain gages were attached to the hooked reinforcing bars at approximately ½ in. from the surface of the precast concrete where they extended out of the deck panels as shown in Figure 4.27. Then, No. 4 bars were tied on the bottom of each hook and No. 5 bars were tied on top of each hook in accordance with the construction drawings.

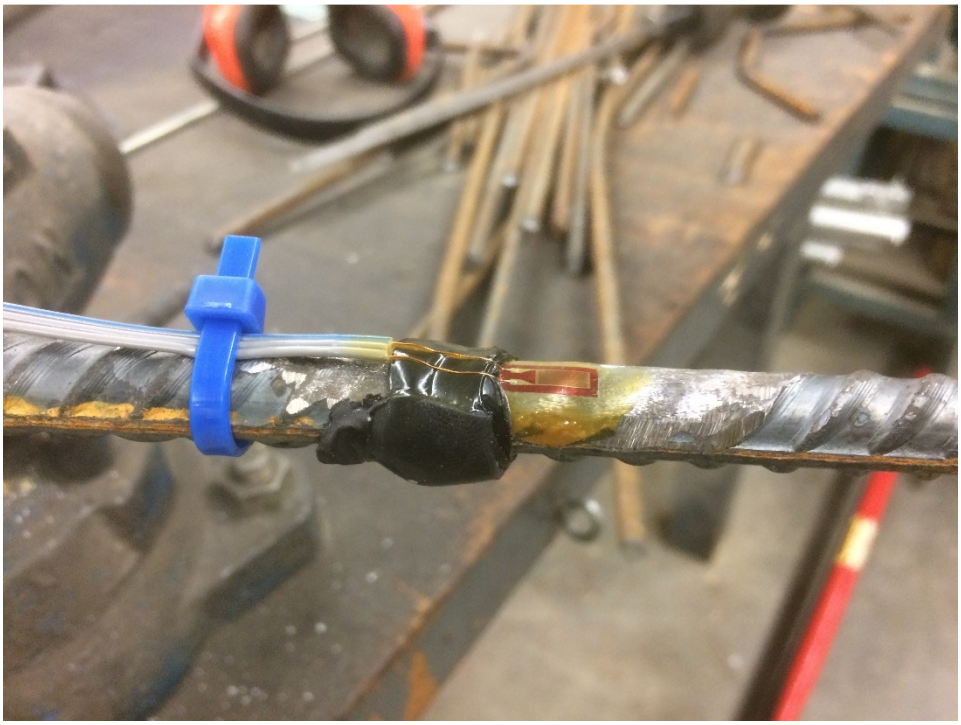

**Figure 4.25: Strain Gage**

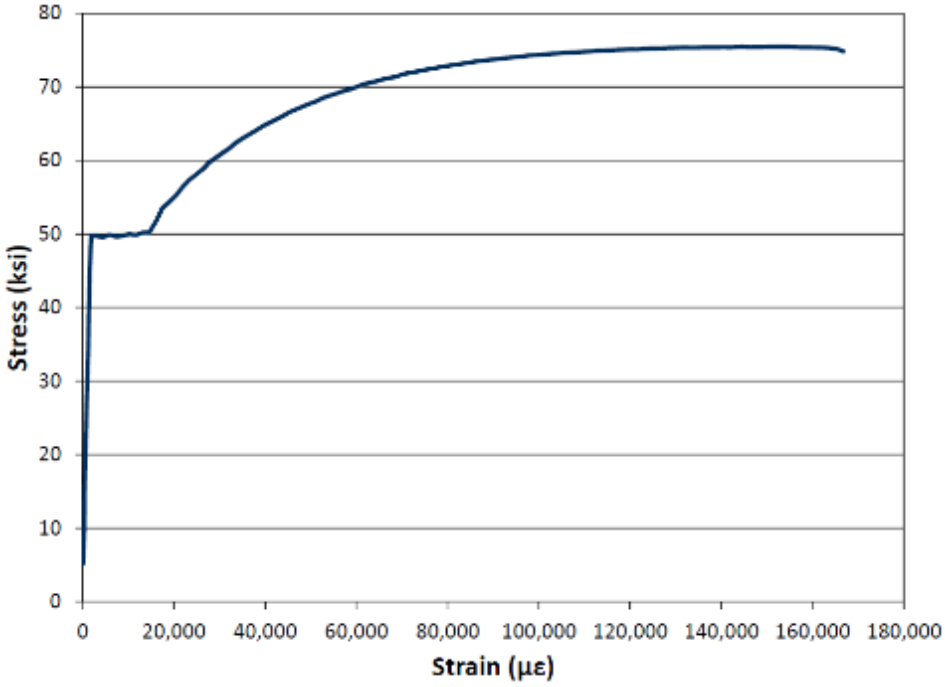


**Figure 4.26: Stress-Strain Relationship for Steel Reinforcement**

**Figure 4.27: Attached Strain Gages to Hooked Reinforcing Steel**

### 4.5.2 Formwork

Next, 1 ½ in. diameter open-cell foam backer rods were placed on the bottom of each unreinforced shear key joint to serve as the bottom of the joint. Similarly, 16 gage hot-rolled sheets were placed at the bottom of each staggered hook reinforced joint.

The forms for the unreinforced shear key joint and staggered hook reinforced joint were recycled from the panel forms. Figure 4.28 shows the joint formwork set-up.

**Figure 4.28: Joint Formwork**

### 4.5.3 Placement

The grout material for joining the precast specimens required specific strength standards. MasterEmaco T 1060 Very Rapid Setting Mortar fulfilled these requirements. Mixing of the grout was conducted with a handheld electric drill and paddle mixing bit in a tin tub. Each joint was

mixed and poured individually due to the short setting time of the grout. A mechanical vibrator consolidated the material in the joint to avoid air pockets. These steps are shown in Figure 4.29.

To increase the volume of the material, coarse aggregate was permitted to extend the grout. Pea Gravel with maximum diameter of 3/8 in. was selected. The grout manufacturer stated that for applications with a thickness of 2-4 in. the grout may be extended 30-50%. Applications with a thickness greater than 4 in. may be extended 50-100%. The unreinforced shear key joint was extended 30% while the staggered hook reinforced joint was extended 100%.

Also, six 3 in. x 6 in. cylinders were cast for each joint to test the ASTM 28-day compressive strength as well as the compressive strength at the time the panel was tested. The 28-day cylinders were moist cured while the test-day cylinders were cured in the lab environment. Table 4.5 and 4.6 summarize the unreinforced shear key joint and staggered hook reinforced joint compressive strength results, respectively. The compressive strength of the grout used for the unreinforced shear key joint was considerably larger than that used for the staggered hook reinforced joint. This may be due to the different amounts of pea gravel added to each mixture. The difference in compressive strengths likely did not greatly affect the results of the jointed specimens in the positive bending, negative bending, and shear reversal tests since critical cracks formed within the precast concrete or at the joint-deck interface and not within the joint grout.

Due to oversight, “Test-Day” cylinder samples were not cast for the following joints: U-NEG-B, U-REV-B, and R-REV-B. This omission did not negatively affect the research project since the cylinder samples only represented the “backup” specimens that were not tested.


**Figure 4.29: Mixing and Vibrating the Grout**

**Table 4.5: Grout Compressive Strength for Unreinforced Shear Key Joints**

| | 28-Day Compressive Strength (psi) | Test-Day Compressive Strength (psi) |
|---|---|---|
| U-POS-Q | 7,860 | 9,620 |
| U-POS-F | 3,160 | 4,020 |
| U-POS-B | 7,910 | 10,740 |
| U-NEG-Q | 5,690 | 10,090 |
| U-NEG-F | 4,450 | 5,430 |
| U-NEG-B | 8,970 | - |
| U-REV-Q | 8,490 | 10,150 |
| U-REV-F | 8,340 | 10,330 |
| U-REV-B | 8,960 | - |

**Table 4.6: Grout Compressive Strength for Staggered Hook Reinforced Joints**

| | 28-Day Compressive Strength (psi) | Test-Day Compressive Strength (psi) |
|---|---|---|
| R-POS-Q | 4,880 | 7,080 |
| R-POS-F | 4,070 | 6,180 |
| R-POS-B | 3,880 | 5,500 |
| R-NEG-Q | 4,500 | 5,680 |
| R-NEG-F | 3,890 | 5,500 |
| R-NEG-B | 3,370 | 4,990 |
| R-REV-Q | 4,400 | 5,950 |
| R-REV-F | 4,690 | 6,190 |
| R-REV-B | 5,440 | - |

### 4.5.4 Curing Procedure

Wet burlap was placed over the specimens as soon as the grout was poured. On average the grout achieved 3,500 psi compressive strength within 2 hours. The wet burlap was removed after 24 hours. After 7 days, the forms were removed. Figure 4.30 shows the joints after the forms were removed.

**Figure 4.30: Unreinforced Shear Key and Staggered Hook Reinforced Joints**

# CHAPTER 5: RESULTS AND DISCUSSION

## 5.1 Overview

This chapter covers the test results from the twelve specimens tested. First, the quasi-static test results are presented which include the unreinforced shear key joint and staggered hook reinforced joint in positive bending, negative bending, and shear reversal. Next, the fatigue test results are presented which also include the unreinforced shear key joint and staggered hook reinforced joint in positive bending, negative bending, and shear reversal. For each test the results are presented in the form of visual inspection, external instrumentation, and internal instrumentation. Finally, comparisons and discussions of the tests will conclude the chapter.

## 5.2 Quasi-Static Tests

This section covers the quasi-static test results for both the unreinforced shear key and staggered hook reinforced joints. This section is separated into three main subsections: positive bending, negative bending, and shear reversal test results.

### 5.2.1 Positive Bending Test Results

This first subsection covers quasi-static positive bending results for the unreinforced shear key joint (U-POS-Q) and staggered hook reinforced joint (R-POS-Q) specimens.

#### 5.2.1.1 Unreinforced Shear Key Joint (U-POS-Q)

The U-POS-Q test was conducted per the prescribed loading procedure. For each load step the applied load was cycled five times up to the calculated value and down to the minimum value. If the specimen did not fail at the current load step, then the load was increased to the next load step and the test continued.

##### 5.2.1.1.1 Visual Inspection

The condition of the joint before versus after the test is shown in Figure 5.1. Crack propagation was documented by marking and labeling the cracks after each load step. The labels corresponded to the force applied by the actuator onto the specimen. Cracks formed north and south of the joint within the deck concrete. During the first load step (1.44 kips), cracks originated at the top of the steel WT section. During the second load step (2.86 kips), the cracks extended and widened. During the third load step (4.30 kips), additional cracks formed. Finally, during the fourth load step (5.72 kips), the specimen failed along the bottom of the steel WT section on the south side.


**Figure 5.1: U-POS-Q Joint Before and After**

#### 5.2.1.1.2 External Instrumentation

As discussed earlier, external instrumentation consisted of wirepots attached to the top of the specimen to measure midspan deflection, wirepots attached to the bottom of the joint to measure large midspan deflection, and wirepots attached to the side of the specimen to measure crack opening at the joint-panel interface.

Figure 5.2 shows the behavior of the moment at joint versus midspan deflection. Note at each load step as the moment at the joint increased, more cracks formed in the specimen and the midspan deflection increased. The bottom wirepots were utilized to capture the specimen behavior after the top wirepots exceeded their stroke limit.

Figure 5.3 shows the behavior of the side crack opening versus moment at joint. Similarly, as noted above, at each load step as the moment at the joint increased, the side cracks opened wider.

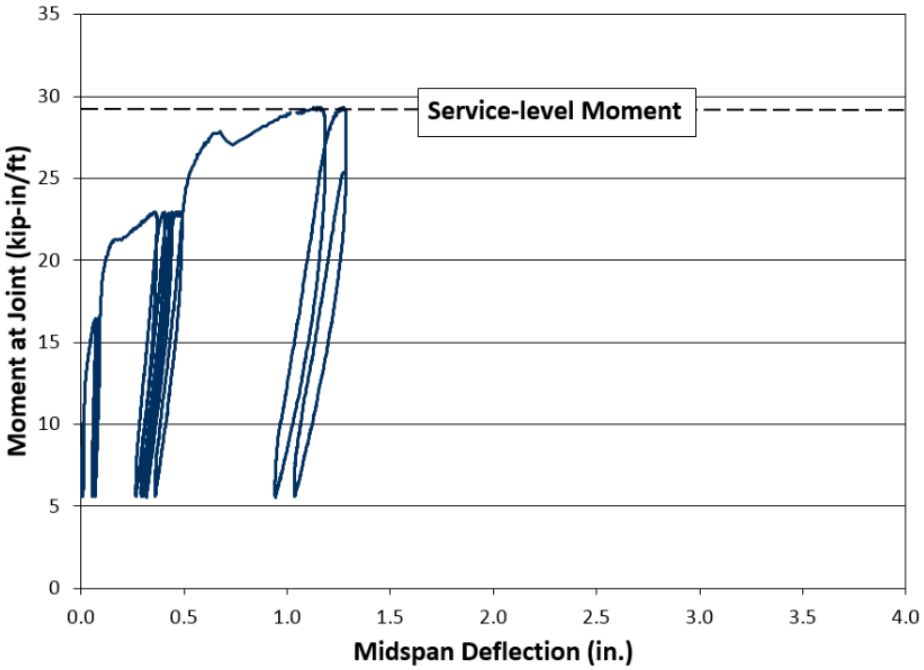


**Figure 5.2: Moment at Joint versus Midspan Deflection (U-POS-Q)**

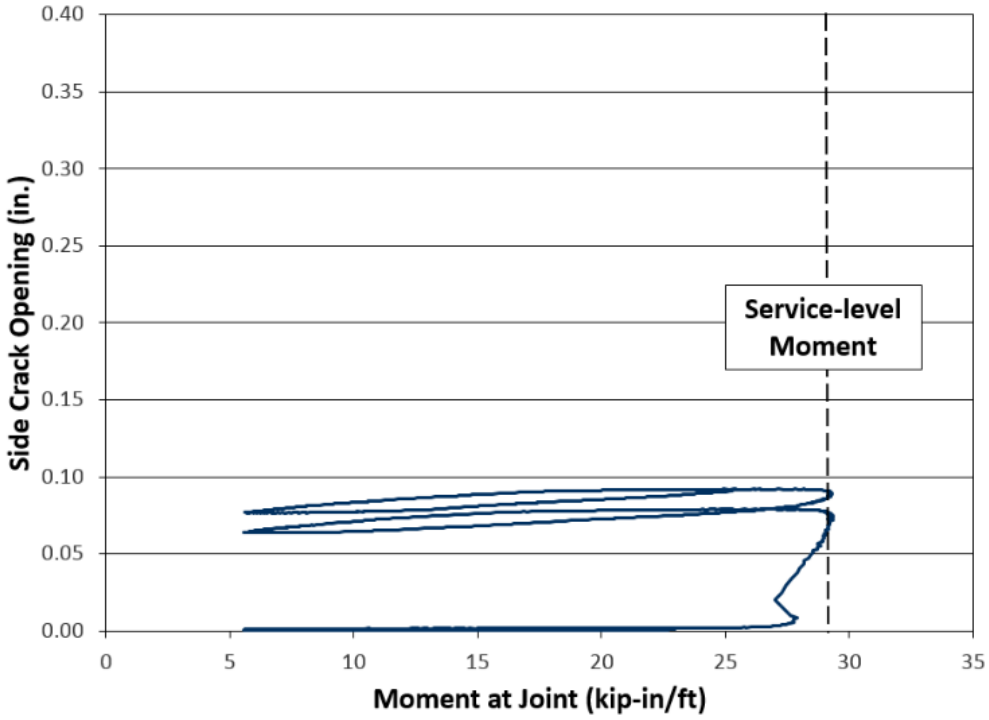


**Figure 5.3: Side Crack Opening versus Moment at Joint (U-POS-Q)**

#### 5.2.1.2 Staggered Hook Reinforced Joint (R-POS-Q)

The R-POS-Q test was conducted per the prescribed loading procedure. For each load step the applied load was cycled five times up to the calculated value and down to the minimum value. If the specimen did not fail at the current load step, then the load was increased to the next load step and the test continued.

##### 5.2.1.2.1 Visual Inspection

The condition of the joint before versus after the test is shown in Figure 5.4. Crack propagation was documented by marking and labeling the cracks after each load step. The labels corresponded to the force applied by the actuator onto the specimen. During the first load step (1.44 kips) and the second load step (2.86 kips) no noticeable cracks occurred. When loading up to the third load step (4.30 kips), cracks formed at the south joint interface. When loading up to the fourth load

step (5.72 kips), the cracks extended and widened. Finally, when loading up to the fifth load step (7.16 kips), the specimen failed.


**Figure 5.4: R-POS-Q Joint Before and After**

#### 5.2.1.2.2 External Instrumentation

As discussed earlier, external instrumentation consisted of wirepots attached to the top of the specimen to measure midspan deflection, wirepots attached to the bottom of the specimen to measure large midspan deflection, and wirepots attached to the side of the specimen to measure crack opening at the joint-panel interface.

Figure 5.5 shows the behavior of the moment at joint versus midspan deflection. Note at each load step as the moment at the joint increased, more cracks formed in the specimen and the midspan deflection increased.

Figure 5.6 shows the behavior of the side crack opening versus moment at joint. Similarly, as noted above, at each load step as the moment at the joint increased, the side cracks opened wider.

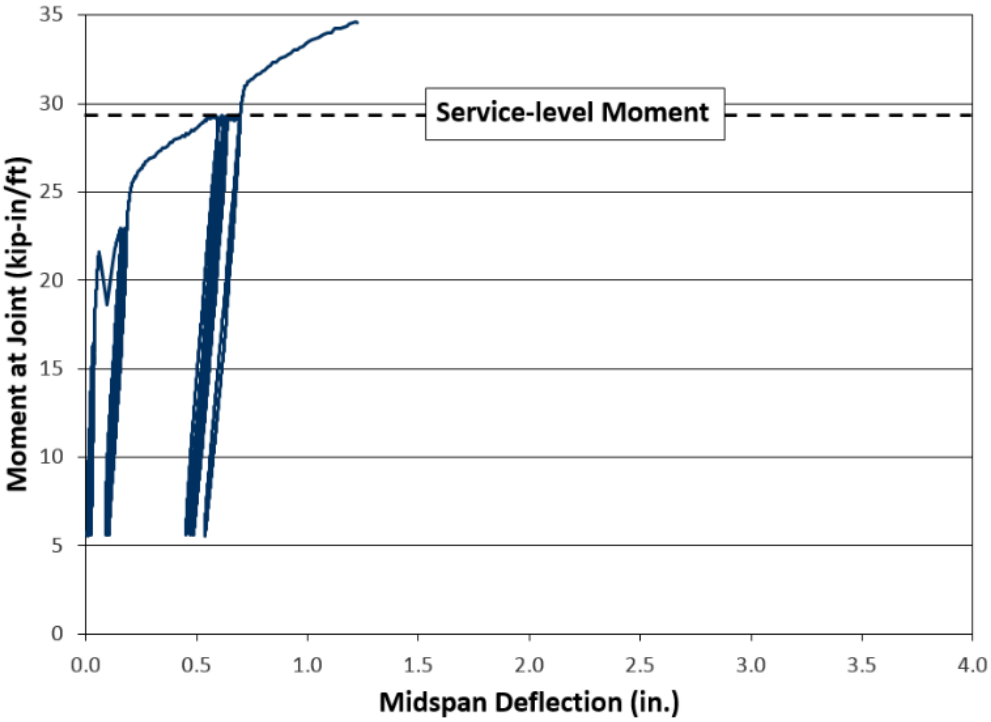


**Figure 5.5: Moment at Joint versus Midspan Deflection (R-POS-Q)**

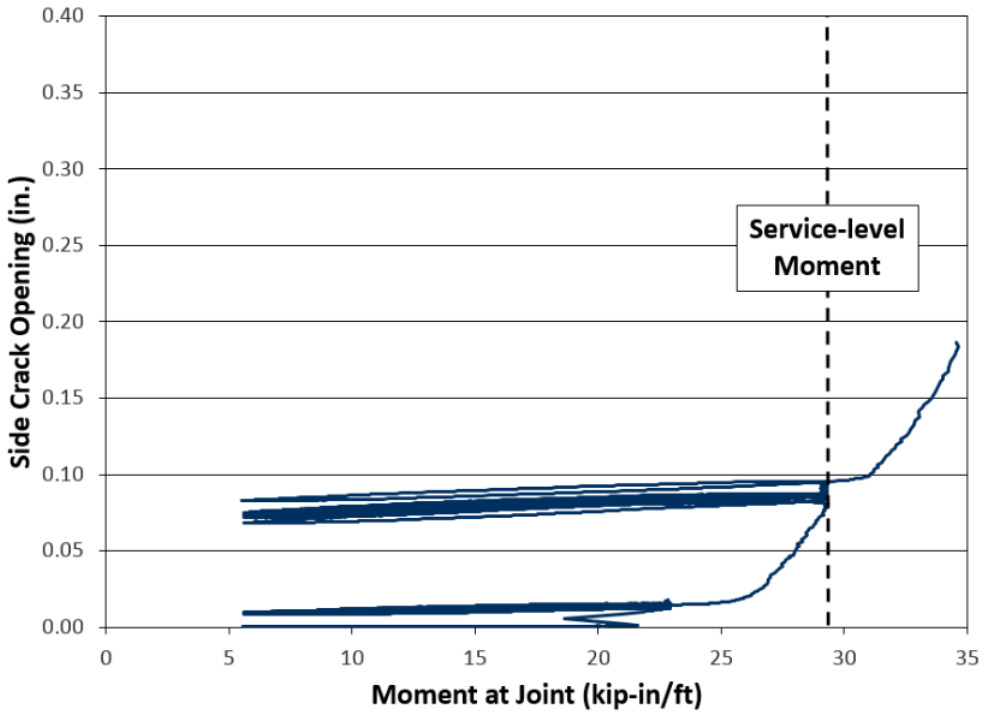


**Figure 5.6: Side Crack Opening versus Moment at Joint (R-POS-Q)**

#### 5.2.1.2.3 Internal Instrumentation

As discussed earlier, internal instrumentation consisted of strain gages attached to each of the four hooked reinforcing bars within the joint.

Figure 5.7 shows the behavior of the strain in reinforcing steel versus moment at joint. At each load step as the moment at the joint increases, more cracks form in the specimen and the strain in the reinforcement increases. Note that the SE and SW strain gages increased significantly between the third and fourth load step compared to the NE and NW strain gages. This shows that the south reinforcing steel yielded at 25.7 kip-in/ft. The strain gages reached their limit at approximately 19,000 με.

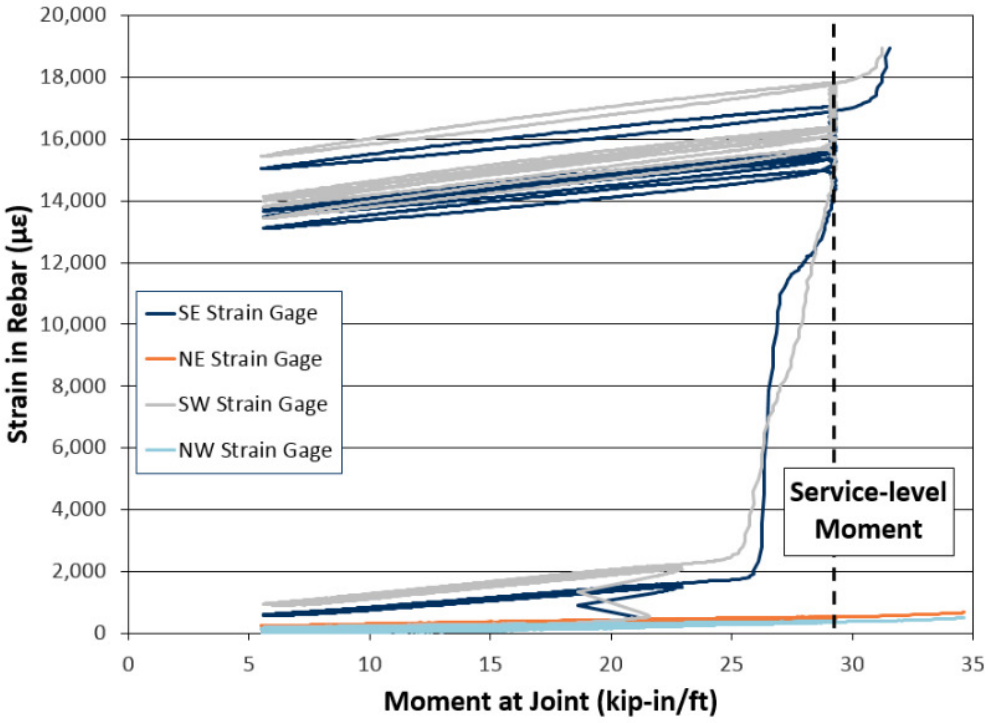


**Figure 5.7: Strain in Reinforcing Steel versus Moment at Joint (R-POS-Q)**

### 5.2.2 Negative Bending Test Results

This second subsection covers quasi-static negative bending results for the unreinforced shear key joint (U-NEG-Q) and staggered hook reinforced joint (R-NEG-Q) specimens.

#### 5.2.2.1 Unreinforced Shear Key Joint (U-NEG-Q)

The U-NEG-Q test was conducted per the prescribed loading procedure. For each load step the applied load was cycled five times up to the calculated value and down to the minimum value. If the specimen did not fail at the current load step, then the load was increased to the next load step and the test continued.

##### 5.2.2.1.1 Visual Inspection

The condition of the joint before versus after the test is shown in Figure 5.8. Crack propagation was documented by marking and labeling the cracks after each load step. The labels corresponded to the force applied by the actuator onto the specimen. During the first load step (1.44 kips) and second load step (2.86 kips) there were no noticeable cracks. When loading up to the third load step (4.30 kips), the specimen failed along the south joint interface.

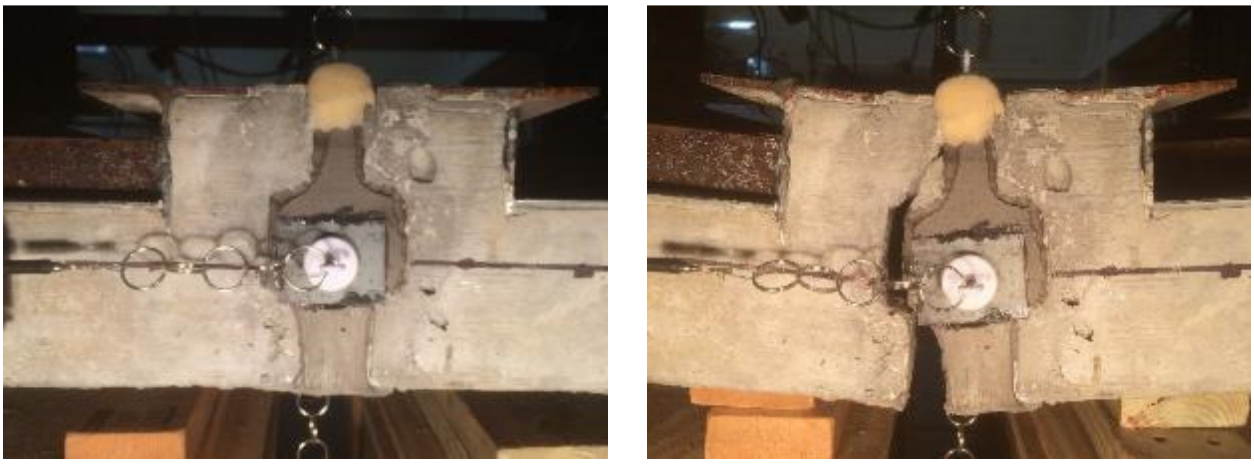

**Figure 5.8: U-NEG-Q Joint Before and After**

#### 5.2.2.1.2 External Instrumentation

As discussed earlier, external instrumentation consisted of wirepots attached to the top of the specimen to measure midspan deflection, wirepots attached to the bottom of the specimen to measure large midspan deflection, and wirepots attached to the side of the specimen to measure crack opening at the joint-panel interface.

Figure 5.9 shows the behavior of the moment at joint versus midspan deflection. Since the specimen failed suddenly along the south joint interface, the load steps are not visible in the graph. Therefore, only a single line depicted the failure occurring. There was not a significant amount of midspan deflection before the specimen failed.

Figure 5.10 shows the behavior of the side crack opening versus moment at joint. Similarly, as noted above, there was not any sign of side crack opening before the specimen failed.

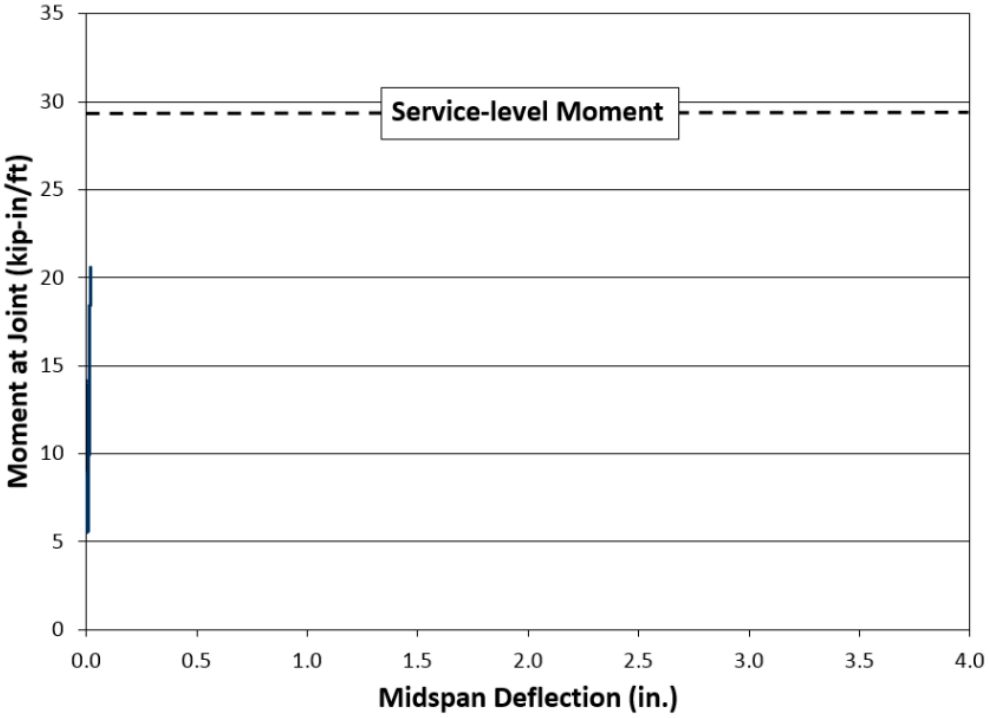


**Figure 5.9: Moment at Joint versus Midspan Deflection (U-NEG-Q)**

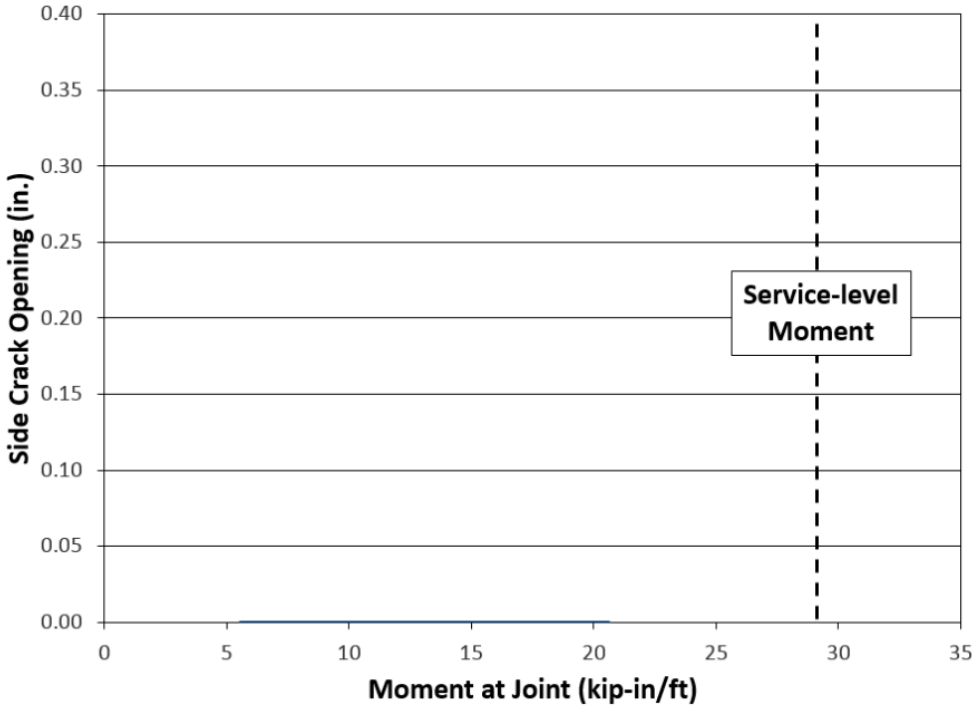


**Figure 5.10: Side Crack Opening versus Moment at Joint (U-NEG-Q)**

#### 5.2.2.2 Staggered Hook Reinforced Joint (R-NEG-Q)

The R-NEG-Q test was conducted per the prescribed loading procedure. For each load step the applied load was cycled five times up to the calculated value and down to the minimum value. If the specimen did not fail at the current load step, then the load was increased to the next load step and the test continued.

##### 5.2.2.2.1 Visual Inspection

The condition of the joint before versus after the test is shown in Figure 5.11. Crack propagation was documented by marking and labeling the cracks after each load step. The labels corresponded to the force applied by the actuator onto the specimen. At the first load step (1.44 (kips), there were no noticeable cracks. When loading up to the second load step (2.86 kips), cracks formed and extended up to the reinforcing steel height at the south joint interface. When loading up to the

third load step (4.30 kips), cracks extended on the south joint interface up to the steel pan, and cracks formed at the north joint interface. When loading up to the fourth load step (5.72 kips), the cracks widened at both the north and south joint interfaces. Finally, when loading up to the fifth load step (7.16 kips), the specimen failed.

It was determined that the distribution bars were part of the load path of the specimen. These bars resisted compressive stresses and ultimately failed by buckling as shown in Figure 5.12.

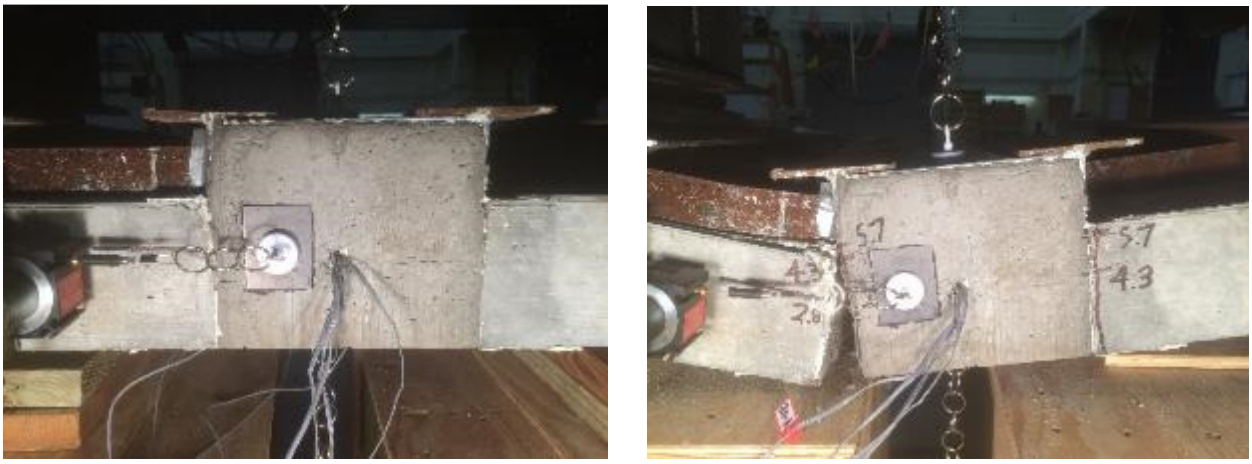


**Figure 5.11: R-NEG-Q Joint Before and After**

**Figure 5.12: R-NEG-Q Buckled Distribution Bars**

#### 5.2.2.2.2 External Instrumentation

As discussed earlier, external instrumentation consisted of wirepots attached to the top of the specimen to measure midspan deflection, wirepots attached to the bottom of the specimen to measure large midspan deflection, wirepots attached to the side of the specimen to measure crack opening at the joint-panel interface, and crack gages attached below the reinforcing steel locations to measure the crack opening at the joint interface. The bottom wirepots were utilized to capture the specimen behavior after the top wirepots exceeded their stroke limit.

Figure 5.13 shows the behavior of the moment at joint versus midspan deflection. Note at each load step as the moment at the joint increased, more cracks formed in the specimen and the midspan deflection increased. The bottom wirepots were utilized to capture the specimen behavior after the top wirepots exceeded their stroke limit.

Figure 5.14 shows the behavior of the side crack opening versus moment at joint. Similarly, as noted above, at each load step as the moment at the joint increased, the side cracks opened wider.

Figure 5.15 shows the behavior of crack gage opening versus moment at joint. Note that the SE and SW crack gages increased significantly during the third load step compared to the NE and NW crack gages. This shows the larger crack opening along the south joint interface compared to the north joint interface. The crack gages were removed after the third load step to avoid any potential damage to the gages.

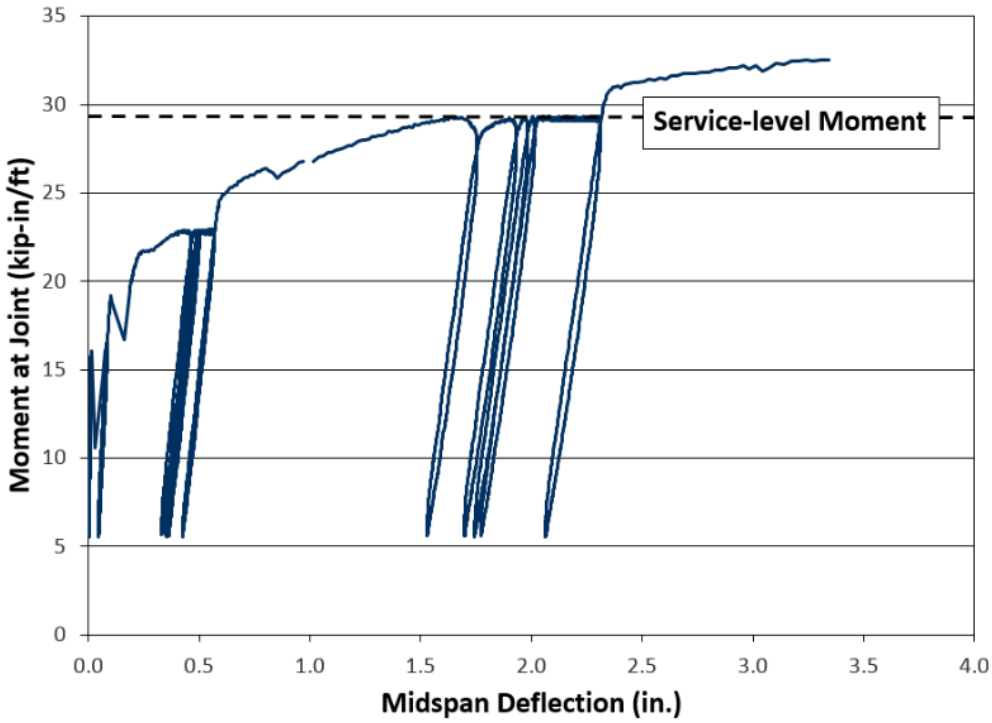


**Figure 5.13: Moment at Joint versus Midspan Deflection (R-NEG-Q)**

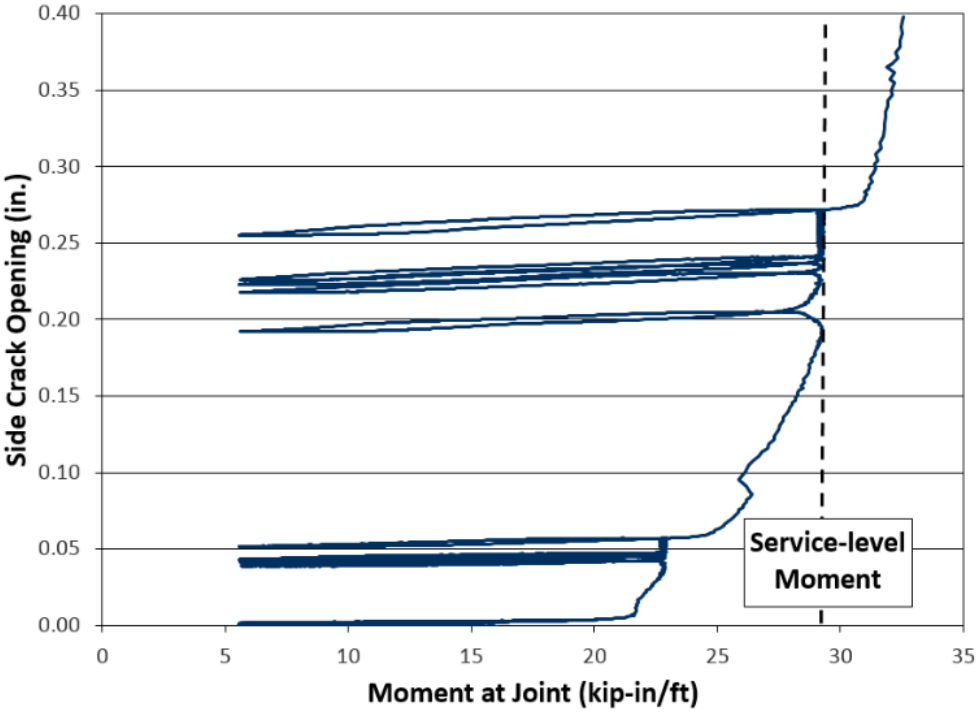


**Figure 5.14: Side Crack Opening versus Moment at Joint (R-NEG-Q)**

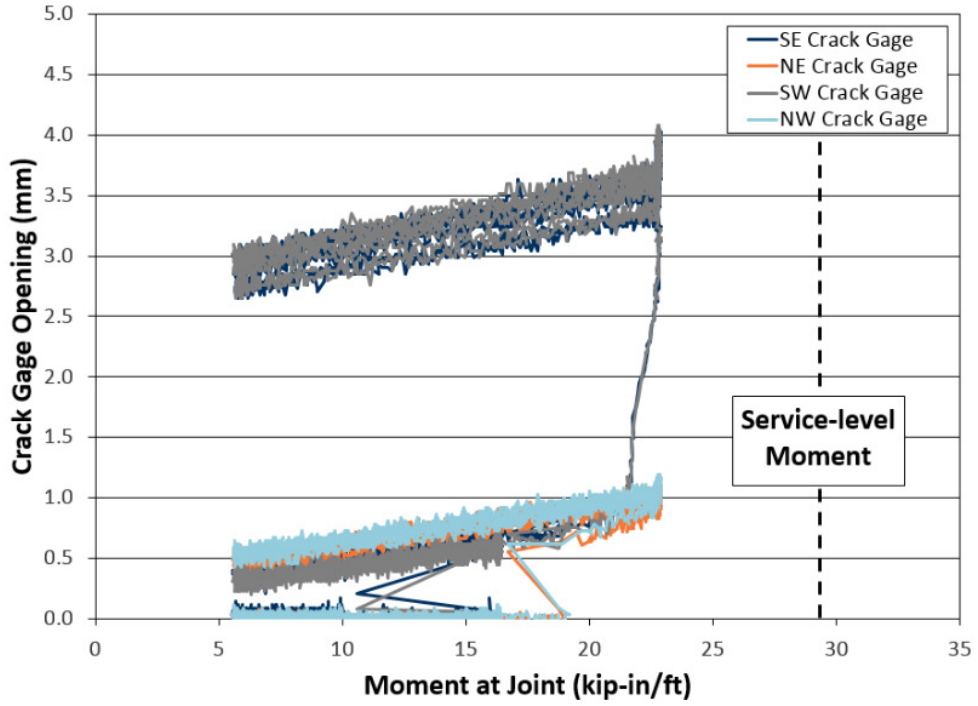


**Figure 5.15: Crack Gage Opening versus Moment at Joint (R-NEG-Q)**

#### 5.2.2.2.3 Internal Instrumentation

As discussed earlier, internal instrumentation consisted of strain gages attached to each of the four hooked reinforcing bars within the joint.

Figure 5.16 shows the behavior of the strain in reinforcing steel versus moment at joint. At each load step as the moment at the joint increased, more cracks formed in the specimen and the strain in the reinforcing steel increased. Note that when loading up to the third load step (23.0 kip-in/ft) a crack formed at the south joint interface and the SE and SW bars yielded resulting in a significant increase in the strain. The NE bar yielded later when the crack at the north joint interface widened when loading up to the fourth load step (29.2 kip-in/ft). The strain gages reached their limit at approximately 19,000 με.

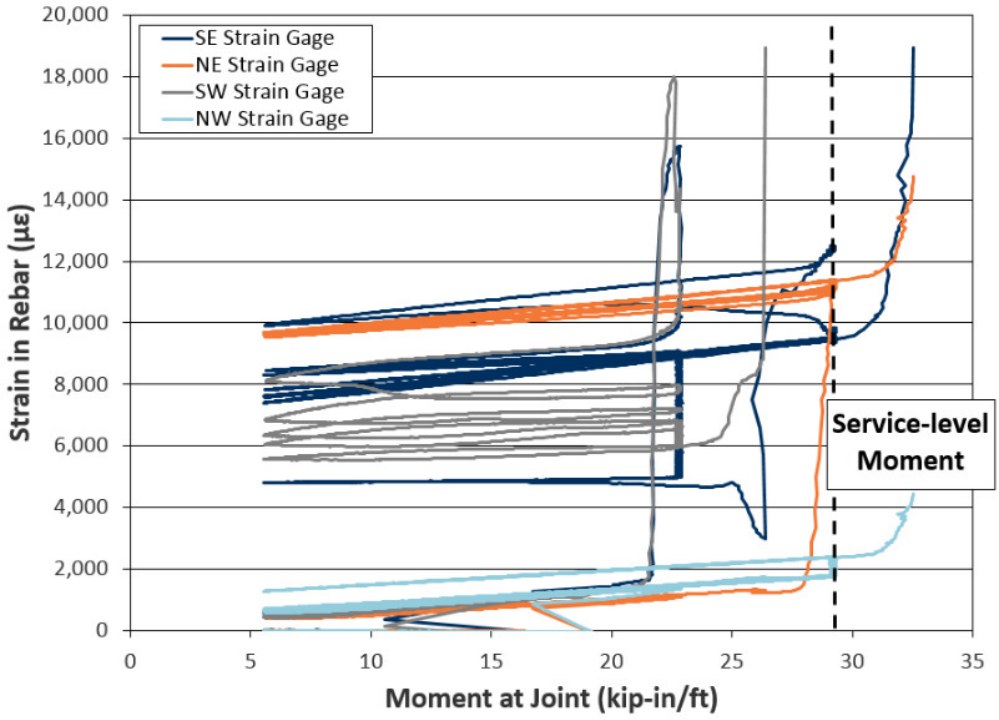


**Figure 5.16: Strain in Reinforcing Steel versus Moment at Joint (R-NEG-Q)**

### 5.2.3 Shear Reversal Test Results

This third subsection covers quasi-static shear reversal results for the unreinforced shear key joint (U-REV-Q) and staggered hook reinforced joint (R-REV-Q) specimens.

#### 5.2.3.1 Unreinforced Shear Key Joint (U-REV-Q)

The U-REV-Q test was conducted per the prescribed loading procedure. For each load step the applied load was cycled five times up to the calculated value and down to the minimum value. If the specimen did not fail at the current load step, then the load was increased to the next load step and the test continued.

##### 5.2.3.1.1 Visual Inspection

The condition of the joint before versus after the test is shown in Figure 5.17. Crack propagation was documented by marking and labeling the cracks after each load step. The labels corresponded to the force applied by one of the actuators onto the specimen. At the first load step (1.32 kips) and second load step (2.15 kips) no noticeable cracks formed. After the third load step (3.80 kips), cracks formed within the deck concrete on the north and south side of the joint originating at the top of the WT steel sections. After the fourth load step (4.62 kips), the cracks extended. During the fifth load step (5.45 kips), several more cracks formed within the deck concrete reaching up to the top surface of the specimen. Finally, during the sixth load step (6.27 kips), the specimen failed.


**Figure 5.17: U-REV-Q Joint Before and After**

#### 5.2.3.1.2 External Instrumentation

As discussed earlier, external instrumentation consisted of wirepots attached to the top of the specimen to measure midspan deflection, wirepots attached to the bottom of the specimen to measure large midspan deflection, and wirepots attached to the side of the specimen to measure crack opening at the joint-panel interface.

Figure 5.18 shows the behavior of the shear at joint versus midspan deflection. Note at each load step as the shear at the joint increased, more cracks formed in the specimen and the midspan deflection increased. The bottom wirepots were utilized to capture the specimen behavior after the top wirepots exceeded their stroke limit.

Figure 5.19 shows the behavior of the side crack opening versus shear at joint. Similarly, as noted above, at each load step as the shear at the joint increased, the side cracks opened wider. The graph depicts the behavior of the south as well as the north joint interfaces.

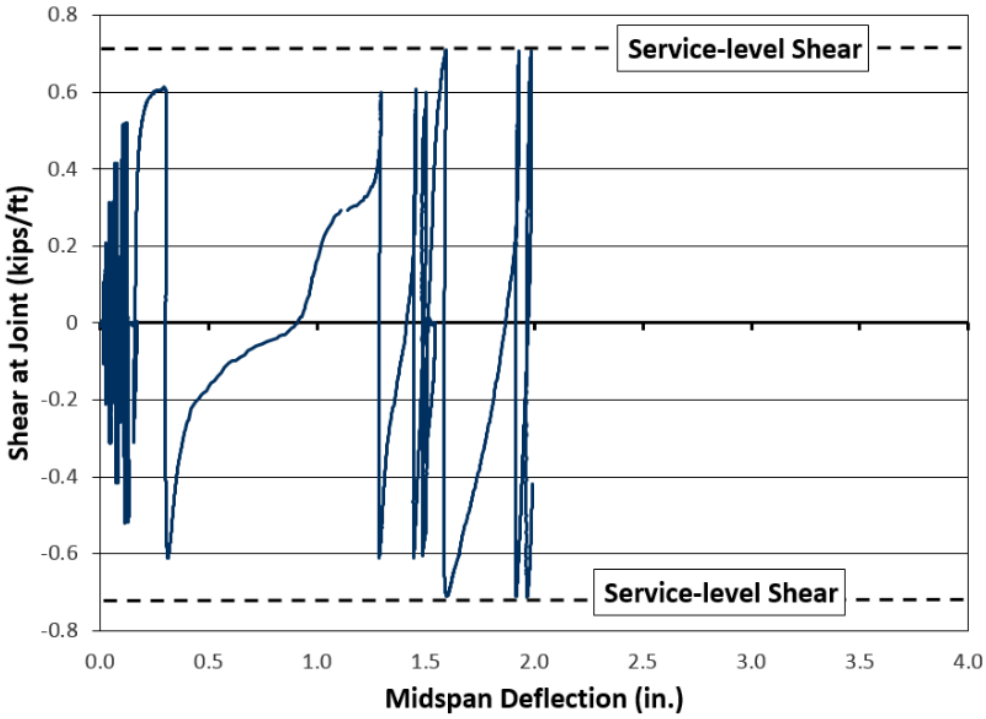


**Figure 5.18: Shear at Joint versus Midspan Deflection (U-REV-Q)**

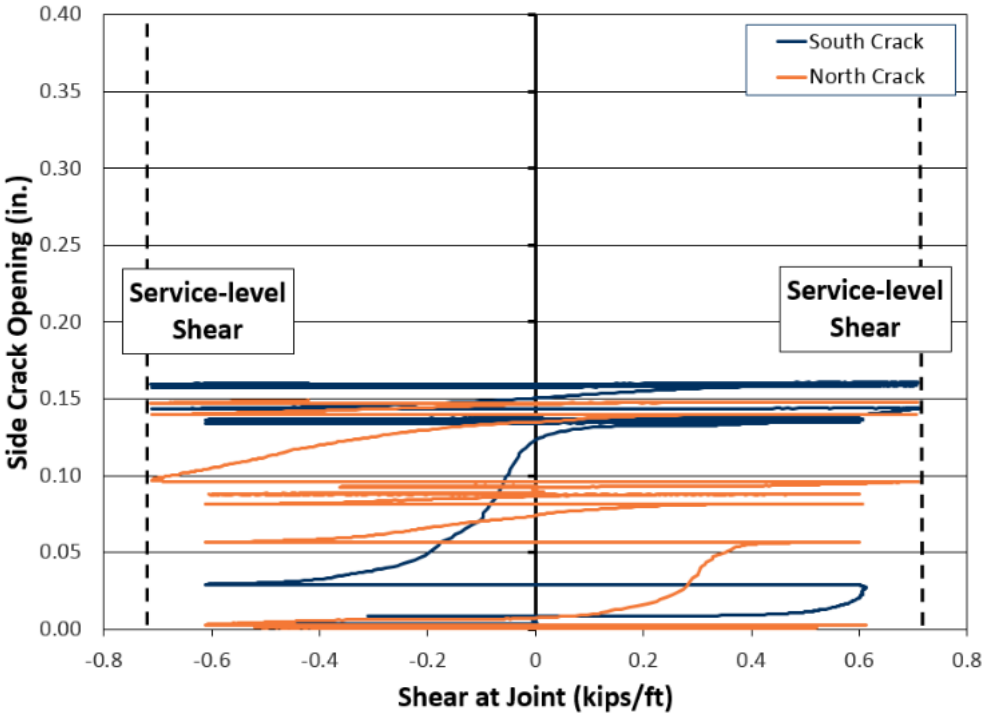


**Figure 5.19: Side Crack Opening versus Shear at Joint (U-REV-Q)**

#### 5.2.3.2 Staggered Hook Reinforced Joint (R-REV-Q)

The R-REV-Q test was conducted per the prescribed loading procedure. For each load step the applied load was cycled five times up to the calculated value and down to the minimum value. If the specimen did not fail at the current load step, then the load was increased to the next load step and the test continued.

##### 5.2.3.2.1 Visual Inspection

The condition of the joint before versus after the test is shown in Figure 5.20. Crack propagation was documented by marking and labeling the cracks after each load step. The labels corresponded to the force applied by one of the actuators onto the specimen. During the first load step (1.32 kips), second load step (2.15 kips), and third load step (2.97 kips), no noticeable cracks formed. During the fourth load step (3.80 kips), a crack formed along the north joint interface extending up to the reinforcing steel height. When loading up to the fifth load step (4.62 kips), the cracks extended along the north joint interface and new cracks formed along the south joint interface extending up towards the top surface of the specimen. During the middle of the fifth load step, the specimen deflected significantly and rested on wood blocks intended to catch specimen when it failed. It was determined that the specimen may be able to resist additional force so the load was removed momentarily to remove the blocks below, and then the test continued as planned. During the sixth load step (5.45 kips), the specimen failed.

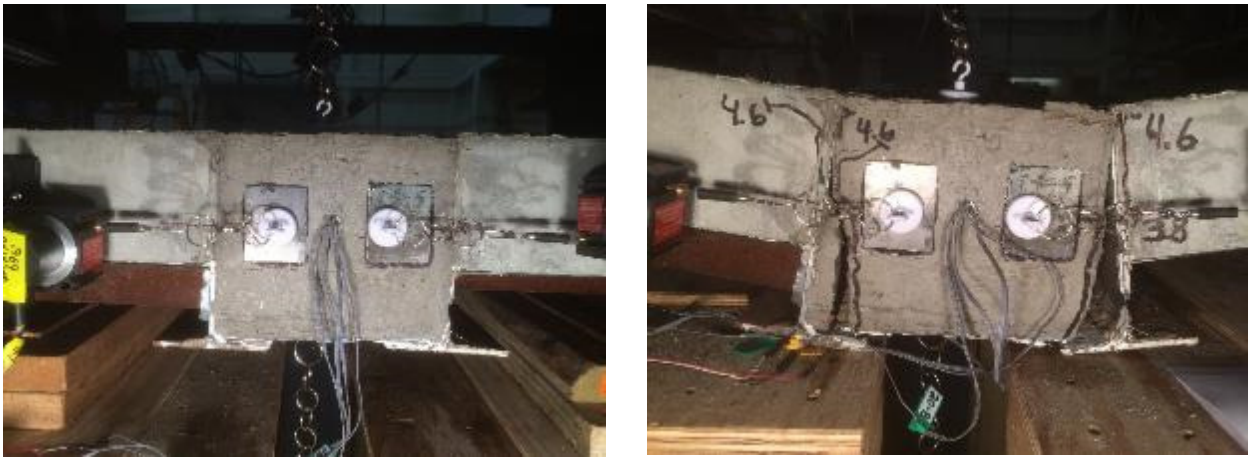


**Figure 5.20: R-REV-Q Joint Before and After**

#### 5.2.3.2.2 External Instrumentation

As discussed earlier, external instrumentation consisted of wirepots attached to the top of the specimen to measure midspan deflection, wirepots attached to the bottom of the specimen to measure large midspan deflection, and wirepots attached to the side of the specimen to measure crack opening at the joint-panel interface.

Figure 5.21 shows the behavior of the shear at joint versus midspan deflection. Note at each load step as the shear at the joint increased, more cracks formed in the specimen and the midspan deflection increased. The bottom wirepots were utilized to capture the specimen behavior after the top wirepots exceeded their stroke limit.

Figure 5.22 shows the behavior of the side crack opening versus shear at joint. Similarly, as noted above, at each load step as the shear at the joint increased, the side cracks opened wider. The graph depicts the behavior of the south joint interface as well as the north joint interface.

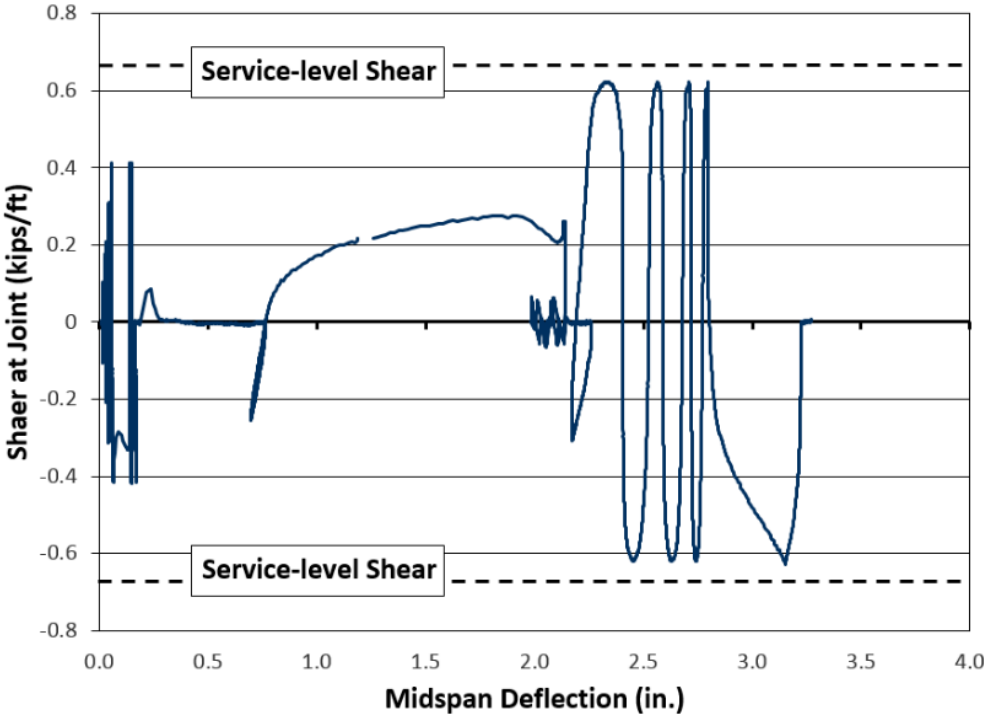


**Figure 5.21: Shear at Joint versus Midspan Deflection (R-REV-Q)**

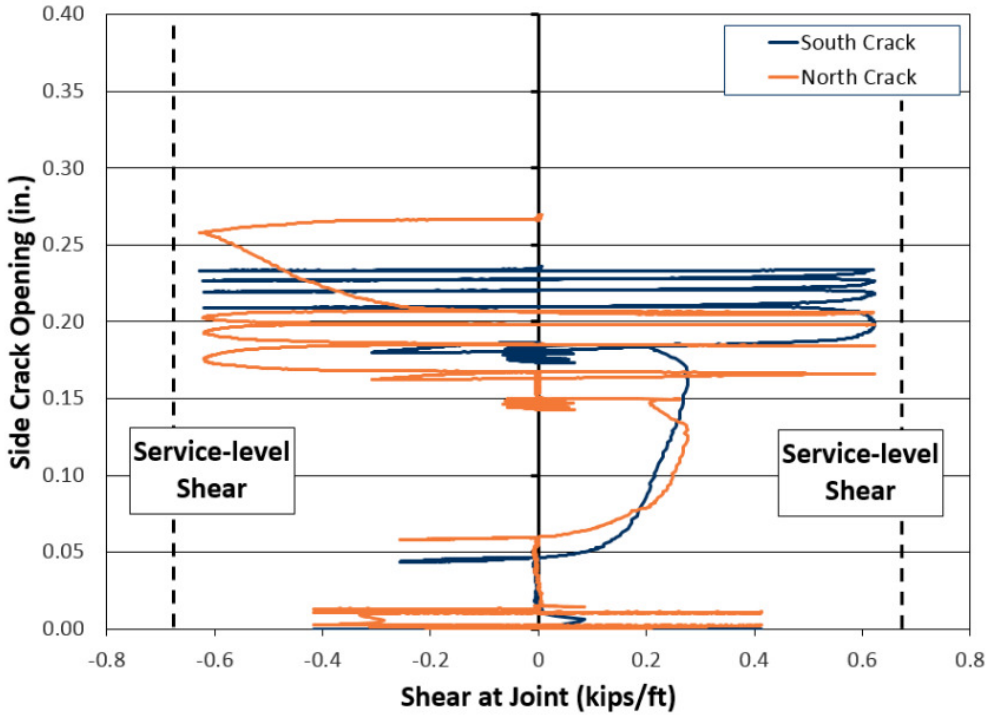


**Figure 5.22: Side Crack Opening versus Shear at Joint (R-REV-Q)**

#### 5.2.3.2.3 Internal Instrumentation

As discussed earlier, internal instrumentation consisted of strain gages attached to each of the four hooked reinforcing bars within the joint.

Figure 5.23 shows the behavior of the strain in reinforcing steel versus shear at joint. At each load step as the shear at the joint increased, more cracks formed in the specimen and the strain in the reinforcing steel increased. Note that during the fourth load step (+/- 0.41 kips/ft) a crack formed at the north joint interface and the NE and NW bars yielded resulting in a significant increase in the strain. During the fifth load step (+/- 0.62 kips/ft) a crack formed at the south joint interface and the SW bars yielded resulting in a significant increase in the strain. Meanwhile, the SE and NW strain gages exceeded their range. The strain gages reached their limit at approximately 19,000 με.

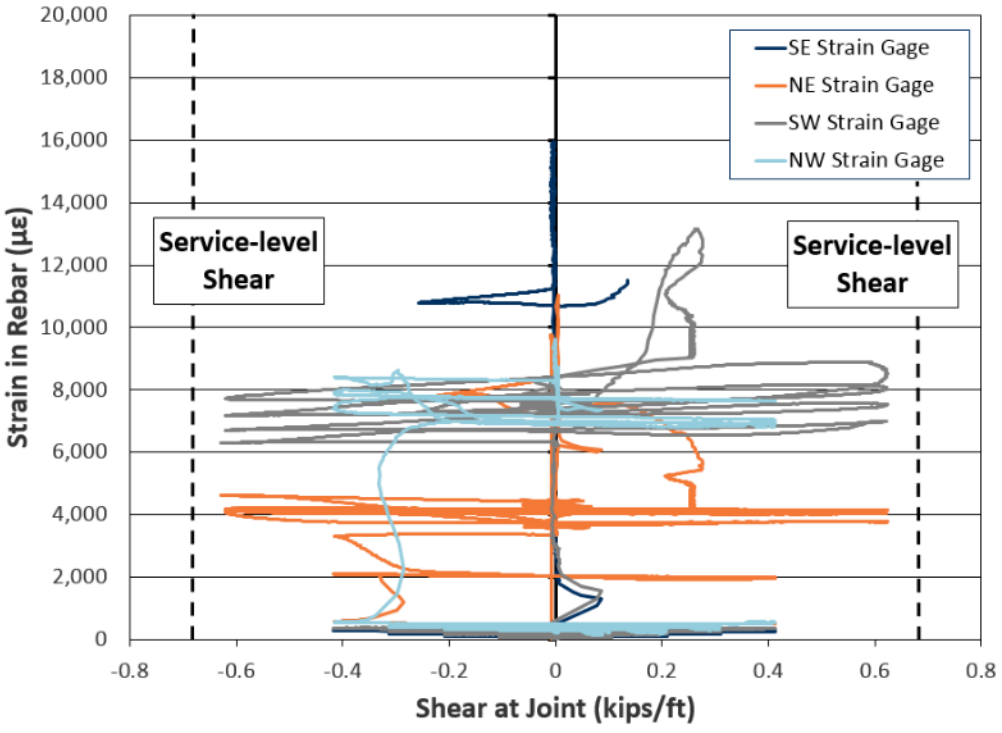


**Figure 5.23: Strain in Reinforcing Steel versus Shear at Joint (R-REV-Q)**

## 5.3 Fatigue Tests

This section covers the fatigue test results for both the unreinforced shear key and staggered hook reinforced joints. This section is separated into three main subsections: positive bending, negative bending, and shear reversal test results.

### 5.3.1 Positive Bending Test Results

This first subsection covers fatigue positive bending results for the unreinforced shear key joint (U-POS-F) and staggered hook reinforced joint (R-POS-F) specimens.

#### 5.3.1.1 Unreinforced Shear Key Joint (U-POS-F)

The U-POS-F test was conducted per the prescribed loading procedure. The test was scheduled to run for 2,000,000 cycles and pause at discrete intervals to record the degradation of the joint at the $1^{st}$, $10^{th}$, $100^{th}$, $1{,}000^{th}$, $10{,}000^{th}$, $100{,}000^{th}$, $1{,}000{,}000^{th}$, and $2{,}000{,}000^{th}$ cycle.

##### 5.3.1.1.1 Visual Inspection

The condition of the joint at each discrete interval is shown in Figure 5.24. Crack propagation was documented by marking the cracks after each discrete interval. Cracks formed north and south of the joint within the deck concrete. After the $1^{st}$ cycle, cracks originated at the top of the steel WT section. After the $10^{th}$ cycle, no new cracks formed. After the $100^{th}$ cycle, cracks extended and widened slightly. After the $1{,}000^{th}$ cycle, additional cracks formed on the south side of the joint within the deck concrete originating at the steel WT section. After the $10{,}000^{th}$ cycle, no new cracks formed. During the $51{,}477^{th}$ cycle, the specimen failed along the south side of the joint within the deck concrete. The crack originated at the flange of the steel WT section and extended up to the top of the specimen.

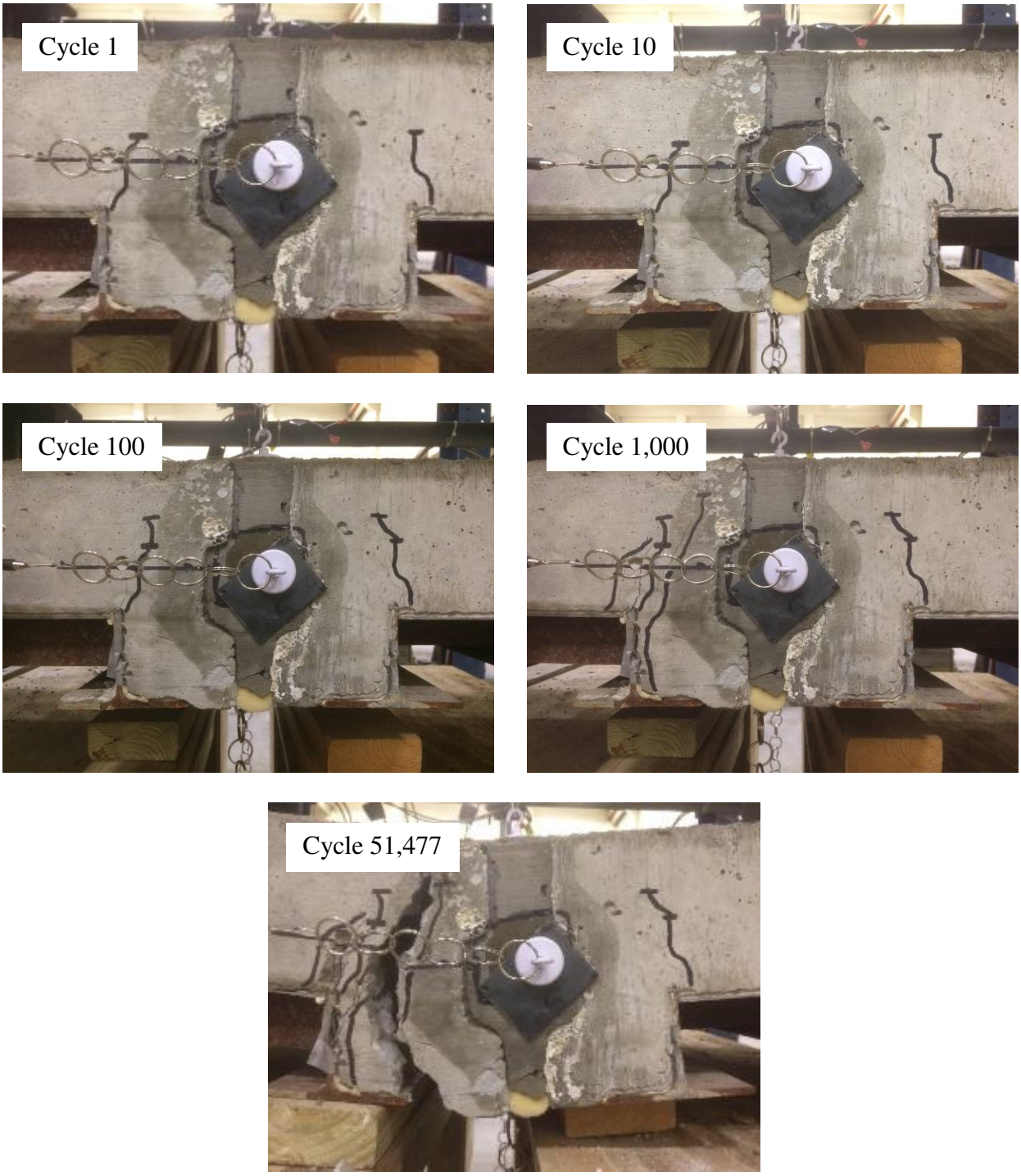


**Figure 5.24: U-POS-F Joint at Discrete Intervals**

#### 5.3.1.1.2 External Instrumentation

As discussed earlier, external instrumentation consisted of wirepots attached to the top of the specimen to measure midspan deflection, wirepots attached to the bottom of the specimen to measure large midspan deflection, and wirepots attached to the side of the specimen to measure crack opening at the joint-panel interface.

Figure 5.25 shows the behavior of the moment at joint versus midspan deflection. Note at each discrete interval, as the test continued and more cracks formed, the stiffness of the specimen weakened and the midspan deflection increased. Figure 5.26 shows the moment versus midspan deflection of each discrete interval superimposed on top of each other to demonstrate the loss of stiffness of the joint as the test progressed.

Figure 5.27 shows the behavior of the side crack opening versus moment at joint. Similarly, as noted above, as the test continued and more cracks formed, the side cracks opened wider.

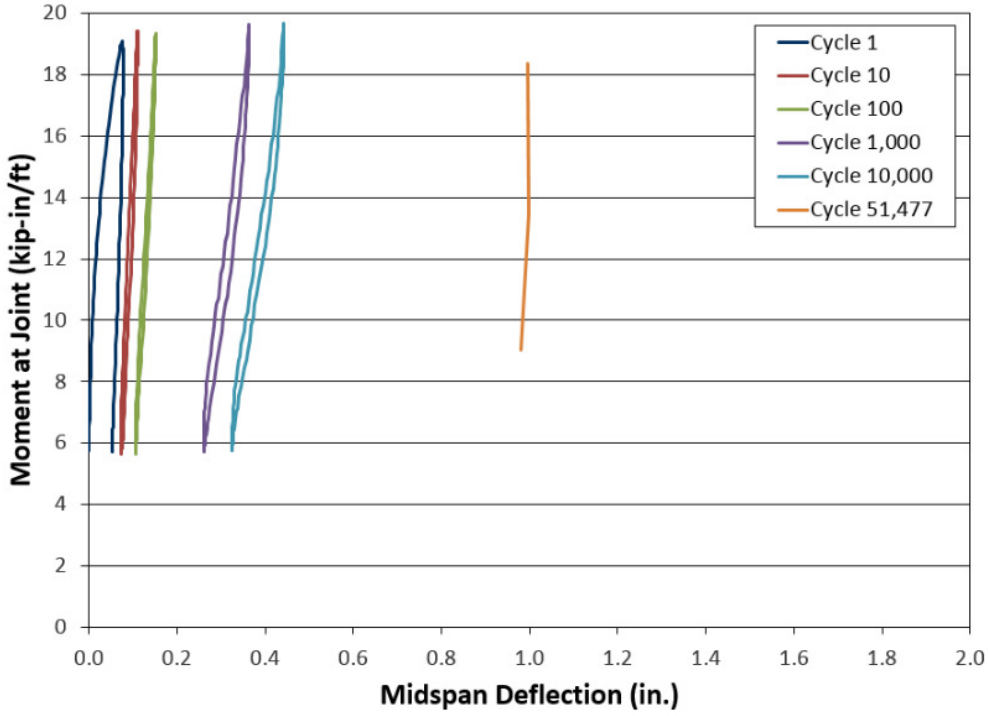


**Figure 5.25: Moment at Joint versus Midspan Deflection (U-POS-F)**

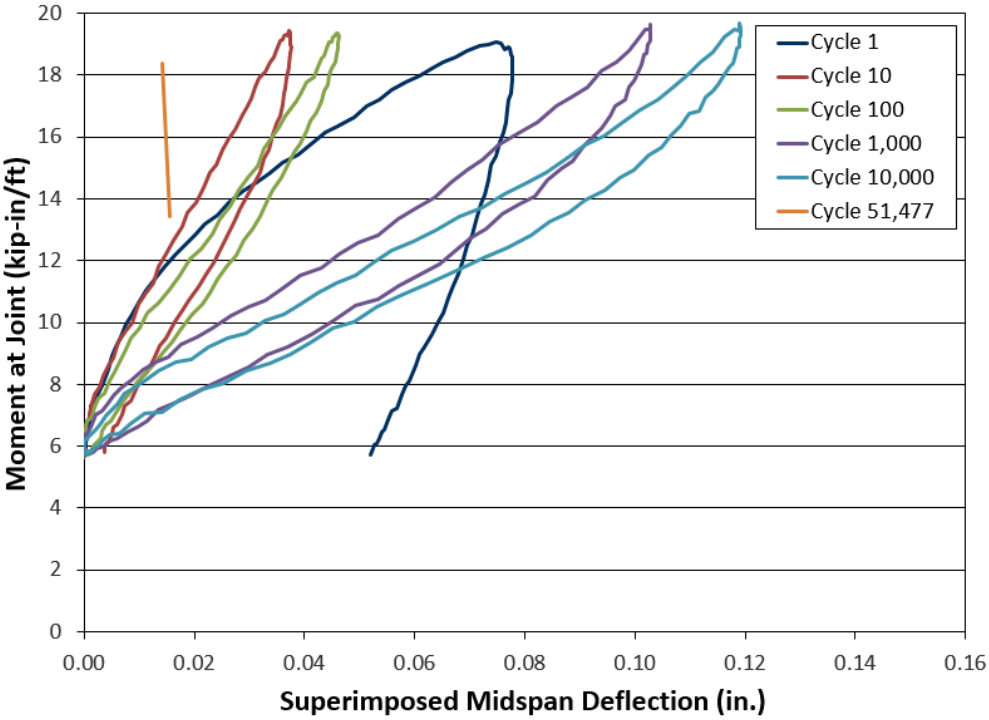


**Figure 5.26: Moment at Joint versus Superimposed Midspan Deflection (U-POS-F)**

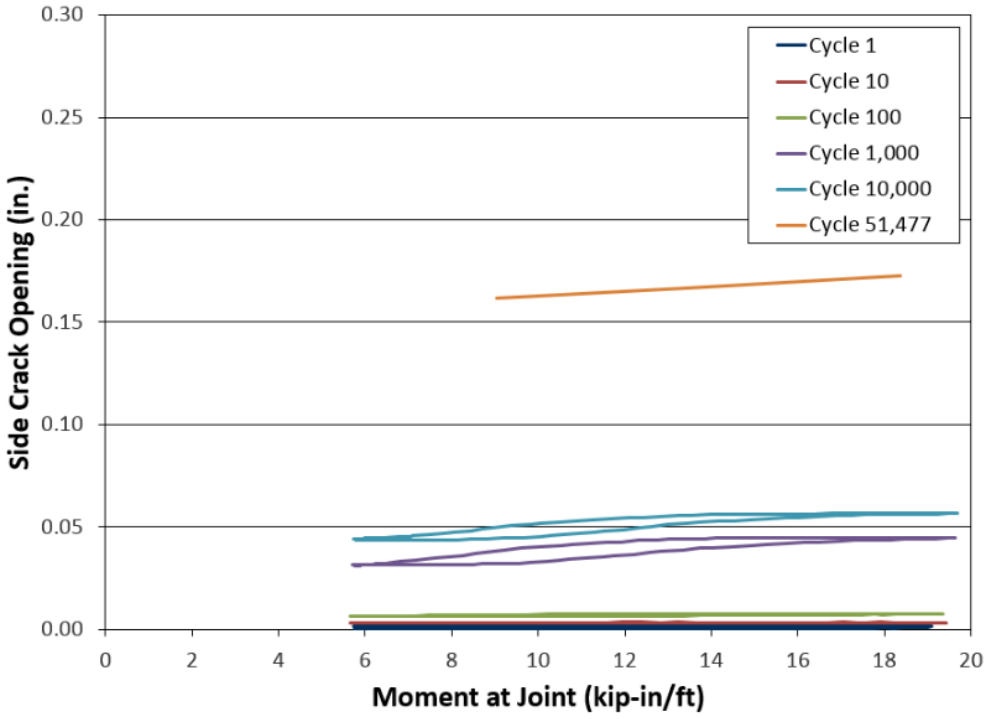


**Figure 5.27: Side Crack Opening versus Moment at Joint (U-POS-F)**

#### 5.3.1.2 Staggered Hook Reinforced Joint (R-POS-F)

The R-POS-F test was conducted per the prescribed loading procedure. The test was scheduled to run for 2,000,000 cycles and pause at discrete intervals to record the degradation of the joint at the 1st, 10th, 100th, 1,000th, 10,000th, 100,000th, 1,000,000th, and 2,000,000th cycle.

##### 5.3.1.2.1 Visual Inspection

The condition of the joint at each discrete interval is shown in Figure 5.28. Crack propagation was documented by marking the cracks after each discrete interval. After the 1st, 10th, and 100th cycle, no noticeable cracks formed. After the 1,000th cycle, cracks formed at the south side within the joint extending up to the reinforcing steel height. The test continued without any new cracks forming until the test was concluded after the 2,000,000th cycle.

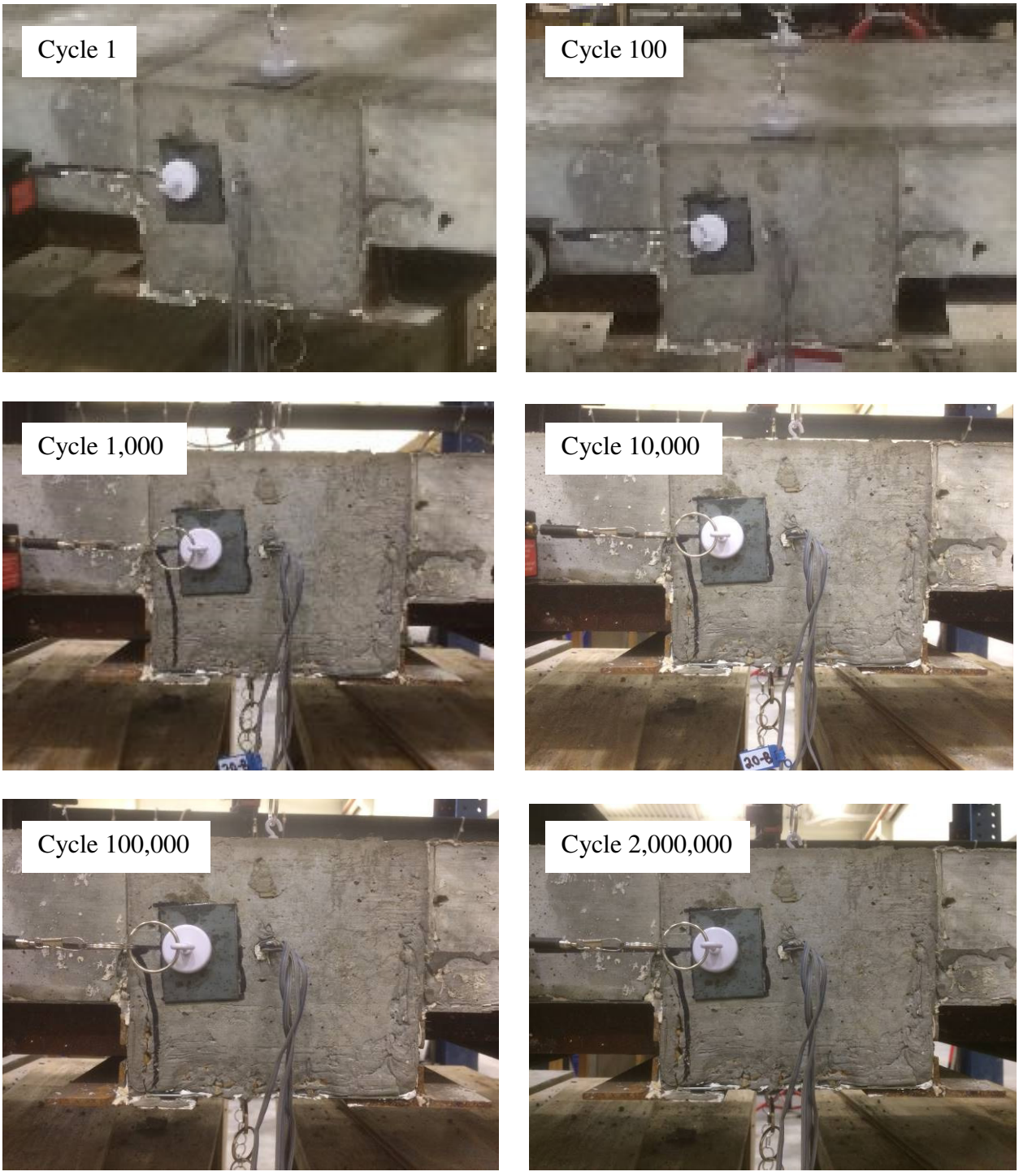


**Figure 5.28: R-POS-F Joint at Discrete Intervals**

#### 5.3.1.2.2 External Instrumentation

As discussed earlier, external instrumentation consisted of wirepots attached to the top of the specimen to measure midspan deflection, wirepots attached to the bottom of the specimen to measure large midspan deflection, and wirepots attached to the side of the specimen to measure crack opening at the joint-panel interface.

Figure 5.29 shows the behavior of the moment at joint versus midspan deflection. Note at each discrete interval, as the test continued and more cracks formed, the stiffness of the specimen weakened and the midspan deflection increased. Between the $100^{th}$ and $1{,}000^{th}$ cycle, there was a significant increase in midspan deflection. This corresponded to a crack that formed in the south side of the joint at the time. Figure 5.30 shows the moment versus midspan deflection of each discrete interval superimposed on top of each other to demonstrate the loss of stiffness of the joint as the test progressed.

Figure 5.31 shows the behavior of the side crack opening versus moment at joint. Similarly, as noted above, as the test continued and more cracks formed, the side cracks opened wider. The south joint interface did not widen significantly when compared to other tests.

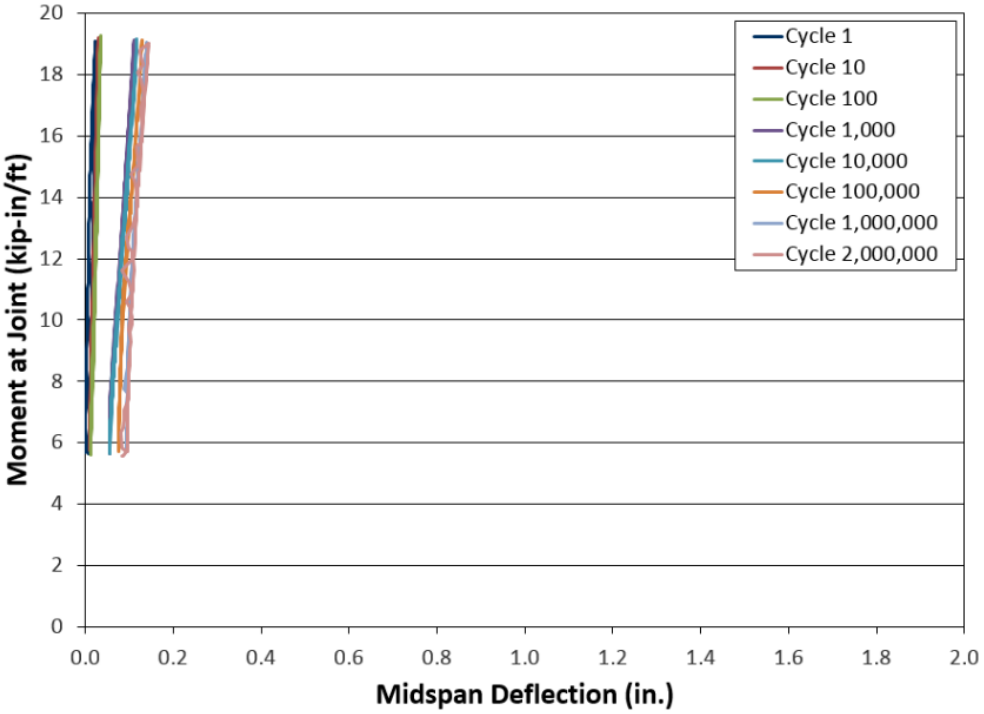


**Figure 5.29: Moment at Joint versus Midspan Deflection (R-POS-F)**

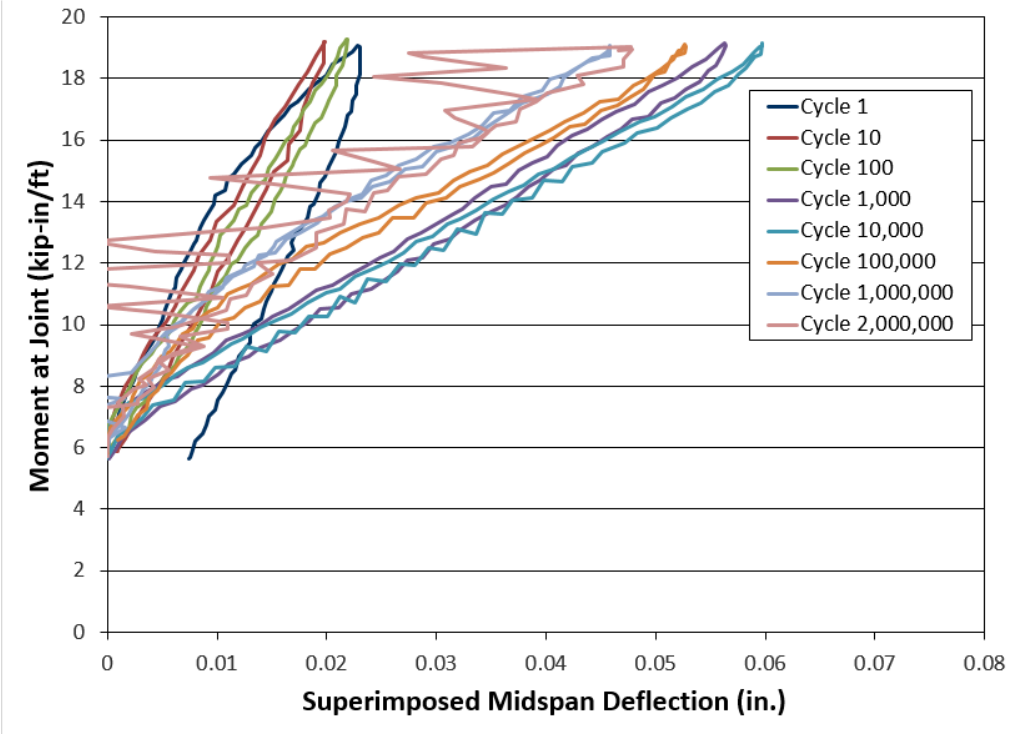


**Figure 5.30: Moment at Joint versus Superimposed Midspan Deflection (R-POS-F)**

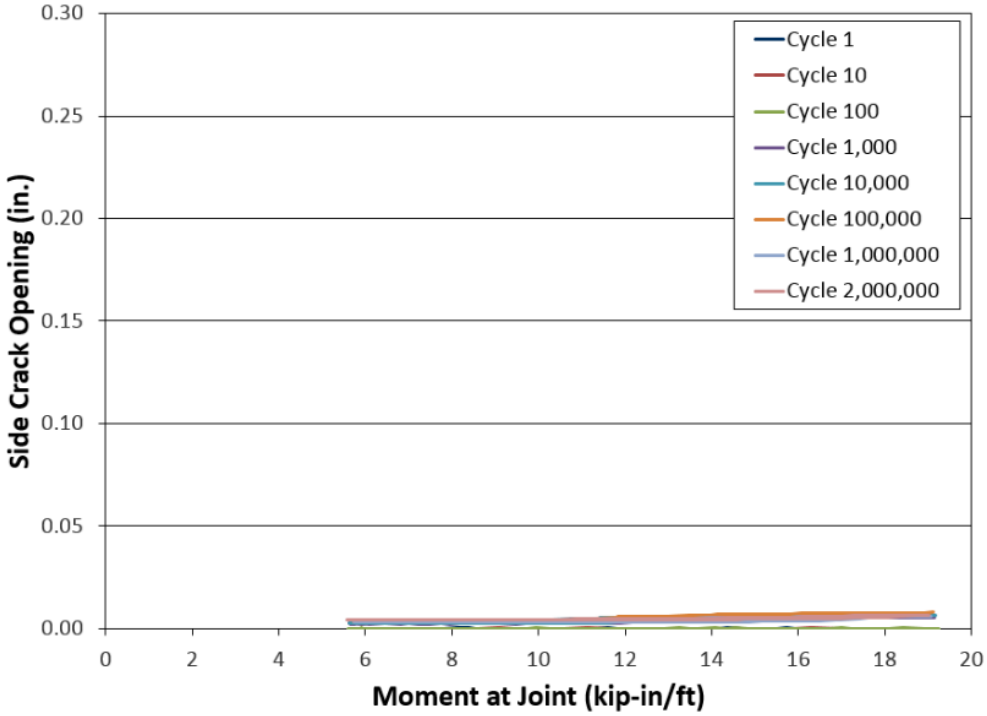


**Figure 5.31: Side Crack Opening versus Moment at Joint (R-POS-F)**

#### 5.3.1.2.3 Internal Instrumentation

As discussed earlier, internal instrumentation consisted of strain gages attached to each of the four hooked reinforcing bars within the joint.

Figure 5.32, 5.33, 5.34, and 5.35 show the behavior of the SE, NE, SW, and NW strain in reinforcing steel versus moment at joint, respectively. At each discrete interval, as the test continued and more cracks formed, the stiffness of the specimen weakened and the midspan deflection increased. Between the 100$^{th}$ and 1,000$^{th}$ cycle, there was a significant increase in strain for the SE and SW bars. This corresponded to a crack that formed at the south joint interface.

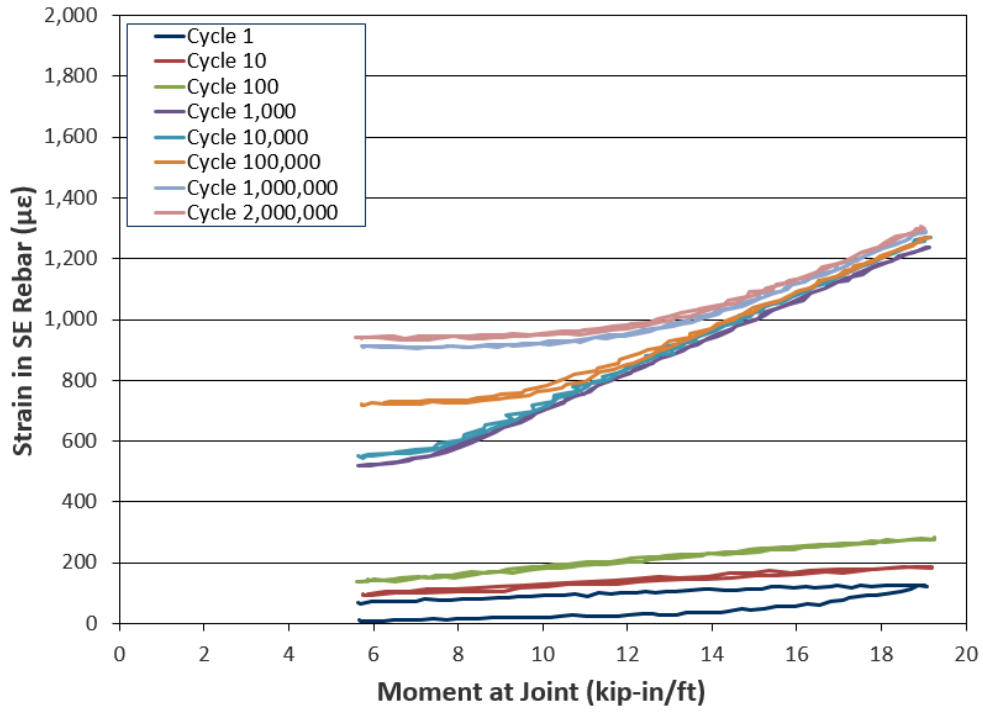


**Figure 5.32: Strain in SE Reinforcing Steel versus Moment at Joint (R-POS-F)**

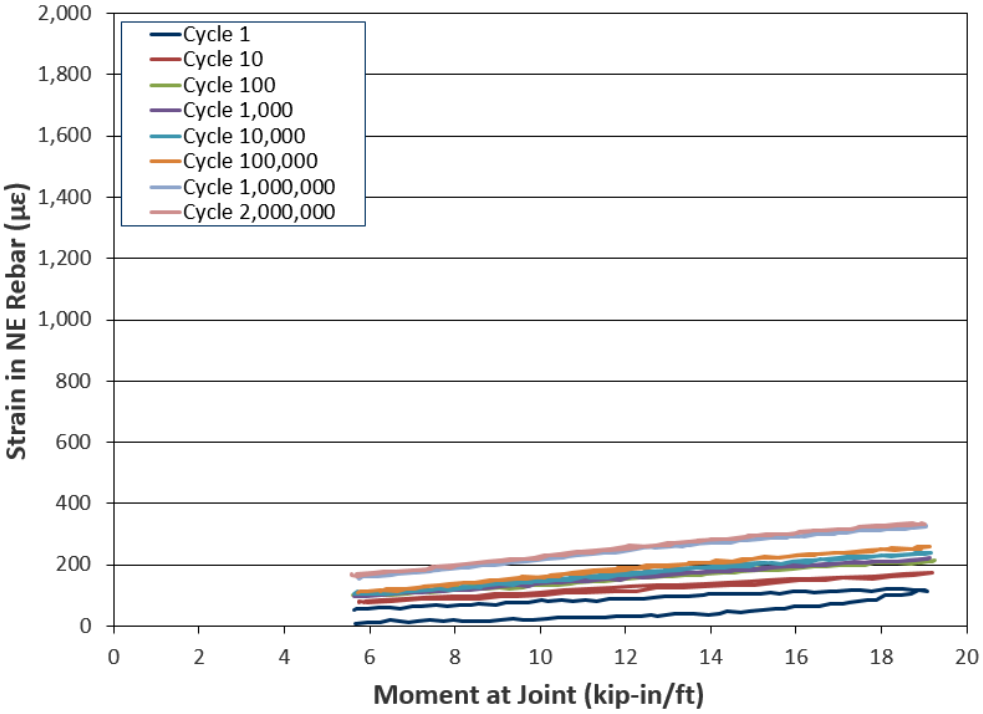


**Figure 5.33: Strain in NE Reinforcing Steel versus Moment at Joint (R-POS-F)**

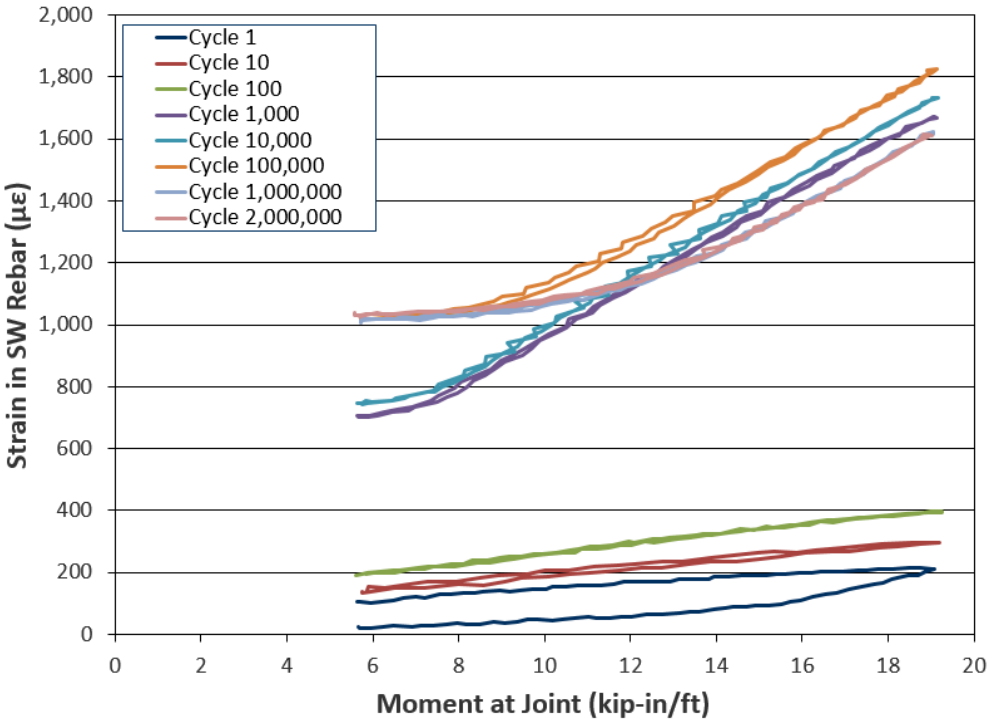


**Figure 5.34: Strain in SW Reinforcing Steel versus Moment at Joint (R-POS-F)**

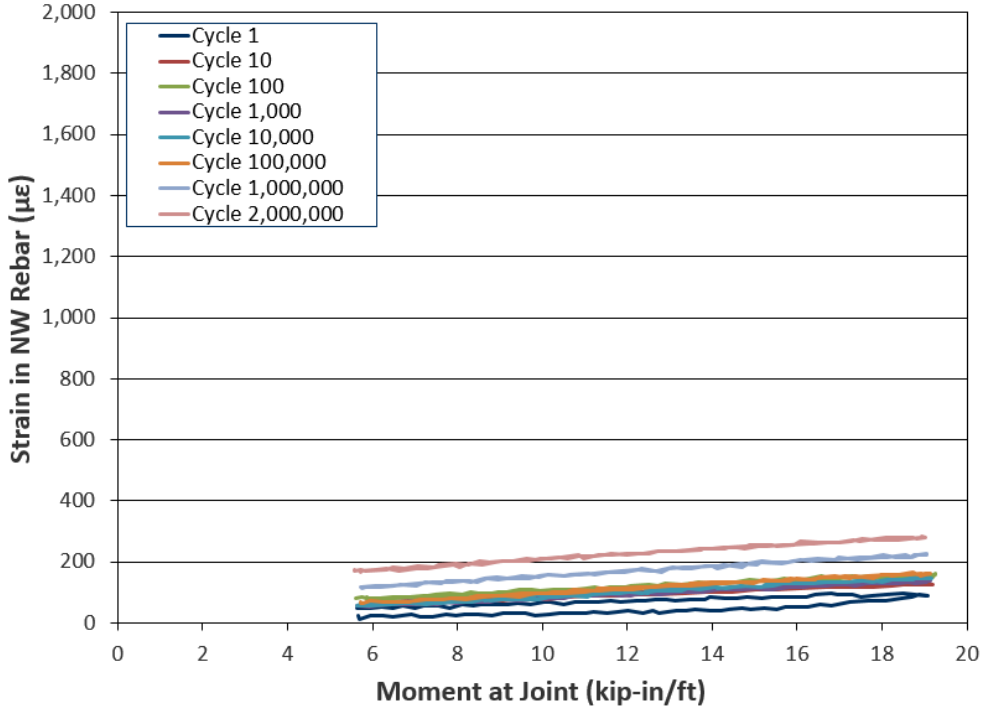


**Figure 5.35: Strain in NW Reinforcing Steel versus Moment at Joint (R-POS-F)**

### 5.3.2 Negative Bending Test Results

This second subsection covers fatigue negative bending results for the unreinforced shear key joint (U-NEG-F) and staggered hook reinforced joint (R-NEG-F) specimens.

#### 5.3.2.1 Unreinforced Shear Key Joint (U-NEG-F)

The U-NEG-F test was conducted per the prescribed loading procedure. The test was scheduled to run for 2,000,000 cycles and pause at discrete intervals to record the degradation of the joint at the $1^{st}$, $10^{th}$, $100^{th}$, $1{,}000^{th}$, $10{,}000^{th}$, $100{,}000^{th}$, $1{,}000{,}000^{th}$, and $2{,}000{,}000^{th}$ cycle.

##### 5.3.2.1.1 Visual Inspection

The condition of the joint at each discrete interval is shown in Figure 5.36. Crack propagation was documented by marking the cracks after each discrete interval. After the $1^{st}$ cycle, no noticeable cracks formed. After the $10^{th}$ cycle, cracks formed within the deck concrete on the north side of the joint directly below the steel WT section. During the $14^{th}$ cycle, the specimen failed at a new crack location on the north side of the joint within the deck concrete.

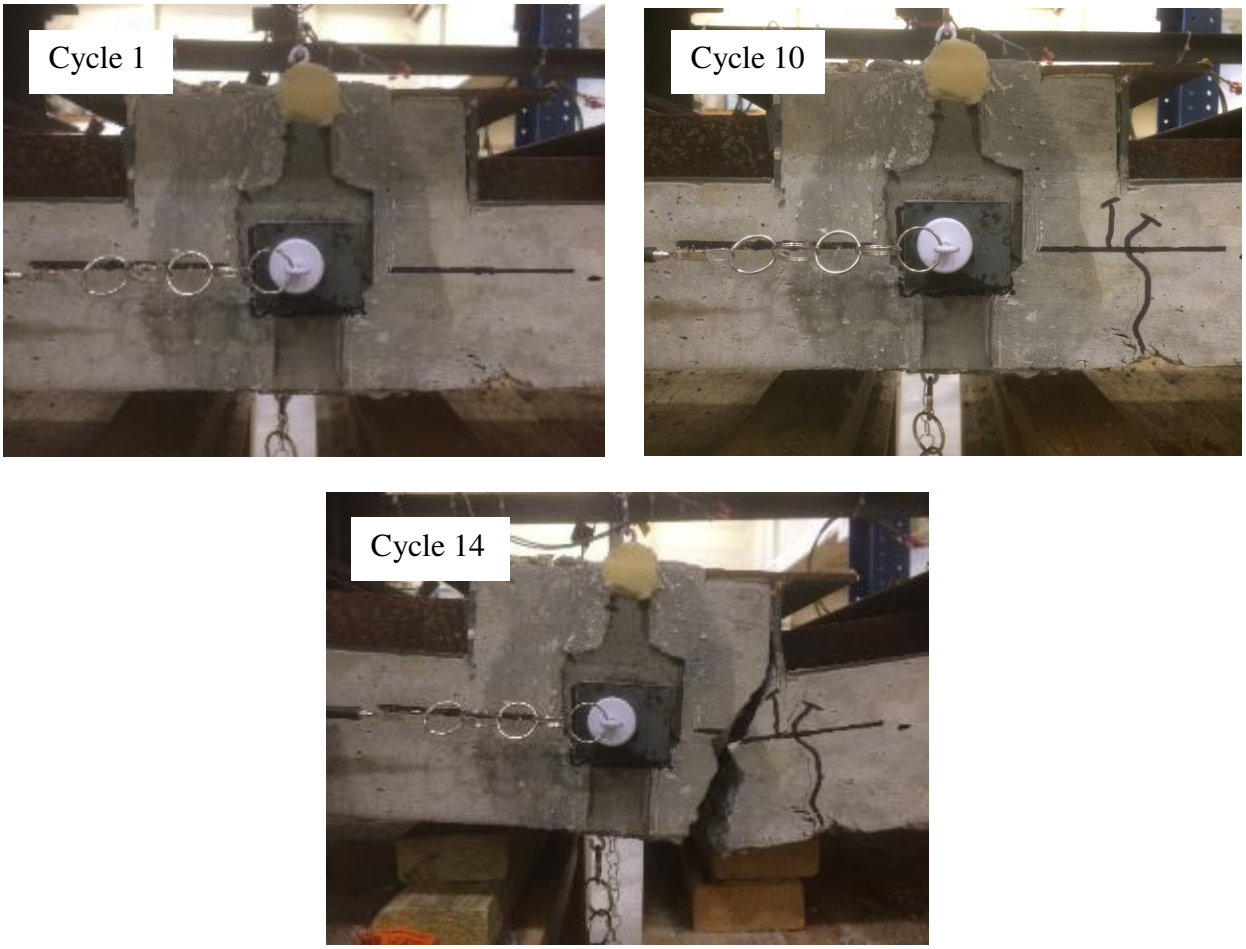


**Figure 5.36: U-NEG-F Joint at Discrete Intervals**

#### 5.3.2.1.2 External Instrumentation

As discussed earlier, external instrumentation consisted of wirepots attached to the top of the specimen to measure midspan deflection, wirepots attached to the bottom of the specimen to measure large midspan deflection, and wirepots attached to the side of the specimen to measure crack opening at the joint-panel interface.

Figure 5.37 shows the behavior of the moment at joint versus midspan deflection. Note at each discrete interval, as the test continued and more cracks formed, the stiffness of the specimen weakened and the midspan deflection increased. Figure 5.38 shows the moment versus midspan

deflection of each discrete interval superimposed on top of each other to demonstrate the loss of stiffness of the joint as the test progressed.

Crack formation and failure occurred to the north of the joint. Unfortunately, the failure was expected to occur to the south of the joint so the side wirepots were attached at this location. Therefore, no useful data was recorded with these instruments to compare side crack opening versus moment at joint.

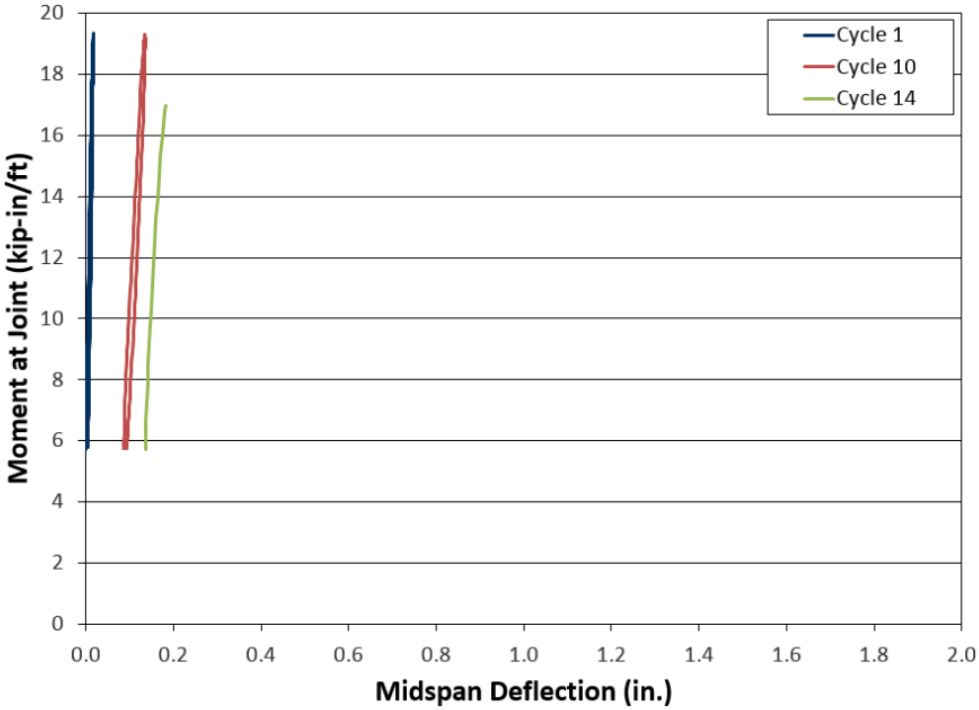


**Figure 5.37: Moment at Joint versus Midspan Deflection (U-NEG-F)**

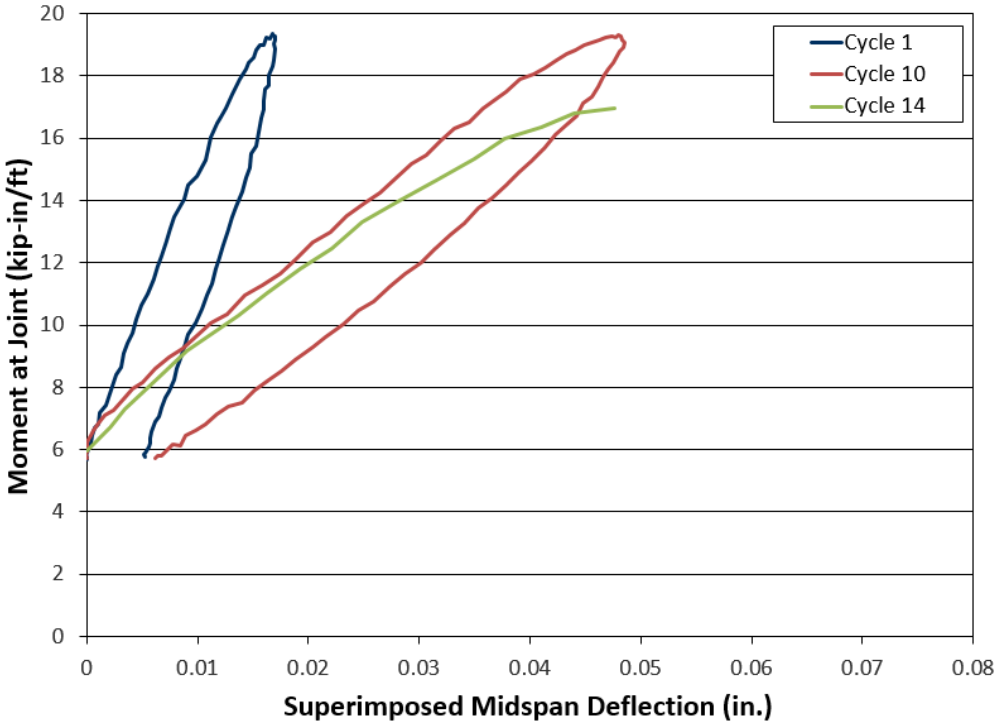


**Figure 5.38: Moment at Joint versus Superimposed Midspan Deflection (U-NEG-F)**

#### 5.3.2.2 Staggered Hook Reinforced Joint (R-NEG-F)

The R-NEG-F test was conducted per the prescribed loading procedure. The test was scheduled to run for 2,000,000 cycles and pause at discrete intervals to record the degradation of the joint at the 1$^{st}$, 10$^{th}$, 100$^{th}$, 1,000$^{th}$, 10,000$^{th}$, 100,000$^{th}$, 1,000,000$^{th}$, and 2,000,000$^{th}$ cycle.

##### 5.3.2.2.1 Visual Inspection

The condition of the joint at each discrete interval is shown in Figures 5.39 and 5.40. Crack propagation was documented by marking the cracks after each discrete interval. After the 1$^{st}$ cycle, cracks formed at the north and south joint interfaces. After the 10$^{th}$ cycle, cracks extended up to the reinforcing steel height. After the 100$^{th}$, 1,000$^{th}$, and 100,000$^{th}$ cycle, no new cracks formed. After the 499,528$^{th}$ cycle, the specimen failed.

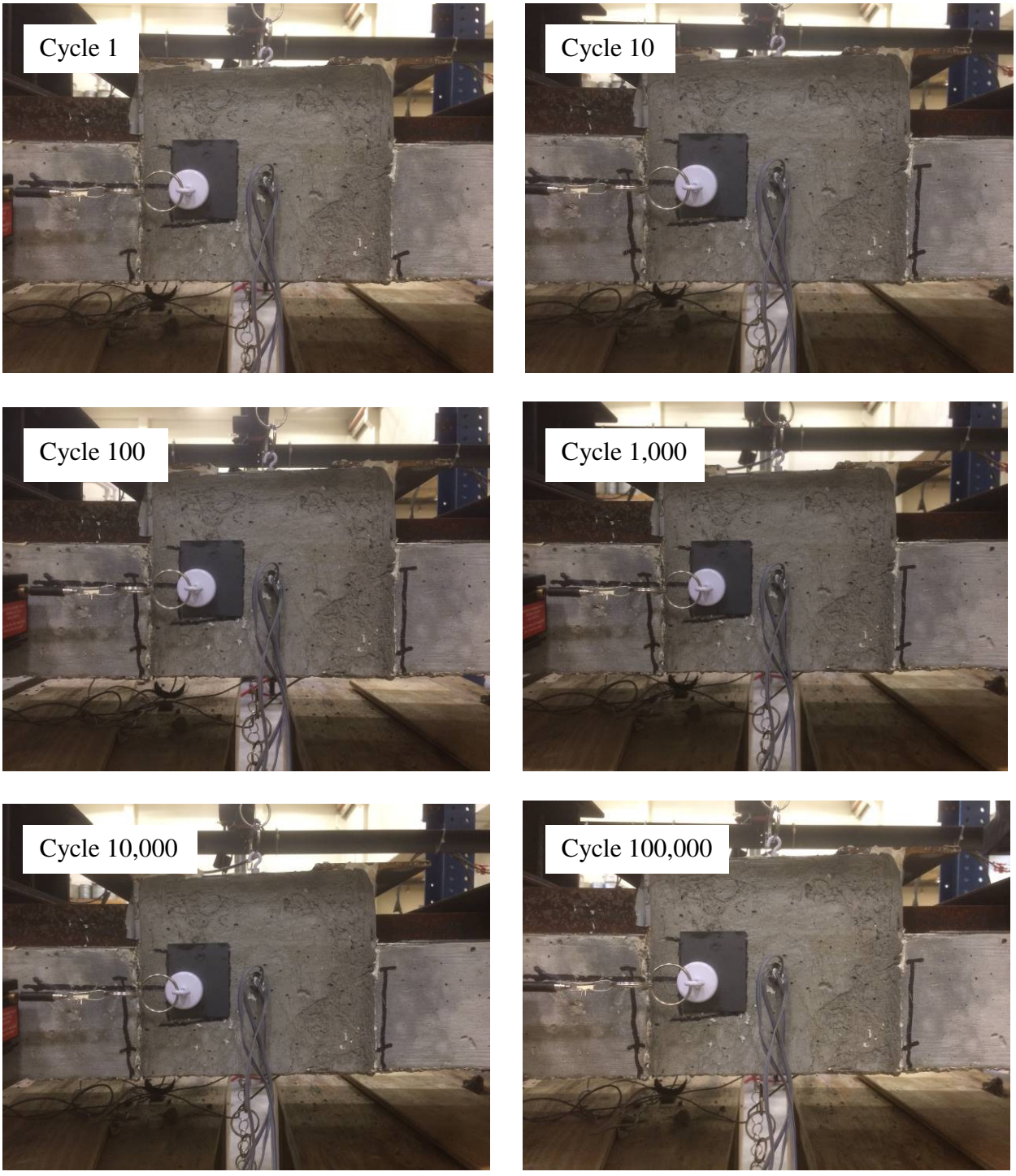


**Figure 5.39: R-NEG-F Joint at Discrete Intervals (Part 1 of 2)**


**Figure 5.40: R-NEG-F Joint at Discrete Intervals (Part 2 of 2)**

#### 5.3.2.2.2 External Instrumentation

As discussed earlier, external instrumentation consisted of wirepots attached to the top of the specimen to measure midspan deflection, wirepots attached to the bottom of the specimen to measure large midspan deflection, wirepots attached to the side of the specimen to measure crack opening at the joint-panel interface, and crack gages attached below the reinforcing steel locations to measure the crack opening at the joint interface. The bottom wirepots were utilized to capture the specimen behavior after the top wirepots exceeded their stroke limit.

Figure 5.41 shows the behavior of the moment at joint versus midspan deflection. Note at each discrete interval, as the test continued and more cracks formed, the stiffness of the specimen weakened and the midspan deflection increased. Figure 5.41 shows the moment versus midspan deflection of each discrete interval superimposed on top of each other to demonstrate the loss of stiffness of the joint as the test progressed.

Figure 5.43 shows the behavior of the side crack opening versus moment at joint. Similarly, as noted above, as the test continued and more cracks formed, the side cracks opened wider.

Figure 5.44 shows the behavior of the average of the SE and SW crack gages represented as the south crack gage opening versus moment at joint while Figure 5.45 shows the behavior of the average of the NE and NW crack gages represented as the north crack gage opening versus moment at joint. Note that the south crack gages increased significantly throughout the test compared to the north crack gages. This shows larger crack opening along the south joint interface compared to the north. The crack gages were removed after the 100,000$^{th}$ cycle to avoid any potential damage to the gages.

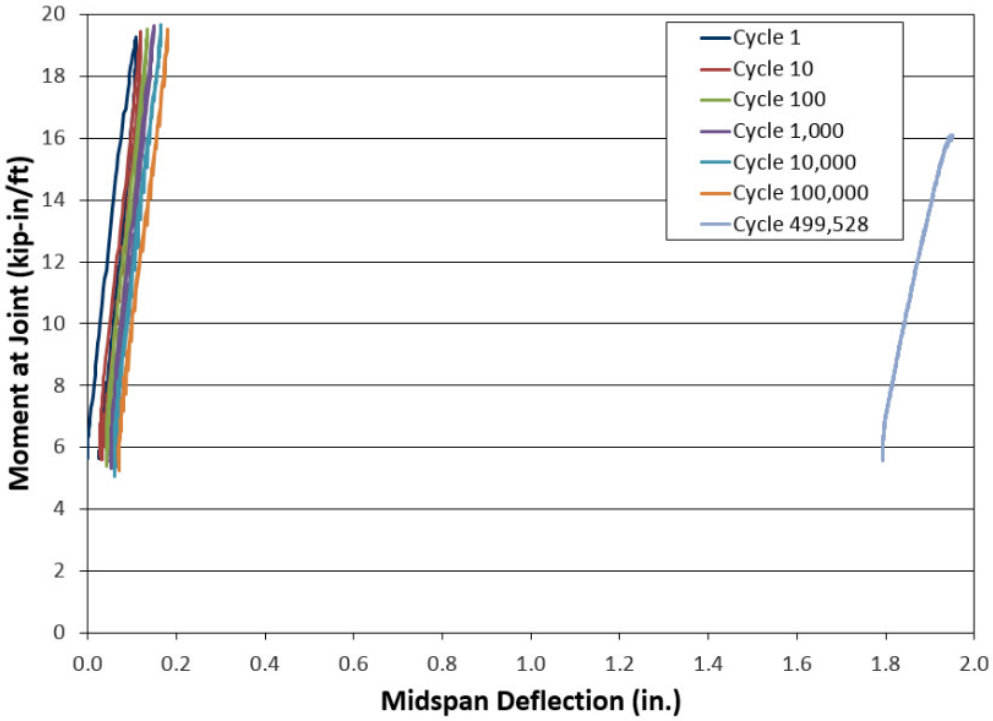


**Figure 5.41: Moment at Joint versus Midspan Deflection (R-NEG-F)**

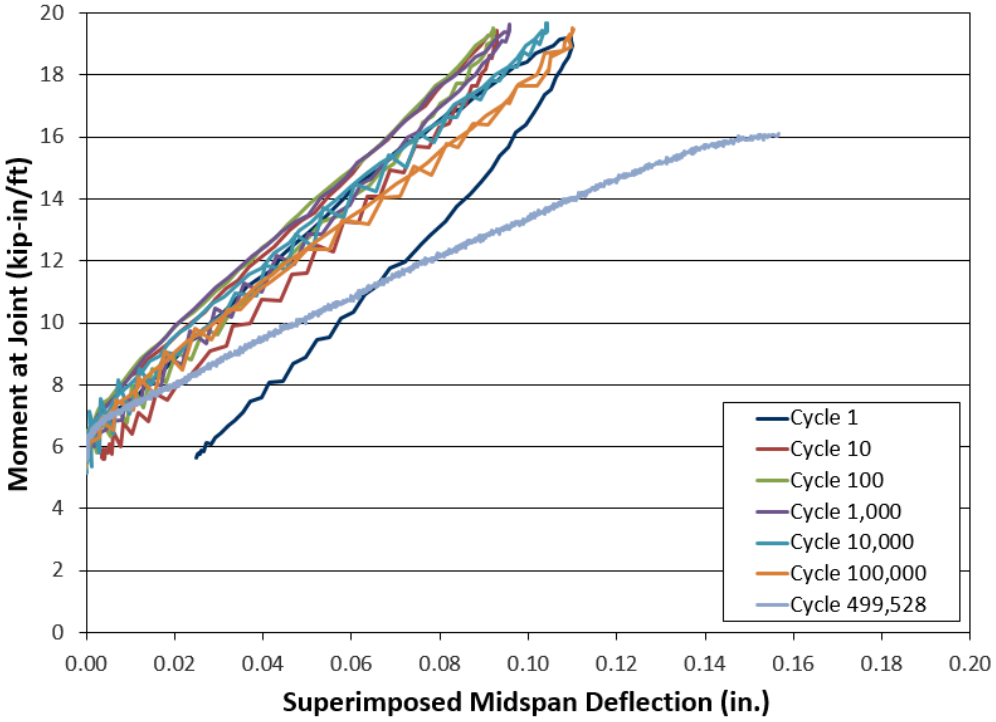


**Figure 5.42: Moment at Joint versus Superimposed Midspan Deflection (R-NEG-F)**

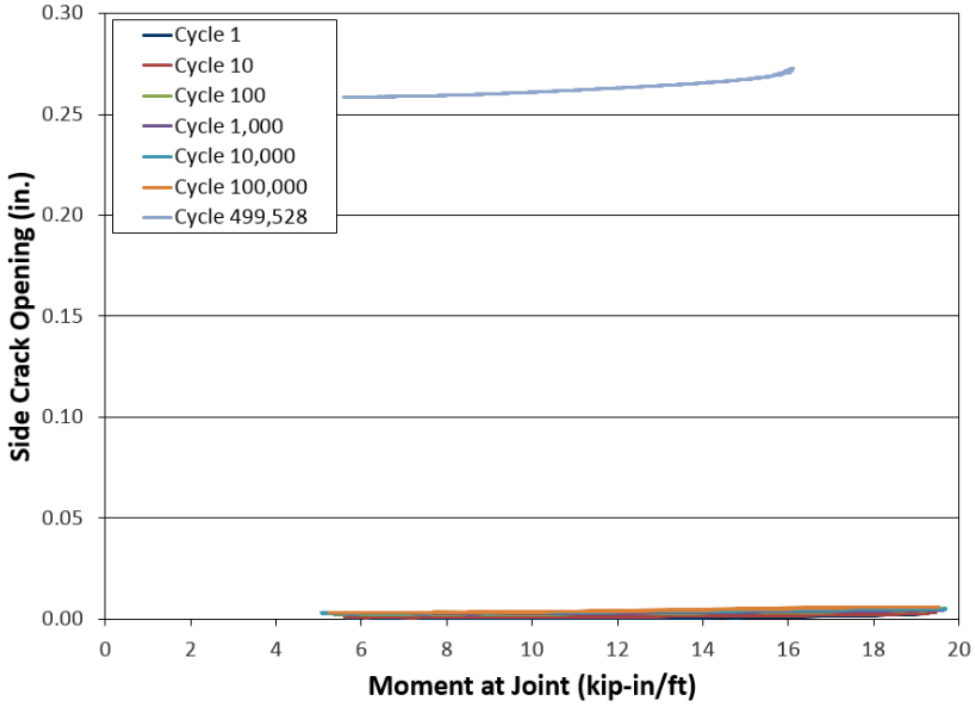


**Figure 5.43: Side Crack Opening versus Moment at Joint (R-NEG-F)**

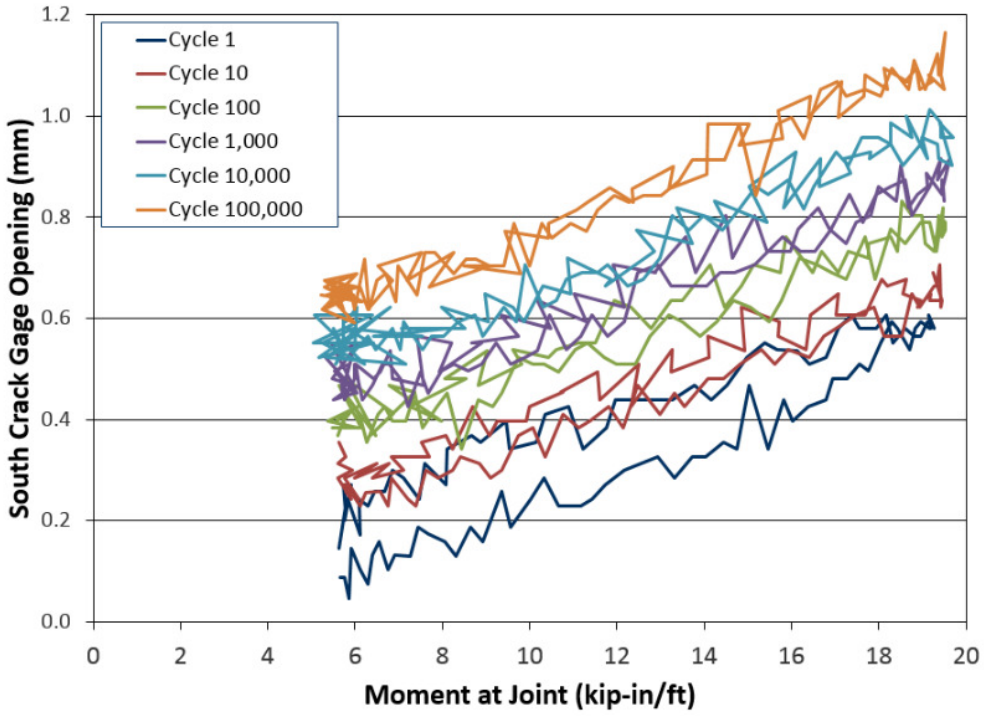


**Figure 5.44: South Crack Gage Opening versus Moment at Joint (R-NEG-F)**

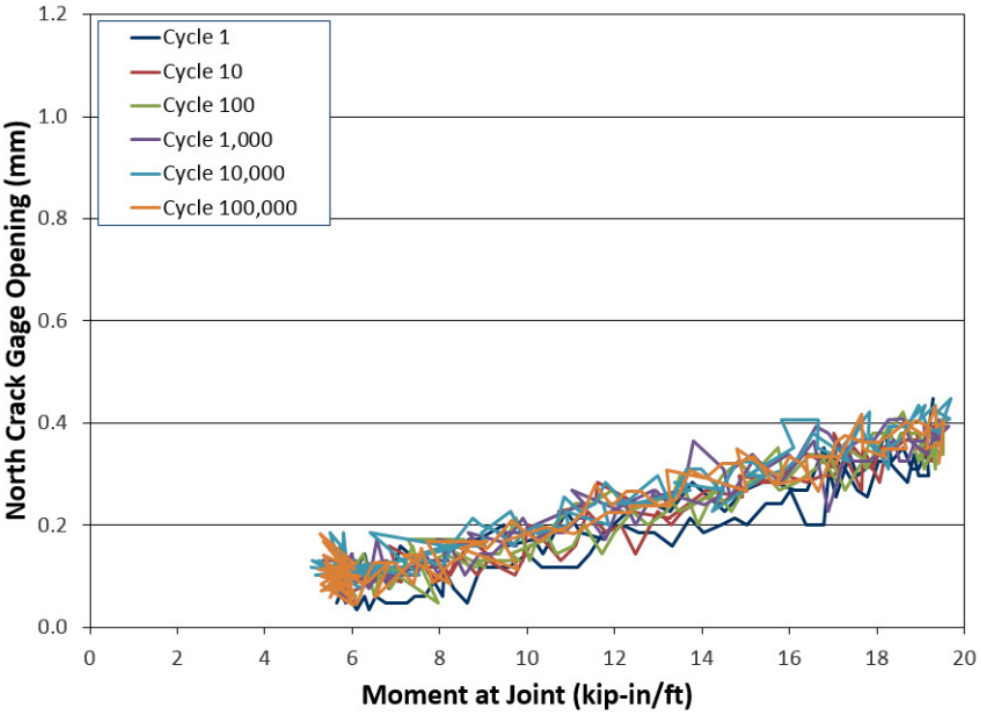


**Figure 5.45: North Crack Gage Opening versus Moment at Joint (R-NEG-F)**

#### 5.3.2.2.3 Internal Instrumentation

As discussed earlier, internal instrumentation consisted of strain gages attached to each of the four hooked reinforcing bars within the joint.

Figure 5.46, 5.47, 5.48, and 5.49 show the behavior of the SE, NE, SW, and NW strain in reinforcing steel versus moment at joint, respectively. At each discrete interval, as the test continued and more cracks formed, the stiffness of the specimen weakened and the reinforcing steel strain increased.

Each of the four reinforcement bars behaved differently during this test. The slope in the SE and SW strain gages were similar. The SW strain gage showed significant increases in strain at each discrete interval when compared to the SE gage. The gages exceeded their limit after the $10{,}000^{th}$ discrete interval either due to reinforcement yielding or instrumentation failure. The strain gage limit was approximately 19,000 με. The slope in the NE and NW strain gages were also similar. The difference between the two north gages was that the NE bar experienced compressive strains originally. This maybe because the specimen experienced slight torsion effects during the test or because the load path of the joint required the NE bar to provide compressive resistance.

After the test was concluded an investigation into the condition of the reinforcing steel was instigated. From visually inspecting the south joint interface crack opening it was determined that the SE bar had fractured. To inspect the condition of the SW bar, the SW bar was cut with a reciprocating saw to separate the north and south decks. Figure 5.50 shows the two decks separated. The north deck is on top and exposes the SE and SW bars. Figure 5.51 shows the condition of the SE and SW bars. The SE bar experienced a ductile fracture while the SW had not failed, yet there were signs of significant necking.

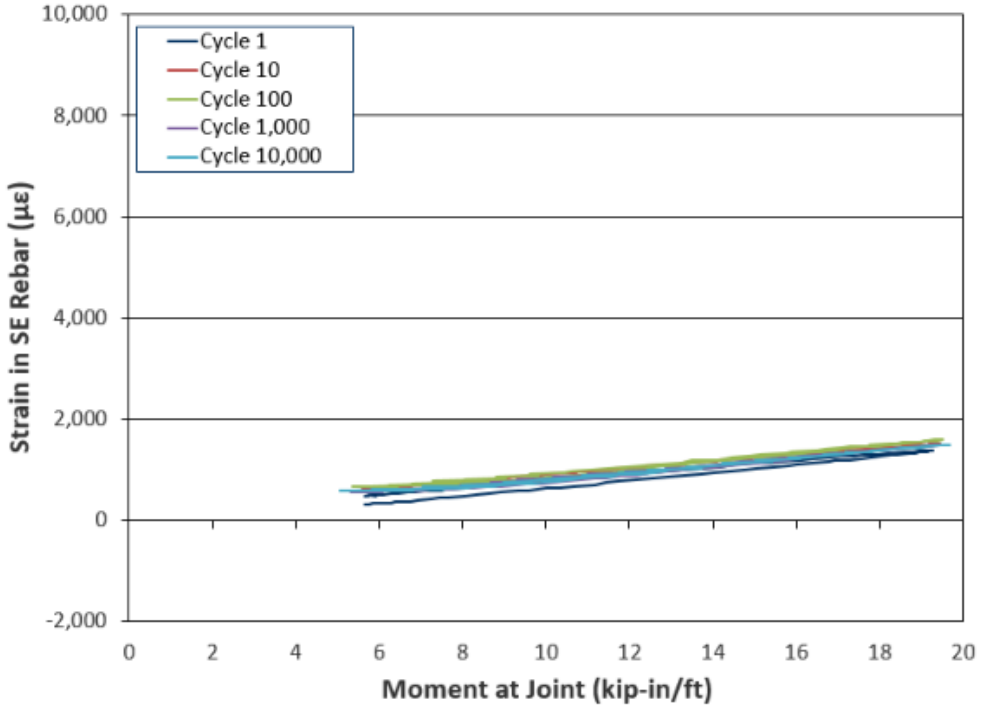


**Figure 5.46: Strain in SE Reinforcing Steel versus Moment at Joint (R-NEG-F)**

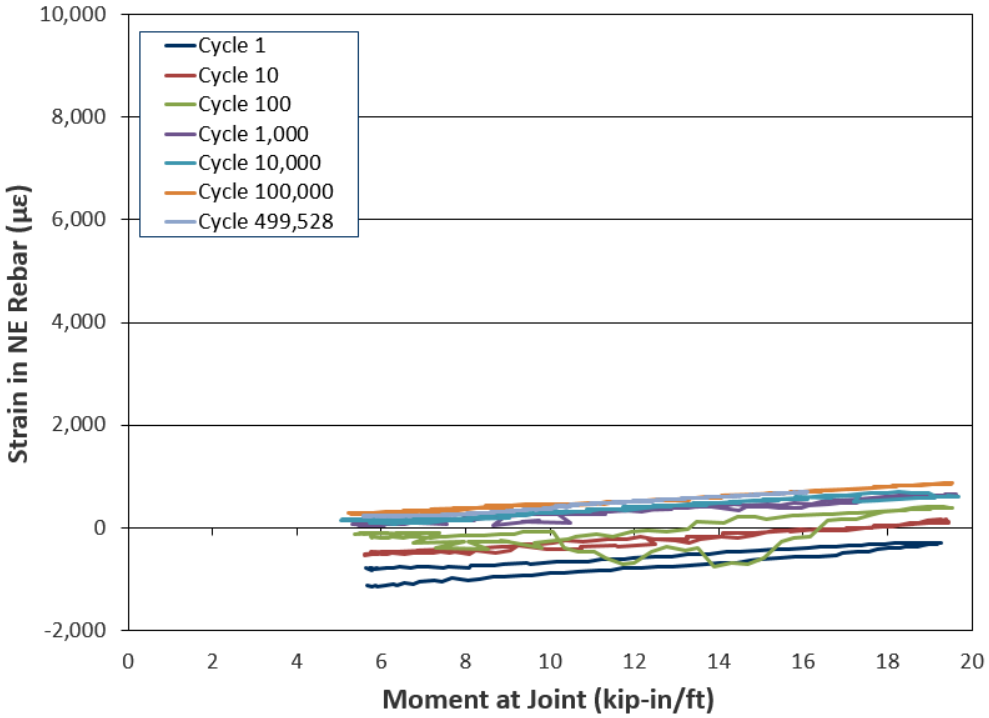


**Figure 5.47: Strain in NE Reinforcing Steel versus Moment at Joint (R-NEG-F)**

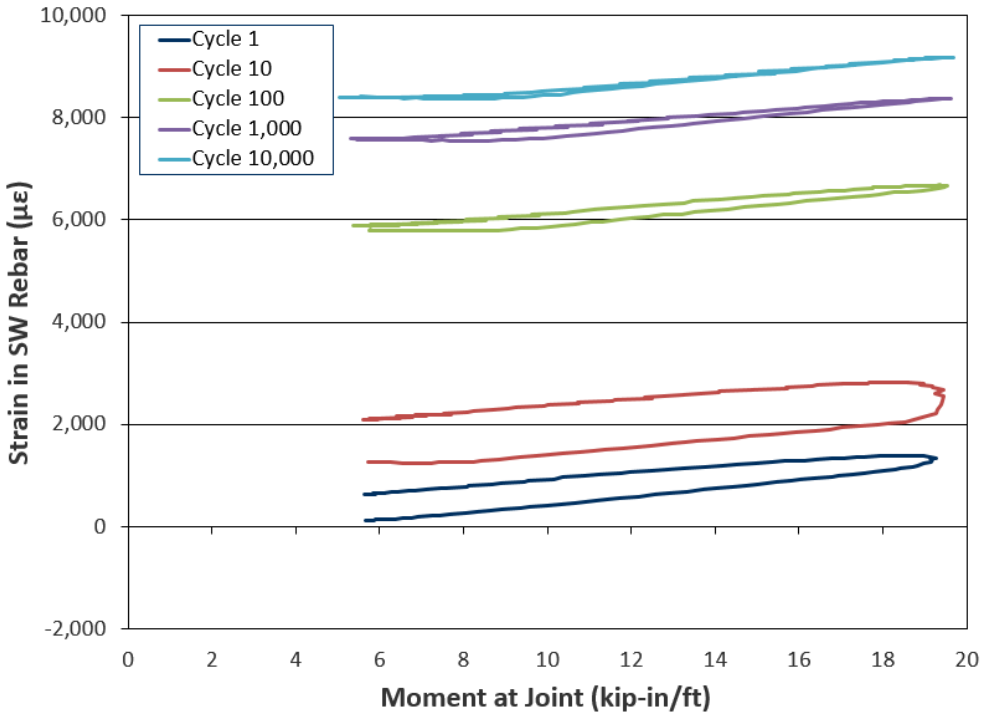


**Figure 5.48: Strain in SW Reinforcing Steel versus Moment at Joint (R-NEG-F)**

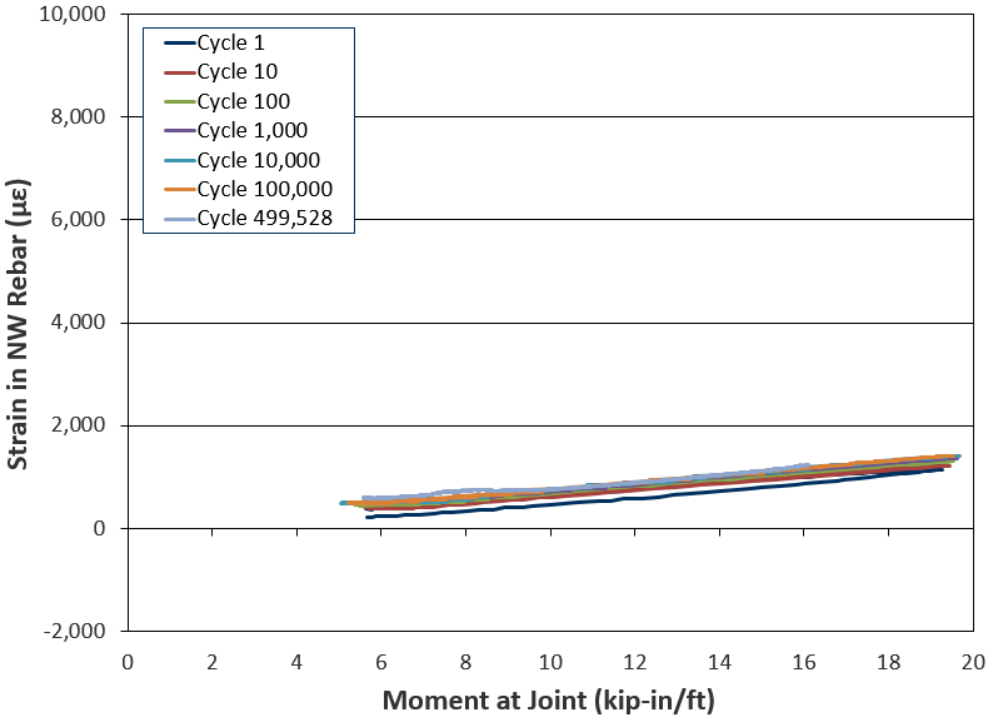


**Figure 5.49: Strain in NW Reinforcing Steel versus Moment at Joint (R-NEG-F)**

**Figure 5.50: Separated Deck Panels (R-NEG-F)**

**Figure 5.51: SE and SW Reinforcing Steel Failure Condition (R-NEG-F)**

### 5.3.3 Shear Reversal Test Results

This third subsection covers fatigue shear reversal bending results for the unreinforced shear key joint (U-REV-F) and staggered hook reinforced joint (R-REV-F) specimens.

#### 5.3.3.1 Unreinforced Shear Key Joint (U-REV-F)

The U-REV-F test was conducted per the prescribed loading procedure. The test was scheduled to run for 2,000,000 cycles and pause at discrete intervals to record the degradation of the joint at the 1st, 10th, 100th, 1,000th, 10,000th, 100,000th, 1,000,000th, and 2,000,000th cycle.

##### 5.3.3.1.1 Visual Inspection

The condition of the joint of the joint at each discrete interval is shown in Figures 5.52 and 5.53. Crack propagation was documented by marking the cracks after each discrete interval. Before testing began, cracks were marked within the deck concrete on the north and south side of the joint starting at the steel WT section and extending up to the reinforcing steel height. These cracks may have formed due to shrinkage or handling of the specimen. After the 1st cycle, no new cracks formed. After the 10th cycle, cracks extended upwards. After the 100th cycle, cracks on the north side of the joint extended and widened. After the 1,000th cycle, additional cracks on the north side of the joint formed. After the 10,000th cycle cracks extended and widened on the north and south side of the joint. After the 100,000th cycle, cracks widened and some extended. After the 1,000,000th cycle, cracks widened. After the 2,000,000th cycle, cracks continued to widen, and the test was concluded without the specimen failing.

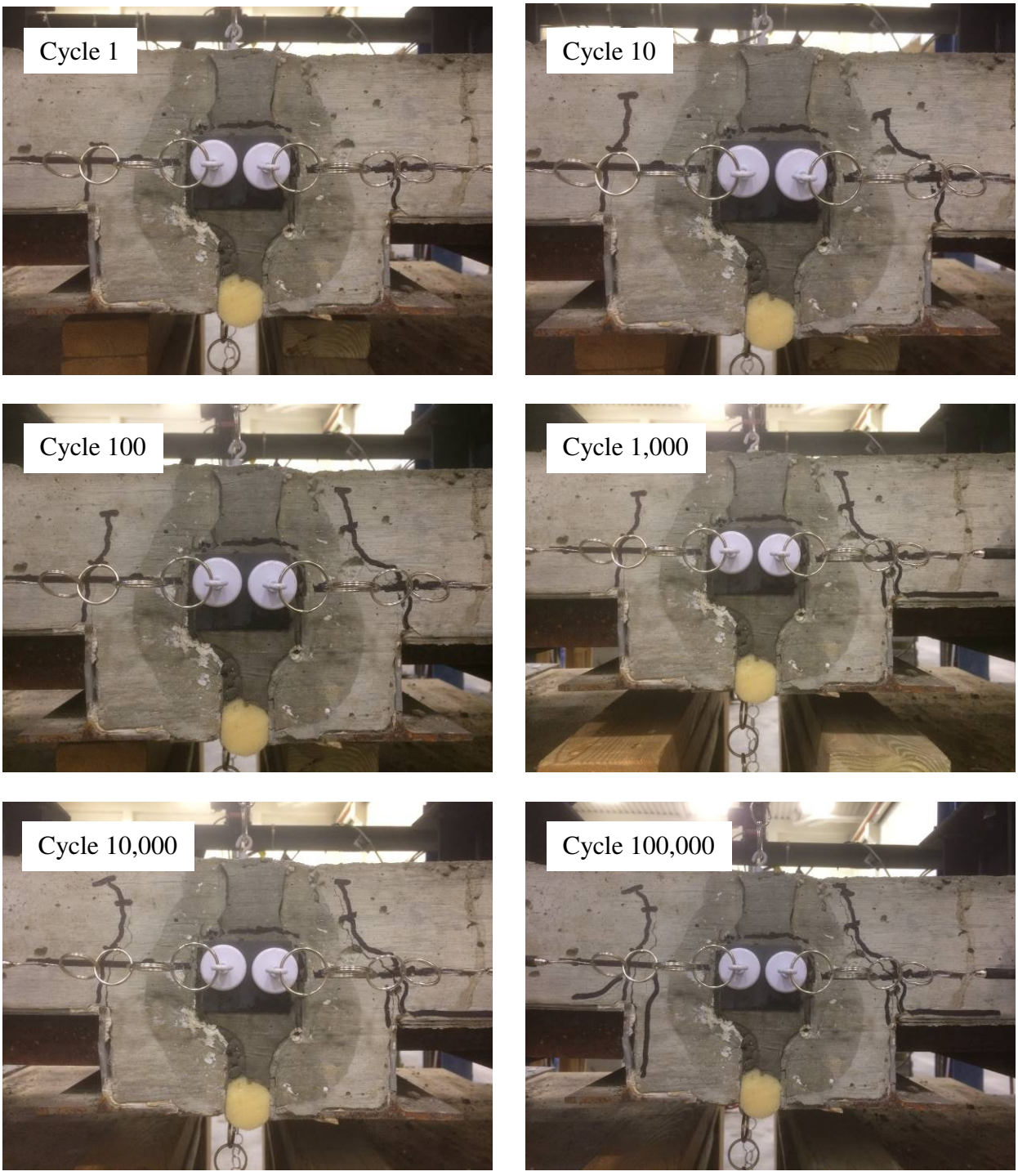


**Figure 5.52: U-REV-F Joint at Discrete Intervals (Part 1 of 2)**

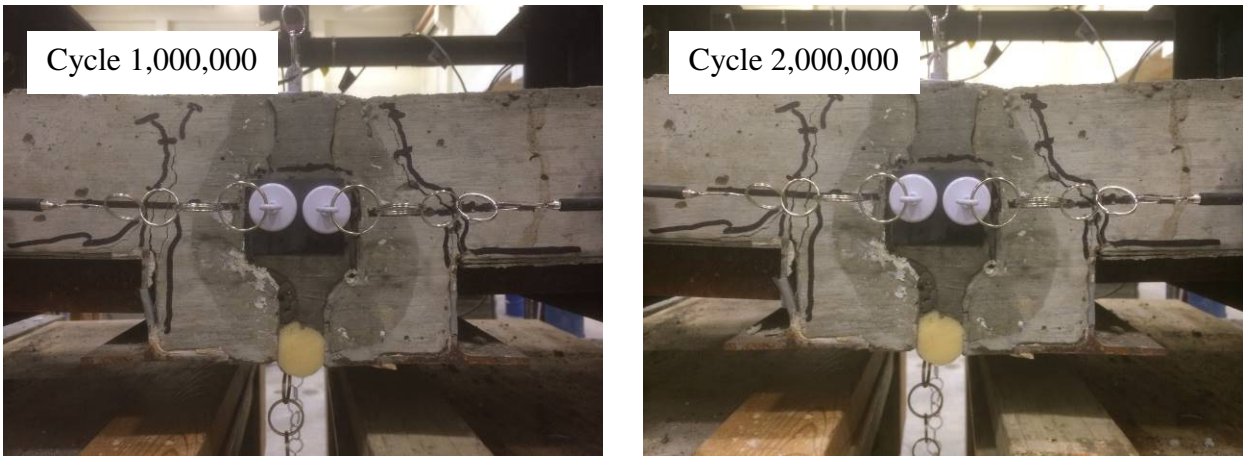


**Figure 5.53: U-REV-F Joint at Discrete Intervals (Part 2 of 2)**

#### 5.3.3.1.2 External Instrumentation

As discussed earlier, external instrumentation consisted of wirepots attached to the top of the specimen to measure midspan deflection, wirepots attached to the bottom of the specimen to measure large midspan deflection, and wirepots attached to the side of the specimen to measure crack opening at the joint-panel interface.

Figure 5.54 shows the behavior of the shear at joint versus midspan deflection. Note at each discrete interval, as the test continued and more cracks formed, the stiffness of the specimen weakened and the midspan deflection increased. Figure 5.55 shows the shear versus midspan deflection of each discrete interval superimposed on top of each other to demonstrate the loss of stiffness of the joint as the test progressed.

Figure 5.56 shows a graph of the south side crack opening versus shear at joint while Figure 5.57 shows a graph of the north side crack opening versus shear at joint. Similarly, as noted above, as the test continued and more cracks formed, the side cracks opened wider. The south and north sides of the joint degraded at similar rates.

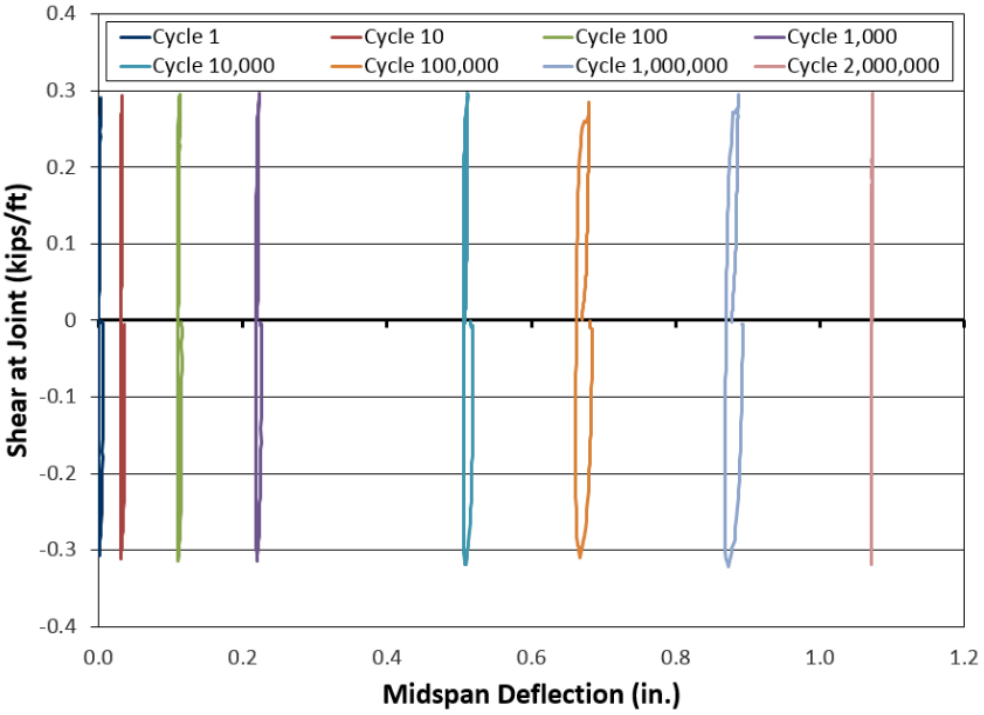


**Figure 5.54: Shear at Joint versus Midspan Deflection (U-REV-F)**

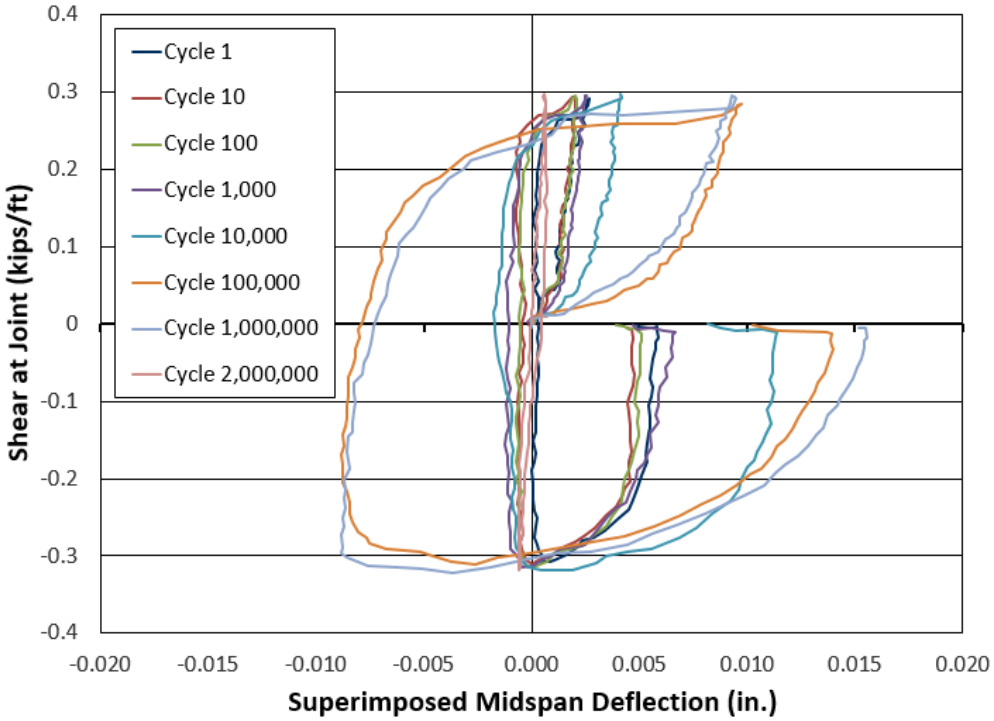


**Figure 5.55: Shear at Joint versus Superimposed Midspan Deflection (U-REV-F)**

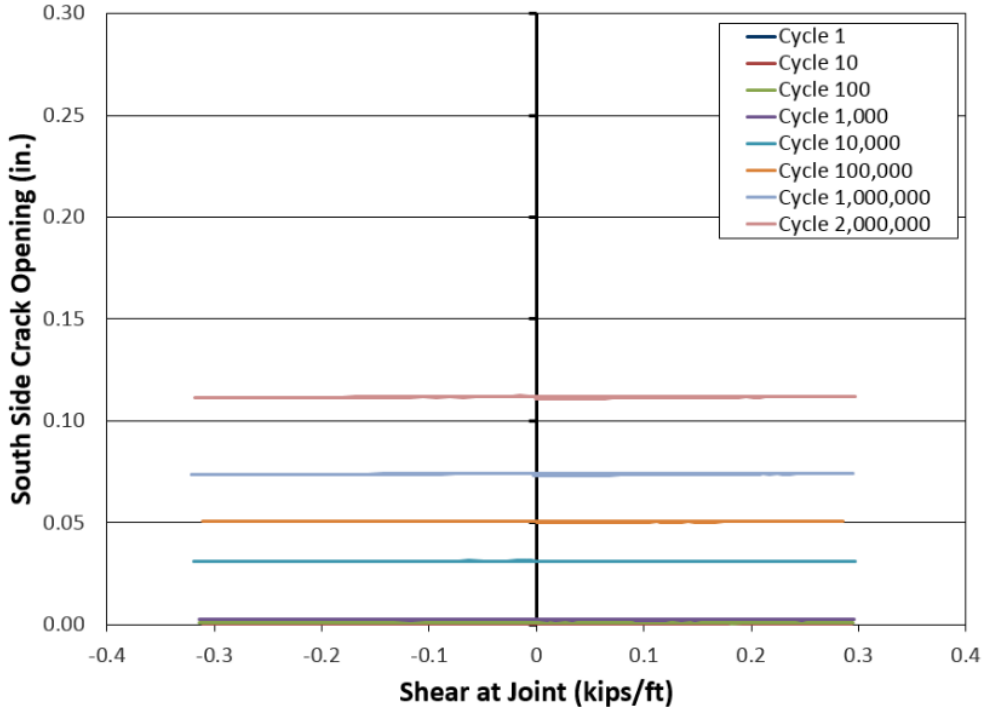


**Figure 5.56: South Side Crack Opening versus Shear at Joint (U-REV-F)**

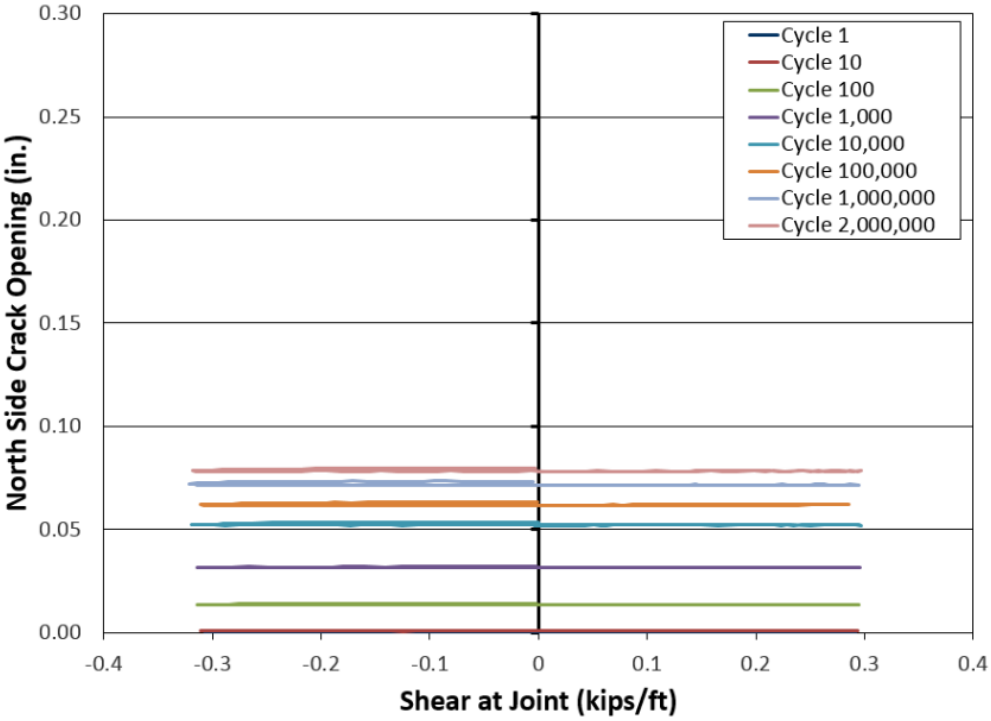


**Figure 5.57: North Side Crack Opening versus Shear at Joint (U-REV-F)**

#### 5.3.3.2 Staggered Hook Reinforced Joint (R-REV-F)

The R-REV-F test was conducted per the prescribed loading procedure. The test was scheduled to run for 2,000,000 cycles and pause at discrete intervals to record the degradation of the joint at the 1st, 10th, 100th, 1,000th, 10,000th, 100,000th, 1,000,000th, and 2,000,000th cycle.

##### 5.3.3.2.1 Visual Inspection

The condition of the joint at each discrete interval is shown in Figures 5.58 and 5.59. Crack propagation was documented by marking the cracks after each discrete interval. After the 1st, 10th, 100th, 1,000th, and 10,000th cycle, no noticeable cracks formed. After the 100,000th cycle, cracks formed within the joint on the north side extending up to the reinforcing steel height. After the 1,000,000th cycle, cracks formed within the joint on the south side extending up to the reinforcing steel height. After the 2,000,000th cycle, no new cracks formed, and the test was concluded without the specimen failing.

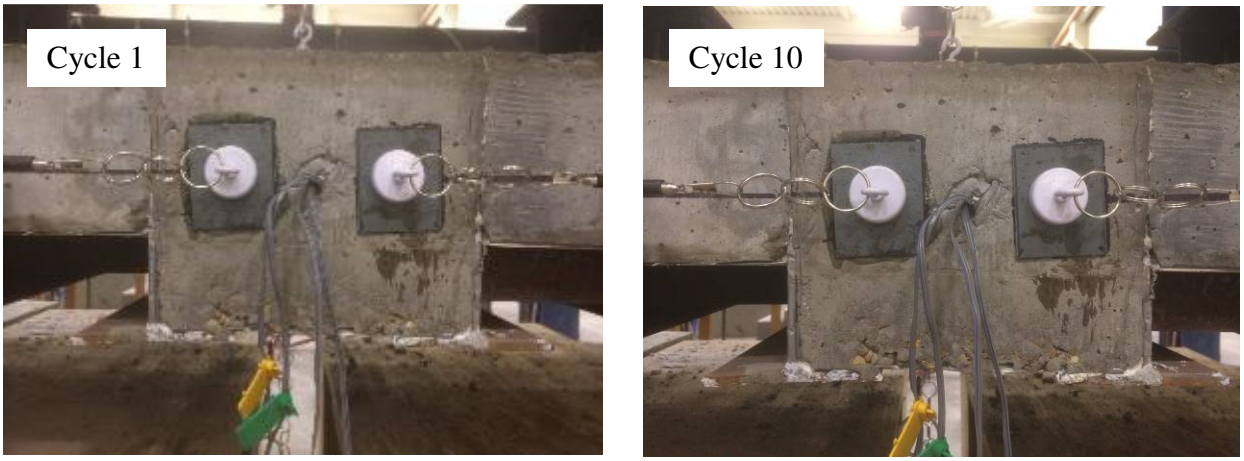


**Figure 5.58: R-REV-F Joint at Discrete Intervals (Part 1 of 2)**

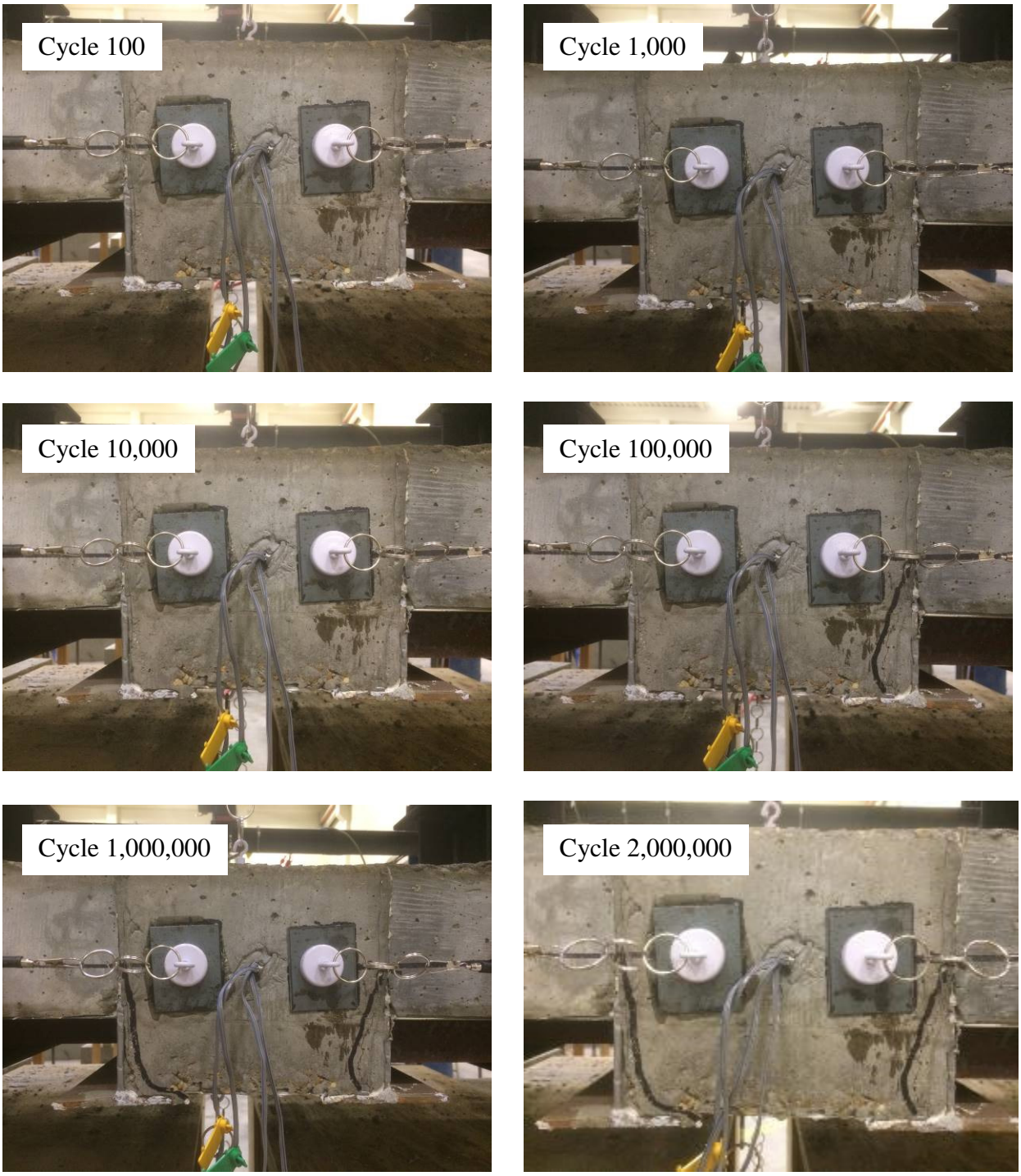


**Figure 5.59: R-REV-F Joint at Discrete Intervals (Part 2 of 2)**

#### 5.3.3.2.2 External Instrumentation

As discussed earlier, external instrumentation consisted of wirepots attached to the top of the specimen to measure midspan deflection, wirepots attached to the bottom of the specimen to measure large midspan deflection, and wirepots attached to the side of the specimen to measure crack opening at the joint-panel interface.

Figure 5.60 shows the behavior of the shear at joint versus midspan deflection. Note at each discrete interval, as the test continued and more cracks formed, the stiffness of the specimen weakened and the midspan deflection increased. Between the 10,000$^{th}$ and 100,000$^{th}$ cycle, there was an increase in midspan deflection. This corresponded to the first crack that formed in the north side of the joint. Figure 5.61 shows the shear versus midspan deflection of each discrete interval superimposed on top of each other to demonstrate the loss of stiffness of the joint as the test progressed.

Figure 5.62 shows a graph of the south side crack opening versus shear at joint while Figure 5.63 shows a graph of the north side crack opening versus shear at joint. Similarly, as noted above, as the test continued and more cracks formed, the side cracks opened wider. The south and north joint interfaces did not widen significantly when compared to other tests.

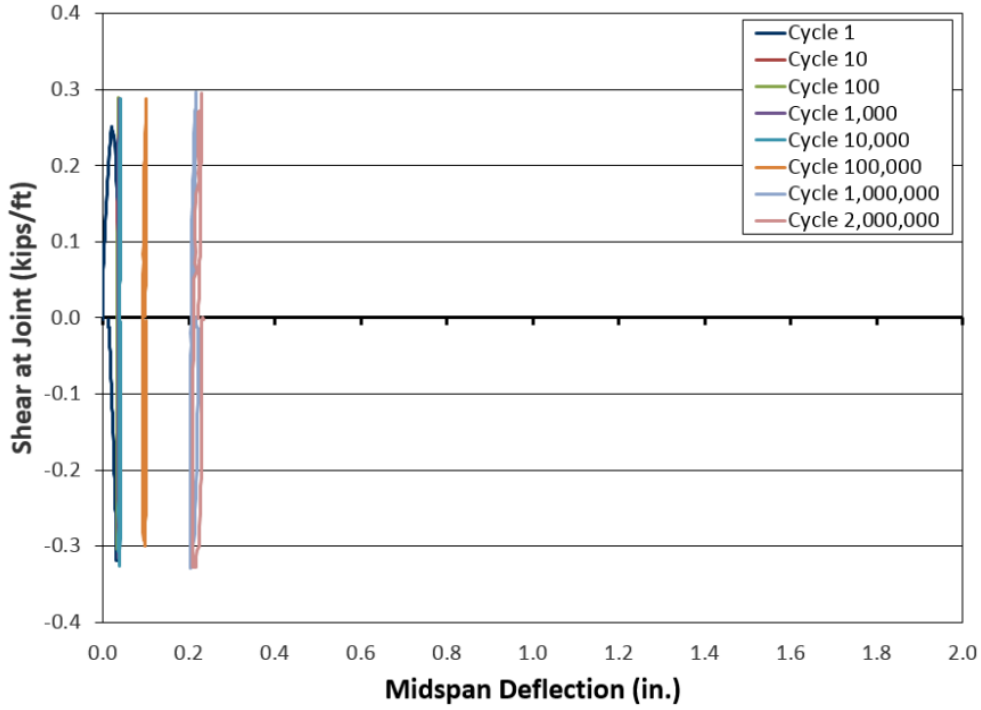


**Figure 5.60: Shear at Joint versus Midspan Deflection (R-REV-F)**

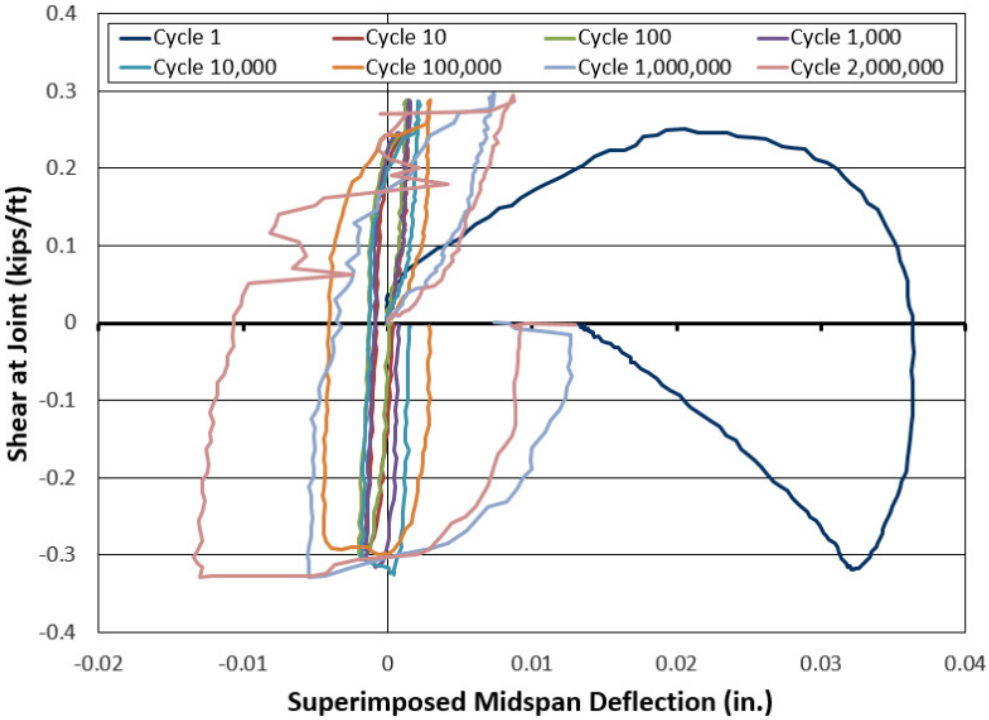


**Figure 5.61: Shear at Joint versus Superimposed Midspan Deflection (R-REV-F)**

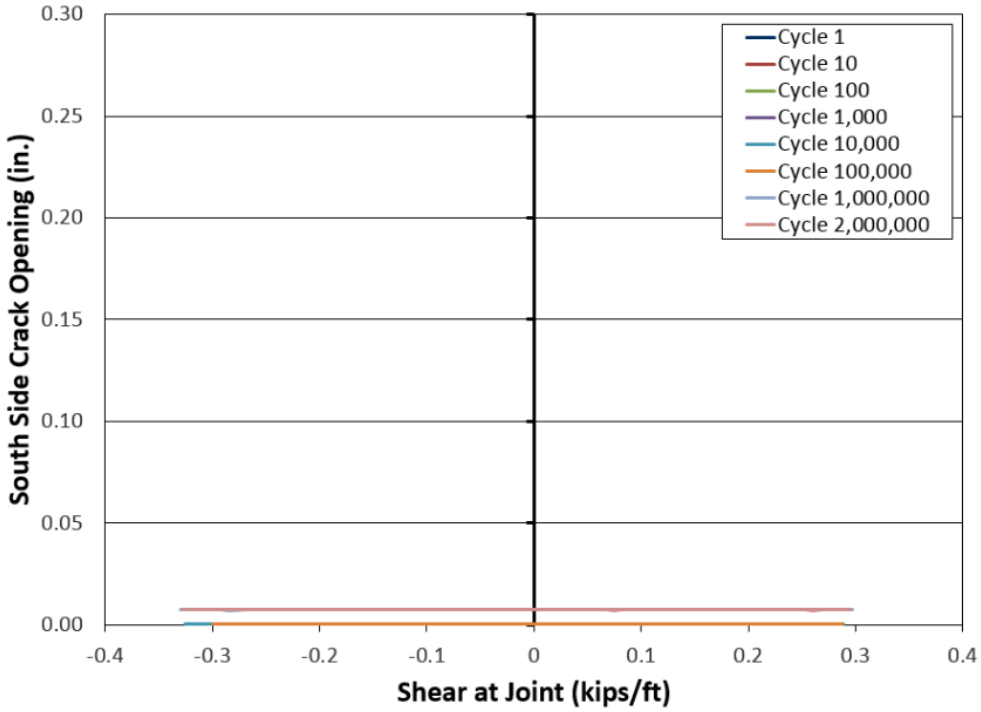


**Figure 5.62: South Side Crack Opening versus Shear at Joint (R-REV-F)**

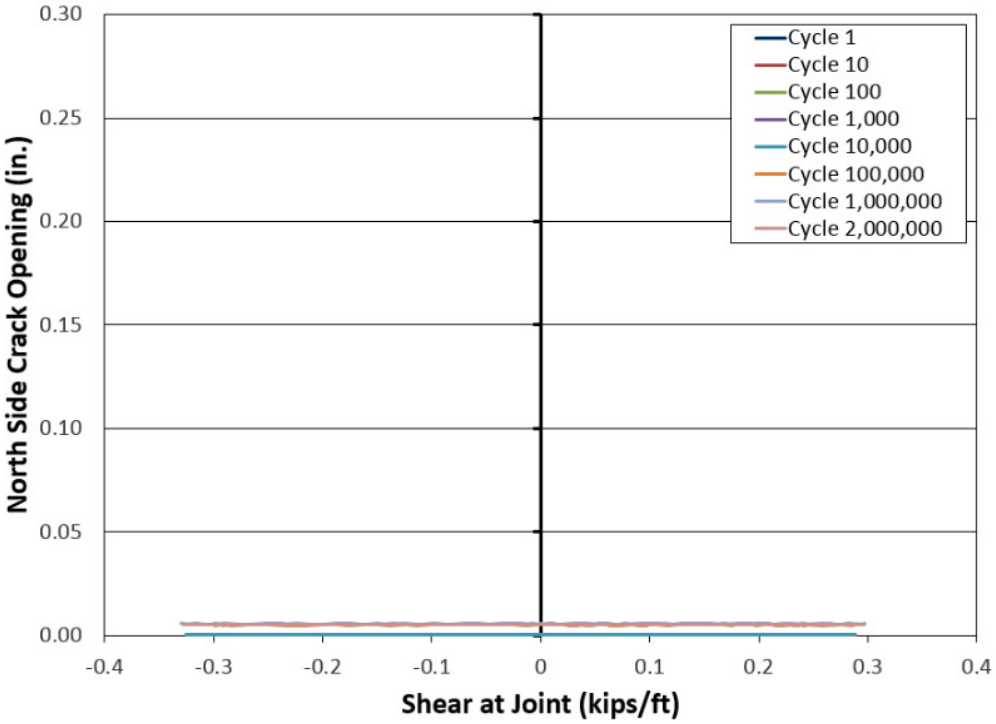


**Figure 5.63: North Side Crack Opening versus Shear at Joint (R-REV-F)**

#### 5.3.3.2.3 Internal Instrumentation

As discussed earlier, internal instrumentation consisted of strain gages attached to each of the four hooked reinforcing bars within the joint.

Figure 5.64, 5.65, 5.66, and 5.67 show the behavior of the SE, NE, SW, and NW strain in reinforcing steel versus shear at joint, respectively. At each discrete interval, as the test continued and more cracks formed, the stiffness of the specimen weakened and the strain in the reinforcement increased. At the 100,000$^{th}$ cycle, there was a significant increase in strain for the NE and NW bars. This corresponded to a crack that formed at the north joint interface. At the 1,000,000$^{th}$ cycle, there was a significant increase in strain for the SE and SW bars. This corresponded to a crack that formed at the south joint interface.

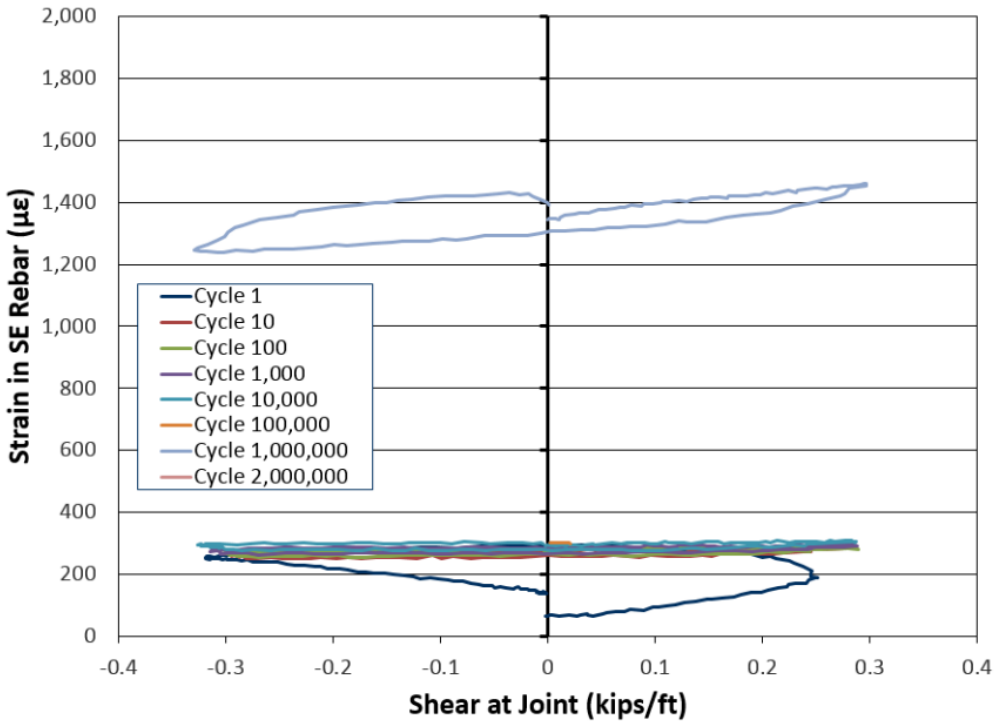


**Figure 5.64: Strain in SE Reinforcing Steel versus Shear at Joint (R-REV-F)**

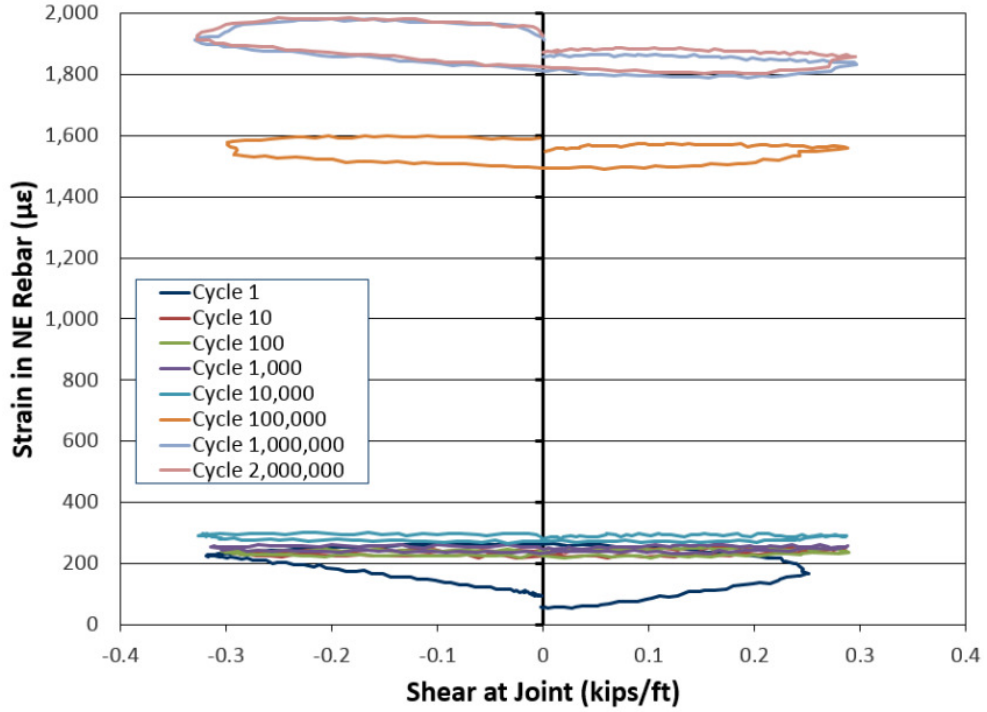


**Figure 5.65: Strain in NE Reinforcing Steel versus Shear at Joint (R-REV-F)**

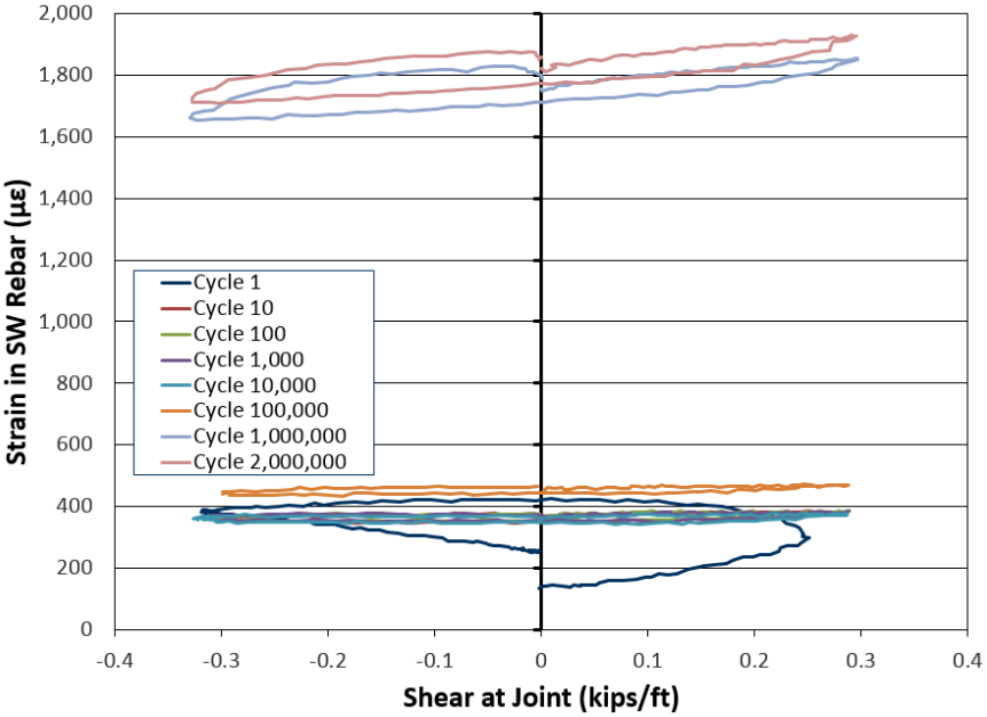


**Figure 5.66: Strain in SW Reinforcing Steel versus Shear at Joint (R-REV-F)**

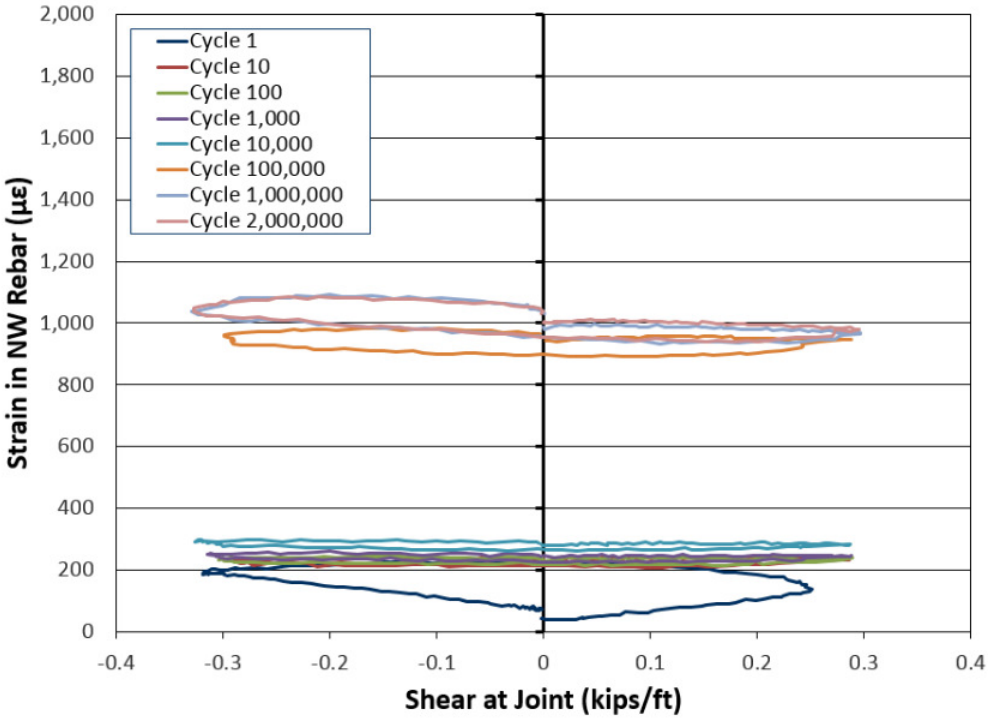


**Figure 5.67: Strain in NW Reinforcing Steel versus Shear at Joint (R-REV-F)**

## 5.4 Discussion

This section summarizes the behavior of the unreinforced shear key joints compared to the staggered hook reinforced joints. Several figures and tables are presented to compare relevant values such as when the first crack formed and when failure occurred. Also, there is a discussion involving the validity of replacing the fatigue test with the shorter, less cumbersome quasi-static test.

### 5.4.1 Flexure Specimens under Quasi-Static Loading

Results of the flexure specimens under quasi-static loading are summarized in Figure 5.68. The moment at the joint and corresponding midspan deflection are shown comparing the specimen behavior at the first crack instance and at failure. It was observed that for the positive bending tests U-POS-Q cracked under less flexural stress than R-POS-Q. The joint moment at the first

crack occurrence for these two specimens was 42% and 75% of $M_{service}$, respectively. Similarly, U-POS-Q failed under less flexural stress than R-POS-Q. The joint moment for these two specimens at failure was 102% and 120% of $M_{service}$, respectively. Both specimens experienced several cracks when loaded and experienced similar values of midspan deflection.

Surprisingly, it was observed that for the negative bending tests U-NEG-Q cracked under more flexural stress than R-NEG-Q. The joint moment at the first crack occurrence for these two specimens was 71% and 56% of $M_{service}$, respectively. However, U-NEG-Q failed under less flexure stress than R-NEG-Q. The moment at the joint for these two specimens at failure was 71% and 112% of $M_{service}$, respectively. The unreinforced shear key joint specimen failed in a brittle manner along the joint interface with no sign of degradation. In contrast, the reinforced staggered hook joint specimen experienced several cracks when loaded, and failed after large amounts of deflection.

The two staggered hook reinforced joint specimens had greater ultimate strength than the unreinforced shear key joint specimens in both the positive bending and negative bending tests. In addition, both the staggered hook reinforced joint specimens exceeded the service-level moment demand, $M_{service}$. This difference in bending capacity between the two specimen types was due to the fact that one type had reinforcing extending out of the deck concrete and into the joint while the other did not.

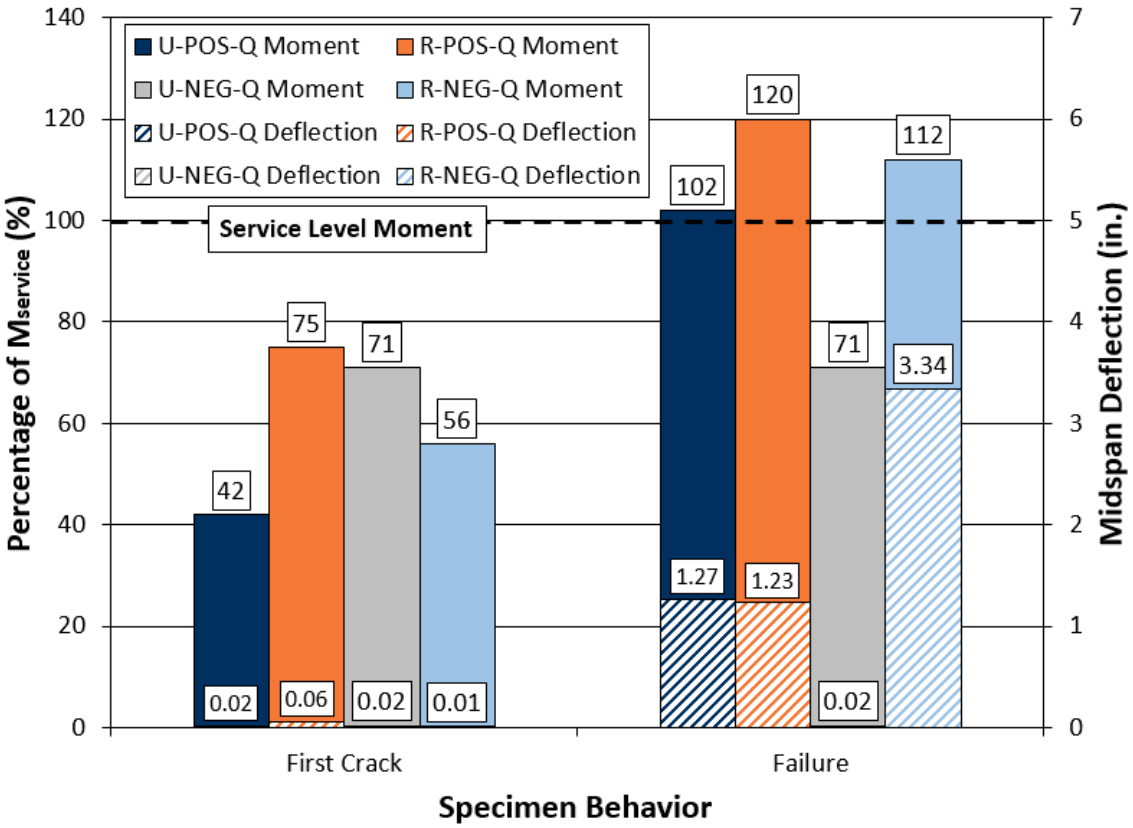


**Figure 5.68: Capacities of Flexure Specimens under Quasi-Static Loading**

### 5.4.2 Shear Reversal Specimens under Quasi-Static Loading

Results of the shear reversal specimens under quasi-static loading are summarized in Figure 5.69. The shear at the joint and corresponding midspan deflection are shown comparing the specimen behavior at the first crack instance and at failure. It was observed that for the shear reversal tests U-REV-Q cracked under similar shear stress as R-REV-Q. The joint shear at the first crack occurrence for these two specimens were both 56% of $V_{service}$. Surprisingly, U-REV-Q failed under slightly more shear stress than R-REV-Q. The joint shear for these two specimens at failure was 99% and 85% of $V_{service}$, respectively. Both specimens experienced several cracks when loaded and experienced large amounts of midspan deflection.

Although the unreinforced shear key joint specimen had greater ultimate strength than the staggered hook reinforced joint specimen, neither one exceeded the service-level shear demand, $V_{service}$. Therefore, comparing the two specimens proved to be inconclusive.

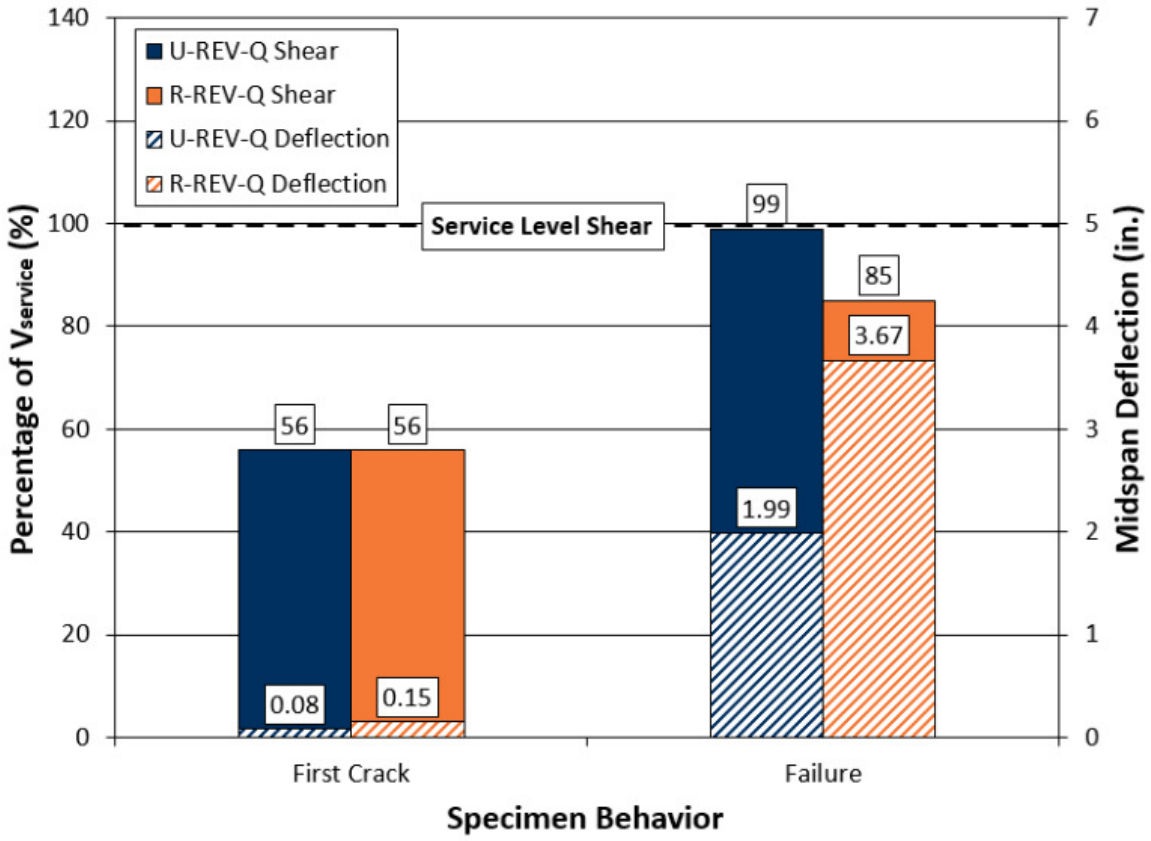


**Figure 5.69: Capacities of Flexure Specimens under Quasi-Static Loading**

### 5.4.3 Flexure Specimens under Fatigue Loading

It is important to recall that the loading for the fatigue tests for this research project was less than what was recommended for future experimental programs. This was because the results from the quasi-static tests showed that on average the test specimens did not have the capacity to resist the service-level stresses. The applied load for fatigue flexure test for this research project corresponded to 30% of $M_{cr}$ which was approximately 67% of $M_{service}$.

Results of the flexure specimens under fatigue loading are summarized in Table 5.1. The cycle count and corresponding midspan deflection are shown comparing the specimen behavior at the first crack instance and at failure. It was observed that for the positive bending tests U-POS-F cracked with less cycles than R-POS-F. The cycle count at the first crack occurrence for these two specimens was 1 and sometime before 1,000 respectively. Similarly, U-POS-F failed with less cycles than R-POS-F. The cycle count for these two specimens was 51,477 and greater than 2,000,000, respectively. The unreinforced shear key joint experienced several cracks when loaded and large midspan deflection due to the gradual degradation of the joint. In contrast, the staggered hook reinforced joint specimen maintained similar stiffness for the duration of the test and had minimal midspan deflection.

Surprisingly, it was observed that for the negative bending tests U-NEG-F cracked with more cycles than R-NEG-F. The cycle count at the first crack occurrence for these two specimens was sometime before 10 and 1, respectively. However, U-NEG-F failed with less cycles than R-NEG-F. The cycle count for these two specimens was 14 and 499,528, respectively. The unreinforced shear key joint specimen failed in a brittle manner with little sign of degradation. In contrast, the staggered hook reinforced joint specimen experienced several cracks when loaded and exhibited a large amount of midspan deflection.

The two staggered hook reinforced joint specimens resisted a significant amount more number of cycles than the unreinforced shear key joint specimens in both the positive bending and negative bending tests. This difference in bending capacity between the two specimen types was due to the fact that one type had reinforcing extending out of the deck concrete and into the joint

while the other did not. However, only the R-POS-F specimen endured the entire 2,000,000 cycle test. Therefore, comparing the two specimens proved to be inconclusive.

**Table 5.1: Capacities of Flexure Specimens under Fatigue Loading**

| | | Cycle Number | Midspan Deflection (in.) |
|---|---|---|---|
| **U-POS-F** | First Crack | 1 | 0.08 |
| | Failure | 51,477 | 1.00 |
| **R-POS-F** | First Crack | 1,000 | 0.02 |
| | Failure | > 2,000,000 | 0.14 |
| **U-NEG-F** | First Crack | 10 | 0.02 |
| | Failure | 14 | 0.18 |
| **R-NEG-F** | First Crack | 1 | 0.11 |
| | Failure | 499,528 | 1.95 |

### 5.4.4 Shear Reversal Specimens under Fatigue Loading

It is important to recall that the loading for the fatigue tests for this research project was less than what was recommended for future experimental programs. This was because the results from the quasi-static tests showed that on average the test specimens did not have the capacity to resist the service-level stresses. The applied load for fatigue shear-reversal tests for this research project corresponded to 3% of $V_n$ which was approximately 42% of $V_{service}$.

Results of the shear reversal specimens under fatigue loading are summarized in Table 5.2. The cycle count and corresponding midspan deflection are shown comparing the specimen

behavior at the first crack instance and at failure. It was observed that for the shear reversal tests U-REV-F cracked with less cycles than R-REV-F. The cycle count at the first crack occurrence for these two specimens was 1 and sometime before 100,000, respectively. Both specimens survived the full 2,000,000 cycle test without failure. The unreinforced shear key joint experienced several cracks when loaded and showed a large amount of midspan deflection. In contrast, the staggered hook reinforced joint specimen maintained similar stiffness for the duration of the test and had minimal midspan deflection.

Since both specimens endured the 2,000,000 cycle test it can be concluded that the staggered hook reinforced joint specimen performed better than the unreinforced shear key joint specimen, because the difference in midspan deflection at the termination of the test was significant. This difference in joint stiffness between the two specimen types was due to the fact that one type had reinforcing extending out of the deck concrete and into the joint while the other did not.

**Table 5.2: Capacities of Shear-Reversal Specimens under Fatigue Loading**

| | | **Cycle Number** | **Midspan Deflection (in.)** |
|---|---|---|---|
| **U-REV-F** | First Crack | 1 | 0.01 |
| | Failure | > 2,000,000 | 1.07 |
| **R-REV-F** | First Crack | 100,000 | 0.03 |
| | Failure | > 2,000,000 | 0.23 |

### 5.4.5 Joint Deterioration and Deck System Performance

Crack formation and failure modes between the two specimen joint types used in this research project differed greatly. Figure 5.70 shows the differences in the crack locations between the two joint types. All the unreinforced shear key joint specimens initially cracked due to cracks originating within the precast deck concrete at the top of the steel WT section. The only exception was U-NEG-Q. It may be concluded that this specimen did not have adequate bonding at the interface between the precast concrete and the closure grout. However, all the staggered hook reinforced joint specimens initially cracked due to cracks originating at the joint-panel interface. The discontinuity between the deck concrete surface, joint grout surface, and WT steel section provided an optimal location for cracks to form.

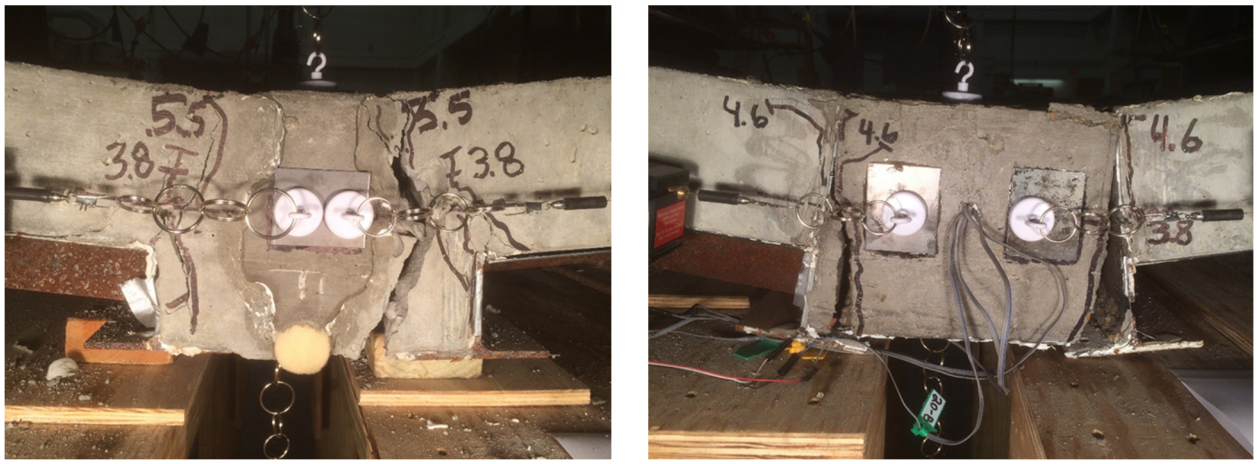


**Figure 5.70: Cracking Behavior in the Unreinforced and Reinforced Joints**

The Exodermic deck system, like many other bridge deck systems, spans in two directions simultaneously (two-way bending) but is primarily designed to transfer loads transversely across girders (one-way bending). For this reason, if cracks form and grow within the transverse joint, load-carrying capacity of the deck system is not necessarily compromised: the loads may be redistributed to the stiffer transverse span between girders. In the extreme, continued deterioration

of the transverse joint would gradually place more flexural and shear demand in the direction spanned by the WT sections from girder to girder, and the deck system would gradually transform into a collection of one-way spanning panels. This joint deterioration could shorten the service life of the bridge via durability and ride quality issues, but collapse would be unlikely. Because of the configuration of WT sections and metal stay-in-place concrete form sheets, initial cracking like that observed during positive flexure and shear reversal tests would not be visible in an actual bridge deck. Deposits of leached material on the bottom surface of the deck system may be the earliest visible indicator of this type of joint cracking.

### 5.4.6 Potential for Replacing the Fatigue Test with the Quasi-Static Test

Overall, the test specimens did not reach satisfactory ultimate strength or fatigue durability. The poor performance in general may be due to the fact that the design of the panels includes a reduction in cross section immediately adjacent to the joint location, which limits the cracking resistance and strength capacity of the joint-panel system. In addition, the panel design only allowed joint reinforcement to have a small effective depth for positive and negative moment resistance.

However, these results do not indicate that the Exodermic deck system lacks adequate strength for use in bridge deck rehabilitation. The laboratory tests were designed as a small set of simple, conservative acceptance-type tests for transverse joint performance that would ideally be applicable to a wide variety of bridge and panel types and configurations. Therefore, the tests were designed to result in stresses at least as large as the maximum possible stresses expected from any location under any truck position of any deck type in any common ALDOT girder-supported bridge deck. Thus, if the jointed specimens exceed the very conservative requirements from the

proposed test methods and performance criteria, then the testing agency can confidently recommend the joint as strong and durable enough for general use.

The converse is not necessarily true. When the panels are installed on a bridge they are composite with the longitudinal girders so there is far less post-cracking deflection experienced by the joint compared to the post-cracking deflections from the laboratory tests. Furthermore, as explained in the preceding section, limited cracking of the transverse joint is expected to result in a gradual transformation to a more one-way load-carrying mechanism between girders. Therefore, if a deck joint type falls short of the performance criteria determined for this trial acceptance testing for general use, it does not indicate that the deck joint system is unsafe for any particular bridge rehabilitation project.

Three out of the four quasi-statically loaded flexure specimens, U-POS-Q, R-POS-Q, and R-NEG-Q, exceeded the full service-level moment at failure with 102%, 120%, and 112% of $M_{service}$, respectively. Neither of the two quasi-statically loaded shear reversal specimens exceeded the designated service-level shear at failure. The U-REV-Q specimen was close since it failed at 99% of $V_{service}$. Only the R-POS-F specimen survived the entire flexure fatigue test. Both the U-REV-F and R-REV-F specimens survived the entire shear-reversal fatigue test. Therefore, only the results from the R-POS-Q and R-POS-F tests can be used to judge the correlation between the quasi-static test and the fatigue test.

Unfortunately for this research project, a larger sample size of successful quasi-static and fatigue tests needed to be completed in order to accurately judge whether there was any correlation between the two test types. So, this research team cannot conclusively recommend future experimental programs based solely on the quasi-static test. There is opportunity for future

research projects to follow the test methods outlined in this research project to perform tests and determine if there is any correlation. As of this writing, it is recommended to perform both the quasi-static tests and the fatigue tests to determine the acceptability of proposed bridge deck joint systems.

# CHAPTER 6: SUMMARY, CONCLUSIONS, AND RECOMMENDATIONS

## 6.1 Summary

ALDOT does not have any standards to test or evaluate the performance of transverse joints in precast-panel bridge deck systems. This research project developed test methods and performance criteria to compare the behavior of various precast-panel transverse joints and determine their acceptability. The test methods and performance criteria were developed by testing a proprietary deck system in the laboratory. The two joint types for the Exodermic deck system were the unreinforced shear key joint and the reinforced staggered hook joint. The transverse joints were tested in quasi-static and fatigue loading for positive bending, negative bending, and shear reversal. Data were collected and analyzed to determine the in-service and long-term performance of the joints. The results were based on capacity, midspan deflection, and crack opening of the specimens.

The performance criteria required that the transverse joints reach an ultimate strength of at least 100% of $M_{service}$ for quasi-statically loaded flexure specimens and at least 100% of $V_{service}$ for quasi-statically loaded shear-reversal specimens. The $M_{service}$ was 28.9 kip-in/ft and $V_{service}$ was 0.728 kips/ft, which were based on stress demands in a deck joint determined from finite element analysis of a standard ALDOT bridge (Rhett 2012). The performance criteria also required that the transverse joints reach a fatigue durability of at least 2,000,000 cycles before failure for the flexure and shear reversal specimens.

## 6.2 Conclusions

The results of this research project yielded the following conclusions:

- The load configuration outlined in Chapter 3 conservatively produces peak realistic stresses on joint specimens due to positive bending, negative bending, and shear reversal as determined from finite-element analyses of a range of standard ALDOT bridges.
- The loading procedure outlined in Chapter 3 provides an efficient and adequate procedure to determine the ultimate strength and fatigue durability of transverse joints.
- Overall, the transverse joints tested in this research project did not satisfy the conservative proposed performance criteria.
- Joint grout materials and proportions should be pre-qualified prior to use in precast deck rehabilitation projects.
- Grout should be tested prior to transverse joint testing to ensure grout meets project design requirements.
- A larger sample size of successful quasi-static and fatigue tests using a variety of panel types need to be completed in order to accurately judge whether there is any useful correlation between the quasi-static test and the fatigue test.
- This research team cannot conclusively recommend transverse joint acceptance based solely on the quasi-static test described in Chapter 3.

## 6.3 Recommendations

Several laboratory tests were conducted in this research project to develop test methods and performance criteria for acceptance of precast-panel bridge-deck transverse joints. To better understand the performance of various deck systems for implementation in ALDOT bridges, the following future work is recommended:

- Conduct small-scale laboratory tests of post-tensioned full-depth precast deck transverse joints and non-post-tensioned full-depth precast deck transverse joints to compare ultimate strength and fatigue durability.
- Conduct full-scale laboratory tests of precast deck panels composite with steel girders to compare the performance of various transverse joint types.
- Compare precast deck transverse joints with different surface preparation techniques such as sandblasting or epoxy coating the joint surfaces.
- Compare precast deck transverse joints with different types of grout materials.
- For future experimental programs testing the acceptability of proposed deck joint specimens, the following test method should be followed:
    - Simply supported span length of 72 in.
    - Specimen width of at least 12 in., but 24 in. is recommend. Width must be adequate to reflect representative joint reinforcing details, if any.
    - Apply load at location so that moment-shear ratio is 40 in. or smaller.

- Apply load for flexure tests so that service-level moment at joint is 28.9 kip-in per ft of joint specimen width.
- Apply load for shear reversal tests so that service-level shear at joint is 0.728 kips per ft of joint specimen width.
- For all tests measure the applied load (including the calculated moment and shear at the joint) and midspan deflection (at the joint location).
- For quasi-static tests:
    - For flexure tests the "load steps" should be 10% of $M_{cr}$, 20% of $M_{cr}$, 30% of $M_{cr}$, etc. where $M_{cr}$ is a function of measured compressive strength of the deck concrete and the dimension of a unit width of deck joint.
    - For shear reversal tests the "load steps" should be 1% of $V_n$, 2% of $V_n$, 3% of $V_n$, etc. where $V_n$ is a function of measured compressive strength of the deck concrete and the dimension of a unit width of deck joint.
    - The load should be cycled five times at 0.02 Hz up to the calculated value and down to a minimum load of 0.25 kips per ft of joint specimen width before advancing to the next load step.
- For fatigue tests:
    - For flexure tests apply load so that service-level moment at joint is 28.9 kip-in per ft of joint specimen width.
    - For shear reversal tests apply load so that service-level shear at joint is 0.728 kips per ft of joint specimen width.

- All fatigue tests should be cycled up to the service-level value and down to a minimum load of 0.25 kips per ft of joint specimen width. The test should run for 2,000,000 cycles at 1.0 to 2.0 Hz and pause at discrete intervals to record the degradation of the joint at the $1^{st}$, $10^{th}$, $100^{th}$, $1{,}000^{th}$, $10{,}000^{th}$, $100{,}000^{th}$, $1{,}000{,}000^{th}$, and $2{,}000{,}000^{th}$ cycle.

## References


Ahmadi, Ahmad K. 1997. *Splicing Grid Reinforced Concrete Bridge Deck Panels Without Welding Using Conventional Rebar Methods.* BGFMA.

American Association of State Highway and Transportation Officials. 2007. *AASHTO LRFD Bridge Design Specifications. 4th Edition.* Washington, D.C.

American Society for Testing and Materials. 2015. *ASTM A1064 - Standard Practice for Carbon-Steel Wire and Welded Wire Reinforcement, Plain and Deformed, for Concrete.* West Conshohocken, PA: ASTM International.

—. 2016. *ASTM C138 - Standard Test Method for Density (Unit Weight), Yield, and Air Content (Gravimetric) of Concrete.* West Conshohocken, PA: ASTM International.

—. 2016. *ASTM C143 - Standard Test Method for Slump of Hydraulic-Cement Concrete.* West Conshohocken, PA: ASTM International.

—. 2014. *ASTM C172 - Standard Practice for Sampling Freshly Mixed Concrete.* West Conshohocken, PA: ASTM International.

—. 2014. *ASTM C231 - Standard Test Method for Air Content of Freshly Mixed Concrete by the Pressure Method.* West Conshohocken, PA: ASTM International.

—. 2012. *ASTM C31 - Standard Practice for Making and Curing Concrete Test Specimens in the Field.* West Conshohocken, PA: ASTM International.

—. 2015. *ASTM C39 - Standard Test Method for Compressive Strength of Cylindrical Concrete Specimens.* West Conshohocken, PA: ASTM International.

—. 1998. *ASTM D6275 - Standard Practice for Laboratory Testing of Bridge Decks.* West Conshohocken, PA: ASTM International.

Au, Alexander, Clifford Lam, and Bala Tharmabala. 2011. *Investigation of Closure-Strip Details for Connecting Prefabricated Deck Systems.* PCI Journal, Summer 2011: 75-93.

Battaglia, Irene K., and Deb Bischoff. 2010. *Exodermic Bridge Deck Performance Evaluation.* Report Number: FEP-06-10, Madison, WI: Wisconsin Department of Transportation.

Bettigole, Neal, and Rita Robison. 1997. *Bridge Decks: Design, Construction, Rehabilitation, Replacement.* New York: ASCE Press.

Bettigole, Robert A. 1998. *Exodermic Dexks and Steel Bridges.* Modern Steel Construction.

Biswas, Mrinmay. 1986. *Precast Bridge Deck Design Systems* PCI Journal, March-April 1986: 40-94.

Bowers, Susan E. 2007. *Recommendations for Longitudinal Post-Tensioning in Full-Depth Precast Concrete Bridge Deck Panels.* Master's thesis, Virginia Polytechnic Institute and State University.

Bridge Grid Flooring Manufacturers Association. 2013. "Grid Reinforced Concrete and Exodermic Bridge Decks." *BGFMA.* Accessed January 29, 2015. www.bgfma.org.

Chapman, Cheryl Elizabeth. 2010. *Behavior of Precast Bridge Deck Joints with Small Bond Diameter U-Bars.* Master's thesis, University of Tennessee, Knoxville.

Culmo, Michael. 2000. *Rapid Bridge Deck Replacement with Full-Depth Precast Concrete Slabs* Transportation Research Record: Journal of the Transportation Research Board. Paper No. 00-1220: 139-146.

D.S. Brown Company. 2007. *An Introduction to: Exodermic Bridge Decks. Exodermic Bridge Deck.* Accessed January 29, 2015. www.exodermic.com.

—. 2017a. *Design Overview - How It Works.* Accessed June 8, 2017. http://www.exodermic.com/Design/HowItWorks.aspx.

—. 2017b. *Representative Exodermic Bridge Deck Projects: Tappan Zee Bridge, Tarrytown, NY.* Accessed June 9, 2017. http://www.exodermic.com/Projects/.

Federal Highway Administration. 2016. *Deficient Bridges by Highway System 2016.* Accessed June 8, 2017. https://www.fhwa.dot.gov/bridge/nbi/no10/defbr16.cfm.

Harvey, Bryan Edward. 2011. *Design & Construction Planning of Rapid Bridge Deck Replacement Systems for I-59 Bridges at Collinsville, AL.* Master's thesis, Auburn University, Alabama.

Issa, Mohsen A., Alfred A. Yousif, and Mahmoud A. Issa. 2000. *Experimental Behavior of Full-Depth Precast Concrete Panels for Bridge Rehabilitation* ACI Structural Journal, May-June 200: 397-407.

Ma, Zhongguo John, Samuel Lewis, Qi Cao, Zhiqi He, Edwin G. Burdette, and Catherine E.W. French. 2012. *Transverse Joint Details with Right Bend Diameter U-Bars for Accelerated Bridge Construction* Journal of Structural Engineering, June 2012: 697-707.

Porter, Scott D. 2009. *Laboratory Testing of Precast Bridge Deck Panel.* Master's thesis, Utah State University, Utah.

Ramey, G. Ed, and Russell S. Oliver. 1998. *Rapid Rehabilitation/Replacement of Bridge Decks.* Final Report-ALDOT Research Project 930-376, Highway Research Center, Auburn University.

Rao, Chetana, Armen Tajirian, and Richard Stubstad. 2003. *Lessons Learned from the Tappan Zee Bridge, New York.* Sacramento, CA: State of California Department of Transportation.

Rhett, Brian Mark. 2012. *An Analytical Investigation of Transverse Joints in Precast-Panel Bridge-Deck Replacement Systems.* Master's thesis, Auburn University, Alabama.

Ryu, Hyung-Keun, Young-Jin Kim, and Sung-Pil Chang. 2007. *Experimental Study on Static and Fatigue Strength of Loop Joints* Engineering Structures, No. 29: 145-162.

Sullivan, Sean R. 2003. *Behavior of Transverse Joints in Precast Deck Panel Systems.* Master's thesis, Ohio University, Ohio.

Umphrey, Joshua Matthew. 2006. *Documentation of the Rapid Replacement of Four GDOT Bridge Decks.* Master's thesis, Auburn University, Alabama.

Zhu, Peng, Zhongguo John Ma, Qi Cao, and Catherine E. French. 2012. *Fatigue Evaluation of Transverse U-Bar Joint Details for Accelerated Bridge Construction* Journal of Bridge Engineering, March-April 2012: 191-200.

# Appendix A: Exodermic Bridge Deck Properties

## Grid Deck Properties - Design and Specification Data

### Exodermic™ Deck with 2" Concrete Cover Over Rebar

- High Strength to Weight Ratio
- Rapid Construction
- Light Weight
- Low Cost to Strength Ratio
- Cast-in-Place or Precast



| | Main Bars | Top Rebar | Positive Moment Region | | Negative Moment Region | | | | Approximate Weight (psf) | | | * Maximum Spans (LRFD 4.6.2.1.8) | |
|---|---|---|---|---|---|---|---|---|---|---|---|---|---|
| | | | Section Modulus (in³/ft) | | Section Modulus (in³/ft) | | | | | | | | |
| | Spacing (in.) | Size and Spacing | Top of Concrete (compression) | Bottom of Steel (tension) | Top Rebar (tension) | Top of Distribution Bar Weld (tension) | Bottom of Steel (compression) | Total Height (in.) | Weight of Grid with Pans | Total Weight with Concrete | Main Bars Perpendicular to Traffic (ft) | Main Bars Parallel to Traffic (ft) |
| Shallow W7x45 | 8 | #5 @ 4" | 61.7 | 6.8 | 3.8 | 15.8 | 4.9 | 6.3 | 12.2 | 62.8 | 9.5 | 7.6 |
| | 10 | #5 @ 5" | 55.9 | 5.6 | 3.0 | 12.6 | 3.9 | 6.3 | 10.7 | 61.0 | 7.2 | 5.5 |
| | 12 | #5 @ 4" | 52.0 | 4.7 | 3.6 | 32.0 | 3.4 | 6.3 | 9.7 | 60.5 | 5.1 | 4.2 |
| Standard W7x45 | 8 | #5 @ 4" | 80.0 | 8.1 | 4.5 | 13.0 | 6.2 | 7.1 | 11.5 | 63.8 | 10.7 | 9.7 |
| | 10 | #5 @ 5" | 72.4 | 6.6 | 3.6 | 10.4 | 4.9 | 7.1 | 10.0 | 61.9 | 10.1 | 7.7 |
| | 12 | #5 @ 4" | 67.5 | 5.6 | 4.3 | 18.5 | 4.3 | 7.1 | 9.0 | 61.4 | 7.4 | 5.9 |
| Standard W10x5 | 8 | #6 @ 4" | 112.6 | 10.5 | 7.8 | 20.5 | 8.4 | 8.2 | 13.9 | 66.6 | 13.4 | 12.2 |
| | 10 | #6 @ 5" | 101.2 | 8.6 | 6.2 | 16.4 | 6.8 | 8.2 | 12.1 | 66.3 | 12.5 | 11.3 |
| | 10 | #5 @ 5" | 96.7 | 8.4 | 4.5 | 9.7 | 6.4 | 8.1 | 12.1 | 64.0 | 9.2 | 7.0 |
| | 12 | #6 @ 4" | 94.8 | 7.3 | 7.5 | 28.5 | 5.8 | 8.2 | 10.9 | 65.7 | 11.7 | 9.7 |
| | 12 | #5 @ 4" | 90.6 | 7.1 | 5.3 | 13.9 | 5.6 | 8.1 | 10.9 | 63.3 | 11.6 | 9.7 |
| Standard W10x7 | 8 | #6 @ 4" | 147.4 | 13.6 | 9.3 | 18.9 | 11.0 | 9.2 | 15.4 | 70.1 | 15.6 | 14.4 |
| | 10 | #6 @ 5" | 132.7 | 11.1 | 7.5 | 15.2 | 8.8 | 9.2 | 13.3 | 67.5 | 13.9 | 11.7 |
| | 10 | #5 @ 5" | 126.8 | 10.9 | 5.5 | 9.8 | 8.2 | 9.1 | 13.3 | 65.2 | 8.1 | 6.7 |
| | 12 | #6 @ 4" | 125.0 | 9.4 | 8.9 | 21.9 | 7.6 | 9.2 | 11.9 | 66.7 | 13.9 | 12.7 |
| | 12 | #5 @ 4" | 119.3 | 8.2 | 6.4 | 12.9 | 7.3 | 9.1 | 11.9 | 64.3 | 11.9 | 10.3 |

**Design Notes:**

**WT Shape main bars:** ASTM A992 (Fy=50 ksi). **Plate and flat bars:** ASTM A709 Grade 36 or 50. **Rebar:** ASTM A615 (Fy=60 ksi)

**Concrete:** f'c=4000 psi, n=8, (n=24 for sustained dead load). Top 0.5" of concrete is sacrificial. Concrete not considered in tension regions.

Total weights shown are with normal concrete and exclusive of "haunch" concrete (between top of beams and top of distribution bars), additional full depth concrete at connections between panels, and any additional deck overlay. Further weight reduction is possible by using lightweight concrete.

* Designs in accordance with 2010 AASHTO LRFD Bridge Design Specifications. Meets deflection criteria of L/800.

All punched holes or slots in steel members are deducted when computing section properties.

Other configurations are available. Contact The BGFMA for more information.

## Appendix B: Exodermic Steel Grid Drawings

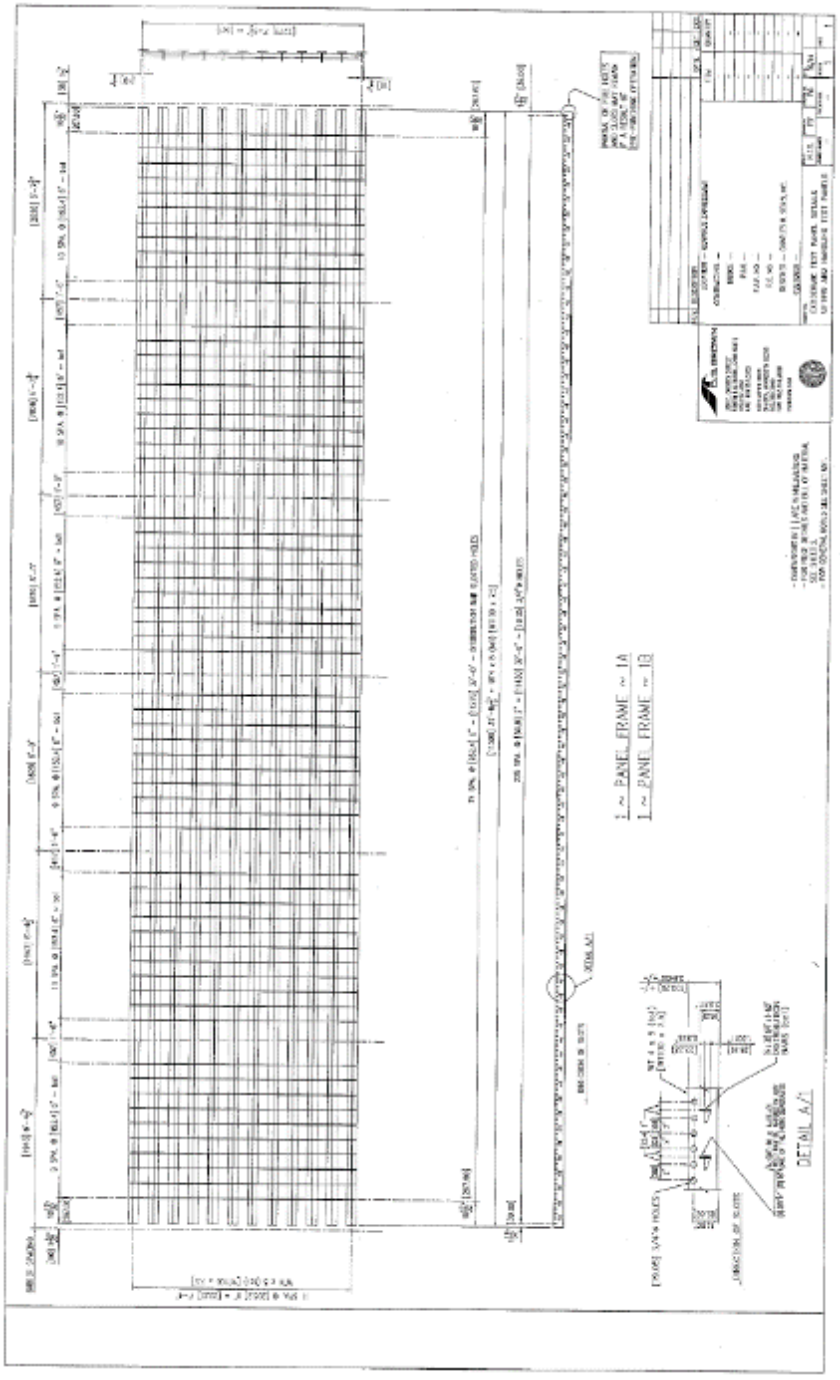

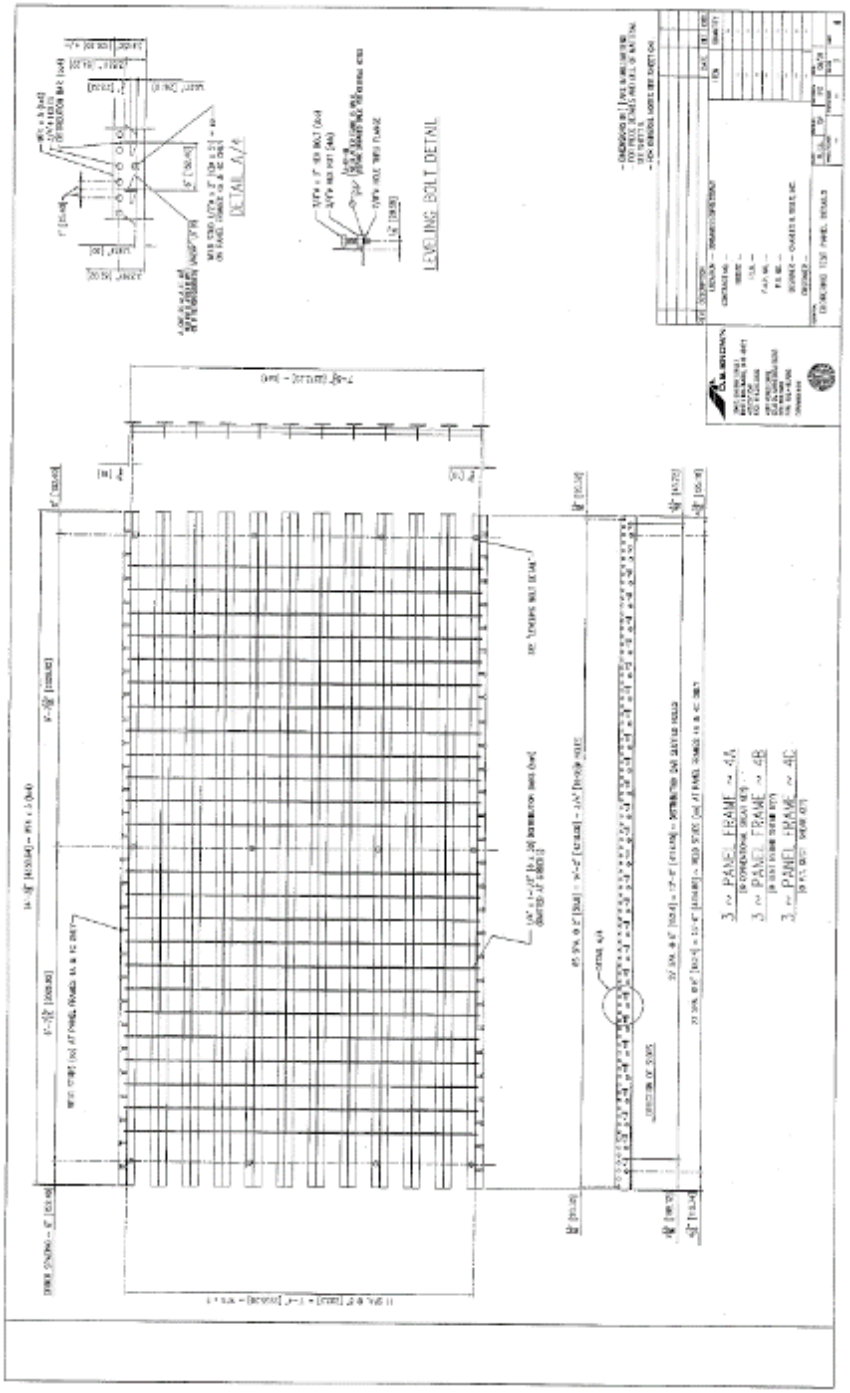
DETAIL A/4
LEVELING BOLT DETAIL

## Appendix C: Specification for Exodermic Deck Systems

### SPECIFICATION FOR EXODERMIC™ DECK SYSTEMS

[Note: Highlighted regions require input from the author or provide guidance. Highlighting should not be visible on the completed document]

1. DESCRIPTION

[For Precast Decks]

1.01 Contractor shall furnish, deliver, and install the precast Exodermic™ deck panels, reinforcing steel, and rapid-setting concrete as shown in the contract drawings and in accordance with the manufacturer's recommendations.

[Or, For Cast-in-Place Decks]

1.01 Contractor shall furnish, deliver, and install the steel grid panels, any miscellaneous metal forms (or other related forming materials), reinforcing steel, and structural concrete as shown in the contract drawings and in accordance with the manufacturer's recommendations. All concrete required for this item shall be placed in the field.

2. MATERIALS

2.01 The materials for this work shall meet the quality requirements of [the relevant portions of the owner's Standard Specifications], unless the same are altered by any specific requirements under any Special Provision, or by notes shown on the contract drawings, or in the Proposal.

[For Precast Decks]

Within 10 days after the contract is awarded, the contractor shall notify the Engineer of the name, address, telephone number, and contact person of the steel grid fabricator and precaster of all deck panels to be manufactured, supplied, and installed. The product under this item is patented. All royalty payments are paid by the authorized manufacturers.

[Or, For Cast-in-Place Decks]

Within 10 days after the contract is awarded, the contractor shall notify the Engineer of the name, address, telephone number, and contact person of the steel grid fabricator of all deck panels to be manufactured, supplied, and installed. The product under this item is patented. All royalty payments are paid by the authorized manufacturers.

2.02 The steel grid deck system must be purchased from one of the following participating BGFMA members:

| | | |
|---|---|---|
| Bailey Bridges, Inc. | Contact: Gene Gilmore | (256) 845-7575 |
| IDSI | Contact: Chris Davis | (412) 682-3041 |
| LB Foster | Contact: Mike Riley | (412) 928-3452 |

Further information may be obtained from:

BGFMA
Attn: Mark Kaczinski
300 East Cherry Street
North Baltimore, OH 45872
Tel: 1-877-257-5499
Fax: 419-257-0332
mkaczinski@dsbrown.com

2.03 The main bearing bars of the steel grid deck shall be fabricated from WT structural shapes using ASTM A992 steel [A588/A709 Grade 50W [A588M/A709M Grade 345W] may also be specified as an alternate for uncoated applications], and distribution bars and miscellaneous plates shall meet the requirements of A572/A709 Grade 50 [A572M/A709M Grade 345] steel [A588/A709 Grade 50W [A588M/A709M Grade 345W] may also be specified as an alternate]. Welding shall be in conformance with established grid industry practice, including the permitted use of Gas Metal Arc Welding (MIG). Weld qualification and weld procedures in accordance with AWS D1.5 [or per the relevant portions of the owner's Standard Specifications] shall be approved prior to deck panel fabrication.

2.04 The panel layout shown on the Contract plans is suggested. The fabricator shall develop the layout and detail it on the shop drawings.

2.05 Concrete shall be in conformance with [the relevant portions of the owner's Standard Specifications], except that maximum coarse aggregate shall not exceed 3/8" [9.5mm] in size.

2.06 Reinforcing steel shall be in conformance with ASTM A615 Grade 60 [A615M Grade 400].

2.07 Galvanized coatings shall conform to ASTM A123/A123M. Any defects in galvanizing shall be repaired as specified in ASTM A780. Repair materials containing aluminum shall not be used to restore defective areas.

2.08 Unless specified otherwise, leveling bolts, nuts, and washers shall conform to the specifications of ASTM A307, ASTM A563 and ASTM F844 respectively.

Leveling bolts need not be galvanized if minimum top cover over the bolts of 2.5 inches [63.5 mm] is provided.

2.09 The vertical steel sheet metal form pans installed in the grid prior to galvanizing shall conform to the latest specification for ASTM A366/A366M or A1011/A1011M. Galvanized steel sheet metal forms installed following grid panel galvanizing shall conform to the latest specification for ASTM A653/A653M, furnished in the gauge specified on the contract drawings. All metal forms shall be protected during shipment and site storage to retain their shape until deck panel installation.

[Include 2.10 for Precast Panels]

2.10 Rapid-setting concrete for the field closure pours shall conform to [the relevant portions of the owner's Standard Specifications]. Coarse aggregate shall not exceed 3/8" [9.5 mm] in size. Prior to opening to traffic, the design compressive strength of the closure pour concrete shall be attained, or other design strength allowable in accordance with the manufacturer's recommendations. Where no overlay is specified and to the extent feasible, rapid-setting concrete color shall match that of the precast concrete surface of the precast panel.

## 3. CONSTRUCTION DETAILS

### 3.01 **Steel Grid Deck**

A. The steel grid deck shall be fabricated to the dimensions and properties as shown on the plans, shop drawings, and in accordance with [the relevant portions of the owner's Standard Specifications]. The use of tertiary or supplemental bars to develop composite action between the concrete deck and steel grid shall not be allowed. Weld sizes shall be in conformance with established grid industry practice unless otherwise indicated on the contract plans. It shall be the contractor's responsibility to field verify all dimensions in order to make necessary changes prior to fabrication. Due consideration shall be given to the placement of leveling devices to provide adequate clearance for their field adjustment from above using a socket wrench and for adequate clearance for field placement of headed shear studs. After the attachment of edge bars, leveling devices, vertical form pans, and other components as described in the plans and specifications, the grid deck shall be galvanized in accordance with ASTM A123/A123M [or the relevant portions of the owner's Standard Specifications].

B. The dimensional tolerances for each steel grid panel shall be in accordance with the most recent version of BGFMA TS-01, "Fabrication Tolerances for Grid Decks", published by the Bridge Grid Flooring Manufacturers Association.

[Or]

B. The steel grid deck panels shall be fabricated within the following tolerances:

| | |
|---|---|
| Panel Length (L) | ±0.25"[6.4mm] (in the direction of main bar) |
| Panel Width (W) | +0, -0.125"[-3.2mm] (in the direction of distribution bar) |
| Squareness (Diagonals 'D1' and 'D2') | $\lvert D1-D2 \rvert \leq 0.5$"[12.7mm] |
| Longitudinal Camber | 0.003*L |
| Transverse Camber | 0.004*W |
| Sweep (side bow) ('L' in feet, tolerance in inches)<br>['L' in meters, tolerance in millimeters] | 0.025*L (for L ≤ 40'-0")<br>$0.00065*L^2$ (for L > 40'-0")<br>[20.83*L (for L ≤ 12.192m)]<br>[$0.178*L^2$ (for L > 12.192m)] |
| Main Bar Verticality | 0.04*H ('H' = full bar height) (See Note 1) |
| Distribution Bar Verticality | 0.04*H ('H' = full bar height) (See Note 1) |
| Bar Spacing (Main Bar & Dist. Bar) | ±0.125"[3.2mm] center to center (See Note 1) |

Note 1: No more than 1% of all locations can violate specified tolerance.

C. Sheet metal forms shall be installed in such a manner as to minimize leakage.

D. Lifting locations and lifting procedures shall be included on the shop drawing submission. Care shall be taken to avoid twisting of the panels or bending of the panels in the weak (perpendicular to main bar) direction. [Use of multiple pick points is recommended.] Steel grid panels must be properly blocked with wood (with due regard to built-in panel camber) during transportation and storage in order to avoid distortion or other damage.

3.02 **Precast Concrete**

A. A concrete mix design, to be approved by the owner, shall be submitted along with the shop drawings prior to commencing work. The concrete mix provided shall produce concrete that shall attain a minimum 28-day compressive strength of 4000 psi [27.6 MPa] [or other design strength specified]. 3/8" [9.5 mm] maximum coarse aggregate shall be used in the mix.

B. Rebar layout shall consider the location of the leveling bolts, providing sufficient clearance for adjustment in the field using a socket wrench. Main (top) rebar, which runs in the same direction as the main bearing bars of the steel grid, shall be placed a minimum of 1" from the web of the main bearing bars. Minimum cover between rebar and exposed surfaces of precast concrete shall be 1" unless otherwise shown on the plans.

C. The top surface of the roadway shall be given a textured finish as designated by the Engineer.

D. The casting bed and forms shall have provisions for straightening and holding the steel grid panels flat and square prior to placing concrete. The steel grid panels shall be checked for conformity with the required dimensions as to cross slope, and must be supported to prevent displacement during precasting operations to obtain the proper concrete thickness.

E. Precast panels shall not be removed from the forms or moved until the concrete has reached the greater of 3500 psi [24.1 MPa] or 75% of the concrete design compressive strength.

F. Precast panels shall be properly cured until the concrete reaches its 28-day design strength.

G. The dimensional tolerances of a completed precast panel in any direction shall be ±1/4 inch [±6.4 mm].

H. After curing, all form release material and any other forming materials adhering to the vertical faces of concrete shall be removed. Precast concrete vertical faces shall be sandblasted, with care taken to avoid damage to the galvanized or epoxy coatings.

I. A rigid lifting frame should be used whenever the precast panels are moved. Lifting locations must be positioned to limit stresses in the panel and analysis should consider stresses caused by deflection of the lifting frame. Proposed handling methods must limit the actual concrete tensile stresses to the concrete modulus of rupture based upon the proposed support locations and expected dynamic loading during handling, storage, and transportation of the panels. Particular care shall be taken to avoid twisting of the panels or bending of the panels in the weak (perpendicular to the main bar) direction.

J. The completed panels shall be marked with their proper identification number. Panels shall be stored and shipped right side up, and wood lagging shall be used (with due regard to built-in panel camber) to prevent steel, concrete, sheet metal, or galvanized coating damage. At a minimum, lagging shall be placed immediately adjacent to the proposed lifting locations and at the ends of the panel. Preferably, blocking should be placed at all stringer (floor beam) block-outs and at the ends of the panel. Blocking between stacked panels must be in vertical alignment across the panel width. Stack no more than four precast panels high.

[Or, For Cast-in-Place Decks]

3.02 **Concrete**

A. A concrete mix design, to be approved by the owner, shall be submitted for approval prior to commencing work. The concrete mix provided shall produce concrete which shall attain a 28-day compressive strength of 4000 psi [27.6 MPa]

[or other design strength specified]. 3/8" [9.5 mm] maximum coarse aggregate shall be used.

B. The top surface of the roadway shall be given a non-skid texture as designated by the Engineer.

3.03 **Field Installation** [For Precast Panels]

A. Installation and installation tolerances shall be in accordance with this specification and the most recent version of BGFMA TS-03, "Installation Tolerances and Guidelines for Grid Reinforced Concrete Bridge Decks," published by the Bridge Grid Flooring Manufacturers Association.

[Or]

A. Installation shall be in accordance with this specification and the most recent version of BGFMA TS-03, "Installation Tolerances and Guidelines for Grid Reinforced Concrete Bridge Decks," published by the Bridge Grid Flooring Manufacturers Association. The steel grid deck panels shall be installed within the following tolerances:

1.) Alignment: Main bearing bar misalignment between adjacent grid deck panels shall be no more than 1/2" [12.7mm].
2.) Gap: Distance between main bearing bars between adjacent grid deck panels shall be as specified, ±1/2" [±12.7mm] but shall not exceed 8" [203.2mm].

B. Panels will be delivered to the job site free from any defects and bearing the proper identifying marks.

C. When rehabilitating a structure, and prior to deck panel installation, blast clean the top surfaces of beam flanges and the surfaces of concrete and uncoated reinforcing steel that will be in contact with new rapid-setting concrete according to [the relevant portions of the owner's Standard Specifications].

D. The panels shall be placed on the structure with careful consideration given to the alignment of each adjacent panel. Measure from fixed points to avoid cumulative error. Lifting panels from the leveling devices, rebar, or distribution bars is prohibited.

E. Adjustment to proper elevation shall be made through the use of the built-in leveling bolts if specified, or shims or other means.

F. After all panels have been adjusted to their proper elevation, and all haunch and miscellaneous forms have been installed, the contractor shall install the welded headed shear studs to the steel stringers, girders, and/or floor beams as detailed on the plans through the openings provided in the deck panels. Alternatively, with

careful layout, studs may be installed prior to placing deck panels. A separate welding generator shall be used to furnish power to each stud gun in order to assure acceptable welds.

G. After all studs have been installed, the Contractor shall clean the top surface of all flanges before any concrete is placed, including breaking the ceramic ferrules around the welded studs.

H. At haunches and areas of full-depth concrete, the contractor shall seal the openings in the main bars using duct tape or other similar material prior to concrete placement. Seal the openings from the haunch or full-depth side.

I. Rapid setting concrete for field closure pours shall be placed, finished, and cured in accordance with [the relevant portions of the owner's Standard Specifications]. Maximum coarse aggregate size shall be 3/8" [9.5 mm]. A pencil vibrator shall be used in the haunch and transverse panel connection areas to assure good consolidation.

[Or, For Cast-in-Place Decks]

3.03 **Field Installation**

A. Installation and installation tolerances shall be in accordance with this specification and the most recent version of BGFMA TS-03, "Installation Tolerances and Guidelines for Grid Reinforced Concrete Bridge Decks," published by the Bridge Grid Flooring Manufacturers Association.

[Or]

A. Installation shall be in accordance with this specification and the most recent version of BGFMA TS-03, "Installation Tolerances and Guidelines for Grid Reinforced Concrete Bridge Decks," published by the Bridge Grid Flooring Manufacturers Association. The steel grid deck panels shall be installed within the following tolerances:

1.) Alignment: Main bearing bar misalignment between adjacent grid deck panels shall be no more than 1/2" [12.7mm].
2.) Gap: Distance between main bearing bars between adjacent grid deck panels shall be as specified, ±1/2" [±12.7mm] but shall not exceed 8" [203.2mm].

B. Panels will be delivered to the job site free from any defects and bearing the proper identifying marks. Check the panels for defects and identification. Repair or replace the grid panels or metal forms damaged during shipment and storage, to the satisfaction of the Engineer.

C. When rehabilitating a structure, and prior to deck panel installation, blast clean the top surfaces of existing beam flanges and the surfaces of concrete and uncoated reinforcing steel that will be in contact with new concrete according to [the relevant portions of the owner's Standard Specifications].

D. Position panels on the beams and align with adjacent panels. Measure from fixed points to avoid cumulative error. Adjustment to proper elevation shall be made through the use of the built-in leveling bolts if specified, or shims or other means. Square up panels as necessary.

E. After all haunch and miscellaneous forms have been installed, the contractor shall install the welded headed shear studs to the steel stringers, girders, and/or floor beams as detailed on the plans through the openings provided in the deck panels. Alternatively, with careful layout and the Engineer's permission, studs may be installed prior to placing deck panels. A separate welding generator shall be used to furnish power to each stud gun in order to assure acceptable welds.

F. After all studs have been installed, the Contractor shall clean the top surface of all flanges before any concrete is placed, including breaking the ceramic ferrules around the welded studs.

G. Gaps between the main bars and the horizontal form pans shall be field sealed by the contractor with silicone caulk as required to prevent excessive concrete and grout leakage.

H. At haunches and areas of full-depth concrete, the contractor shall seal the openings in the main bars using duct tape or other similar material prior to concrete placement. Seal the openings from the haunch or full-depth side.

I. No concrete shall be placed until all grid panels are in place on the bridge, and secured in proper position and all welded [and bolted, if any] headed shear studs and reinforcing steel is installed in accordance with [the relevant portions of the owner's Standard Specifications]. Main (top) rebar, which runs in the same direction as the main bearing bars of the steel grid, shall be placed a minimum of 1" from the web of the main bearing bars.

J. Concrete shall be placed, finished, and cured in accordance with [the relevant portions of the owner's Standard Specifications]. A pencil vibrator shall be used in the haunch and full depth areas between grid panels to assure good consolidation.

K. The vertical surfaces of any construction joints shall be thoroughly coated with a Portland cement mortar bonding grout [or other suitable material].

L. Where feasible, a worker with a high-pressure water hose shall be stationed under the deck during all concrete pouring and finishing to wash any drips off of the

structural steel. Care must be taken not to disturb the form pans in the grid deck with the high-pressure stream.

M. Damaged or defective concrete shall be repaired or replaced in accordance with [the relevant portions of the owner's Standard Specifications].

4. METHOD OF MEASUREMENT

4.01 Precast Exodermic™ panels shall be measured as the total gross square footage of the deck slab panel installed and inspected in accordance with the plans and specifications. Measurements shall be taken from the outside edge to outside edge of the top surface of the deck slab in both directions. No deduction shall be made for joints, block-outs, or openings.

[Or, For Cast-in-Place Decks]

4.01 Exodermic™ panels shall be measured as the total gross square footage of the grid deck panel installed and inspected in accordance with the plans and specifications. Measurements will be taken from the outside edge to outside edge of the grid panel in both directions. No deduction will be made for joints, block-outs, or openings.

5. BASIS OF PAYMENT

5.01 The unit bid price shall include the cost of furnishing all labor, materials, and equipment necessary to complete the work, including the furnishing and installation of all deck panels, which also includes the cost of transportation, storage, and protection from damage to the deck panels.

# COMMENTARY TO SPECIFICATION FOR EXODERMIC™ DECK SYSTEMS

C2.05 Aggregate size greater than 3/8" could potentially prevent consolidation of concrete in and around fabrication punches critical for the development of composite action with the grid. Additionally, as the clearance between the bottom of the WT main bearing bar and top flange of the supporting steel decreases; it becomes more difficult to obtain full consolidation of concrete under the WT. The recommended minimum design haunch is 1-1/2". However, this is not always achievable, and site conditions will dictate the height. For haunch heights less than the minimum, it is suggested that a high strength grout be poured to the bottom of the WT main bars over the supporting member prior to placement of field placed concrete. In this way, complete transfer of the load is ensured.

C2.07 ASTM A780 allows for three methods of repair: Zinc-Based Solders (Hot-Stick), Paints Containing Zinc Dust, or Sprayed Zinc (Metalization). Although some states include repair procedures within construction specifications, fabricators should have the ability to select which method of repair in accordance with A780 is most convenient.

C2.10 Due to the inherent cold joints associated with precast panel construction, an overlay is always recommended to reduce the potential for intrusion of harmful brine from deicing salts. If an overlay is not specified, a "plaid" appearance is expected from the different shades of concrete. This is the result of different materials that were used to batch the precast and closure pour concretes at separate locations and times. An exact match is impossible to obtain, however, a close match is possible if samples of both precast and closure pour concrete are submitted in advance.

C3.02A The strength of a grid reinforced concrete deck system is determined by the transformed area method. Although 28-day compressive strength requirements vary among owners, 4000 psi is generally the lowest strength specified for concrete bridge decks. Therefore, fabricators have developed design tables and literature for their systems using a concrete design compressive strength of 4000 psi. Specification of compressive strengths less than 4000 psi could alter the modular ratio and therefore affect the strength of the composite system and deviate from published design tables.

In general, when specifying concrete for bridge decks, a low W/C (< 0.4) is preferred. Low W/C ratios result in higher strength, low permeability concrete. Low W/C ratios and air entrainment increase the durability of the concrete. Although a low W/C ratio results in a lower slump and therefore reduced workability, plasticizers have been used successfully to increase the workability without sacrificing strength.

C3.02F (Precast only) Allowable curing methods vary among owners; however, water curing is certainly the most widely accepted method. Continued hydration through water curing allows a supply of water to react with the cement for the concrete to gain strength. A minimum period of seven days is often specified.

## Appendix D: MasterEmaco T 1060 Technical Data Guide

BASF
We create chemistry

Technical Data Guide

3 | 03 01 00
Maintenance of Concrete

# MasterEmaco® T 1060

## Very rapid-setting cement-based concrete repair mortar

FORMERLY 10-60 RAPID MORTAR

**PACKAGING**
50 lb (22.6 kg) polyethylene-lined bags
3,000 lb (1,360 kg) bulk bags

**YIELD**
0.43 ft³ (0.012 m³) per 50 lb (22.6 kg)
- WHEN EXTENDED 50%:
0.57 ft³ (0.016 m³)
- WHEN EXTENDED 100%:
0.77 ft³ (0.022 m³)

**STORAGE**
Store in unopened containers in cool, clean, dry conditions

**SHELF LIFE**
- 50 LB BAGS:
1 year when properly stored
- 3,000 LB BULK BAGS:
6 months when properly stored

**VOC CONTENT**
0 g/L less water and exempt solvents

**DESCRIPTION**
MasterEmaco T 1060 is a onecomponent shrinkage-compensated very rapid-setting cement-based mortar. It is designed for repairing horizontal concrete surfaces where high early strength gain is required.

**PRODUCT HIGHLIGHTS**
- Extra low permeability helps minimize chloride intrusion
- Very rapid-setting so that structures can be opened to vehicular traffic in 1 hour
- Low residual moisture, can be coated in as little as 4 hours
- Excellent resistance to freeze/thaw cycling
- Shrinkage compensated, minimizing cracking from drying shrinkage reducing stress at the bond line
- Can be extended up to 100% by weight providing higher yields
- Proprietary cement blend bonds to carbonated and noncarbonated concrete substrates

**APPLICATIONS**
- Interior and exterior
- Horizontal surfaces
- Applications requiring high early-strength gain
- Structural concrete repairs
- Partial and full-depth repairs

**SUBSTRATES**
- Concrete

**HOW TO APPLY**

**SURFACE PREPARATION**

CONCRETE

1. Concrete must be structurally sound and fully cured (28 days).
2. Saw cut the perimeter of the area being repaired into a square with a minimum depth of ½" (13 mm).
3. Refer to current ICRI Guideline no. 310.2R for surface prep requirements to permit proper bond.

REINFORCING STEEL

1. Remove all oxidation and scale from the exposed reinforcing steel in accordance with ICRI Technical Guideline No. 310.1R.
2. For additional protection from future corrosion, coat the prepared reinforcing steel with MasterProtect P 8100 AP.

Master Builders Solutions by BASF
www.master-builders-solutions.basf.us

MASTER® BUILDERS SOLUTIONS

## Technical Data

### Composition

MasterEmaco T 1060 is a blend of cement, graded aggregate, shrinkage-compensating agents, and set-control additives.

### Compliances

- ASTM C 928

### Test Data

The following results were obtained with a water / powder ratio of 5.5 pints (2.6 L) of water to 50 lbs (22.7 kg) of MasterEmaco T 1060 at 73° F (23° C).

| PROPERTY | RESULTS | TEST METHOD |
|---|---|---|
| **Fresh wet density,** lb/ft³ (kg/m³) | 130 (2,082) | ASTM C 138 |
| **Set time,** min, at 72° F (22° C) | | ASTM C 191 |
| Initial | 16 | |
| Final | 28 | |
| **Working time,** min | 8 | |
| **Length change,** % (µstrain) | | ASTM C 928 |
| Drying shrinkage | –0.05 (–500) | |
| Wetting expansion | +0.03 (+300) | |
| **Coefficient of thermal expansion,** in/in/° F (cm/cm/° C) | 7.0 x $10^{-6}$ (12.6 x $10^{-6}$) | CRD C 39 |
| **Modulus of elasticity,** psi (GPa) | 4.4 x $10^6$ (19.5) | ASTM C 469 |
| **Rapid chloride permeability,** coulombs | < 300 | ASTM C 1202 |
| **Freeze/thaw resistance,** % RDM, at 300 cycles | 100 | ASTM C 666, (Procedure A) |
| **Scaling resistance,** at 25 cycles | 0 rating; no scaling | ASTM C 672 |
| **Slant shear bond strength,** psi (MPa) | | ASTM C 882, modified[1] |
| 1 day | 2,300 (16) | |
| 28 days | 2,600 (18) | |
| **Splitting tensile strength,** psi (MPa) | | ASTM C 496 |
| 1 day | 400 (3) | |
| 28 days | 450 (3) | |
| **Flexural strength,** psi (MPa) | | ASTM C 348 |
| 1 day | 700 (5) | |
| 28 days | 850 (6) | |
| **Compressive strength,** psi (MPa), 2" cubes | | ASTM C 109 |
| 1 hr | 2,000 (14) | |
| 1 day | 4,000 (28) | |
| 28 days | 8,000 (55) | |
| **Compressive strength,** psi (MPa), 3 by 6" cylinders, at 28 days | 7,400 (51) | ASTM C 39 |

[1]No bonding agent used; mortar scrubbed into substrate.

All application and performance values are typical for the material, but may vary with test methods, conditions, and configurations.

**MIXING**

1. Precondition material to 70° F ±5° (21° C ±3°) before mixing.
2. Add 5½ pints (2.6 L) of potable water to the mixing container for each bag of MasterEmaco T 1060. If required, add the correct amount of aggregate to the mixer. Add the powder to the water while continuously mixing with a slow-speed drill and paddle, mortar mixer, or other forced action mixer.
3. Mix for a minimum of 3 minutes until fully homogeneous.

AGGREGATE EXTENSION

1. For repair areas 2–4" (51–102 mm) in depth, the minimum recommended addition is 15–25 lbs (6.8–11.4 kg) of ⅜" (10 mm) washed, graded, rounded, SSD, low-absorption, high-density aggregate per 50 lb (22.6 kg) bag.
2. For areas greater than 4" (102 mm) in depth, the minimum recommended addition is 25–50 lbs (11.4–22.6 kg) of ⅜" (10 mm) washed, graded, rounded, SSD, low-absorption, high-density aggregate per 50 lb bag.
3. The maximum aggregate extension is 50 lbs (22.6 kg) of pea gravel per bag.
4. Aggregate must comply with the requirements of ASTM C 33.

**APPLICATION**

1. After removing all standing water, thoroughly scrub a thin layer of bond coat into the saturated surface with a stiff-bristled broom or brush. Do not dilute the bond coat with water. Do not apply more of this bond coat than can be covered with mortar before the bond coat dries. Do not retemper the bond coat.
2. Immediately place the repair mortar from one side of the prepared area to the other. Work the material firmly into the bottom and sides of the patch to ensure good bond. Level the MasterEmaco T 1060 and screed it to the elevation of the existing concrete. Apply the appropriate finish.
3. Finish the completed repair, as required, taking care not to overwork the surface.
4. The recommended application range of MasterEmaco T 1060 is from 40 to 85° F (4 to 29° C). Follow ACI 305 and 306 for hot or cold weather.
5. A maximum of 15 minutes should be allowed to mix, place, and finish MasterEmaco T 1060 at 70° F (21° C).

**CURING**

Cure with an approved curing compound compliant with ASTM C 309 or preferably ASTM C 1315.

**CLEAN UP**

Clean tools and equipment with clean water immediately after use. Cured material must be removed mechanically.

**FOR BEST PERFORMANCE**

- Minimum ambient, surface, and material temperature is 40° F (4° C) and rising.
- Do not mix longer than 5 minutes.
- Minimum application thickness is ½" (13 mm).
- Neat MasterEmaco T 1060 can be applied to a minimum of ¼" (6 mm) if intended for use under deck membranes on balconies subject to pedestrian traffic.
- Consult coating supplier for overcoating requirements.
- Do not mix partial bags.
- Do not add plasticizers, accelerators, retarders, or other additives.
- For professional use only; not for sale to or use by the general public.
- Make certain the most current versions of product data sheet and SDS are being used; visit www.master-builders-solutions.BASF.us to verify the most current versions.
- Proper application is the responsibility of the user. Field visits by BASF personnel are for the purpose of making technical recommendations only and not for supervising or providing quality control on the jobsite.

**HEALTH, SAFETY AND ENVIRONMENTAL**

Read, understand and follow all Safety Data Sheets and product label information for this product prior to use. The SDS can be obtained by visiting www.master-builders-solutions.basf.us, e-mailing your request to basfbscst@basf.com or calling 1(800)433-9517. Use only as directed.

**For medical emergencies only, call ChemTrec® 1(800) 424-9300.**

**LIMITED WARRANTY NOTICE**

BASF warrants this product to be free from manufacturing defects and to meet the technical properties on the current Technical Data Guide, if used as directed within shelf life. Satisfactory results depend not only on quality products but also upon many factors beyond our control. BASF MAKES NO OTHER WARRANTY OR GUARANTEE, EXPRESS OR IMPLIED, INCLUDING WARRANTIES OF MERCHANTABILITY OR FITNESS FOR A PARTICULAR PURPOSE WITH RESPECT TO ITS PRODUCTS. The sole and exclusive remedy of Purchaser for any claim concerning this product, including but not limited to, claims alleging breach of warranty, negligence, strict liability or otherwise, is the replacement of product or refund of the purchase price, at the sole option of BASF. Any claims concerning this product must be received in writing within one (1) year from the date of shipment and any claims not presented within that period are waived by Purchaser. BASF WILL NOT BE RESPONSIBLE FOR ANY SPECIAL, INCIDENTAL, CONSEQUENTIAL (INCLUDING LOST PROFITS) OR PUNITIVE DAMAGES OF ANY KIND.

Purchaser must determine the suitability of the products for the intended use and assumes all risks and liabilities in connection therewith. This information and all further technical advice are based on BASF's present knowledge and experience. However, BASF assumes no liability for providing such information and advice including the extent to which such information and advice may relate to existing third party intellectual property rights, especially patent rights, nor shall any legal relationship be created by or arise from the provision of such information and advice. BASF reserves the right to make any changes according to technological progress or further developments. The Purchaser of the Product(s) must test the product(s) for suitability for the intended application and purpose before proceeding with a full application of the product(s). Performance of the product described herein should be verified by testing and carried out by qualified experts.

**BASF Corporation**
**Construction Systems**

889 Valley Park Drive, Shakopee, MN 55379
**www.master-builders-solutions.basf.us**

**Customer Service** 1(800) 433.9517
**Technical Service** 1(800) 243.6739